THE CONTRIBUTION OF CORTICAL FEATURE PROCESSING TO OCULOMOTOR TARGET SELECTION

DEVIN HEINZE KEHOE

A THESIS SUBMITTED TO
THE FACULTY OF GRADUATE STUDIES
IN PARTIAL FULFILLMENT OF THE REQUIREMENTS
FOR THE DEGREE OF
DOCTOR OF PHILOSOPHY

GRADUATE PROGRAM IN PSYCHOLOGY
YORK UNIVERSITY
TORONTO, ONTARIO

Abstract

We effortlessly move our eyes to objects with specific features and avoid objects with other features. This feature-guided target selection behavior has been studied extensively in experimental psychology and systems neuroscience. By now, the visual and cognitive factors that mediate target selection and the neural signatures of target selection in oculomotor substrates are clear. For example, neural activation encoding targets and distractors gradually divergences over time therefore signalling stimulus identity, while visual/cognitive factors like bottom-up salience or top-down priority modulate the precise time of this divergence. But despite the extensive research on oculomotor target selection, little research has examined how neural activation in oculomotor substrates encoding potential eye movements vectors is reweighted to indicate stimulus identity. Meanwhile, a parallel branch of systems neuroscience has thoroughly examined the function and anatomy of the visual processing pipeline distributed throughout the neocortex of mammals. Heretofore, however, there has been little if any attempt to characterize the relationship between cortical visual feature processing and oculomotor vector encoding during feature-guided target selection.

This dissertation presents a series of behavioral experiments that provide several insights into this relationship. In these experiments, I measure the perturbation of target-directed saccades elicited by competitive remote distractors as a function of (1) the feature-space distance between targets and distractors and/or (2) distractor processing time. Given the close correspondence between saccade perturbation metrics and the underlying physiology of the oculomotor system, this methodology offers a non-invasive analog to examining the time course of oculomotor distractor activation during feature-guided target selection. In one set of experiments, I observed that distractor activation encodes the feature-space distance between targets and distractors in a

manner consistent with attentional pruning of visual features observed in cortical feature representations during feature-based attentional deployment. In another set of experiments, I observed that the pattern of visual onset response latencies across distractor features mimics the pattern robustly observed between the cortical modules specialized for processing the respective features. These results indicate a close representational and temporal parity between feature encoding in oculomotor and (cortical) perceptual systems. I therefore propose a broad theory of oculomotor feature encoding whereby eye movement vectors in oculomotor substrates are dynamically and continuously reweighted by the feature-dependent network of cortical modules in the perceptual system necessary for representing the relevant feature set of the potential eye movement target.

Dedication

To Erin,

Thanks for convincing me to go to university all those years ago.

Acknowledgements

First and foremost, I need to thank my supervisor, Maz. He has been unwavering in his support and guidance over the years. I have always been able to rely on his impressively ready insights, responsiveness, patience, encouragement, and compassion. I couldn't have possibly asked for a better graduate mentor. Thank you so much for everything, Maz.

The research in this dissertation would never have been possible if not for the help of many awesome RAs who were tremendously helpful with data collection and analysis over the years. It was a pleasure working with all of you and I know for certain you're off doing awesome and exciting things. In chronological order, thank you and shout out to Maryam, René, Jenn, Hassaan, and Lukas.

I also need to extend a very warm thank you to the lovely folks in the Psychology Graduate Office: Lori, Freda, Barb, Suzanne, and Adrienne. You guys are superhumanly helpful and show such compassion for the grad students. I'm forever grateful. Thank you!

I owe a special thank you to Richard for going out of his way to be my *pro forma* supervisor at York these last couple of years. Thank you, Richard. I really appreciate you doing that for me. And it's truly been a pleasure taking your courses and working with you on my minor area project. Those have easily been my favourite non-dissertation-related academic activities at York.

Cyan, you make life way more fun, and without exaggerating, you're the kindest human I've ever met. You've been extremely gracious in lending an ear or a backrub when things get stressful. And you're also a nerd: I love being able to blather on about the details of my work or even to work through technical problems with you. You've made this process so much easier, and I love you even more for it. Thank you so very kindly. Together, we will conquer the world.

Or something. Also, special shoutout to Brody for being the greatest (and worst) personal support animal (pet).

Thank you to family and friends, namely Mom, Dad, Erin, Mary, Kam, Rose, and KP, for all the times you've checked in on my dissertation progress and readily offered uplifting words of encouragement. I know this dissertation means almost as much to each of you as it does to me. No worries, though, I won't insist that you read it.

I was very fortunate to start graduate school alongside an awesome cohort of fellow BBCS students/postdocs, many of whom are my closest friends to this day. I'm extremely fortunate to have fallen in with such a wonderful group of people. And the love and support from fellow grad students surely helped make the daunting task of grad school possible. BBCS nerds: maybe the real PhD was the friends we made along the way.

Thanks very much to my committee: Denise and Erez. I have really appreciated your guidance and support over the years. Your advice has certainly helped me reach some big decisions. And our thoughtful discussions have revealed to me interesting new aspects of my research that I hadn't considered. Thank you.

Recently, I've had the wonderful fortune to find myself doing exciting work in the Ebitz lab at the Université de Montréal. Becket, I have really appreciated all your great career advice, and although I was nearly over the finish line when I joined, it's really helped me a lot to get there. Thank you. And to the students/postdocs in the NOISE lab, you guys rock and have always been super encouraging. To more shenanigans!

Table of Contents

List of Tables

List of Figures

Chapter 1. Vision and Eye Movements

1.1. Introduction

Vision is unique compared to our other senses in at least two regards. First, while other sensory organs are affixed to our bodies, our visual sensory organs, the retinas, can be redirected and aligned to a particular location in the environment independently of the rest of our body. This redirection and alignment of the retina is possible because our retinas are affixed to the back of our approximately spherical eyes, which are free to move within their orbit. The eyes are connected to three pairs of antagonist extraocular muscles in which each pair affords rotational movement around one of three bodily cardinal axes (i.e., superior/inferior, medial/lateral, and anterior/posterior. Second, vision is an endlessly cyclical process whereby neurocognitive processing of the available visual information is used to select a target location for the realignment of our gaze. Then, by virtual of realigning our gaze to the selected location, visual processing of that location is enhanced. As such, visual processing relies on eye movements, which relies on visual processing, *ad infinitum*.

The reciprocal nature of visual processing and eye movements is attributable to the fact that the density of our photoreceptors—specialized cells that transduce light energy into neurobiological signals—is highest in the centermost region of the retina called the *fovea centralis* and drops off exponentially at greater eccentricities (Curcio et al., 1990). Such retinal organization is evolutionarily adaptive as uniformly distributing photoreceptors across the retina limits an organism to moderate visual processing across the entire visual environment, whereas densely clustering photoreceptors in one retinal area provides excellent visual processing in a small portion of the visual environment without requiring additional anatomical resources. The trade-off is that high visual acuity is afforded to only a narrow subset of the entire visual environment (the fovea only subtends approximately 1 degree of arc[1] across the visual

environment), but as alluded to, this limitation is mitigated by our ability to redirect the retinas: moving the eyes about the visual environment allows us to serially process the environment with high visual acuity, but consequently requires many eye movements (e.g., primates typically make around 2-3 eye movements a second).

Since time and metabolic resources are expended for each eye movement, careful planning of eye movements is required. Evolutionary pressures have undoubtedly ensured that animals must prioritize their eye movements so to direct them to only the most biologically and behaviorally relevant objects or locations in the environment (e.g., a predator or food, in that order). Unsurprisingly, then, a great amount of visual and cognitive processing is dedicated to selecting targets for eye movements, a process aptly called *target selection*. While immense research has *identified* the visual and cognitive factors that mediate target selection, less research has examined *when* visual and cognitive information is incorporated into impending eye movements and from *where* these visual and cognitive inputs originate. The current dissertation will address this limitation by focusing on the context-dependent time course of cortical inputs into the oculomotor system that mediates target selection. In the following sections of this chapter, I will briefly review fundamental concepts related to visual and oculomotor processing, and then outline how these processes reciprocally contribute to oculomotor target selection.

1.2. Visual Processing

In this section, I will provide an overview of critical concepts related to how primate visual systems process the visual environment and then give an anatomical and functional summary of the primate visual system.

---

[1]In vision science, a degree of arc is more commonly referred to as a *degree of visual angle*. This concept is herein more simply referred to as “degree”.

1.2.1. Receptive Fields

When the eyes are steadily fixated, a certain portion of the environment is visible, which is referred to as the visual field. The human visual field encompasses about 135 degrees vertically and 160 degrees horizontally with overlap between both eyes in the central 60 degrees horizontally (Spector, 1990). Each visible point of space in the environment corresponds to a unique location on the retina and is therefore encoded by a specific population of photoceptors. We can invert this relationship to say that each photoreceptor is responsive to incoming light information from a particular region of space; this region of space defines the *receptive field* of the cell.

Visual receptive fields are pooled together to form larger receptive fields via neural summation: the neural activity levels in a collection of visually receptive neurons additively modulate the activity of an upstream neuron. As such, the upstream neuron inherits the visual receptive fields of the downstream neurons. This pooling starts in the retina as photoreceptors are pooled into retinal ganglion cells (RGCs). RGCs project visual representations out of the retina to visual neurons in the central nervous system, where pooling continues and creates increasingly large visual receptive fields. Spatially specific visual encoding is present throughout the widely distributed visual processing areas of the primate central nervous system (Benson et al., 2018).

1.2.2. Feature Specificity

In addition to spatial selectivity, visual neurons are also characterized by visual feature selectivity. Visual features are the visual constitutes of the visual environment and vary continuously along some psychophysical dimension, called a visual attribute. For example, color is a real-valued physical—and psychological—continuum. Color is therefore an example of a visual attribute, and any one particular color is therefore a visual feature. When a visual neuron

becomes active for some visual features and inactive for other visual features along the same attribute, this neuron is feature selective. For example, a visual neuron may be very active for red, but inactive for green. As such, the neuron is selective for the feature red and encodes the attribute color. Conversely, a visual neuron may be equally active for all colors, and therefore, is not color selective.

In addition to color, primate visual systems encode myriad simple (i.e., one-dimensional) visual attributes with obvious underlying psychophysical continuums, such as line orientation, sinusoidal spatial frequency, motion direction, velocity, etc. Visual attributes are successively pooled together forming increasingly complex (i.e., multi-dimensional) visual attributes, allowing for encoding of complex visual stimuli like faces, words, and even complex novel objects (Kehoe et al., 2018a). Decades of visual neuroscience research has revealed that the primate visual system consists of dozens of anatomically and functionally distinct visual areas specialized for processing a specific set of attributes of varying complexity.

1.2.3. Visual Processing Hierarchy

The various visual processing areas of the primate nervous system and their rich interconnections form a tangled web. This network has been meticulously catalogued by neuroanatomists into approximately 300 connections between approximately 30 nodes (DeYoe & Van Essen, 1988; Felleman & Van Essen, 1991; Van Essen et al., 1992; Van Essen & Maunsell, 1983) (see Figure 1.1 to better appreciate the impressive combinatorial complexity of the primate visual processing network). Interestingly, the primate visual processing network has obvious linear properties, as visual processing areas are hierarchically distributed on a functional and anatomical basis. In each successive layer of the visual processing hierarchy, the constituent

visual neurons have an increased (1) receptive field size, (2) representational complexity, (3) visual onset latency, and (4) posterior-to-anterior anatomical position (see Figure 1.2):

1. Cells in the highest levels of the visual processing hierarchy have massive receptive fields that span most of the visual field, while cells in the lowest levels of the hierarchy have small receptive fields that span a small fraction of the visual field. This property emerges because spatially contiguous receptive fields from downstream neurons are pooled together into an upstream neuron. Given this principle, visual receptive field size increases somewhat linearly as a function of position in the visual processing hierarchy.
2. Visual feature representations from downstream neurons are pooled and transformed so that increasingly complex visual features of the environment are encoded in each successive layer of the hierarchy. For example, if a stimulus consists of two intersecting lines, and the orientation of each individual line is encoded by one of two visual neurons, then these representations can be pooled together into an upstream visual neuron to encode the angle of the lines.
3. Neurons in lower levels of the hierarchy will encode a stimulus faster than will neurons in higher levels. This property emerges because visual representations are propagated between cortical visual modules with a transmission time of approximately 10 ms, the so called *10 ms rule-of-thumb* (Nowak & Bullier, 1997). As such, the latency of neuronal responses to visual stimuli increases by approximately 10 ms for each downstream module that relayed the signal.
4. The cortical visual processing hierarchy is anatomically distributed so that lower levels occupy locations in posterior sites of the cerebrum, while higher levels occupy sites that are further anterior.

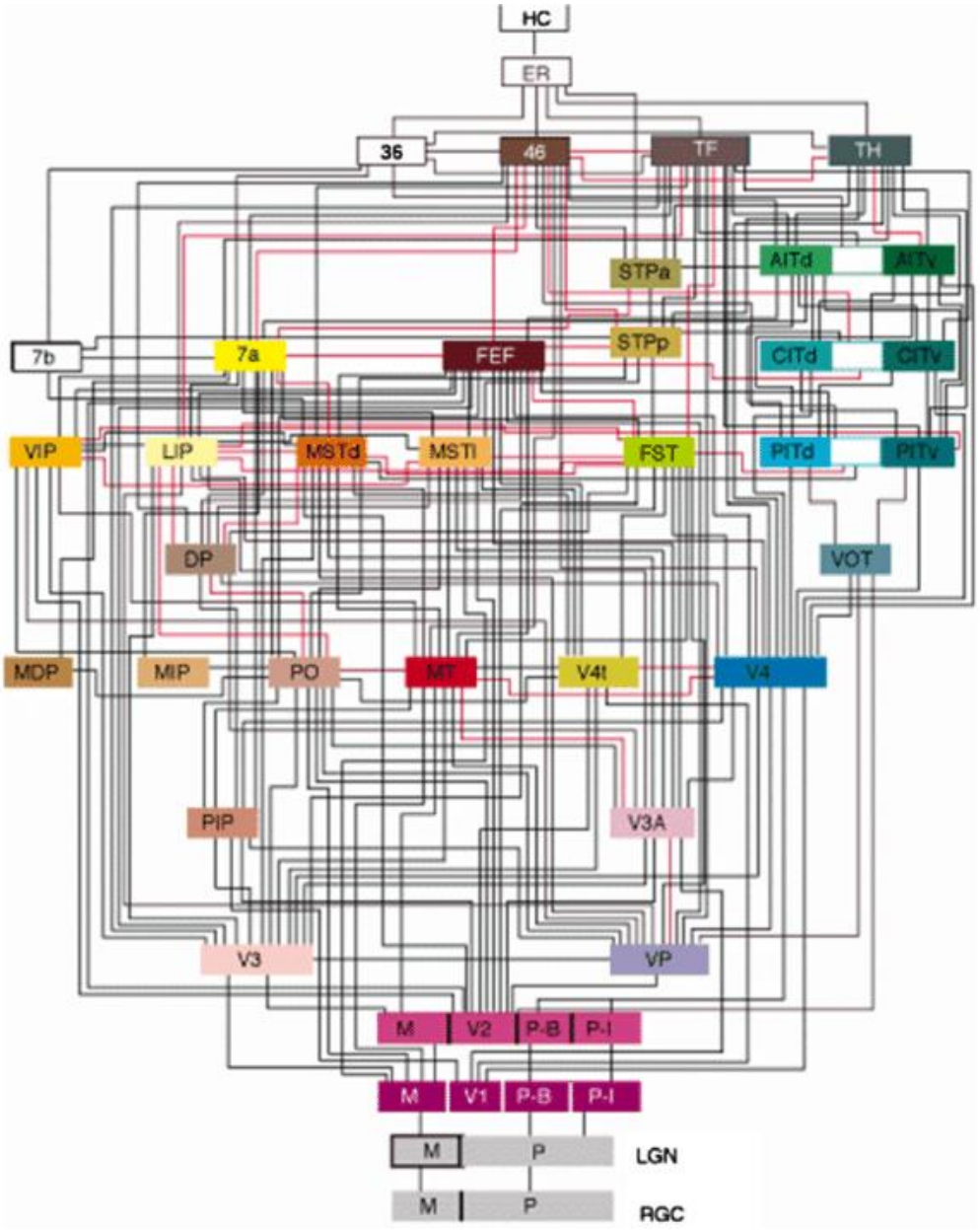

Figure 1.1. Macaque cortical visual processing network. Visual processing areas (nodes) are indicated by text-labelled squares. Connections between nodes are indicated by horizontal and vertical lines. The hierarchical position of nodes is indicated by their height in the figure. Note: Several subcortical visual substrates are not included in this diagram. Reprinted from Felleman, D. J., & Van Essen, D. C. (1991). Distributed hierarchical processing in the primate cerebral cortex. *Cerebral Cortex*, *1*(1), 1-47. https://doi.org/10.1093/cercor/1.1.1.

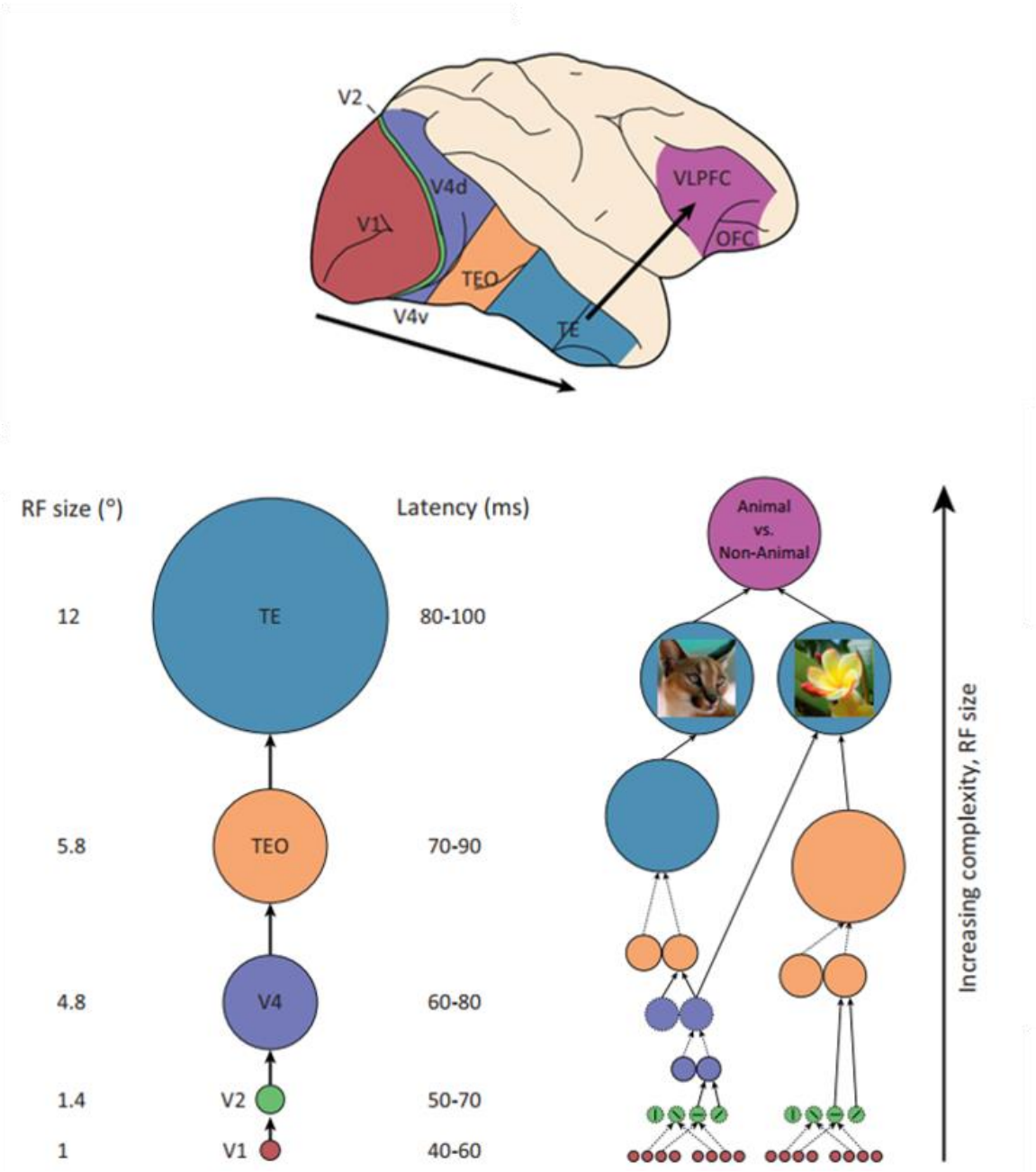

Figure 1.2. Visual processing hierarchy of the macaque ventral stream. Visual processing areas are indicated by color. Diagram of brain (top) indicates the posterior-to-anterior hierarchical distribution of some connected visual processing areas of the ventral stream. Bottom diagram indicates (from left to right) the increase in receptive field size, visual onset latency, and visual representational complexity from lower-to-higher levels of the visual processing hierarchy. Reprinted from Kravitz, D. J., Saleem, K. S., Baker, C. I., Ungerleider, L. G., & Mishkin, M.

(2013). The ventral visual pathway: an expanded neural framework for the processing of object quality. *Trends in Cognitive Sciences, 17*(1), 26-49. https://doi.org/10.1016/j.tics.2012.10.011

The visual processing hierarchy can be further segmented into three functionally and anatomically distinct, yet interconnected, parallel hierarchies: the retinotectal pathway (not illustrated in Figure 1.1), the dorsal stream (hot colors in Figure 1.1), and the ventral stream (cool colors in Figure 1.1). Segmentation into three parallel visual processing hierarchies begins in the retina, where three functionally and anatomically distinct types RGCs project visual information into the central nervous system: koniocellular cells feed the retinotectal pathway, parasol cells feed the dorsal stream, and midget cells feed the ventral stream.

1.2.3.1. Retinotectal pathway. The retinotectal pathway primarily subserves rapid orienting responses by carrying visual input from the RGCs to the extraocular muscles with fewer synapses than in any other visual pathway. This affords primates gross orienting responses with latencies at least as short as 50 ms. This pathway bypasses cortex and therefore forgoes higher visual and cognitive processing and is entirely reflexive. However, the reflexive sensitivity of this system can up- or downregulated by executive control signals largely mediated through the basal ganglian network (Hikosaka et al., 2000).

1.2.3.2. Dorsal stream. The dorsal processing stream is classically referred to as the "where" pathway, as it largely subserves spatial vision (Ungerleider & Mishkin, 1982). Generally, visual cells in this pathway have large receptive fields, poor spatial contrast sensitivity, high temporal contrast sensitivity, nearly absent color sensitivity, and fast conduction velocities. These traits allow the substrates of the dorsal stream to optimally subserve quickly directing focused attention and purposeful motor behavior towards objects and regions in space.

Lesions of the dorsal stream are typically associated with hemilateral visual neglect, impaired visually-guided motor behavior, and perceptual deficits in spatial localization.

1.2.3.3. Ventral stream. The ventral processing stream is classically referred to as the "what" pathway, as it largely subserves featural vision and object recognition (Ungerleider & Mishkin, 1982). Visual cells in the ventral stream generally have smaller receptive fields than corresponding stages in the dorsal stream, high spatial contrast sensitivity, low temporal contrast sensitivity, slow conduction velocities, and a subset of cells encode color. These traits allow the substrates of the ventral stream to encode the precise visual details of the environment subserving the representation and recognition of objects. Lesions of the ventral stream are associated with a wide range of agnosies for specific visual attributes or types of objects. For example, achromatopia, the inability to perceive color; or prosopagnosia, the inability to perceive faces.

1.3. Oculomotor Processing

In this section, I will provide functional distinctions between types of eye movements, an overview of some critical concepts related to how primate oculomotor systems encode the visual environment and how this processing subserves target selection, how oculomotor processing manifests into overt behavior, and then give an anatomical and functional summary of the primate oculomotor system.

1.3.1. Types of Eye Movements

Eye movements are typically categorized according to their functional role in oculomotor behaviour (Sparks, 2002). *Vergence eye movements* are reflexive, disconjugate horizontal eye movements that ensure that a particular location in the visual field is simultaneously foveated (i.e., at the center of gaze) in both eyes. *Vestibular optokinetic responses* (VOR) and *optokinetic*

nystagmus responses (OKN/R) are reflexive, conjugate eye movements that maintain fixational stability while the observer or image (respectively) are in motion. *Smooth pursuit eye movements* (SEM) and *saccades* are voluntary, conjugate eye movements that redirect gaze to a new location in the visual field. As a functional distinction, SEMs allow us to stably track a moving visual stimulus, while saccades allow us to redirect the location of our gaze to a stationary stimulus. SEMs and saccades can also be differentiated according to their velocities, with SEM ranging from 0-30 degrees/second and saccades ranging from 50-1000 degrees/second, and their reaction time latencies contingent on stimulus onset, with an average SEM latency of 125 milliseconds (ms) and an average saccade latency of 200 ms (Sparks, 2002). Despite these functional and kinematic differences, SEMs and saccades are both encoded according to retinotopic spatial mapping as with visual information. The current dissertation will primarily focus on oculomotor processing of saccades.

1.3.2. Motor Fields

Since eye movements redirect the location of gaze, they have a start point (initial fixation location) and an endpoint (post-movement fixation location) and can be conveniently conceptualized as polar vectors having both a direction and an amplitude. In much the same way that visual neurons have retinotopic visual receptive fields, oculomotor cells encode potential eye movement vectors as retinotopic *motor fields* AKA *movement fields*. Specifically, when activation levels in a specific population of oculomotor cells surpasses some threshold, an eye movement with a specific direction and amplitude is elicited. This direction and amplitude define the motor field of that population of oculomotor cells. Interestingly, this spatial encoding scheme is utilized by other movement systems such as those involved in manual reaching (Georgopolous et al., 1982, 1988; Kettner et al., 1988; Schwartz et al., 1988). Populations of cells encoding

contiguous saccade vectors in retinotopic space are located on contiguous portions of neural tissue, thus forming orderly motor maps (Anderson et al., 1998; Robinson, 1972; Robinson & Fuchs, 1969). This oculomotor mapping is nowhere more apparent than in the intermediate layers of the superior colliculus (SCi) and the frontal eye fields (FEF) where saccades and SEMs are encoded on orderly spatial maps of potential movement vectors, as demonstrated by meticulous microstimulation experiments (Gottlieb et al., 1993; Robinson & Fuchs, 1969; Robinson, 1972) (see Figure 1.3 for an example of the motor map encoded in SCi). One distinguishing characteristic of the constituent cells in neural substrates encoding oculomotor maps is that they possess a variety of motor and/or visual sensitivities (i.e., they may have a visual receptive and/or motor field).

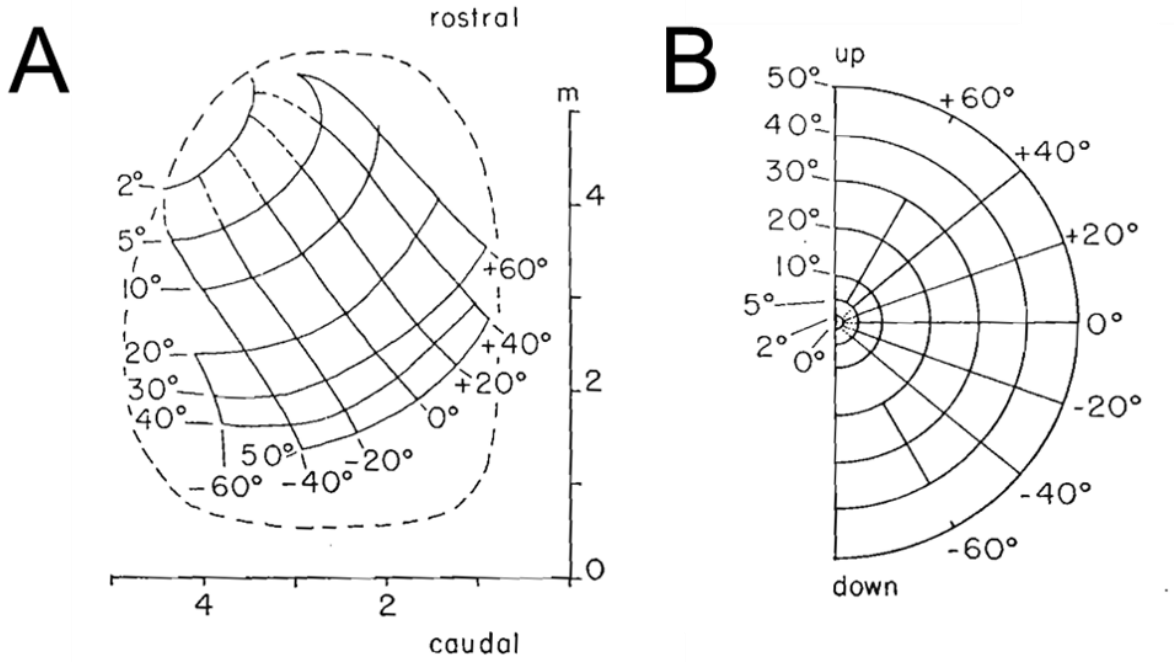

Figure 1.3. Macaque oculomotor map in the intermediate layers of the superior colliculus (SCi). **A:** 2-dimensional slice of neural tissue in SCi where horizontal grid lines indicate motor field amplitudes and vertical grid lines indicate motor field directions. Scale indicates millimeters. **B:** Corresponding saccade vectors in retinotopic space to

those neurally represented in A. Reprinted from Robinson, D. A. (1972). Eye movements evoked by collicular stimulation in the alert monkey. *Vision Research*, *12*(11), 1795-1808. https://doi.org/10.1016/0042-6989(72)90070-3

1.3.2.1. Vector averaging. Oculomotor vectors are spatially and temporally averaged. If two oculomotor vectors are simultaneously activated, the elicited movement is the average of the two vectors weighted by the strength of microstimulation delivered to each vector (Robinson, 1972; Robinson & Fuchs, 1969). This also observed when a behaving primate executes a saccade to one stimulus and only the secondary oculomotor vector is invasively stimulated (Glimcher & Sparks, 1993). If suprathreshold stimulation of two oculomotor vectors are offset in time by ≤ 30 ms, then the first saccade vector is elicited, but some portion of it is mechanically interfered with and replaced by the second saccade vector (Robinson, 1972; Robinson & Fuchs, 1969). Suprathreshold stimulation of two oculomotor vectors offset in time by >30 ms merely elicits two sequential saccades. If a behaving primate executes a saccade but subthreshold microstimulation is delivered to a secondary saccade vector ≤ 30 ms prior to saccade execution, then the saccade is initially directed towards the stimulated vector, but then deviates back towards the target and thus has a distinctly curved trajectory (McPeek, 2006; McPeek et al., 2003; Port & Wurtz, 2003). Given these observations, the interval between saccade execution and 30 ms prior to saccade execution has been deemed the *critical period* (McPeek et al., 2003), as the susceptibility of an impending saccade trajectory to be modulated by competing oculomotor activity is confined to this interval. These spatiotemporal vector averaging properties are robust enough to be accurately modelled mathematically (Ottes et al., 1986; Port & Wurtz, 2003; Van Gisbergen & Van Opstal, 1987; Van Opstal & Van Gisbergen, 1989).

Inhibition introduces a negative contribution in the vector average computation. Inhibitory pharmacological injections into oculomotor maps shifts saccadic endpoints away from

the inhibited oculomotor locus (Lee et al., 1988) and saccades trajectories curve away from the inhibited locus (Aizawa & Wurtz, 1998). However, in the absence of inhibitory injections, saccades curved away from a visual stimulus are not associated with sustained inhibition of the stimulus, but rather a transient decrease in activity encoding the stimulus during the critical period (White et al., 2012).

1.3.3. Cell Types

Cells in oculomotor substrates are classically categorized into 6 types: pure movement, visual burst, visual tonic, visuomotor burst, visuomotor tonic, and fixation (cf. Lowe & Schall, 2018). *Pure movement cells* have no sensitivity to light stimulation but become very active immediately prior to a saccade executed into their motor fields (Schall et al., 1995a; Seagraves & Goldberg, 1987; Wurtz & Goldberg, 1972). Conversely, visual burst and visual tonic cells are sensitive to light stimulation but lack any saccade-related sensitivity (Goldberg & Wurtz, 1972; Wurtz & Mohler, 1976). *Visual burst cells* become very active immediately after the onset of a visual stimulus located in their visual receptive field, but this activation quickly drops back to baseline levels (McPeek & Keller, 2002). *Visual tonic cells* also become very active immediately after the onset of a visual stimulus inside their receptive field. This activation level quickly decreases but is maintained at above baseline levels for as long as the stimulus remains in the visual receptive field (Hanes et al., 1998; Mays & Sparks, 1980). Visuomotor burst and visuomotor tonic cells are sensitive to both light stimulation in their receptive fields and saccades executed into their motor fields (Munoz & Wurtz, 1995a; Schall et al., 1995a). In these cells, there is a close spatial correlation between the visual receptive and motor fields (Rodgers et al., 2006). *Visuomotor burst cells* become very active after the onset of a visual stimulus into their receptive fields, but this activity quickly drops back down to baseline levels. These cells become

very active again immediately prior to the execution of a saccade into their motor field (McPeek & Keller, 2002). *Visuomotor tonic cells* have the same properties as visuomotor burst cells, except that they maintain a certain level of activation between stimulus onset and saccade execution, typically referred to as the delay period (Basso & Wurtz, 1998; Hanes et al., 1998; Glimcher & Sparks, 1992; Munoz & Wurtz, 1995a). *Fixation cells* are tonically active during fixation periods and briefly become inactive immediately prior to saccade execution (Dorris et al., 1997; Hanes et al., 1998; Munoz & Wurtz, 1993).

1.3.4. Target Selection

1.3.4.1. Neurophysiology. Target selection is the process whereby, over time, the neural representation of a target is gradually enhanced, while simultaneously the neural representations of all other stimuli are gradually suppressed, until eventually, the target representation surpasses threshold and is thus selected for a saccadic eye movement (see Figure 1.4). When a visual stimulus appears in visual receptive field of an oculomotor cell, the cell responds with a rapid swell of activation (i.e., a *burst*). The latency of this *visual onset burst* is typically 50-60 ms (Boehnke & Munoz, 2008) reflecting afferent signal transmission times from the retina to the oculomotor substrates. Across all visual and visuomotor cell types, the magnitude and latency of the visual onset burst does not distinguish whether a target or non-target (in a vision experiment, these are typically called distractors) is in the receptive field of the cell (Fecteau & Munoz, 2006). After the initial visual onset burst, tonic visual and tonic visuomotor oculomotor cells maintain above baseline levels of activation, so called *tonic activity*, in an interval of time referred to as the *delay period*, which is the interval of time between visual onset burst and saccade execution. For visual tonic and visuomotor tonic cells encoding non-target locations, tonic activity gradually decreases to baseline levels in the delay period. Conversely, tonic

activity is maintained for visual tonic cells encoding a target location in the delay period, while tonic activity gradually increases in the delay period for visuomotor cells encoding a target. The point in time after stimulus onset at which neural activation levels have diverged between oculomotor cells encoding target and distractor locations is called the target discrimination time. After sufficient processing time, visuomotor tonic, visuomotor burst, and pure movement cells discharge a burst of activity time-locked to the execution of a saccade to the target, called a *motor burst*. The latency of the saccade after the motor burst onset is approximately 10 ms, which likely reflects the efferent transmission time between oculomotor substrates and brainstem saccade generators (Miyashita & Hikosaka, 1996). During saccade execution, otherwise tonically active fixation cells transiently deactivate to release tension on the extraocular muscles and allow the eye to move (Munoz & Wurtz, 1993). After the saccade, fixation cell tonic active resumes to anchor gaze on the newly selected fixation point (i.e., the saccade target). However, the level of post-saccadic tonic activity has stepped, as a different amount of tension is required to anchor the extraocular muscles on this new location.

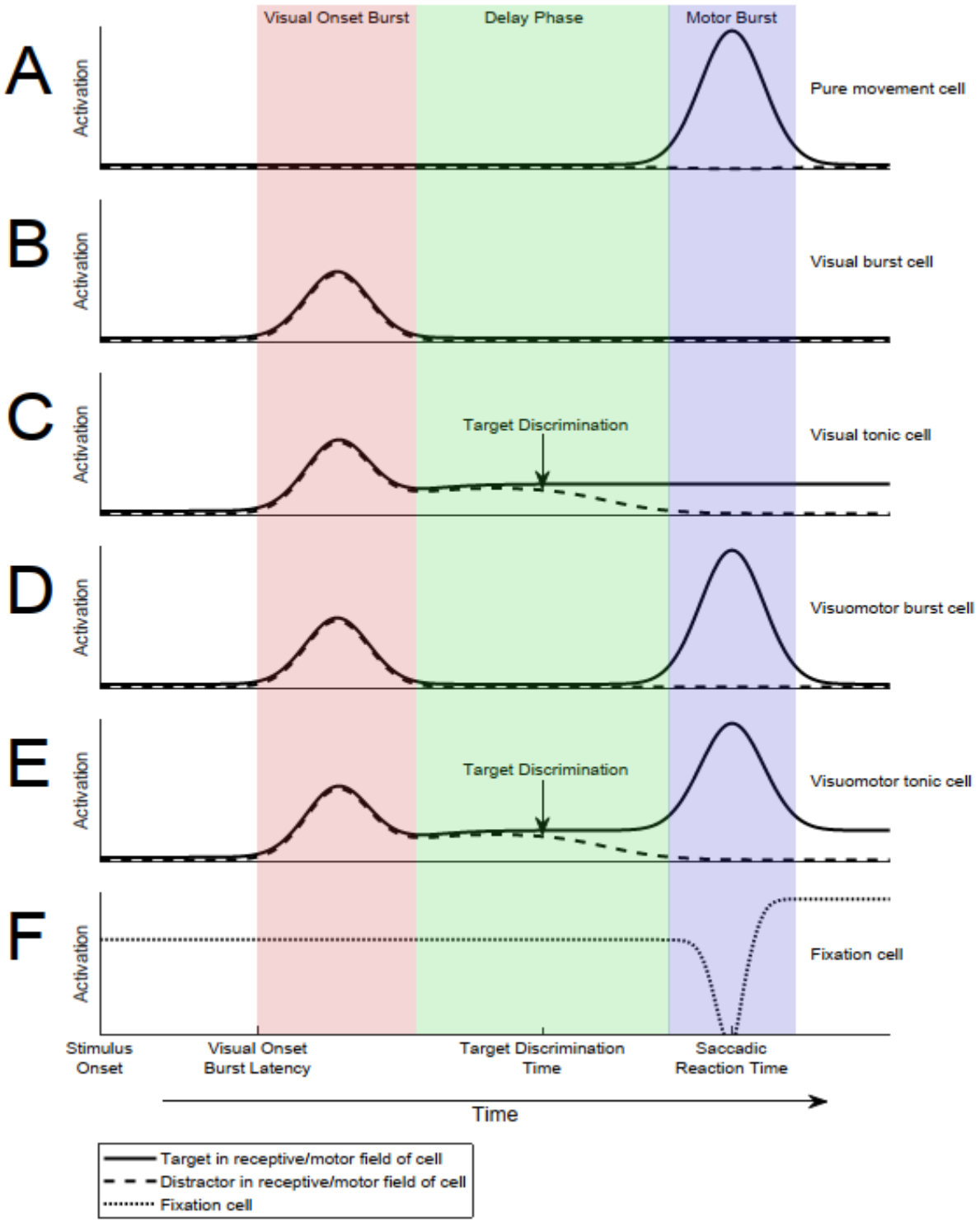

Figure 1.4. Generic oculomotor target selection time course. The visual onset bursting phase is indicated by the red shaded region. The delay phase is indicated by the green shaded area. The motor burst phase is indicated by the blue shaded region. **A,B,C,D,E:** Oculomotor cellular activation levels when either the target (solid line) or a non-target

(dashed line) is in the visual receptive/motor field of the cell. **C,E:** Target discrimination time is indicated by the arrow and accompanying text. **A:** Neural activation levels for pure movement cells. **B:** Neural activation levels for visual burst cells. **C:** Neural activation levels for visual tonic cells. **D:** Neural activation levels for visuomotor burst cells. **E:** Neural activation levels for visuomotor tonic cells. **F:** Neural activation levels for fixation cells (dotted line).

1.3.4.1.1. Stimulus identity encoding. Target selection processing can be disaggregated into visual processing and motor processing components, as the motor command signal is related exclusively to the motor burst and activity prior to the motor burst is sometimes uncorrelated with the eventual target choice. For example, target and distractor representations are identical during the visual onset burst and for some portion of the delay phase (Fecteau & Munoz, 2006), and interestingly, target discrimination time is entirely uncorrelated with saccade latency in approximately 50% of VM tonic cells in SCi (McPeek & Keller, 2002). Conversely, trajectory modulation of an impending saccade by competing oculomotor activity is limited to the critical period immediately prior to saccade execution during the motor burst period (Glimcher & Sparks, 1993; McPeek, 2006; McPeek et al., 2003; Port & Wurtz, 2003; Robinson, 1972; Robinson & Fuchs, 1969). As such, we can conclude that, broadly speaking, activity prior to the motor burst is related to visual processing, while activity during the motor burst is related to the motor command signal for saccade execution. Since oculomotor cell activation levels are different between cells encoding targets versus those encoding non-targets during the delay phase, we can also conclude that these cells encode stimulus identity, where stimulus identity can be defined by a variety of visual and cognitive factors. A general principle of oculomotor encoding during target selection processing arises from these observations: if there are differences in the activation level of oculomotor cells encoding two different stimuli during

visual processing phases, then the factors that identify those stimuli are encoded by the oculomotor cells. The factors encoded by oculomotor cells may be entirely unrelated to the oculomotor task of the observer. For example, the visual onset bursts and delay phase activation levels may differ between distractors based on their level of inherent visual salience (White et al., 2017b). In such a context, the activation level differences observed between distractors do not distinguish a target from a distractor and are thus unrelated to the task of saccadic localization of the target. Alternatively, the factors that uniquely identify a target may be encoded by VM cells, thus these cells encode the behavioral relevance of the stimulus in their visual receptive/motor field.

1.3.4.1.1.1. Salience and priority. Two features that are sharply distinct from each other along their respective visual attribute dimension are perceptually high contrast. For example, the perceptual conspicuity between a vertical line and a horizontal line is visually striking, whereas the perceptual conspicuity between a vertical line and nearly vertical line is visually subtle and difficult to perceive. In the former case, vision scientists refer to this featural relation as characterized by high salience, while the latter case is characterized by low salience. *Salience* can therefore be defined as the inherent perceptual conspicuity of a feature given its featural context. The aggregation of salience across all the relevant visual attributes in the visual environment is called a salience map and indicates all the perceptually conspicuous locations in the visual environment. The concept of a salience map was first introduced by cognitive psychologists and incorporated into highly influential theories of attentional processing (Tresiman & Gelade, 1980; Wolfe, 1994; Wolfe et al., 1989) and later incorporated into highly successful predictive models of task-free oculomotor target selection (Itti & Koch, 2000; Itti et al., 1998; Parkhurst et al., 2002), as sensory salience can reflexively capture attentional (Yantis

& Jonides, 1984) and oculomotor (Theeuwes et al., 1998) selection. However, primate behavior is often goal-oriented and therefore cannot be influenced by featural contrasts alone. For example, if your task is to localize a red color patch, then the perceptually striking contrast between neighboring blue and yellow color patches may be highly salient but is behaviorally irrelevant. As such, our neurocognitive executive control system prioritizes sensory representations based on their behavioral relevance to the organism, which is called *priority* encoding. Thus, priority is the re-weighting of salience based on behavioral relevance (see Figure 1.5). This priority control signal originates in the fronto-parietal network of executive neural substrates and is propagated downstream where it modulates more posterior visual and oculomotor representations (Corbetta & Shulman, 2002; Serences & Yantis, 2006, 2007; Serences et al., 2005; Yantis et al., 2002).

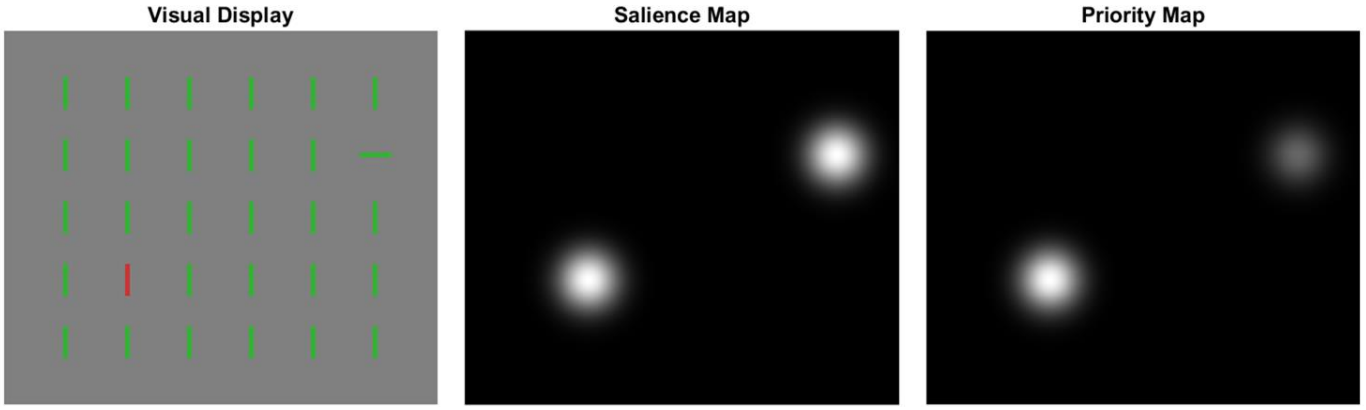

Figure 1.5. Salience and priority maps for an example visual display. Assume the observer's task is to localize the red stimulus. The left panel illustrates an example visual display containing a uniform field of green/vertical lines, except for one red/vertical line and one green/horizontal line. The red/green and vertical/horizontal perceptual contrasts are both very salient given their featural context. The middle panel illustrates the salience map of the display where salience is indicated by brightness. The areas of high salience correspond to the locations of the red/green and vertical/horizontal contrasts. The right panel illustrates the priority map of the display where priority is indicated by brightness. Although the vertical/horizontal contrast is highly salient, it receives a lower priority

weighting as these features are irrelevant for the task, whereas the red/green contrast receives a higher priority weighting since these features are task relevant.

1.3.4.2. Behavior. During oculomotor target selection processing, distractor activation levels often do not fully return to baseline and some residual distractor-related activation persists to the time of saccade execution. If there is residual distractor activity at the time of saccade execution, then by the vector averaging principle observed in oculomotor substrates, saccades curve and/or land in between targets and non-targets (i.e., *the global effect*). As such, systematic saccade curvature or global effect reveals that there is systematic unresolved competition between targets and distractors. Systematic saccade curvature and global effect differences between visual stimuli and cognitive contexts thus reveals the wide variety of visual and cognitive factors encoded on priority maps in oculomotor substrates.

1.3.4.2.1. Saccade curvature. Saccade curvature is any deviation from a straight line between the start and endpoint of a saccade. Various methods have been proposed to quantify this phenomenon (Ludwig & Gilchrist, 2002; Tudge et al., 2017). In the *remote distractor paradigm* in which saccades are executed to a target with a task-irrelevant distractor located somewhere in the periphery, saccades tend to curve towards the distractor at SRTs less than 200 ms and begin to curve away from the distractor at SRTs greater than 200 ms (McSorley et al., 2006), although saccades tend to curve away from the distractor on average (Doyle & Walker, 2001; Tipper et al., 2001). Saccades require approximately 70 ms of distractor processing time before curving towards a distractor (Kehoe & Fallah, 2017) similar to saccade amplitude shifts (Becker & Jürgens, 1979; Ludwig et al., 2007). Saccade curvature studies corroborate neurophysiological studies in suggesting that features are encoded in oculomotor substrates and affect the priority weightings of saccade vectors (Kehoe et al., 2018a, 2018b; Ludwig &

Gilchrist, 2003; Mulckhuyse et al., 2009). As such, distractors that are spatially (McSorley et al., 2004) and priority balanced (Kehoe et al., 2018a) elicit baseline saccade curvature likely because unresolved competition sums to zero. Behavioral studies reveal a long list of visual and cognitive factors that can affect the vector priority weightings (discussed in greater detail below).

1.3.4.2.2. Global effect. The global effect is the spatial averaging of possible saccade vectors in which saccade endpoints land in between potential targets. This occurs for visual stimuli separated by between 20 and 45 polar degrees (Findlay & Blythe, 2009; Van der Stigchel & Nijboer, 2013; Van der Stigchel et al., 2012; Walker et al., 1997). The global effect occurs for saccades with short latencies (<250 ms) and is resolved at longer latencies (Coëffé & O'Regan, 1987; Findlay, 1982; Heeman et al., 2014; Van der Stigchel & Theeuwes, 2005). Unlike saccade curvature, the saccade endpoints do not usually deviate in the opposite direction from a distractor. Saccade vector averaging seems to be under top-down control of the observer, as the global effect can be eliminated with explicit task instructions (Findlay & Blythe, 2009; Findlay & Kapoula, 1992; Heeman et al., 2014).

1.3.4.2.3. Flash saccade inhibition. During saccade planning, a transient flash of light represses the initiation of saccades after a latency of about 60 ms (Reingold & Stampe, 2002). This effect is also observed for microsaccades (Engbert & Kliegl, 2003; Hafed & Clark, 2002). The flash may be a global, spatially homogenous luminance flux (Reingold & Stampe, 2002) or the spatially specific onset of a visual stimulus (Kehoe et al., 2020). The likely causes of saccade inhibition from transient visual onsets may be from fixation cell engagement (Munoz & Wurtz, 1993) or lateral inhibitory networks in colliculus (Munoz & Istvan, 1998), although the latter mechanism is more likely given the that flash saccade inhibition can be elicited from spatially-specific peripheral stimuli (Kehoe et al., 2020).

1.4. Disaggregating Visual and Oculomotor Substrates

For this dissertation, I will adopt the following distinction between visual and oculomotor processing substrates with the following criteria:

1. Oculomotor substrates are those which, when microstimulated at low currents, elicit saccades in the absence of a visual stimulus. Conversely, visual substrates are those which do not elicit saccades when microstimulated, except at extreme amperages (e.g., $\mu A \geq 200$), which is almost certainly a bleeding effect of current into oculomotor substrates (see Schiller, 1977). Stimulation of visual areas induces visual perceptual phenomena (Lee et al., 2000; Schiller et al., 2011).
2. Oculomotor areas exhibit spatially-specific and dissociable visual and motor activity, while neuronal activity in cortical visual areas do not exhibit spatially-specific modulation associated with eye movements.
3. Oculomotor areas are those which when lesioned, produce deficits in saccade generation, while sparing any perceptual function. This is doubly dissociable with visual area lesions, which show perceptual deficits following lesions without discernible motor deficits.

1.5. Interplay of Visual and Oculomotor Processing

Although the visual and oculomotor processing neural substrates can be meaningfully disaggregated, there is considerable interplay between these systems, which subserves the wide range of visual and oculomotor behaviors observed in primates. These interactions between visual and oculomotor substrates are reciprocal: oculomotor substrates alter the sensory/perceptual representations in cortex, while oculomotor substrates select movements from the priority-weighted sensory representations projected from relevant visual cortices.

1.5.1. How Oculomotor Processing Modulates Vision

Abundant single unit recording experiments have demonstrated that sensory representations in visual cortical neurons are modulated by the deployment of spatial attention into the receptive field of the neurons (Connor et al., 1996; Connor et al., 1997; Martinez-Trujillo & Treue, 2004; McAdams & Maunsell, 1999a, 1999b; Perry et al., 2014; Recanzone & Wurtz, 2000; Reynolds et al., 2000; Spitzer et al., 1988; Treue & Martinez-Trujillo, 1999; Treue & Maunsell, 1996). Critically, it has been demonstrated that the modulatory effects of attention on visual sensory representations are rooted in oculomotor substrates (reviewed by Awh et al., 2006; Moore et al., 2003). For example, microstimulation in FEF causes increased luminance (Moore & Fallah, 2001, 2004) and motion direction (Gold & Shadlen, 2000) sensitivity, while microstimulation in SCi causes increased change detection performance (Cavanaugh & Wurtz, 2004) and motion direction sensitivity (Müller et al., 2005). Microstimulation in oculomotor substrates replicates the modulatory effects of covert attention on downstream visual representations in visual cortices (Armstrong et al., 2006; Monosov et al., 2011; Moore & Armstrong, 2003). Conversely, reversible inactivation of SCi produces inattentive perceptual judgement deficits (Lovejoy & Krauzlis, 2010). These studies establish the link between oculomotor processing and visual cortical sensory representations.

1.5.2. How Vision Modulates Oculomotor Processing

In the deep layers of SCi, visual responses are eliminated following ablation or reversible cooling of primary visual cortex, extrastriatal cortex, and visual associative cortex (Broadman area 19) (Schiller et al., 1974). This suggests that oculomotor substrates select movement goals from sensory maps projected from visual cortices in a feedforward manner. This account predicts that alteration of cortical sensory representations should also alter oculomotor vector encoding.

Consistent with this prediction, stimulation of V1 biases saccadic target selection for stimuli in the stimulated receptive field (Schiller & Tehovnik, 2005; Tehovnik et al., 2002), while stimulation of MT biases SEM in the direction encoded by the stimulated population of MT cells (Groh et al., 1997; Born et al., 2000). Far and above encoding sensory maps, oculomotor substrates also encode complex priority maps, as demonstrated directly from single unit recordings in which oculomotor cell activation levels are higher for target features than distractor features (Bichot et al., 1996; Carello & Krauzlis, 2004; Herman & Krauzlis, 2017; Horwitz & Newsome, 1999, 2001; Kim & Basso, 2008; McPeek & Keller, 2002, 2004; Sato & Schall, 2003; Sato et al., 2003; Schall & Hanes, 1993; Schall et al., 1995a, 2004; Shen & Paré, 2007, 2012; Thompson et al., 2005). This is corroborated by behavioral studies suggesting that complex priority relationships between targets and distractors have a modulatory influence on oculomotor vector representations. Saccades curvature analyses demonstrate that oculomotor maps encode previous distractor locations (Belopolsky & Van der Stigchel, 2013; Jonikaitis, & Belopolsky, 2014), the locus of visuospatial attention (Scheliga et al., 1994, 1995a, 1995b), salience (Tudge et al., 2018; van Zoest et al., 2012), target-distractor similarity for color (Kehoe et al., 2018b; Ludwig & Gilchrist, 2003; Mulckhuyse et al. 2009) and complex objects (Kehoe et al., 2018a), target probability (Walker et al., 2006), semantic meaning (Weaver et al., 2011), and social relevance (Laidlaw et al., 2015). Saccade endpoint analyses suggest that oculomotor maps encode luminance (Deubel, Wolf, Hauske, 1994), salience (De Vries et al., 2017), stimulus size (Findlay, 1982; Van der Stigchel et al., 2012), and target probability (He & Kowler, 1989).

Another prediction from this view of oculomotor processing pertains to the temporality of oculomotor vector representations. As features become increasingly complex, they require processing in increasingly higher levels in the visual processing hierarchy, which requires

additional processing time (Nowak & Bullier, 1997; Schmolesky et al., 1998). If oculomotor substrates relied on cortical sensory representations of the available stimuli to select a target, then as the visual stimuli or cognitive factors increased in complexity, oculomotor visual onset burst latencies should increase. Consistent with this prediction, the visual onset burst latencies in SCi for achromatic and chromatic stimuli are offset by ~30 ms (White et al., 2009), which corresponds to the visual onset latency differences between the magno- and parvocellular layers in V1 and V2 (Nowak & Bullier, 1997; Nowak et al., 1995; Schmolesky et al., 1998).

Kehoe and Fallah (2017) developed an experimental paradigm to non-invasively infer oculomotor visual onset response latencies. We measured saccade curvatures elicited by task irrelevant, peripheral distractors as a function of distractor processing time while human observers executed saccades to a target (saccade-distractor onset asynchrony [SDOA]), which reveals the time course of oculomotor distractor processing. Consistent with White et al. (2009), our novel SDOA behavioral paradigm has demonstrated that saccade curvature is elicited by color-modulated distractors ~20 ms later than it is for luminance-modulated distractors. These results demonstrate that sensory representations are projected into oculomotor substrates from relevant cortical sites that process the stimulus features, and thus suggests that oculomotor substrates rely on cortical visual and cognitive processing to construct priority-weighted object representations from which to select.

1.6. Current Research

The purpose of the current dissertation is to investigate the theory that oculomotor substrates are necessary but insufficient for feature-based target selection, as cortical sensory representations must be projected into the oculomotor substrates from relevant visual cortices where these representations are dynamically reweighted according to behavioral priority. In

chapters 2 and 3, I show that complex priority weights associated with computations in visual and executive cortices are apparent in the oculomotor maps of available saccade goals. In chapter 2, I show that saccade curvatures vary as a Mexican hat shaped function of the CIE1931 *Yxy* colorspace distance between targets and distractors (Kehoe et al., 2018b), consistent with attentional pruning of visual features outside the attentional focus of a target stimulus, as predicted by the selective tuning (ST) model of visual attention (Tsotsos, 2011; Tsotsos et al., 1995). In chapter 3, I show that the priority weights assigned to sets of complex, novel objects is apparent in oculomotor vectors during visual search for complex objects. In chapters 3 and 4, I examine how the visual features and cognitive factors that characterize stimuli have a modulatory influence on visual onset response latencies in oculomotor substrates encoding vector maps. In chapter 3, I extend the SDOA paradigm to complex object selection and demonstrate that visual onset response latencies for these complex objects are consistent with cortical processing in the latest stages of the visual processing hierarchy (e.g., IT, V4) (Kehoe et al., 2020). In chapter 4, I replicate the original SDOA experiment using achromatic static and motion distractors and show that visual onset latencies are shorter for strictly dorsal stream features than the ventral stream features in the original paradigm, and that visual onset latencies are in order of visual complexity even within the dorsal processing stream itself.

Chapter 2. Perceptual Color Space Representations in the Oculomotor System are Modulated by Surround Suppression and Biased Selection

This manuscript has been published in *Frontiers in Systems Neuroscience*:

Kehoe, D. H., Rahimi, M., & Fallah, M. (2018). Perceptual color space representations in the oculomotor system are modulated by surround suppression and biased selection. *Frontiers in Systems Neuroscience*, *12*, 1. https://doi.org/10.3389/fnsys.2018.00001

2.1. Abstract

The oculomotor system utilizes color extensively for planning saccades. Therefore, we examined how the oculomotor system actually encodes color and several factors that modulate these representations: attention-based surround suppression and inherent biases in selecting and encoding color categories. We measured saccade trajectories while human participants performed a memory-guided saccade task with color targets and distractors and examined whether oculomotor target selection processing was functionally related to the CIE (*x*,*y*) color space distances between color stimuli and whether there were hierarchical differences between color categories in the strength and speed of encoding potential saccade goals. We observed that saccade planning was modulated by the CIE (*x*,*y*) distances between stimuli thus demonstrating that color is encoded in perceptual color space by the oculomotor system. Furthermore, these representations were modulated by (1) cueing attention to a particular color thereby eliciting surround suppression in oculomotor color space and (2) inherent selection and encoding biases based on color category independent of cueing and perceptual discriminability. Since surround suppression emerges from recurrent feedback attenuation of sensory projections, observing oculomotor surround suppression suggested that oculomotor encoding of behavioral relevance results from integrating sensory and cognitive signals that are pre-attenuated based on task demands and that the oculomotor system therefore does not functionally contribute to this process. Second, although perceptual discriminability did partially account for oculomotor processing differences between color categories, we also observed preferential processing of the red color category across various behavioral metrics. This is consistent with numerous previous studies and could not be simply explained by perceptual discriminability. Since we utilized a memory-guided saccade task, this indicates that the biased processing of the red color category

does not rely on sustained sensory input and must therefore involve cortical areas associated with the highest levels of visual processing involved in visual working memory.

2.2. Introduction

Color processing plays an important role in many oculomotor behaviors like pursuit eye movements (Tchernikov & Fallah, 2010), saccadic eye movements (Itti & Koch, 2000; Ludwig & Gilchrist, 2003; McPeek & Keller, 2001; Mulckhuyse et al., 2009), visual search (Bauer et al., 1996a, 1996b, 1998; D'Zmura, 1991; Green & Anderson, 1956; Lindsey et al., 2010; Treisman & Gelade, 1980), and attentional selection (Folk et al., 1992, 1994; Pomerleau et al., 2014; Wolfe & Horowitz, 2004). Examinations of these behaviors have provided evidence that the color representations that influence oculomotor planning are encoded in multi-dimensional color space similar to how perceived color is encoded. For example, it has been demonstrated that the speed of pursuit eye movements to one of two differently-colored, superimposed random dot kinematograms (RDKs) moving in opposite directions is linearly proportional to the distance between the colors in CIE (*x*,y) color space (Tchnerikov & Fallah, 2010). Similarly, it has been demonstrated that the discriminability of a target from distractors in color visual search is determined by the linear discriminability of the target from the distractors in CIE (*x*,*y*) color space (Bauer et al., 1996a, 1996b, 1998; D'Zmura, 1991; c.f. Lindsey et al., 2010). However, whether the color representations utilized for saccade planning are also encoded in a multi-dimensional color space remains unclear.

There is physiological (Bichot et al., 1996; Sato et al., 2003; Sato & Schall, 2003) and behavioral (Ludwig & Gilchrist, 2003; McPeek & Keller, 2001; Mulckhuyse et al., 2009) evidence that color, at least categorically, modulates saccade planning. Additionally, there is preliminary evidence to suggest that the oculomotor system encodes potential saccade goals in

perceptual color space: First, White et al. (2009) demonstrated that neurons in the intermediate layers of the superior colliculus (SCi)—a critical neural substrate for the generation of saccades (Robinson, 1972; Wurtz & Goldberg, 1972) and oculomotor target selection processing (Basso & Wurtz, 1997, 1998; McPeek & Keller, 2002, 2004)—have inherent color sensitivities characterized by very broad tuning profiles in DKL color space. Second, the color representations in the oculomotor system almost certainly originate from cortex as the alternative retinotectal pathway is colorblind (Schiller et al., 1979) and the long onset latencies of color signals in SCi (~80-90 ms; White et al., 2009) are inconsistent with the characteristically short onset latencies of the retinotectal pathway (11-27 ms; Schiller & Malpeli, 1977). Furthermore, the latency differences between color and luminance signals in the oculomotor system observed either physiologically (White et al., 2009) or inferred from psychophysics (Kehoe & Fallah, 2017) are very similar to the latency differences observed between the cortical dorsal and ventral visual processing streams (Schmolesky et al., 1998). This suggests that color representations in the oculomotor system are processed through the ventral processing stream specifically, along which wavelength representations are transformed into perceived color representations in area V4 (Conway et al., 2007; Conway & Livingstone, 2006; Schein & Desimone, 1990). The ventral visual processing stream is also richly interconnected with the frontal eye field (FEF) (Schall et al., 1995b; Felleman & Van Essen, 1991), another critical neural substrate for oculomotor target selection processing (Dassonville et al., 1992; Schlag-Rey et al., 1992; Segraves & Goldberg, 1987) that integrates complex visual representations and higher cognitive factors (Bichot et al., 1996; Kastner et al., 2007; Moore & Fallah, 2001, 2004; Sato et al., 2003; Thompson et al., 2005). Third, there is an extensive degree of overlap in the neural circuitry that subserves saccadic eye movements, pursuit eye movements, and visual search (Awh et al., 2006; Krauzlis,

2005; Schiller & Tehovnik, 2001), and previous experiments have demonstrated that pursuit eye movements (Tchernikov & Fallah, 2010) and visual search (Bauer et al., 1996a, 1996b, 1998; D'Zmura, 1991) are influenced by the color space relationships between stimuli. These observations suggest that perceptual color space representations could mediate saccadic target selection processing; however, whether and how they do so warrant further investigation.

One informative method to examine the factors that mediate saccadic target selection is to examine saccade curvature elicited from remote distractors. Physiological studies have demonstrated that saccade curvature is elicited from unresolved competition between potential saccade goals in the epoch immediately prior (~30 ms) to the initiation of saccades (McPeek et al., 2003; McPeek, 2006). Saccade curvature towards a distractor reflects distractor-related excitation (McPeek, 2006; McPeek et al., 2003), while curvature away from a distractor likely reflects distractor-related inhibition (Aizawa & Wurtz, 1998). Critically, the magnitude of unresolved activity encoding a distractor vector in this epoch is proportional to the magnitude of saccade curvature for saccades curved both towards (McPeek et al., 2003; McPeek, 2006; Port & Wurtz, 2003) and away from a distractor (White et al., 2012). Therefore, saccade curvature provides an index of the inherent competitiveness of a non-target stimulus during target selection processing. In fact, behavioral studies have demonstrated that saccade curvatures are greater when the color of a task irrelevant, peripheral distractor is congruent with a saccade target than when it is incongruent (Ludwig & Gilchrist, 2003; Mulckhuyse et al., 2009). However, these studies do not provide insight into whether potential saccade goals are encoded in perceptual color space, as with pursuit (Tchernikov & Fallah, 2010). This could be examined by measuring the magnitude of saccade curvature as a continuous function of the distance between a cued saccade target and a peripheral distractor in perceptual color space. Interestingly, under such

experimental conditions, previous research suggests that two possible phenomena may arise: (1) feature-based surround suppression and (2) hierarchical color selection.

Researchers have demonstrated that there is an inhibitory annulus surrounding the locus of attention giving the "beam" of attention a difference of Gaussians (DoG) or Mexican hat wavelet spatial profile (Hopf et al., 2006; Müller & Kleinschmidt, 2004; Slotnick et al., 2002). This so-called "surround suppression" was first predicted by Tsotsos (1990) and incorporated into the computational theory of visual attention "selective tuning" (ST) (Tsotsos et al., 1995; Tsotsos, 2011). Critically, however, ST predicts that surround suppression should also be observed in the feature domain of an attended feature, which has been confirmed for orientation (Loach et al., 2010; Tombu & Tsotsos, 2008), and more recently, for color (Strömer & Alvarez, 2014).

Strömer and Alvarez (2014) utilized a perceptual discrimination task in which human participants covertly monitored two differently colored RDKs located in opposite hemifields and discriminated whether coherent motion emerged in one of the RDKs. They observed that discrimination performance was highest when the colors of the two attended RDKs were close *or far* in color space and was lowest when colors were at an intermediate distance. This result is characteristic of attention-based surround suppression in the feature domain of the attended feature (i.e., color) as predicted by ST (Tsotsos et al., 1995; Tsotsos, 2011). We therefore predict that if attention is cued to a color saccade target and the inherent competitiveness of a color distractor during target selection processing is measured, saccade curvature should vary as a function of the distance between target and distractor in color space with a DoG profile.

Research examining the influence of color on oculomotor processing has provided evidence for a color hierarchy of attentional selection, first proposed by Tchernikov and Fallah

(2010). They observed that when participants executed a saccade to an aperture containing two superimposed RDKs with equal luminance and velocity, but with different directions and colors, participants made smooth pursuit eye movements to one of the two colors in the absence of any task instructions to do so, demonstrating automatic selection. Critically, however, they also observed a color hierarchy of selection in which red was selected over green, yellow, and blue; there was a weak preference of green over yellow and blue; and blue was not preferred over other colors. Lindsey et al. (2010) then demonstrated that visual search for desaturated color targets imbedded amongst saturated and white distractors that were equidistant from the target in CIE (*x*,*y*,*Y*) color space was more efficient for "reddish" targets than "purplish" targets. These effects were independent of target luminance differences, the perceptual similarity between targets and distractors, linear discriminability of targets from distractors in CIE (*x*,*y*,*Y*) color space, and lexical color category membership. In addition to these behavioral results, Pomerleau et al. (2014) measured event-related potentials during a visual search task and observed that the N2pc subcomponent, which is indicative of the contralateral deployment of attention (Luck, 2014), had a shorter latency for red and blue than green and yellow targets. This result provided the first electrophysiological evidence for hierarchical differences in the attentional selection of color. Even more recently, Blizzard et al. (2016) demonstrated that red stop signals elicited faster response inhibition than green stop signals on a stop signal task, thus demonstrating hierarchical color selection involvement in higher stages of cognitive processing.

These results strongly suggest that reddish hues receive preferential or biased processing in the visual system compared to other colors. However, these few studies of the color hierarchy give conflicting accounts of the level in the visual processing hierarchy at which biased color selection occurs. For example, Lindsey et al. (2010) provided evidence that the varying

proportions of color signals from the L, M, and S color channels in the earliest stages of color processing explain the selection bias, whereas the results of Blizzard et al. (2017) suggested that the biased selection of certain colors must take place at higher levels of cognitive processing associated with attentional deployment and executive function.

The purpose of the current research was to (1) investigate whether color representations are encoded in perceptual color space by the oculomotor system. This was examined with a memory-guided saccade task in which participants were instructed to saccade to the remembered location of a color target displayed amongst color distractors. We then measured saccade curvature as a function of the CIE (*x*,*y*) color space distance between the target and an isolated distractor to determine if saccade planning is systematically modulated by the perceptual color space relations between potential saccade goals. We utilized CIE (*x*,*y*) color space as it represents color encoding in cortical structures like V4 (Schein & Desimone, 1990) and is therefore more appropriate for studying the role of color in higher-order cognitive processes such as sustained memory representations than other color space conceptualizations representing lower-level color representations in, for example, lateral geniculate nucleus such as Derrington-Krauskopf-Lennie color space (Derrington et al. 1984). We analyzed saccade curvatures as they are proportional to distractor-related unresolved competition immediately prior to the initiation of saccades and are therefore indicative of the inherent competitiveness of a distractor (McPeek et al., 2003; McPeek, 2006; Port & Wurtz, 2003; White et al., 2012). Furthermore, saccade curvatures are modulated by color (Ludwig & Gilchrist, 2003; McPeek & Keller, 2001; Mulckhuyse et al., 2009) and are elicited by remembered stimuli (Belopolsky & Theeuwes, 2011; Belopolsky & Van der Stigchel, 2013). Saccade curvature direction (i.e., towards vs. away from distractors) is largely indicative of distractor processing time (Kehoe & Fallah, 2017; McSorley et al., 2006, 2009), which likely

due to the transition from excitatory to inhibitory oculomotor distractor-related processing over time (McPeek & Keller, 2002). As we were specifically interested in examining potential differences in the inherent competitiveness of color distractors in the current study, we analyzed absolute saccade curvature. If the color space distance between targets and distractors functionally modulates absolute saccade curvatures, this would provide evidence that the oculomotor system encodes color stimuli in perceptual color space. (2) We examined whether the competitiveness of distractors was modulated by surround suppression in the color feature-domain by examining whether inherent competition (i.e., saccade curvature) varied as a function of color space distance specifically with a Mexican hat or quadratic polynomial mathematical profile, as surround suppression is characterized by a DoG (Tsotsos et al., 1995; Tsotsos, 2011) and since a Mexican hat approximates a DoG as does a quadratic function within a limited range. (3) We investigated whether there was a hierarchical, biased selection of certain color categories (red > green > yellow > blue) for saccades as with pursuit eye movements (Tchernikov & Fallah, 2010) by examining overall color selection differences between color categories. We then examined whether this was accompanied by hierarchical differences in the strength and speed of saccadic vector encoding by examining whether there were any hierarchical differences in the inherent competitiveness (i.e., saccade curvature) of isolated distractors, error proportion, mean saccadic reaction time (SRT), and saccadic precision as a hierarchical function of color category. (4) We examined whether the biased selection of color stimuli that characterizes the color hierarchy occurs at low or high levels of color representation. We therefore utiliized a memory-guided saccade task. First, because it relies on sustained visual working memory representations in the anterior most areas of the frontoparietal network like dorsolateral prefrontal cortex (Goldman-Rakic, 1995) as supposed to sustained sensory input. Therefore any hierarchical color

effects would indicate that color selection biases either occur or are maintained at the highest levels of visual processing. Second, target selection processing in the delayed saccade paradigm is highly similar to visually-guided target selection processing (Schall, 2004; Segraves & Goldberg, 1987) and our results can therefore be generalized to the broader oculomotor target selection literature.

2.3. Methods

2.3.1. Subjects

30 York University undergraduate students (17 to 48-year-olds, 9 males) participated in the experiment for course credit. Participants had normal or corrected-to-normal visual acuity and had normal color vision as assessed by Ishihara color plates (Ishihara, 2006). Written informed consent was obtained prior to participation in accordance with the Declaration of Helsinki. York University's Human Participants Review Committee approved all experimental procedures.

2.3.2. Visual stimuli

The saccade target was a red (x =.63, y = .33, L = 12.07 cd/m^2), green (x =.29, y = .59, L = 12.00 cd/m^2), yellow (x = .40, y =.50, L = 12.09 cd/m^2), or blue (x =.15, y = .07, L = 12.04 cd/m^2) square that subtended 2.0^o × 2.0^o (see Figure 2.1). Placeholders were grey (x = .28, y = .30, L = 11.20 cd/m^2) squares that subtended 2.0^o × 2.0^o. Stimuli were embedded in a black (x = .26, y = .24, L = 0.22 cd/m^2) background displayed on 21-inch CRT monitor (60 Hz, 1024 × 768). Color and luminance were calibrated using a spectrophotometer (PR-655, Photo Research, Syracuse, NY). Participants observed stimuli in a dimly lit room from a distance of 57 cm with a headrest used to stabilizing their head position.

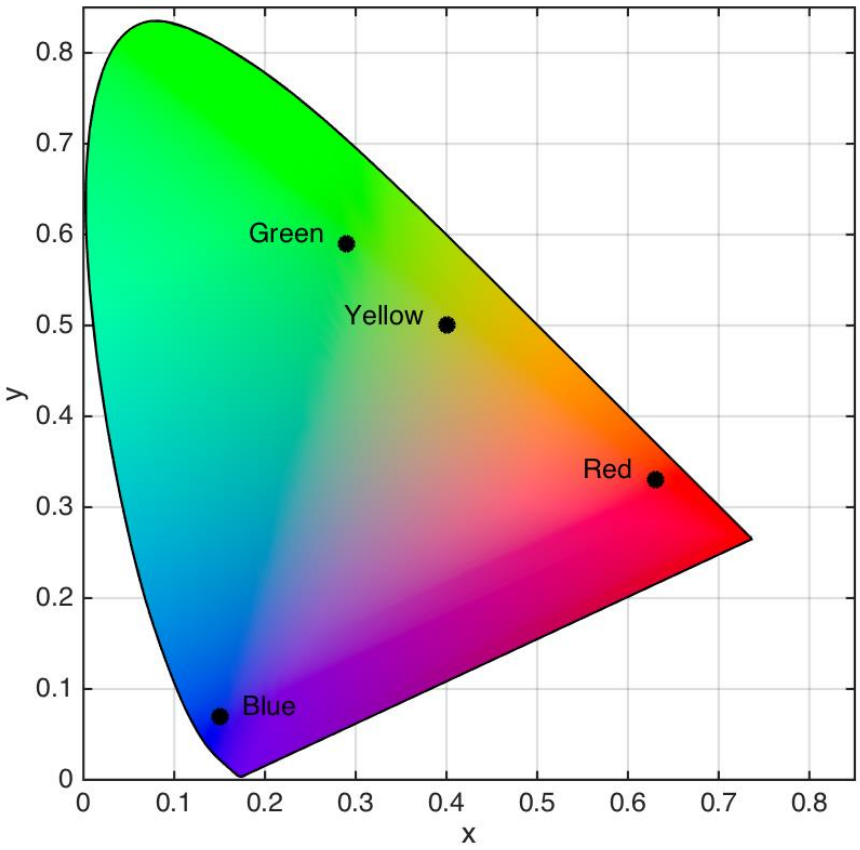

Figure 2.1. Locations of isoluminant target color categories in CIE (*x*,*y*) color space. Black dots with associated labels denote color category locations.

2.3.3. Apparatus

Stimulus presentation was controlled on a computer running Presentation software (Neurobehavioral Systems, Berkeley, CA) and a serial response box (Cedrus, San Pandro, CA). Eye position was sampled using an infrared eye tracker (500 Hz, Eyelink II, SR Research, Ontario, Canada). The camera was calibrated using a nine-point grid. Calibration was conducted at the beginning of each experimental run. Drift-corrections were conducted prior to each block and as needed.

2.3.4. Procedure

Trials were initiated by a button press on the serial response box and then maintaining fixation (1.89^o square window) on a white central fixation cross ($0.4^o \times 0.4^o$) for 200 ms (see Figure 2.2). Eight placeholders centered to the circumference of an imagery circle (radius = 7.5^o) at positions along the cardinal and oblique axes were displayed for 200 ms to indicate all potential target positions (spatial phase). A randomly sampled subset of 4 placeholders was then replaced with red, green, yellow, and blue squares and displayed for 200ms (color display). The colored squares then reverted back to grey placeholders and were displayed for 200 ms (mask phase). The placeholders and fixation cross were removed from the display creating a blank, grey background displayed for 1000 ms (delay phase). A target color was randomly selected from the four colors and a target cue was displayed at central fixation for 200 ms. The offset of the central target cue served as the go-signal to execute a saccade to the remembered location of the target color from the previous color display. Participants were instructed to maintain fixation throughout the trial until presented with the go-signal. The trial was complete when a saccade was made to the location of the target colored square (correct) or a non-target colored square (incorrect) from the color display, or until 500 ms had elapsed since the go-signal (time out). An error tone signified a time-out or failure to maintain fixation. Trials with a timeout or fixation break were reinserted randomly back into the block. There were 8 trials for each of the 4 target colors on every block. Participants completed 10 blocks of 32 trials for a total of 320 trials.

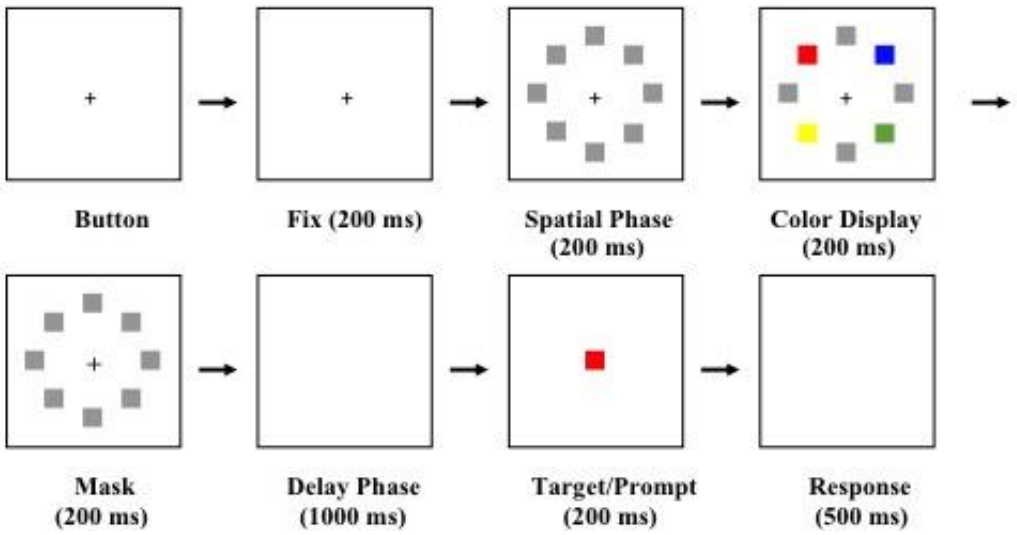

Figure 2.2. Example trial sequence with a red target. Trials were initiated after button pressing and fixating for 200 ms. Grey placeholders then occupied all the potential target positions for 200 ms. Four locations were randomly selected to display colored squares for 200 ms. The colored squares were masked for 200 ms. A blank display was presented for 1000 ms to produce memory-guided saccades. The central target cue appeared for 200 ms. Offset of the target cue was the saccadic go-signal. Participants were given 500 ms to execute a saccade. Note that there was an isolated distractor on this example trial (see section **2.3.5. Saccade Detection and Data Analysis**).

2.3.5. Saccade Detection and Data Analysis

Customized MATLAB (MathWorks, Natick, MA) algorithms were used to detect, visualize, filter and analyze saccades. Trials that contained blinks, corrective saccades, saccade amplitudes < 1^o, endpoint deviations > 6^o from the center of the selected stimulus, or fixation drifts > 1^o during the presaccadic latency period were excluded from further analysis.

To examine unresolved competition between stimuli during saccade planning, we analyzed two saccade curvature metrics: (1) *sum curvature*, the sum of all orthogonal deviations from a straight line between the start and endpoint of saccade trajectories sampled by the eye tracker; and (2) *max curvature*, the maximum orthogonal deviation from a straight line between the start and endpoint of saccade trajectories. To compute these metrics, we first translated the

start point of each saccade to the Cartesian origin and then trigonometrically rotated each saccade so that the endpoint was aligned to the positive *y*-axis. Therefore, the saccade curvature metrics were signed so that a negative sign indicates deviation (i.e., curvature) in the counter-clockwise (CCW) direction, and conversely, a positive sign indicates deviation in the clockwise (CW) direction. This method was ideal for examining saccade curvature on circular displays with randomized target and distractor locations. Saccades with a sum curvature greater than 3 standard deviations from the mean were not analyzed for any curvature analyses.

For all saccade curvature analyses, we only analyzed a subset of correct trials with the following characterizations: (1) a single distractor occupied the stimulus positions 45° or 90° CCW to the target and there were no distractors occupying either of the stimulus positions 45° or 90° CW to the target (subsequently referred to as the CCW condition); (2) a single distractor occupied the stimulus positions 45° or 90° CW to the target and there were no distractors occupying either of the stimulus positions 45° or 90° CCW to the target (subsequently referred to as the CW condition); or (3) no distractors occupied any of the stimulus positions within 90° of the target in either the CCW or CW direction (subsequently referred to as baseline). We refer to trials in the CCW and CW conditions as isolated distractor trials. Unpredictable distractors located 135° from a target position reportedly elicit only a marginal effect on saccade curvature (McSorley et al., 2009) and were therefore not considered in the current analyses. First, we examined whether baseline curvature was significantly biased in a particular direction by comparing baseline curvature to zero. Next, to ensure that the isolated distractor 45° or 90° away from the target position elicited a systematic effect on saccade curvature, we compared saccade curvatures in the CCW and CW conditions relative to baseline (i.e., using unbiased curvatures) to determine if saccades curved away from the isolated distractors as is commonly observed in

the remote distractor paradigm (Doyle & Walker, 2001; Tipper et al., 2001). We used unbiased curvature since a significant bias may uniformly shift curvatures in either the CCW or CW direction such that they do not actually curve in opposite directions (where the sign of the metrics indicates the direction) even though the distractors are located in opposite directions.

Next, to investigate whether potential saccade goals were encoded in CIE (*x*,*y*) perceptual color space, we analyzed whether unresolved competition between potential saccade goals (as indexed by saccade curvature) was modulated by the color space distances between the target and isolated distractors, referred to as *target-distractor color space distance*. This analysis was performed in several steps: First, we computed an exhaustive list of pairwise Euclidian distances between each color stimulus in CIE (*x*,*y*) color space (see Table 2.1) using the Pythagorean equation and categorized the color space distance between the target and the isolated distractor on every trial. Second, we computed mean saccade curvature as a function of target-distractor color space distance separately for the CCW and CW conditions. We then averaged together the absolute, unsigned saccade curvature from the CCW and CW conditions for each target-distractor color space distance, as we were ultimately interested in examining the average magnitude of saccade curvature (i.e., inherent competitiveness of distractors) as a function of target-distractor color space distance regardless of the relative position of the isolated distractor to the target and the direction of the curvature. Furthermore, averaging the CCW and CW conditions would compensate for any curvature bias and thus generalize the current results such that they are not limited to any particular spatial arrangement of a color distractor relative to the target. Third, we examined absolute mean saccade curvature as a function of target-distractor color distance with regression analyses. To determine whether the inherent competitiveness of

isolated distractors was modulated by surround suppression in color space, we fit the data with a Mexican hat wavelet model (a close approximation to the DoG function):

$$f(x|\alpha,\sigma,\kappa) = (\alpha - y_n)\cdot\left(1-\frac{x^2}{\kappa\sigma^2}\right)\cdot e^{-\frac{x^2}{2\sigma^2}} + y_n,$$

where α is the function ceiling, σ is the width of the function, κ was included to scale the depth of the inhibitory annulus, y_n is the baseline of the function and was set to the mean saccade curvature (y_i) observed at the furthest target-distractor color space distance (n), and minima are located at $x = \pm\sqrt{\kappa+2}\sigma$. Next, we fit the data with a generic quadratic polynomial model:

$$f(x|a,b,c) = ax^2 + bx + c.$$

Reducing the number of fitted free parameters in the Mexican hat model ensured an equal number of fitted parameters between models. Functions were fit using a custom implementation of the maximum likelihood estimation method by maximizing the following Gaussian log-likelihood function:

$$l(\theta|y) = \sum_{i=1}^{n} \log[\,\phi(\hat{y}_i|y_i,\sigma_i)\,],$$

where θ is the vector of fitted parameters in either the Mexican hat wavelet [$\theta = (\alpha,\sigma,\kappa)'$] or quadratic [$\theta = (a,b,c)'$] models, n is the number of target-distractor color space distances being fitted to the model, ϕ is the Gaussian normal probability density function, $\hat{y}_i$ is the saccade curvature value predicted by the model with parameters θ for the ith target-distractor color space distance, y_i is the average saccade curvature value observed for the ith target-distractor color space distance, and σ_i is the standard deviation for the ith target-distractor color space distance. The goodness-of-fits were evaluated using an *F*-test. If both models provided a significant fit to the data, the best fitting model was determined by performing an *F*-test on the ratio of the sum of squared residuals from each fitted model with $n-k$ degrees of freedom, where k is the number

of fitted parameters (see Kehoe & Fallah, 2017). Furthermore, to provide further evidence of a functional relationship between saccade curvature and target-distractor color space distance, we analyzed the data with a quadratic planned contrast.

Table 2.1. CIE 1931 (*x*,*y*) distances between stimuli.

	Pairwise CIE (*x*,*y*) Distances				Average Distance
	Red	Green	Yellow	Blue	(Discriminability)
Red	-	0.43	0.29	0.55	0.42
Green	0.43	-	0.14	0.54	0.37
Yellow	0.29	0.14	-	0.50	0.31
Blue	0.55	0.54	0.50	-	0.53

Note: Color space distances between each successive pair of color stimuli are in the first 4 columns. The average distance of each color stimulus from the remaining color stimuli is in the fifth column. The average distance was utilized as an index of target color discriminability.

To examine whether there was an overall selection bias on color categories, we analyzed potential categorical color differences between *overall selection proportion*, which was the proportion of total trials (i.e., correct and incorrect) in which a particular color category was selected as a saccade target. This required us to include the error trials back into the data and then remove them for subsequent analyses.

We then analyzed whether the inherent competitiveness of distractors was hierarchically modulated by the color categories of the isolated distractors. As with target-distractor color space distance, absolute, unsigned saccade curvature was averaged between the CCW and CW conditions for each isolated distractor color. All subsequent analyses were performed on all correct trials of all trial types (i.e., isolated distractors and no isolated distractors).

Next, to examine whether the strength and speed of saccade target color encoding varied as a function of the target color category, we examined three metrics related to the strength and

speed of target encoding: (1) *Proportion of errors*, which was the number of trials for a particular target color in which the saccade was executed to an incorrect location divided by the total number of trials with that target color. (2) *Saccadic reaction time* (SRT), which was the time between the go-signal and saccade initiation for correct saccades. (3) *Saccadic precision*, which was the area of a 95% confidence data ellipse fit to the 2-dimensional displacement between the target center and the saccade endpoints computed for each color and each participant for correct saccades (see Chen et al., 2011). Saccade precision was computed before and after translating the start-point of every saccade back to fixation. Our results demonstrated that this translation did not have a systematic effect on the results and thus we report the results for translated saccades.

Mean differences were analyzed with paired-samples *t*-tests or repeated-measures ANOVAs and Bonferroni *post hocs*. If a Mauchley's test provided insufficient evidence for sphericity, the degrees of freedom of the ANOVA were adjusted using the Greenhouse-Geisser ($\varepsilon \leq 0.7$) or Huynh-Feldt ($\varepsilon > 0.7$) adjustment. To examine whether there were hierarchical differences between color categories (red > green > yellow > blue) consistent with the color hierarchy (Tchernikov & Fallah, 2010), we examined planned polynomial contrasts of the color categories. As we performed parametric analyses, a Shapiro-Wilk test was used to determine whether the data were normally distributed. If this analysis provided insufficient evidence of normally distributed data ($p < .05$), the data was transformed to achieve normality using a $\log(x + 1)$ transformation. If this did not successfully normalize the data, we alternatively utilized a $\sqrt[3]{x}$ transformation. These transformations were chosen because they are ideal for normalizing positively skewed data such as ours.

Lastly, for each categorical analysis discussed above, we performed a complimentary functional analysis to rule out perceptual discriminability as a possible explanation for any potential differences between color categories. First, the discriminability of each color was calculated by averaging the distance between one color category and all remaining color categories in CIE (*x*,*y*) color space (see Average Distance column in Table 2.1). Next, a linear regression analysis using ordinary least squares was performed to assess whether there was a functional relationship between the discriminability of each color category and the means utilized in the aforementioned categorical analyses.

2.4. Results

Chi-squared goodness-of-fit tests were repeated for each participant to analyze the frequencies of correct and incorrect trials and ensure that individual participants correctly discriminated the target above chance on each experimental run (all *p*s <.05). As such, the average task performance of the group (M = 62.89%, SE = 2.71%) was significantly above chance level (25%), $t(29) = 13.96$, $p < .001$, $d = 2.55$. Error trials were removed from the subsequent analyses with the exception of overall selection proportion. There was no difference across target color categories in the number of trials thrown out due to a large displacement (>6^o) from the selected stimulus, $\chi^2(3, N = 420) = 0.59$, $p = .899$ (see section Saccade Detection and Data Analysis).

2.4.1. *Color Space Encoding of Isolated Distractors*

Sum curvature was significantly biased in the CCW direction overall as demonstrated by comparing baseline (M = −0.80°, SE = 0.34°) to zero, $t(29) = 2.32$, $p = .027$, $d = .42$. Critically, however, unbiased sum curvature was significantly different between the CCW (M = 0.74°, SE = 0.38°) and CW (M = −0.75°, SE = 0.43°) isolated distractor conditions, $t(29) = 2.87$, $p = .008$, *d*

= .52 (see Figure 2.3). Similarly, baseline max curvature (M = −0.05°, SE = 0.03°) was also biased in the CCW direction, $t(29) = 2.12$, $p = .042$, $d = .39$; and unbiased max curvature was also significantly different between the CCW (M = 0.03°, SE = 0.03°) and CW (M = −0.07°, SE = 0.03°) isolated distractor conditions, $t(29) = 2.65$, $p = .013$, $d = .48$. Saccade curvature differences between the CCW and CW isolated distractor conditions suggested that isolated distractors systematically modulated saccade curvature and thus validated examining saccade curvature on isolated distractors trials to investigate target selection competition between color stimuli.

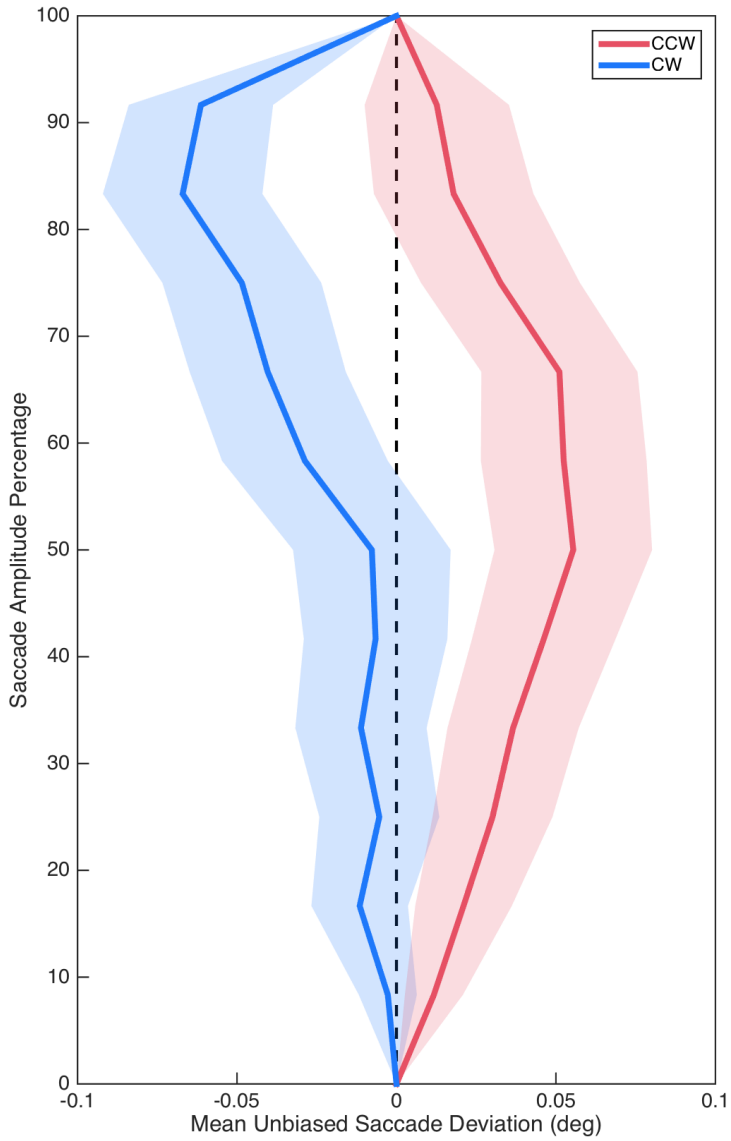

Figure 2.3. Mean unbiased saccade trajectories for saccades in the CCW (red) and CW (blue) conditions. Shading represents standard error.

The Mexican hat model provided a marginal fit of sum curvature as a function of target-distractor color space distance, $F(2,3) = 6.25$, $p = .085$, $R^2 = 0.75$ (see Figure 2.4*A*); as did the quadratic model, $F(2,3) = 7.44$, $p = .069$, $R^2 = 0.77$ (see Figure 2.4*B*). Critically, the minima of the fitted Mexican hat ($x_{min} = .42$) and quadratic ($x_{min} = .41$) models were nearly identical. To provide additional evidence for a functional relationship between sum curvature and target-distractor color space distance, sum curvature was transformed to achieve normality [$log(x + 1)$]

and was analyzed with a quadratic planned contrast, which demonstrated a significant quadratic contrast, $F(1,29) = 5.41$, $p = .027$, $\eta_p^2 = 0.16$. In contrast, the Mexican hat model did not provide a significant fit of max curvature as a function of target-distractor color space distance, $F(2,3) = 5.31$, $p = .103$, $R^2 = 0.76$ (see Figure 2.4*C*). However, the quadratic model provided a marginal fit to the data, $F(2,3) = 7.44$, $p = .069$, $R^2 = 0.81$ (see Figure 2.4*D*). As with sum curvature, the minima of the fitted Mexican hat ($x_{min} = .38$) and quadratic ($x_{min} = .39$) models were nearly identical for the max curvature data. Again, to provide additional evidence for a functional relationship between max curvature and target-distractor color space distance, max curvature was transformed to achieve normality ($\sqrt[3]{x}$) and was analyzed with a quadratic planned contrast, which demonstrated a significant quadratic contrast, $F(1,29) = 4.76$, $p = .037$, $\eta_p^2 = 0.14$.

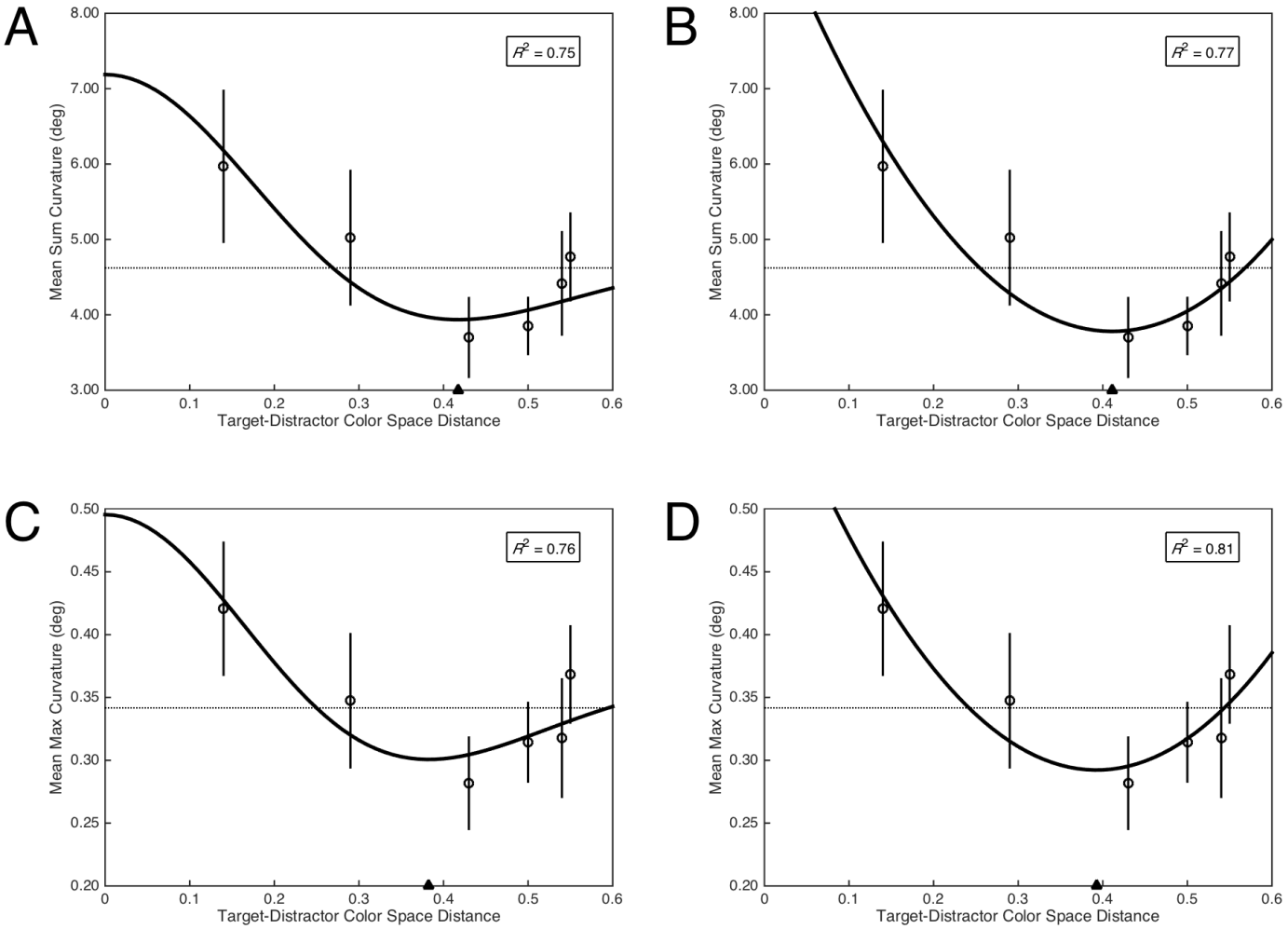

Figure 2.4. Saccade curvature as a function of target-distractor color space distance. Open circles represent mean saccade curvature and error bars represent standard error. Dashed horizontal lines indicate the grand mean across all color space distances. Filled triangle on the abscissa indicates the minima of the fitted models. The coefficient of determination is included in the top right of each plot. *A*: Mean sum curvature fit as a function of the Mexican hat model. *B*: Mean sum curvature fit as a function of the quadratic model. *C*: Mean max curvature fit as a function of the Mexican hat model. *D*: Mean max curvature fit as a function of the quadratic model.

2.4.2 *Hierarchical Differences between Color Categories*

2.4.2.1. Color selection bias. Error trials were added back into the data in order to analyze the proportion of trials on which a particular color was selected regardless of the specified target color (i.e., regardless of task instructions) to investigate whether there was a bias

for the selection of certain colors. We therefore calculated the proportion of total trials on which each color was selected, which is a combination of both the discrimination accuracy and the error selection bias for each color. This analysis demonstrated that there was a significant main effect of color category on overall selection proportion, $F(1.97,57.08) = 9.27$, $p < .001$, $\eta_p^2 = 0.24$ (see Figure 2.5*A*). *Post hoc* analyses demonstrated that overall, red was selected more often than green ($p = .012$) and yellow ($p = .002$). There were no other significant differences (ps > .05). However, red was selected marginally more often than blue ($p = .093$) and blue was selected marginally more often than yellow ($p = .051$). Furthermore, there was a significant linear contrast, $F(0.66,19.03) = 10.72$, $p = .008$, $\eta_p^2 = 0.27$; and quadratic contrast, $F(0.66,19.03) = 12.69$, $p = .005$, $\eta_p^2 = 0.30$. We then examined whether color selection biases can be simply explained by discriminability differences in color space (see Figure 2.5*B*). A linear regression analysis found insufficient evidence of a linear relationship between the overall selection proportion and discriminability in CIE (x,y) color space, $F(1,2) = 1.55$, $p = .340$, $R^2 = 0.52$. This result suggests that the strong bias for red stimulus selection is independent of discriminability in color space.

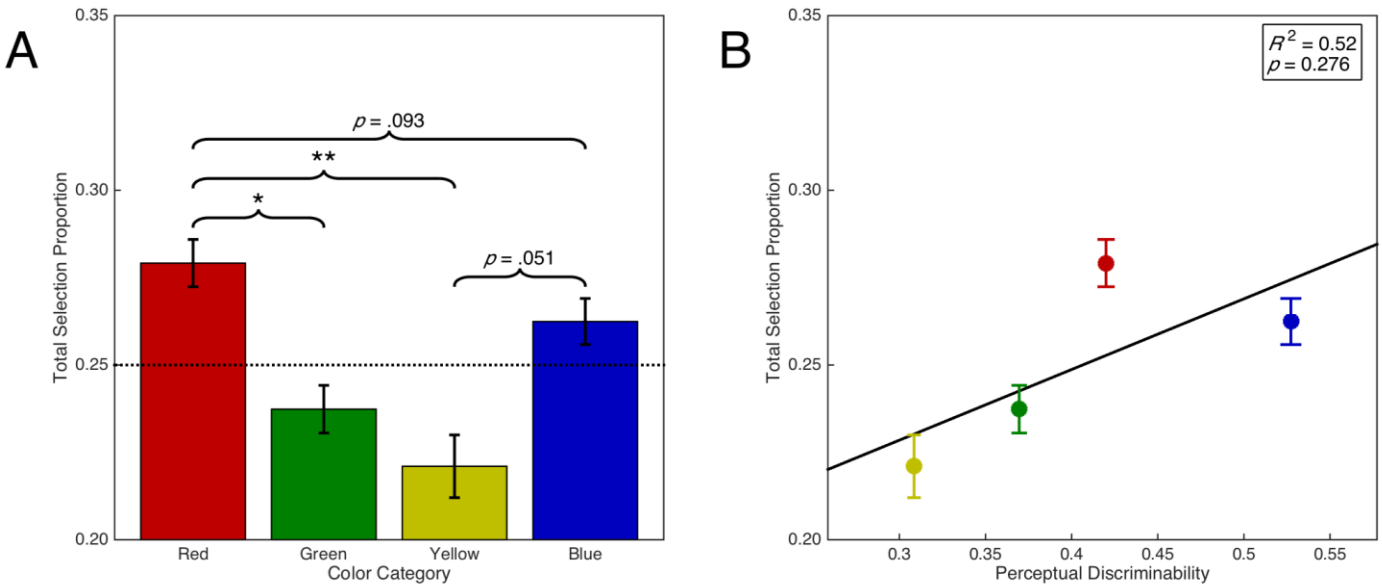

Figure 2.5. Selection bias as a function of color category and discriminability. Error bars represent standard error. Dashed horizontal line indicates chance. *A*: Overall color selection proportion as a function of color category. *B*: Overall color selection proportion as a function of color discriminability in CIE (*x*,*y*) color space. Panel includes line of best fit, the coefficient of determination, and significance level from the regression analysis. *$p < .05$. **$p < .01$.

2.4.2.2. Saccade curvature on isolated distractor trials. Sum and max curvature were both normalized with a $log(x + 1)$ transformation. There was no main effect of isolated distractor color category on sum curvature, $F(3,87) = 1.85$, $p = .144$, $\eta_p^2 = 0.06$; however, there was a marginal linear contrast, $F(1,29) = 3.41$, $p = .075$, $\eta_p^2 = 0.11$ (see Figure 2.6*A*). Furthermore, sum curvature was unrelated to the discriminability of isolated distractors in color space, $F < 1$, $R^2 = 0.06$ (see Figure 2.6*B*). Similarly, there was a marginal main effect of isolated distractor color category on max curvature, $F(3,87) = 2.62$, $p = .056$, $\eta_p^2 = 0.08$; and there was a marginal linear contrast, $F(1,29) = 3.65$, $p = .066$, $\eta_p^2 = 0.11$ (see Figure 2.6*C*). Max curvature was also unrelated to the discriminability of isolated distractors in color space, $F < 1$, $R^2 = 0.19$ (see Figure 2.6*D*).

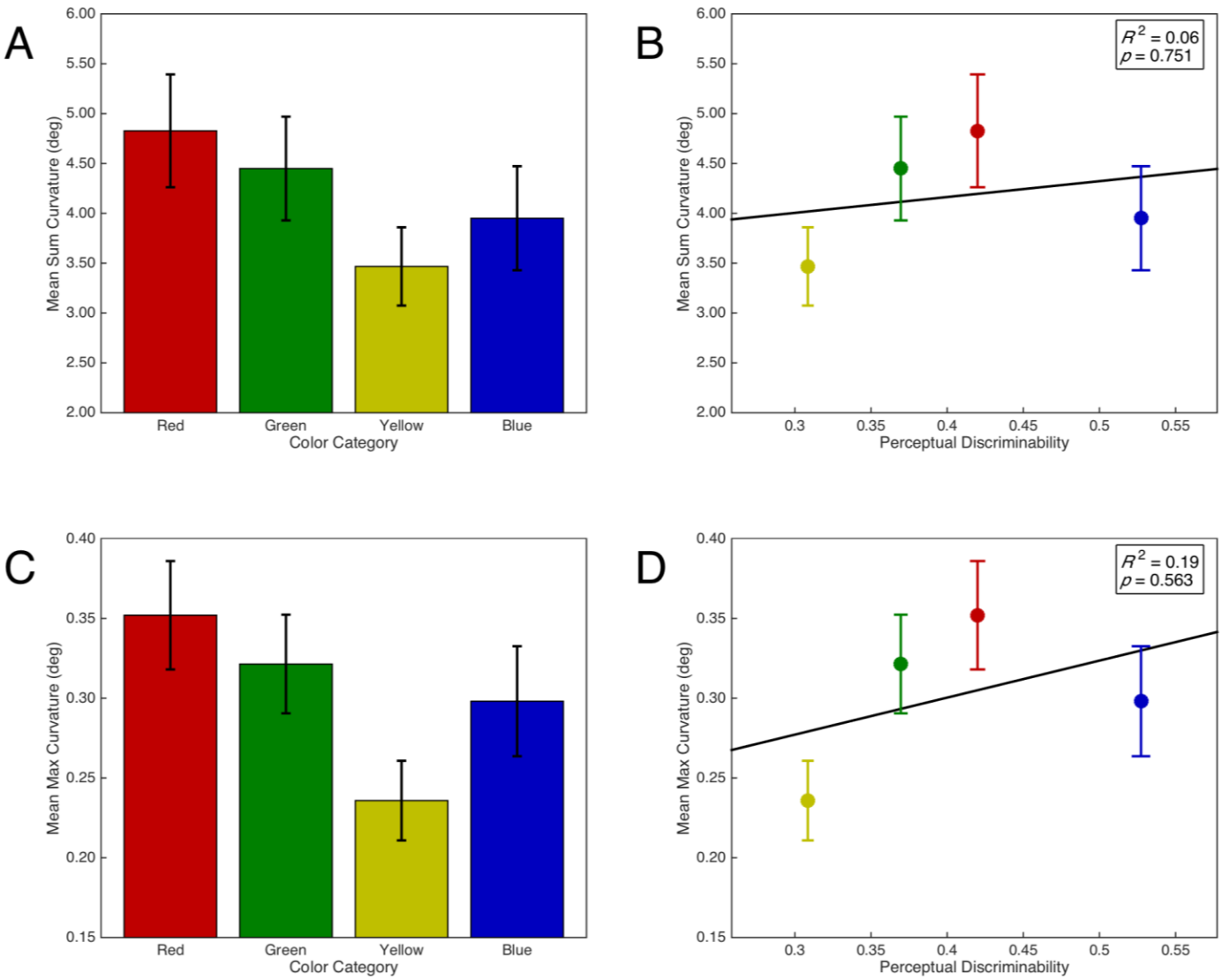

Figure 2.6. Saccade curvature as a function of isolated distractor category and discriminability. Error bars represent standard error. Right panels include line of best fit, the coefficient of determination, and significance level from the regression analyses. *A*: Sum curvature as a function of isolated distractor color category. *B*: Sum curvature as a function of isolated distractor discriminability in CIE (*x*,*y*) color space. *C*: Max curvature as a function of isolated distractor color category. *D*: Max curvature as a function of isolated distractor discriminability in CIE (*x*,*y*) color space.

2.4.2.3. Strength of saccade vector encoding per target color category. There was a significant main effect of target color on the proportion of errors, $F(2.05, 59.52) = 37.11$, $p < .001$, $\eta_p^2 = 0.56$ (see Figure 2.7*A*). *Post hoc* analyses demonstrated that there were fewer errors for red targets than green ($p < .001$) and yellow ($p < .001$) targets. Similarly, there were fewer errors for blue than green ($p < .001$) and yellow ($p < .001$) targets. There were no other significant differences (ps > .05). Additionally, there was a significant quadratic contrast, $F(0.68,19.84) = 59.70$, $p < .001$, $\eta_p^2 = 0.67$; but insufficient evidence for a linear contrast, $F(0.68,19.84) = 1.86$, $p = .263$, $\eta_p^2 = 0.04$. These categorical differences were not explained by a linear relationship between target color space discriminability and proportion of errors, $F(1,2) = 6.53$, $p = .125$, $R^2 = 0.77$ (see Figure 2.7*B*).

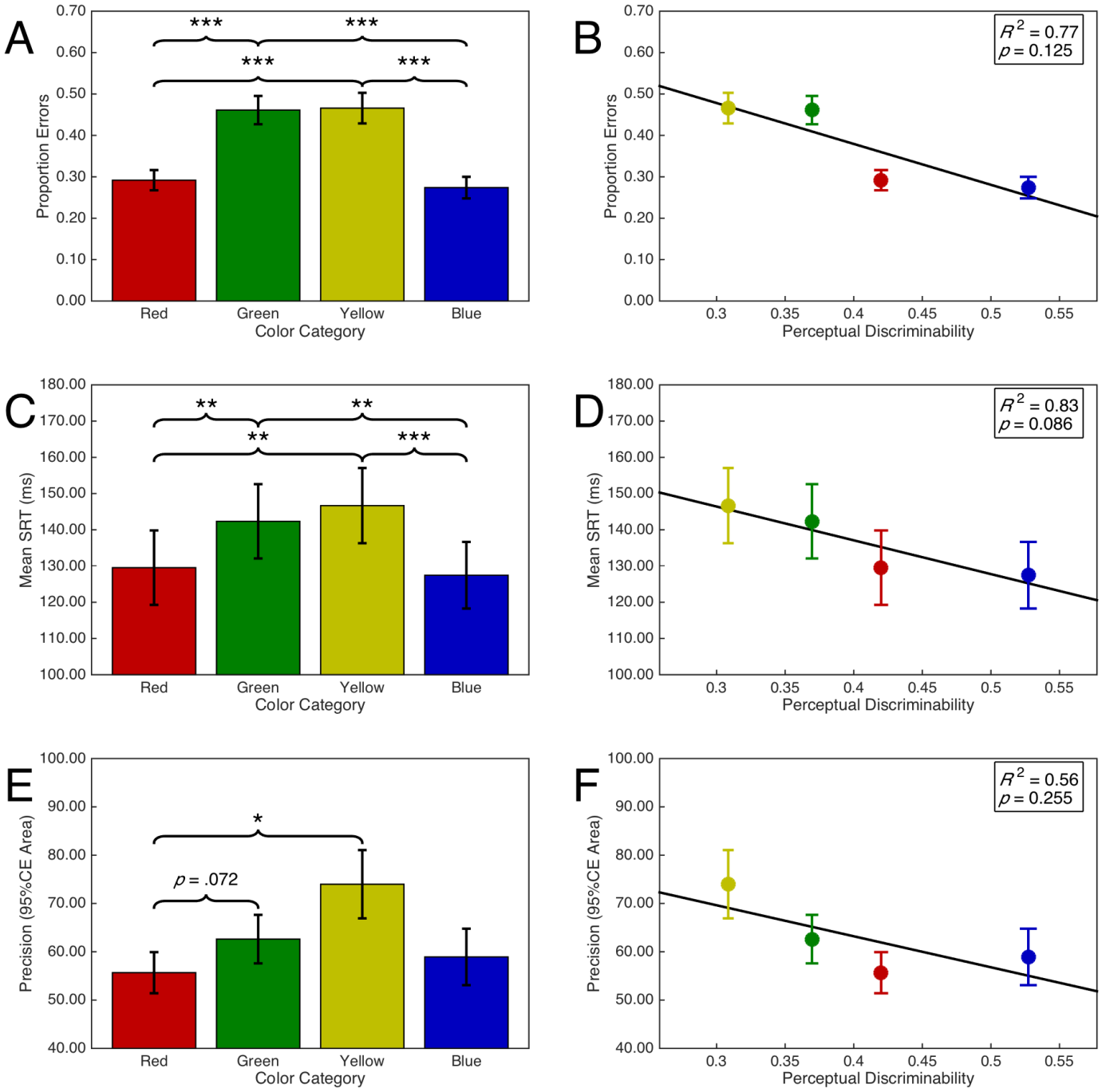

Figure 2.7. Task performance as a function of target color category and discriminability. Error bars represent standard error. Right panels include line of best fit, the coefficient of determination, and significance level from the regression analyses. *A*: Proportion of errors per target color category. *B*: Proportion of errors as a function of discriminability. *C*: Mean SRT per target color category. *D*: Mean SRT as a function of discriminability. *E*: Mean

precision per target color category. *F*: Mean precision as a function of discriminability. *$p < .05$. **$p < .001$.***$p < .001$.

There was a significant main effect of target color category on saccadic reaction time, $F(3,87) = 12.05$, $p < .001$, $\eta_p^2 = 0.29$ (see Figure 2.7*C*). *Post hoc* analyses demonstrated that SRTs were shorter for blue targets than for green ($p = .001$) and yellow ($p < .001$) targets. SRTs for red targets were shorter than for green ($p = .004$) and yellow ($p = .003$) targets. There were no other significant differences (ps > .05). As with proportion errors, there was a significant quadratic contrast, $F(1,29) = 31.30$, $p < .001$, $\eta_p^2 = 0.52$; but insufficient evidence for a linear contrast, $F < 1$. This was accompanied by a marginal, negative linear relationship between discriminability and saccadic reaction time, $F(1,2) = 10.11$, $p = .086$, $R^2 = 0.83$ (see Figure 2.7*D*). The regression line ($\hat{y} = -93.21 \cdot x + 174.38$) indicates that SRTs decreased by 9.32 ms as the average distance between a target color and the remaining color distractors increased by .1 units in CIE (*x*,*y*) color space.

Saccade precision was transformed using a $log(x + 1)$ transformation. There was a significant main effect of target color on saccade precision, $F(1.77,51.21) = 5.96$, $p = .006$, $\eta_p^2 = 0.17$ (see Figure 2.7*E*). *Post hoc* analyses indicated that saccades were more precise for red targets than yellow ($p = .022$) targets and marginally more precise than for green targets ($p = .070$). There were no other significant differences (ps > .05). Furthermore, there was a significant quadratic contrast, $F(0.59,17.07) = 8.57$, $p = .007$, $\eta_p^2 = 0.23$; but insufficient evidence for a linear contrast, $F(0.59,17.07) = 2.56$, $p = .132$, $\eta_p^2 = 0.08$. There was insufficient evidence for a linear relationship between discriminability and saccade precision, $F(1,2) = 2.50$, $p = .255$, $R^2 = 0.56$ (see Figure 2.7*F*).

2.5. Discussion

A memory-guided saccade task with cued color targets and distractors was used to examine the role of color in saccadic target selection processing. We investigated whether color saccade targets are encoded in perceptual color space by the oculomotor system and whether cuing a target color would elicit surround suppression in oculomotor color space. Next, we examined whether there are hierarchical color differences in the selection and encoding of saccade target vectors to color stimuli, as has been observed with the biased automatic selection of colors for pursuit eye movements (Tchernikov & Fallah, 2010), and whether such hierarchical effects can be accounted for simply by differences in perceptual discriminability. This provided insight into the level in the visual processing hierarchy at which the biased selection of certain colors occurs.

2.5.1. *Behavioral Relevance and Featural Encoding in the Oculomotor System*

In our first analysis, we examined whether the color representations utilized by the oculomotor system for saccade planning were encoded in perceptual color space by analyzing trials on which a correct saccade was made to the target and an isolated, peripheral distractor was within 90° of the target. On these isolated distractor trials, we examined saccade curvature elicited by the distractor as saccade curvature is indicative of the competition elicited by a competing saccade goal during target selection processing. This allowed us to determine whether distractor-related competition covaried as a function of the perceptual color space relations between potential saccade goals on the task. We utilized a preliminary analysis to determine whether isolated distractors had a modulatory influence on saccade curvatures. Therefore, we compared saccade curvature between trials on which the distractor appeared counterclockwise (CCW) to the target to trials on which the distractor appeared clockwise (CW) to the target, as

previous experiments suggest that saccades should curve in opposite directions in these two contexts (Dolye & Walker, 2001; Tipper et al., 2001). Furthermore, we also calculated the curvature observed on trials with no isolated distractor to establish a baseline level of inherent saccade curvature, which is expected as saccades are idiosyncratically curved (Bahill & Stark, 1975) and previous studies of saccade curvature report directional biases (Doyle & Walker, 2001; McSorley et al., 2004). As such, we observed a significant curvature bias in the CCW direction. Therefore, to determine if saccades curved in opposite directions in the CCW and CW conditions, we examined the difference in unbiased saccade curvature (i.e., baseline subtracted) between these conditions. This analysis was ideal as it merely introduces a scalar offset between the means, one that makes any potential mean difference more interpretable, but does not change the outcome of any statistical analysis since the variances are unchanged. This analysis demonstrated that saccades curved in opposite directions in the CCW and CW conditions relative to the baseline, thus validating our use of saccade curvatures to examine differences in color encoding by the oculomotor system. As such, we then measured saccade curvature as a function of the CIE (*x*,*y*) color space distance between the target and distractor. Our data demonstrated that saccade curvature elicited by these isolated distractors was functionally related to the color space distance between the target and distractor in CIE (*x*,*y*) color space. This suggested that the color representations that are utilized by the oculomotor system to plan saccadic eye movements are encoded in perceptual color space as with pursuit eye movements (Tchernikov & Fallah, 2010) and visual search (Bauer et al., 1996a, 1996b, 1998; D'Zurma, 1990).

Previous studies have found that remote distractor-related saccade curvature is greater when the featural similarity of the distractor to the target is categorically greater (Ludwig et al., 2003; Mulckhuyse et al., 2009). However, the current results demonstrate that oculomotor

suppression of a distractor can vary continuously along a particular feature dimension that determines the behavioral relevance of the distractor. This continuous relationship between saccade curvature and distractor behavioral relevance may result from a gradient of oculomotor activation/inhibition in critical oculomotor neural substrates such as SCi where the spatiotemporal interactions of multiple saccade vectors can elicit saccade curvature towards a distractor when the target and distractor vectors are co-activated (McPeek et al., 2003) or away from a distractor when the distractor vector is inhibited (Aizawa & Wurtz, 1998). This reasoning is supported by the observation that saccade curvature towards (McPeek et al., 2003) and away (White et al., 2012) from a distractor is correlated with the magnitude of neural activation encoding the distractor vector. Interestingly, in the critical oculomotor substrates that encode movement vectors and have been most strongly associated with saccade curvature, namely SCi (McPeek et al., 2003; Port & Wurtz, 2003; White et al., 2012) and FEF (McPeek, 2006), there are many cells with visuomotor properties and some that are strictly visual (SCi: McPeek & Keller, 2002; FEF: Bruce & Goldberg, 1985; Mohler et al., 1973). Therefore, what is not clear from the current experiment is whether the featural computations necessary to determine the behavioral relevance of the stimuli is performed locally in these oculomotor substrates or whether alternatively these areas integrate visual and cognitive signals to related saccade vectors and select a winner for the movement. The latter mechanism is supported by research demonstrating behavioral relevance or *priority* encoding in SCi (reviewed by Fecteau & Munoz, 2006) and with a winner-take-all saccade triggering mechanism in SCi (see White & Munoz, 2011 for a discussion). Critically, this latter mechanism is also consistent with the current observation of surround suppression.

2.5.2. *Surround Suppression of Oculomotor Representations*

The relationship between saccade curvature and target-distractor color space distance was marginally fit by both Mexican hat and quadratic polynomial functions, and when treating color space distances categorically, there was a quadratic contrast between the means. This is consistent with surround suppression of the cued saccade target color in color space and provides experimental support for selective tuning (Tsotsos et al., 1995; Tsotsos, 2011). Critically, if surround suppression modulates the strength of visuomotor representations in the oculomotor system, this implies that the featural computation necessary to determine the behavioral relevance of potential saccade goals was not performed locally in oculomotor substrates. This is because surround suppression in feature space results from task-based priming of a relevant visual feature at the top level of representation in the visual hierarchy and the subsequent recursive pruning of connections to unrelated features in a recurrent feedback sweep through the visual hierarchy (Tsotsos et al., 1995; Tsotsos, 2011). This theoretical prediction of ST has been well supported by recent behavioral (Boehler et al., 2009; Hopf et al., 2010) and neurophysiological (Buffalo et al., 2010; Mehta et al., 2000; Roelfsema et al., 2007) experiments. Since the oculomotor system does not have intrinsic featural representations, this feedback sweep would not propagate through the oculomotor system. Therefore, surround suppression modulating oculomotor representation implies that sensory signals projected into the oculomotor system have already been attenuated in the respective representational networks from which they originate. The behavioral relevance of a potential oculomotor movement goal is likely then determined by the cumulative strength of the attenuated sensory signals across feature domains. Furthermore, we would not expect similar results had we pre-cued the memory-guided saccade target, as this would have introduced the influence of spatial attention, which over the

considerably lengthy delay period of 1000 ms, likely would have eliminated the featural competition elicited by distractors that we observed.

2.5.3. *Attentional Color Hierarchy*

We examined whether hierarchical differences between color categories were apparent in various aspects of saccadic target selection processing and saccadic vector encoding as they are in the task irrelevant selection of certain color categories for pursuit eye movements (Tchernikov & Fallah, 2010) or the task relevant selection of visual search targets (Lindsey et al., 2010; Pomerleau et al., 2014) and response inhibition signals (Blizzard et al., 2016). We began by examining whether there was an overall selection bias for certain color categories regardless of task instructions by adding error trials back into the dataset and examining the proportion of total trials on which any particular color category was selected. Consistent with the automatic (i.e., task irrelevant) color selection bias observed by Tchernikov and Fallah (2010) in which participants hierarchically selected color RDKs (red > green > yellow > blue) for pursuit despite never being instructed to do so, we observed a strong overall bias for selecting the color red over green and yellow, and marginally over blue, which was accompanied by a significant linear contrast between the aforementioned color categories. Next, we examined if the inherent competitiveness of an isolated distractor was also modulated by the color category of the distractor. Here we observed only a marginal hierarchical effect of color category, but it was qualitatively the same as the overall selection bias above. Neither the overall selection bias nor the marginal modulation of inherent competitiveness by color category could be explained by differences in the discriminability of color categories in CIE (*x*,*y*) color space.

The results from examining overall selection proportion and inherent competitiveness of isolated distractors were qualitatively distinct from those obtained by examining the speed and

strength of saccadic vector encoding of the target color (i.e., SRT and the proportion of error trials respectively). Our data demonstrated that when saccades were cued to red targets, they were faster, more precise, and were executed with fewer errors than saccades directed to green and yellow targets. However, blue demonstrated a similar advantage for the proportion of errors and speed, but not for precision. These results were accompanied by significant quadratic contrasts between the aforementioned color categories for the proportion of errors, saccadic latency, and saccadic precision and with insufficient evidence for a linear contrast across these metrics. Clearly, blue was processed more efficiently or elicited more selection bias than would otherwise be predicted by the original color hierarchy (red > green > yellow > blue) of Tchernikov and Fallah (2010). Recall that overall selection proportion and distractor inherent competitiveness showed no such equal advantage for the blue color category. There are several possible explanations for this discrepancy.

Our data may suggest a fundamental variation on the color hierarchy specifically for the speed and strength of saccade vector encoding (red = blue > green = yellow). For example, faster saccades executed to both red and blue targets is consistent with Pomerleau et al. (2014) who observed faster N2pc ERPs to both red and blue targets than green and yellow targets in visual search. Such results could reflect a fundamental difference in the speed of transmission between red/blue and green/yellow color signals. However, this is unlikely given that red/blue and green/yellow color signals are projected through separate anatomical color channels (De Valois & De Valois, 1993). More plausible is that the proportion of errors and response latency metrics are reflective of the perceptual decision component of the task, which is highly related to the discriminability of the stimuli: a perceptual decision threshold is surpassed faster as the target becomes more easily perceptually discriminable (Ditterich et al., 2007; Gold & Shadlen, 2000;

Hanes & Schall, 1996). We find this explanation more plausible given that subsequent analyses suggested that lower error rates and faster latencies for red and blue saccades might be explained by the perceptual discriminability of these colors in color space, as SRTs showed a marginal linear relationship with the discriminability of the current color categories in color space, and although there was an insignificant relationship for error rates, a subjective inspection of these means suggests that errors might vary as a sigmoidal or step-like function of discriminability in color space. These results were also consistent with previous studies demonstrating that the discriminability of color stimuli in color space facilitates the response latency in visual search (Bauer et al., 1996a, 1996b, 1998, D'Zurma, 1990). Furthermore, higher perceptual discriminability between stimuli also improves the signal-to-noise ratio in the perceptual accumulation process (Gold et al., 1999; Romo et al., 2003), which could account for our observation of fewer errors for red and blue than green and yellow color categories.

The differences may also be explained by the fact that color was strictly task irrelevant in Tchernikov & Fallah and was crucial for the current task. As such, the perceptual discriminability of the stimuli may impede the featural processing of the saccade targets therefore degrading task performance as is observed in visual search (Verghese, 2001; Verghese & Nakayama, 1994). Another possibility is that the current effects were influenced by differences in the strength of visual working memory representations between color categories. Previous studies that have reported preferential processing for red over other color categories have utilized tasks in which color processing occurs during sustained color stimulation (Blizzard et al., 2016; Lindsey et al., 2010; Pomerleau et al., 2014; Tchernikov & Fallah, 2010). Given that the signal-to-noise ratio of prefrontal neural activity is proportional to visual working task performance (Saguchi & Goldman-Rakic, 1991, 1994; Williams & Goldman-Rakic, 1995),

utilizing a task that relies on visual working memory color representations may have introduced the influence of perceptual discriminability on localization performance as decreased perceptual discriminability may have degraded working memory representations. In any case, our data provided evidence for privileged processing of red stimuli, consistent with a growing number of studies (Blizzard et al., 2016; Lindsey et al., 2010; Pomerleau et al., 2014; Tchernikov & Fallah, 2010). Therefore, the current results cannot be simply accounted for just by differences in perceptual discriminability and likely arise from an interaction of inherent selection biases for red and the perceptual discriminability of the color stimuli.

2.5.4. *Representational Level of the Selection Bias*

We were interested in determining where in the visual processing hierarchy does the biased selection and processing of color categories occur. We utilized a memory-guided saccade task and observed clear hierarchical effects in the selection and inherent competitiveness of color categories independent of perceptual discriminability. Given the delay period of 1000 ms, previous research suggests that the color representations that guided this saccade task were those maintained through recurrent projections in the cortical visual system (Lee et al., 2005) perhaps as early as V1 (Supèr et al., 2001), as supposed to feedforward sensory signals from the retina, which would have decayed after this considerable delay. Therefore, the current categorical color effects likely do not arise from differing proportions of chromatic photoreceptors as has been proposed for speeded visual search (Lindsey et al., 2010).

2.5.5. *Conclusion*

We utilized a memory-guided saccade task with color targets and distractors to gain insight into various aspects of how color is encoded and selected for saccades by the oculomotor system. Our results demonstrated that there is a functional relationship between saccade

curvature elicited by an isolated distractor and the CIE (*x*,*y*) color space distance between the target and the distractor suggesting that the oculomotor system encodes color in perceptual color space as with the visual system. Furthermore, cueing attention to a particular color elicited surround suppression in oculomotor color space as the functional relationship between saccade curvature and target-distractor color space distance was characterized by functions that approximate a DoG, which demonstrates attentional facilitation near an attended feature in feature space and suppression at an intermediate distance in feature space. These results suggested that oculomotor behavioral relevance is computed by integrating sensory and cognitive signals that have been attenuated based on task parameters. Our data also suggested that the visual system has an inherent bias for the selection and encoding of the color category red over other categories independent of perceptual discriminability, but the speed and accuracy of responding on a memory-guided saccade task is more related to the perceptual discriminability of the target stimulus relative to distractors. Finally, this experiment suggests that the color hierarchy arises from selection and encoding biases in the later stages of visual processing independent of feedforward sensory input.

Chapter 3. Oculomotor Target Selection is Mediated by Complex Objects

This manuscript has been published in the *Journal of Neurophysiology*:

Kehoe, D. H., Lewis, J., & Fallah, M. (2021). Oculomotor target selection is mediated by complex objects. *Journal of Neurophysiology*, *126*(3), 845-863. https://doi.org/10.1152/jn.00580.2020

3.1. Abstract

Oculomotor target selection often requires discriminating visual features, but it remains unclear how oculomotor substrates encoding saccade vectors functionally contribute to this process. One possibility is that oculomotor vector representations (observed directly as physiological activation or inferred from behavioral interference) of potential targets are continuously re-weighted by task-relevance computed elsewhere in specialized visual modules, while an alternative possibility is that oculomotor modules utilize local featural analyses to actively discriminate potential targets. Strengthening the former account, oculomotor vector representations have longer onset latencies for ventral- (i.e., color) than dorsal-stream features (i.e., luminance), suggesting that oculomotor vector representations originate from featurally-relevant specialized visual modules. Here, we extended this reasoning by behaviorally examining whether the onset latency of saccadic interference elicited by visually complex stimuli is greater than is commonly observed for simple stimuli. We measured human saccade metrics (saccade curvature, endpoint deviations, saccade frequency, error proportion) as a function of time after abrupt distractor onset. Distractors were novel, visually complex, and had to be discriminated from targets to guide saccades. The earliest saccadic interference latency was ~110 ms, considerably longer than previous experiments, suggesting that sensory representations projected into the oculomotor system are gated to allow for sufficient featural processing to satisfy task demands. Surprisingly, initial oculomotor vector representations encoded features, as we manipulated the visual similarity between targets and distractors and observed increased vector modulation response magnitude and duration when the distractor was highly similar to the target.

Oculomotor vector modulation was gradually extinguished over the time course of the experiment.

3.2. Significance Statement

We challenge the role of the oculomotor system in discriminating features during saccadic target selection. Our data suggest that the onset latency of oculomotor vector representations is scaled by task-difficulty and featural complexity, suggesting that featural computations are performed outside of the oculomotor system, which receives the output of these computations only after sufficient visual and cognitive processing. We also challenge the convention that initial oculomotor vector representations are feature-invariant, as they encoded task-relevance.

3.3. Introduction

The oculomotor system encodes visual stimuli (Goldberg & Wurtz, 1972; Mohler et al., 1973) and saccades (Robinson, 1972; Robinson & Fuchs, 1969) as vectors on orderly spatial maps. If multiple potential saccade targets are present, the oculomotor system must select a winner from among the available oculomotor vector representations, a process called target selection. Competition between oculomotor vector representations during target selection can be inferred behaviorally from the spatial biasing of a target-directed saccade by some secondary stimulus, such as in the remote distractor (Doyle & Walker, 2001; Sheliga et al., 1994, 1995; Tipper et al., 1997, 2001) or double-stepping target (Becker & Jürgens, 1979; Findlay and Harris, 1984) paradigms. The modulation of saccade trajectories by competing distractors during target selection is sensitive to the time course of oculomotor planning. Saccade trajectories are typically biased towards distractors at short saccade latencies (Heeman et al., 2014, 2017; McSorley et al., 2006; Tudge et al., 2018; van Zoest et al., 2012), while at longer saccade

latencies, saccades curve away from distractors (McSorley et al., 2006) and endpoint averaging ceases (Heeman et al., 2014, 2017; Tudge et al., 2018).

When visual features define oculomotor targets (e.g., feature-based oddity search or template matching), successful target selection requires discriminating among stimuli on the basis of their constituent features. Behavioral experiments have demonstrated that visual features impose additional competition between oculomotor vector representations. Saccade trajectories are more spatially biased by distractors with task-relevant (Kehoe et al., 2018a, 2018b; Ludwig & Gilchrist, 2003; Mulckhuyse et al., 2009; van der Stigchel et al., 2011) or conspicuous (Tudge et al., 2018; van Zoest et al., 2012) features than distractors with task-irrelevant or inconspicuous features. For example, saccades curvature elicited by distractors that are color-congruent with targets is greater than saccade curvature elicited by incongruent distractors (Ludwig & Gilchrist, 2003; Mulckhuyse et al., 2009). Similarly, saccadic endpoint averaging between stimuli is enhanced for identical stimulus pairs as compared to feature-incongruent stimulus pairs (van der Stigchel et al., 2011). In fact, the magnitude of saccade curvature and endpoint deviation varies continuously as a function of target-distractor similarity for color (Kehoe et al., 2018b) and even complex, meaningless, novel objects (Kehoe et al., 2018a).

Visual features can also modulate the latency of saccadic interference effects. Kehoe and Fallah (2017) developed a non-invasive, behavioral method for estimating the latency of visually-evoked saccadic interference. We measured distractor-elicited saccade curvature as a function of time between an abrupt, task-irrelevant distractor onset and saccade execution. Targets onset prior to distractors allowing us to continuously analyze the entire time course of distractor processing. Conversely, previous studies have been limited to analyzing saccade curvature (McSorley et al., 2006; Mulckhuyse et al., 2009) and saccade endpoint averaging

(Heeman et al., 2014, 2017) at distractor processing times greater than ~150 ms, as targets did not lead distractors. With our paradigm, we observed that the onset latency of saccadic interference elicited by luminance distractors was ~20 ms faster than by color distractors.

The theoretical foundation of this non-invasive technique is rooted in the spatiotemporal oculomotor interactions in the intermediate layers of the superior colliculus (SCi) and frontal eye fields (FEF) associated with curved saccades. In these substrates, oculomotor vector representations are observed directly via neural activation of visuomotor (VM) neurons. Critically, in the perisaccadic interval ~20-30 ms prior to saccade execution, if there is transient excitation (McPeek et al., 2003; McPeek, 2006; Port & Wurtz, 2003) or suppression (White et al., 2012) of VM cells encoding a distractor, saccades curve towards or away (respectively) from the distractor. Furthermore, the magnitude of the excitation or suppression in this epoch is proportional to the magnitude of saccade curvatures (see Figure 3.1). In the excitatory case, this mechanism has been causally demonstrated with microstimulation (McPeek et al., 2003; McPeek, 2006). Conversely, inhibitory injections in SCi elicit saccades curved away from the inactivated motor field (Aizawa & Wurtz, 1998).

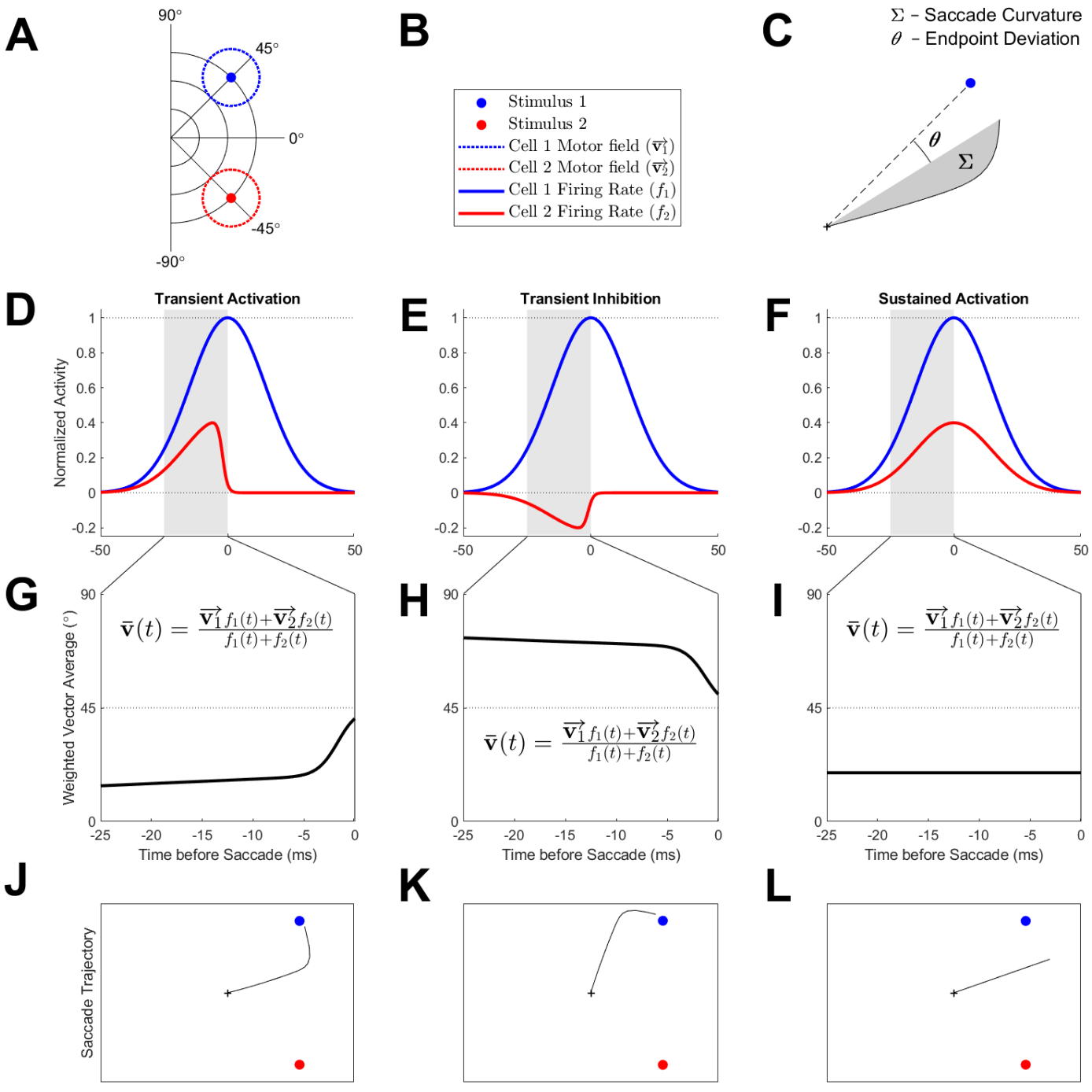

Figure 3.1. Weighted vector average model linking hypothetical oculomotor neural activity to saccade trajectories. *A*: Polar coordinates of two stimuli (blue and red filled circles) of equal eccentricity and the motor fields of two hypothetical oculomotor cells encoding the stimuli (blue and red dotted lines). Motor fields are color-coded in accordance with their encoded stimulus. *B*: Figure legend. *C*: Schematic diagram of saccade curvature and endpoint deviation derivation. *Row D, E, F*: Hypothetical normalized neural firing rate patterns for cells encoding the stimuli.

Firing rates are color-coded in accordance with their encoded stimulus. Shaded region corresponds to the critical epoch (i.e., the interval of time between saccade execution and 25 ms prior to saccade execution). *Row G*, *H*, *I*: Weighted vector average model as a function of time in the critical epoch. *Insets*: Formulation of a weighted vector average model similar to those used previously (e.g., Port & Wurtz, 2003) in which variable *t* is time. *Row J*, *K*, *L*: Resultant saccade trajectory on an example display containing the blue and red stimuli. *Column D*, *G*, *J*: Transient activation during critical epoch for cell encoding red stimulus elicits strongly curved saccade deviating toward the red stimulus. *Column E*, *H*, *K*: Transient inhibition during critical epoch for cell encoding red stimulus elicits strongly curved saccade deviating away from the red stimulus. *Column F*, *I*, *L*: Sustained activation during critical epoch for cell encoding red stimulus elicits straight saccade with endpoint shifted toward the red stimulus.

White et al. (2009) demonstrated that visual onset burst latencies for VM cells in SCi are ~30 ms longer for color targets than for luminance targets. This difference closely corresponds to the visual onset burst latency differences between cells in the magno-/parvocellular or dorsal/ventral processing streams in early visual areas such as the lateral geniculate nucleus (LGN), V1, and V2 (Nowak & Bullier, 1997; Schmolesky et al., 1998). Such close correspondence may suggest that saccade-vector encoding neurons of the oculomotor system receive visual input specifically from visual processing modules specialized for processing task-relevant visual features. In anterior visual cortical modulates specialized for processing complex visual stimuli (e.g., faces), visual onset burst latencies are longer than in more posterior visual cortical modules specialized for processing simpler visual stimuli (e.g., Gabors) (Nowak & Bullier, 1997; Schmolesky et al., 1998). If oculomotor substrates receive visual input specifically from visual modules specialized for processing task-relevant visual features, then oculomotor activation latencies should be longer for more complex stimuli than for simple stimuli. Previous behavioral experiments utilizing double-stepping targets (Becker & Jürgens, 1979), luminance flashes (Reingold & Stampe, 2002), or irrelevant Gabors (Kehoe & Fallah, 2017) have

consistently shown that the onset latency of saccadic interference elicited by simple visual stimuli is 50-70 ms. Here, we utilized our aforementioned behavioral paradigm to non-invasively estimate the onset latency of saccadic interference elicited by task-relevant complex objects.

In the current study, subjects performed a template-matching visual discrimination between complex, novel target and distractor objects and executed saccades to the target. We reason that these stimuli would likely require feature processing in late stages of the ventral visual processing stream. As in Kehoe and Fallah (2017), we randomized the interval between distractor and target onsets (distractor-target onset asynchrony [DTOA]) but ensured feature processing of the stimuli by presenting the distractor before the target on 50% of trials so that the order of stimulus onset did not provide target information. As such, we analyzed saccade curvature as a function of time between saccade initiation and distractor onset for correct trials in which the distractor onset before the target. Additionally, we examined saccade endpoint deviations, saccade frequencies, and error proportions, as they are also indicative of oculomotor excitatory and suppressive processing: (a) subthreshold microstimulation of a secondary saccade vector in SCi or FEF concurrent with saccade initiation causes saccade endpoints to shift towards the stimulated vector and the magnitude of these deviations is proportional to the intensity of the microstimulation (Glimcher & Sparks, 1993; Robinson & Fuchs, 1969; Robinson, 1972) (see Figure 3.1). (b) The abrupt onset of a visual stimulus transiently lowers the behavioral likelihood of saccade initiation ~60 ms after stimulus onset (Reingold & Stampe, 2002). As visual onset latencies in SCi are typically 50-60 ms (Bohenke & Munoz, 2008), this effect may be due to lateral inhibition in SCi whereby collicular stimulation transiently elicits rapid (~5 ms) inhibition in surrounding loci (Munoz & Istvan, 1998). (c) Target selection is guided by the available representations in SCi, as an inhibitory injection at the target locus greatly impairs accurate

target selection (McPeek & Keller, 2004). We also manipulated the visual similarity between targets and distractors to examine when behavioral relevance encoding of stimuli emerged during the oculomotor processing time course. Based on previous investigations of feature-based saccadic target selection, we expected that the initial excitatory response would be feature invariant, while the subsequent suppressive response would vary in latency and magnitude between similarity conditions (Fecteau & Munoz, 2006). Finally, to examine whether perceptual learning modulates oculomotor vector representations, we examined whether distractor processing was similar across the time course of the experimental session.

3.4. Methods

3.4.1. *Participants*

36 York University undergraduate students (17-30 years old, 6 male) participated in the experiment for course credit. Participants had normal or corrected-to-normal visual acuity and were naïve to the purpose and design of the experiment. Informed consent was obtained prior to participation. All research was approved by York University's Human Participants Review Committee.

3.4.2. *Stimuli*

6 stimuli used in a previous experiment (Kehoe et al., 2018a) were constructed offline using MATLAB (MathWorks, Natick, MA) by intersecting 6 or 7 vertical and horizontal line segments (1°× 0.08°) together at right angles in a configuration that did not resemble meaningful alphanumerical characters to an English speaker (similar to Palmer, 1978; see Figure 3.2*A*). Individual line segments occupied 1 of 12 possible locations that were embedded in an imaginary box (2° × 2°). All stimuli were linearly related to one another in the number of line segments differences between them. Stimuli were assigned to an integer-valued location on a conceptual

number line in which the absolute difference in number line position between any two stimuli was equal to the number of line segment differences between them and is therefore inversely proportional to their visual similarity. The difference in number line position between stimuli is herein referred to as objective similarity (OS). The 6 stimuli were divided into 3 subsets of 2 stimuli: {3,4}, {2,5}, and {1,6} (see Figure 3.2*B*). Each subset was characterized by a unique OS value: OS = 1, OS = 3, and OS = 5, referred to herein as OS1, OS3, and OS5 (respectively). Stimuli in each subset were interchangeably assigned as either targets or distractors. The stimuli were white (CIE*xy* = [.29, .30], luminance = 126.02 cd/m^2) and were displayed against a black (CIE*xy* = [.27, .26], luminance = 0.20 cd/m^2) background on a 21-inch CRT monitor (85 Hz, 1024 × 768). Participants viewed stimuli in a dimly lit room from a viewing distance of 57 cm with a headrest stabilizing their head position.

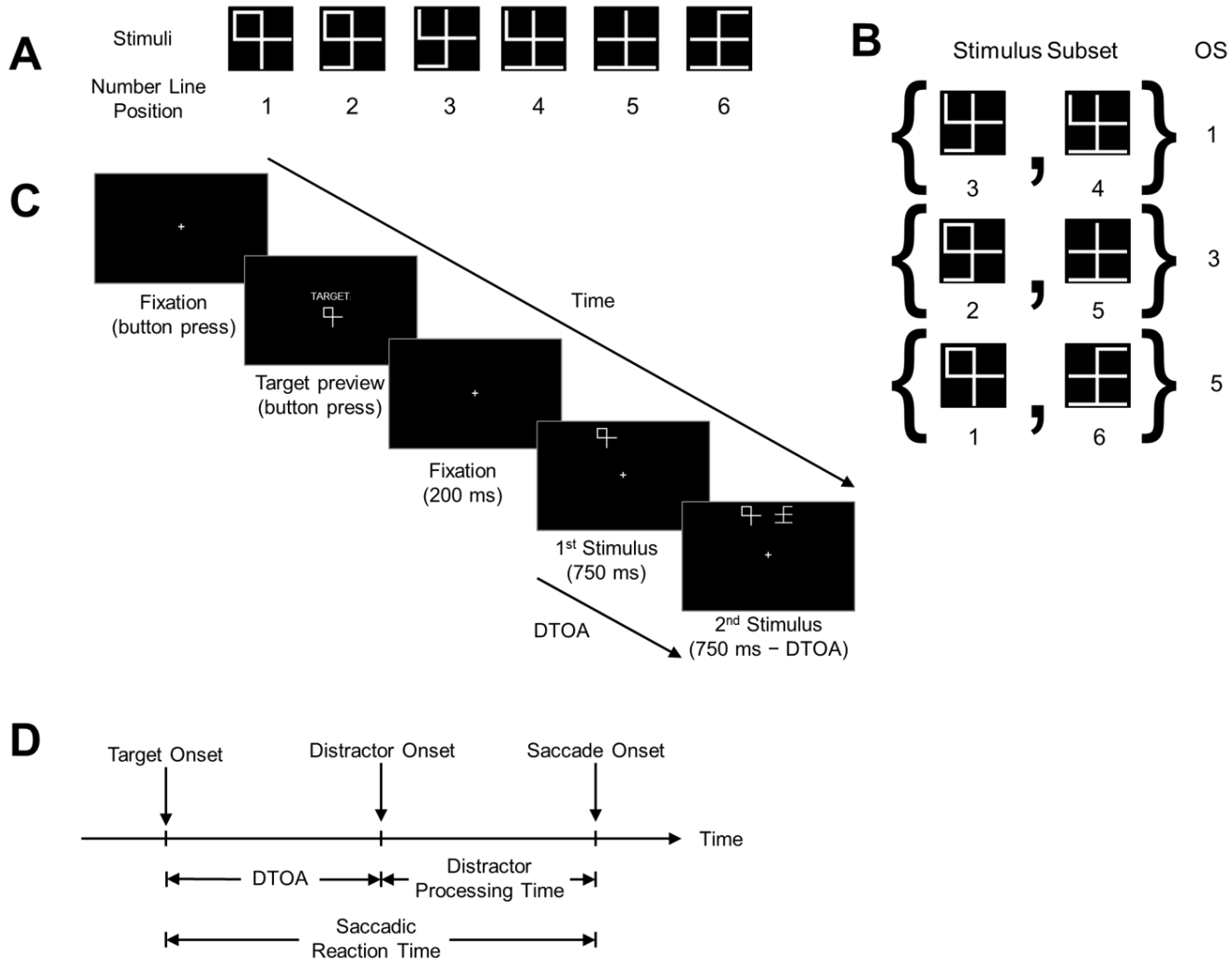

Figure 3.2. Discrimination saccade task stimuli, displays, and temporal schematic. *A*: Stimuli used in the current experiment. Stimuli were placed on an integer-valued conceptual number line in which the absolute difference between number line positions corresponds to the number of line segment differences, referred to as objective similarity (OS). *B*: Stimulus subsets and associated OS. 6 stimuli were uniquely assigned to 3 subsets of 2 stimuli where each subset has a unique OS value. *C*: Trial structure. Participants pressed a button to preview the target stimulus until they were familiar with it. Participants then pressed the button again to initiate the discrimination display. After maintaining fixation for 200 ms, the display was presented for 750 ms or until a saccade to one of the stimuli was detected. The target and distractor onsets were separated by a randomized interval, referred to as distractor-target onset asynchrony (DTOA). *D*: Temporal schematic diagram. Absolute time is represented by the long, rightward horizontal arrow. Critical temporal events (target onset, distractor onset, saccade onset) are indicated

by downward facing arrows and accompanying text labels. Critical temporal intervals are indicated by double-sided, horizontal arrows with accompany text labels. Saccadic reaction time is the interval between target onset and saccade onset. Distractor-target onset asynchrony (DTOA) is the interval between target onset and distractor onset. Distractor processing time is the interval between distractor onset and saccade onset.

3.4.3. *Apparatus and Measurement*

Stimulus presentation was controlled using a computer running Presentation software (Neurobehavioral Systems, Berkeley, CA). Manual button responses were collected on a serial response box (RB-540; Cedrus, San Pedro, CA). Eye position was recorded using infrared eye tracking (500 Hz, EyeLink II; SR Research, Ontario, Canada). The eye tracker was calibrated using a nine-point grid at the beginning and halfway point of each experimental session, and as needed. All data processing and statistical analysis was performed using MATLAB.

3.4.4. *Task Procedure*

Trials were initiated by button pressing (see Figure 3.2*C*). A target preview was presented until participants pressed the button a second time. A white fixation cross (0.4°× 0.4°) then appeared in the center of the display. After participants maintained fixation (1.89° × 1.89° window) for 200 ms, the target and distractor appeared at 1 of 4 locations. The target and distractors were always in the same vertical hemifield, were equidistant from fixation (8° eccentricity), and angularly separated from the vertical meridian by 22.5°. The relative time between distractor and target onsets (distractor-target onset asynchrony [DTOA]) was −150, −100, −50, 0, 50, 100, or 150 ms in which a positive value indicates that the target onset first. To correctly discriminate the target, participants were instructed to maintain fixation, use their peripheral vision to determine which stimulus was the target, and then make a saccade to it. The trial ended when a saccade was made to the target (correct) or distractor (incorrect) or 750 ms

had elapsed from the time of the first stimulus onset (time-out). An error tone and message were used to indicate incorrect and time-out trials. Time-out trials were randomly replaced back into the block. Participants received accuracy feedback at the end of each block.

Participants completed 1 session with 6 blocks of 75 trials for a total of 450 trials. Each block contained 3 repeats of 25 conditions (3 OS conditions × 7 DTOA conditions + 4 no distractor baseline trials, one for each stimulus location) in randomized order. On each trial, the hemifield (upper vs. lower), left/right order of the target and distractor, and target/distractor stimulus assignment (e.g., target = 1, distractor = 6 vs. target = 6, distractor = 1) was randomized with equal probability.

3.4.5. *Saccade Detection*

Saccades were detected, visualized, filtered, and analyzed offline using customized MATLAB algorithms. Saccades were defined as a velocity exceeding 20 °/s for at least 8 ms and a peak velocity exceeding 50 °/s. Saccadic reaction time (SRT) was defined as the time from target onset to saccade initiation (see Figure 3.2*D*). Trials that contained blinks (1.98%), corrective saccades (1.01%), saccade amplitudes < 1° (1.75%), endpoint deviations > 3° from the center of the target (5.26%), fixation drifts > 0.5° during the pre-saccadic latency period (4.27%), or an SRT < 100 ms (3.49%) were excluded from further analysis leaving 82.24% of the data remaining.

Saccade curvatures were quantified as the sum of all orthogonal deviations from a straight line between the start and end of the saccade in degrees visual angle. Endpoint deviations were quantified as the angular separation between the saccade endpoint and the center of the target in polar degrees. See Figure 3.1*C* for a schematic diagram of these definitions. Mean baseline saccade curvature and endpoint deviation for each participant at each target location was

subtracted from the data to reduce idiosyncratic movement. These metrics were coded so that positive values correspond to deviations towards the distractor, while negative values correspond to deviations away from the distractor. This convention conveniently indicates excitatory distractor processing as positively valued saccade curvature/endpoint deviation and inhibitory distractor processing as negatively valued saccade curvature given the relationship between saccade curvature/endpoint deviation direction and excitatory/inhibitory distractor processing in oculomotor substrates (see section **3.3. Introduction**).

3.4.6. *Data Analysis*

3.4.6.1. Task performance. To ensure that the task was performed at above chance levels, a binomial exact test was conducted on the frequency of correct trials for each participant. Participants who did not score above chance ($p < .05$) were removed from subsequent analyses.

3.4.6.2. Distractor processing time. We only analyzed trials on which the target onset prior to or synchronously with distractor onset (DTOA ≥ 0). Distractor processing time was defined as the time between distractor onset and saccade onset and was computed by subtracting DTOA from SRT (see Figure 3.2*D*). We fit a Gaussian kernel smoother with a bandwidth of 10 ms to the saccade curvature and endpoint deviation data from each subject as a function of distractor processing time. A sliding two-tailed, Wilcoxon signed-rank test was used to determine the distractor processing epochs at which saccade curvature and endpoint deviation were significantly different than zero. Similarly, a Gaussian kernel density estimator (KDE) with a bandwidth of 10 ms was fit to the distributions of correct and erroneous saccades for each subject to estimate saccade frequency and error proportion as a function of distractor processing time. Saccade frequencies appeared to be distributed as an exponentially-modified Gaussian (EMG) function of distractor processing time but for a transient decrease in the range of ~125-

250 ms. To estimate the distractor processing time (t) of this transient decrease, we first fit an expectation EMG model to the data outside of this range. The model was defined as

$$g(t) = \alpha \frac{\exp\left(-[t-\mu]^2 / 2\sigma^2\right)}{1+\exp(\lambda[t-\mu])},$$

where α scales the height of the model, μ and σ^2 are the mean and variance parameters for the Gaussian component of the model, and λ scales the skew of the model. We fit the model by maximizing the log-likelihood of the parameters using the normal distribution. We validated the model with a ratio test comparing the fit to a one-parameter null model. Second, a sliding one-tailed Wilcoxon signed-rank test was used to determine the distractor processing time that saccade frequencies were significantly lower than the expectation model. A sliding Wilcoxon signed-rank test was used to determine the distractor processing epochs at which error proportion was significantly greater than the standard error of the proportion. We only analyzed saccade curvature, endpoint deviation, and error proportion for distractor processing times with at least 20 saccades, i.e., KDE $\geq 20 / \sqrt{2\pi\sigma^2}$, where $\sigma = 10$ (KDE bandwidth).

This analysis was repeated to examine (a) the overall distractor processing time course; (b) distractor processing time course differences between OS conditions; and (c) distractor processing time course differences between the first, second, and final 1/3 of experimental blocks. All saccade metrics were compared between conditions with a sliding Friedman test to determine when processing was significantly different between conditions. For all sliding inferential analyses, epochs were considered significant when $p < .05$ for at least 10 ms. Significant epochs separated by ≤ 5 ms were pooled together. Non-parametric Wilcoxon signed-rank and Friedman tests were utilized as the data was often not normally distributed across subjects.

3.4.6.3. Consistency of overall distractor processing time effects across subjects.

We examined whether the pattern of results for the overall data was consistent across individual subjects with a time series analysis that captures inter-subject variability. We generated *b*=1000 bootstrapped resamples of the entire data set. For each subject and for each resample, we computed saccade curvature, endpoint deviation, saccade frequency, and error proportion as a function of distractor processing time using the kernel regression and KDE techniques outlined in the previous section (see *Distractor Processing Time*). Next, we identified significant distractor processing epochs for each metric and for each subject using a sliding non-parametric distribution test. The distribution test empirically examines whether a large distribution of n observations, $Y = (y_1, \ldots, y_n)$, is significantly different from some constant, c. Borrowing the computational formulation of Poe et al. (2005), the one-tailed cumulative probability in the left tail is

$$p_L = \frac{1}{n}\sum_{i=1}^{n} z_i, \quad z_i = \begin{cases} 0, & y_i - c \leq 0 \\ 1, & y_i - c > 0 \end{cases},$$

the one-tailed cumulative probability in the right tail is

$$p_R = \frac{1}{n}\sum_{i=1}^{n} z_i, \quad z_i = \begin{cases} 0, & y_i - c \geq 0 \\ 1, & y_i - c < 0 \end{cases},$$

and the two-tailed cumulative probability is $2 \times \min\{p_L, p_R\}$.

The following analyses were repeated for each subject to detect subject-level significant distractor processing epochs. A sliding two-tailed, distribution test was used to determine the distractor processing epochs at which the saccade curvature and endpoint deviation distributions of resamples were significantly different than zero. A sliding one-tailed, distribution test was used to determine the distractor processing epochs at which the saccade frequency distribution of resamples was significantly less than an EMG expectation model, where the model was fit to the

mean of the saccade frequency distribution of resamples using the method outlined in the previous section (see *Distractor Processing Time*). A sliding one-tailed, distribution test was used to determine the distractor processing epochs at which the error proportion distribution of resamples was significantly greater than the standard deviation of the error proportion distribution of resamples. For all sliding inferential analyses, epochs were considered significant when $p < .05$ for at least 10 ms. Significant epochs separated by ≤ 5 ms were pooled together. We removed subject level epochs that onset < 60 ms after distractor onset, as such short latency effects are likely anticipatory and not visually guided. For saccade curvature and endpoint deviation, we split the subject epochs into positively/negatively signed sets of epochs.

We examined the consistency between the epochs detected at the subject level with the epochs detected at the group level. We analyzed the probability that time bins in the subject level epochs temporally overlap with the temporal interval of each group-level epoch. Finally, we computed the number of subjects with at least one epoch that overlaps with the temporal interval of each group level epoch. We tested whether the number of subjects with epochs consistent with the group level epochs was significant using a binomial exact test.

3.4.6.4. Disentangling SRT and distractor processing time. We performed several analyses to ensure that any potential effects of distractor processing time are not confounded by systematic SRT differences between conditions. First, we examined potential SRT mean differences between DTOA (0, 50, 100, 150), OS (OS1, OS3, OS5), and experimental block (early, middle, late) conditions using a linear mixed-effects model with fixed effects for all conditional main effects and interactions and with random subject intercepts for each fixed effect similar to repeated-measures ANOVA. A marginal *F*-test with planned orthogonal comparisons as *post hocs* was used to analyze all fixed effects. To examine potential speed-accuracy trade-

offs, we repeated this analysis for error proportions with a generalized linear mixed-effects model with a logit link function to the binomial distribution. Second, we repeated our data smoothing procedure (see *Distractor Processing Time*) to analyze saccade metrics as a function of distractor processing time separately across DTOA conditions. This allowed us to investigate whether the latencies of distractor processing effects are consistent across DTOA conditions. Third, we realigned the data to target onset and repeated our data smoothing procedure to analyze saccade metrics as a function of SRT. This allowed us to investigate whether the distractor effects temporally scale with distractor onset, or alternatively, whether distractor effects are fixed with respect to saccade latency. In the second and third analyses, saccade metric differences between DTOA conditions as a function of distractor processing time and SRT were analyzed using a sliding Friedman test with the same inferential conventions used above. Significant epochs in each DTOA condition were identified using sliding Wilcoxon signed-rank tests with the same inferential conventions used above.

3.5. Results

All participants correctly discriminated the target above chance (all ps $\leq .009$), except for one participant ($p = .050$) who was therefore removed from subsequent analyses. The group mean percentage of correct target discriminations was 89.67% ($SE = 0.92\%$).

3.5.1. *Overall Distractor Processing*

We examined whether the duration of distractor processing time (see Figure 3.2*D*) had a systematic influence on saccade trajectories. Figure 3.3 illustrates a random sampling of saccade trajectories uniformly sampled across distractor processing time. As can be seen in Figure 3.3, saccade trajectories appear spatially biased towards distractors at early distractor processing times and spatially biased away from distractors at later distractor processing times. Next, we

examined potential systematic effects of distractor processing time on saccade curvature, endpoint deviation, saccade frequency, and error proportion with kernel regression, KDE, and sliding inferential analyses.

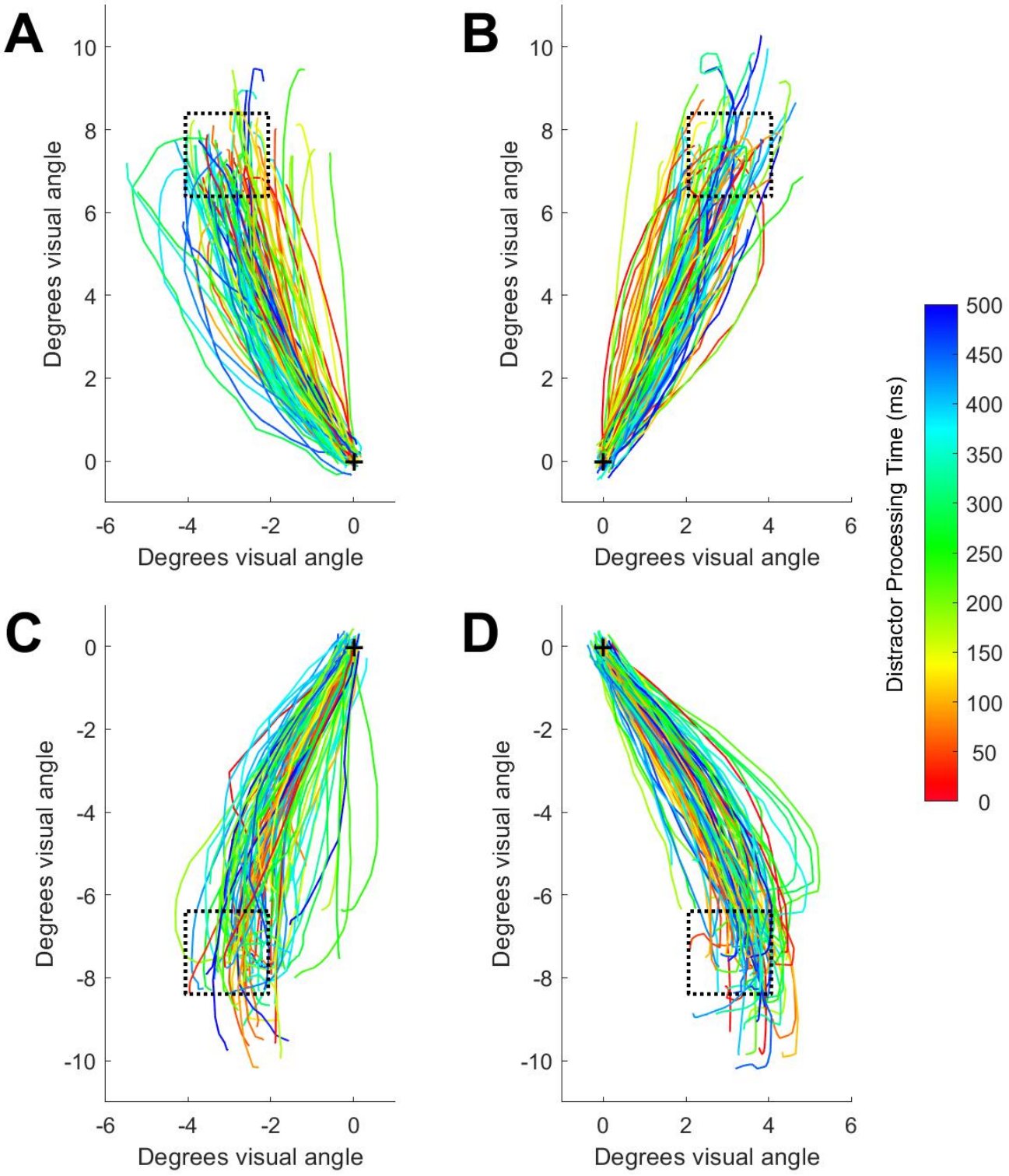

Figure 3.3. Example saccade trajectories. Saccades are color-coded by distractor processing time in milliseconds (see color gradient scale, right side). Dashed-black line indicates target position. Black cross indicates fixation

anchor. Each panel illustrates a subset of n = 100 randomly selected saccades. Saccade random selection was constrained such that saccades were uniformly distributed across distractor processing time. *A*: Saccades elicited to top, left targets. *B*: Saccades elicited to top, right targets. *C*: Saccades elicited to bottom, left targets. *D*: Saccades elicited to bottom, right targets.

We analyzed the behavioral effects of distractor processing time averaged across all conditions (see Figure 3.4). Positively valued saccade curvature indicates curvature towards the distractor, which is indicative of excitatory distractor processing, while negatively valued saccade curvature indicates curvature away from the distractor, which is indicative of inhibitory distractor processing. As such, saccade curvature indicated that there was an initial epoch of gradually decreasing excitatory processing (0-69 ms), followed by a transient excitatory epoch (133-168 ms), and then an extended epoch of inhibitory processing (247-500 ms) (see Figure 3.4*A*). Positively valued endpoint deviation indicates saccade endpoints biased towards the distractor, which is associated with sustained excitatory distractor processing. As such, endpoint deviation indicated that there was an extended excitatory epoch (108-243 ms) (see Figure 3.4*B*). The expectation model provided a good fit to saccade frequency ($p < .001$) and indicated that there was a transient drop in saccade frequency (130-230 ms) (see Figure 3.4*C*). There was an abrupt onset of erroneous saccades that gradually decreased over distractor processing time (154-349 ms) (see Figure 3.4*D*).

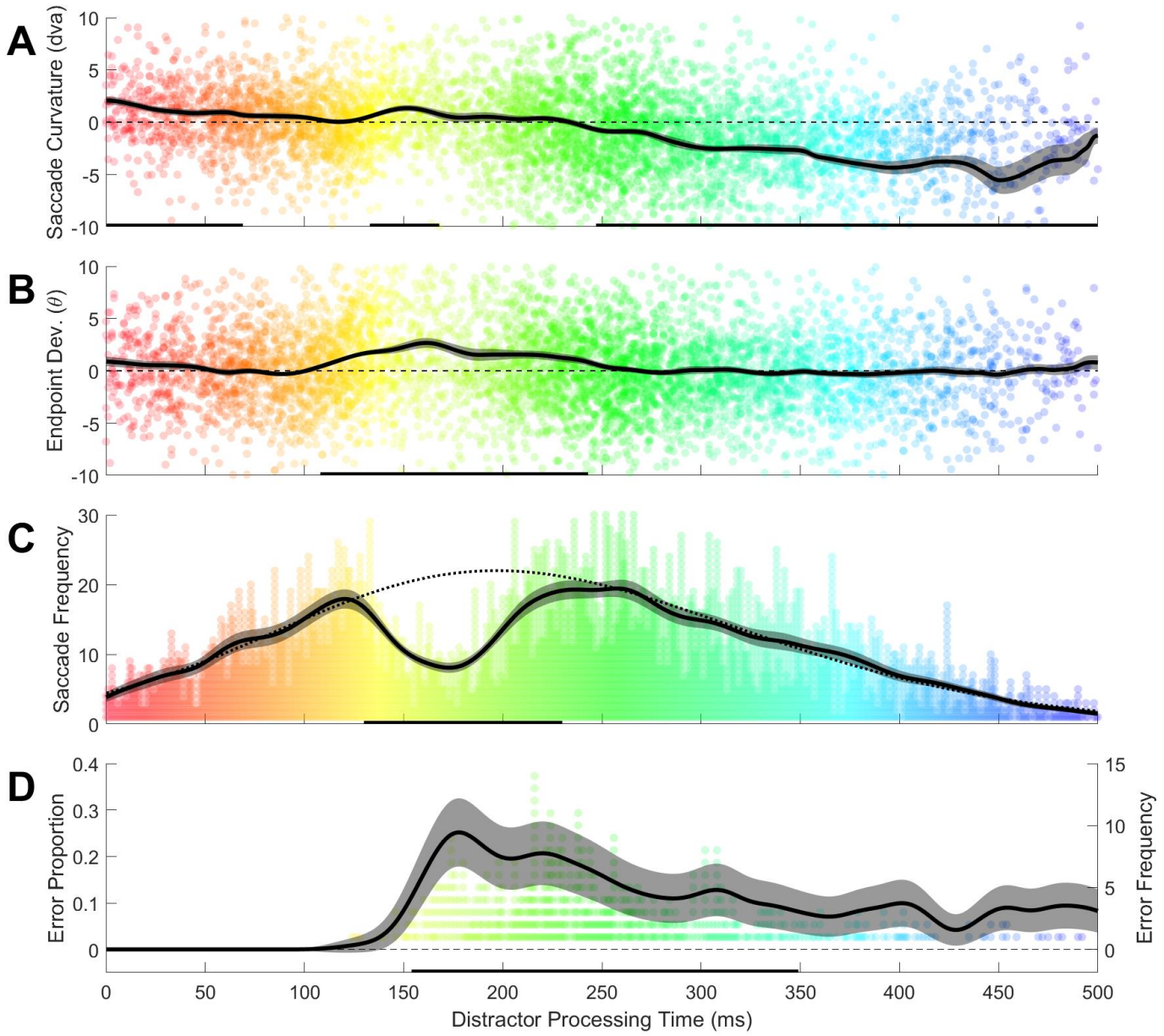

Figure 3.4. Smoothed overall saccade metrics as a function of distractor processing time. Shaded error bars represent standard error across subjects (N = 35). All statistical analyses were considered significant at $p < .05$. Data points indicate individual saccades. Distractor processing time color scale is identical to Figure 3.3. *A*,*B*: Black bars along the abscissa indicate significant differences from zero (two-tailed Wilcoxon signed-rank test). *A*: Mean saccade curvature. *B*: Mean endpoint deviation. *C*: Sum saccade frequency. Dashed line indicates fitted exponentially-modified Gaussian expectation model. Black bars along the abscissa indicate significant differences below expectation (one-tailed Wilcoxon signed-rank test). *D*: Proportion of errors. Black bars along the abscissa indicate significant differences above the standard error of the proportion (one-tailed Wilcoxon signed-rank test).

3.5.2. *Overall Distractor Processing Effects Across Subjects*

We examined whether 5 primary effects observed for the overall data were consistent across subjects: an excitatory effect of saccade curvature, an inhibitory effect of saccade curvature, an excitatory effect of endpoint deviation, an effect of saccade frequency, and an effect of error proportion (see Figure 3.5). All descriptive and inferential statistics for this analysis are presented in Table 3.1. 20 excitatory saccade curvature, 7 inhibitory saccade curvature, and 2 excitatory endpoint deviation anticipatory subject epochs (onset < 60 ms) were removed from this analysis. 26.9% of the distribution of saccade curvature excitatory subject-level epochs overlapped with the group-level epoch (see Figure 3.5*A*). The number of subjects with at least one overlapping epoch with the group-level epoch was 10, which was not statistically greater than chance ($\binom{35}{10}$, $p = .992$). 88.6% of the distribution of saccade curvature inhibitory subject-level epochs overlapped with the group-level epoch (see Figure 3.5*B*). All subjects had at least one overlapping epoch to the group-level epoch, which was statistically greater than chance ($\binom{35}{35}$, $p = 0$). 65.5% of the distribution of endpoint deviation excitatory subject-level epochs overlapped with the group-level epoch (see Figure 3.5*C*). The number of subjects with at least one overlapping epoch to the group-level epoch was 24, which was statistically greater than chance ($\binom{35}{24}$, $p = .008$). 86.0% of the distribution of saccade frequency subject-level epochs overlapped with the group-level epoch (see Figure 3.5*D*). The number of subjects with at least one overlapping epoch to the group-level epoch was 31, which was statistically greater than chance ($\binom{35}{31}$, $p < .001$). 95.4% of the distribution of error proportion subject-level epochs overlapped with the group-level epoch (see Figure 3.5*E*). The number of subjects with at least one overlapping epoch to the group-level epoch was 27, which was statistically greater than chance ($\binom{35}{27}$, $p < .001$). Given this analysis, all group level effects of the

overall data show considerable consistency across subjects, except for saccade curvature excitatory responses. However, this may be due to a much narrower group-level epoch for the saccade curvature excitatory effect relative to other effects in the overall data.

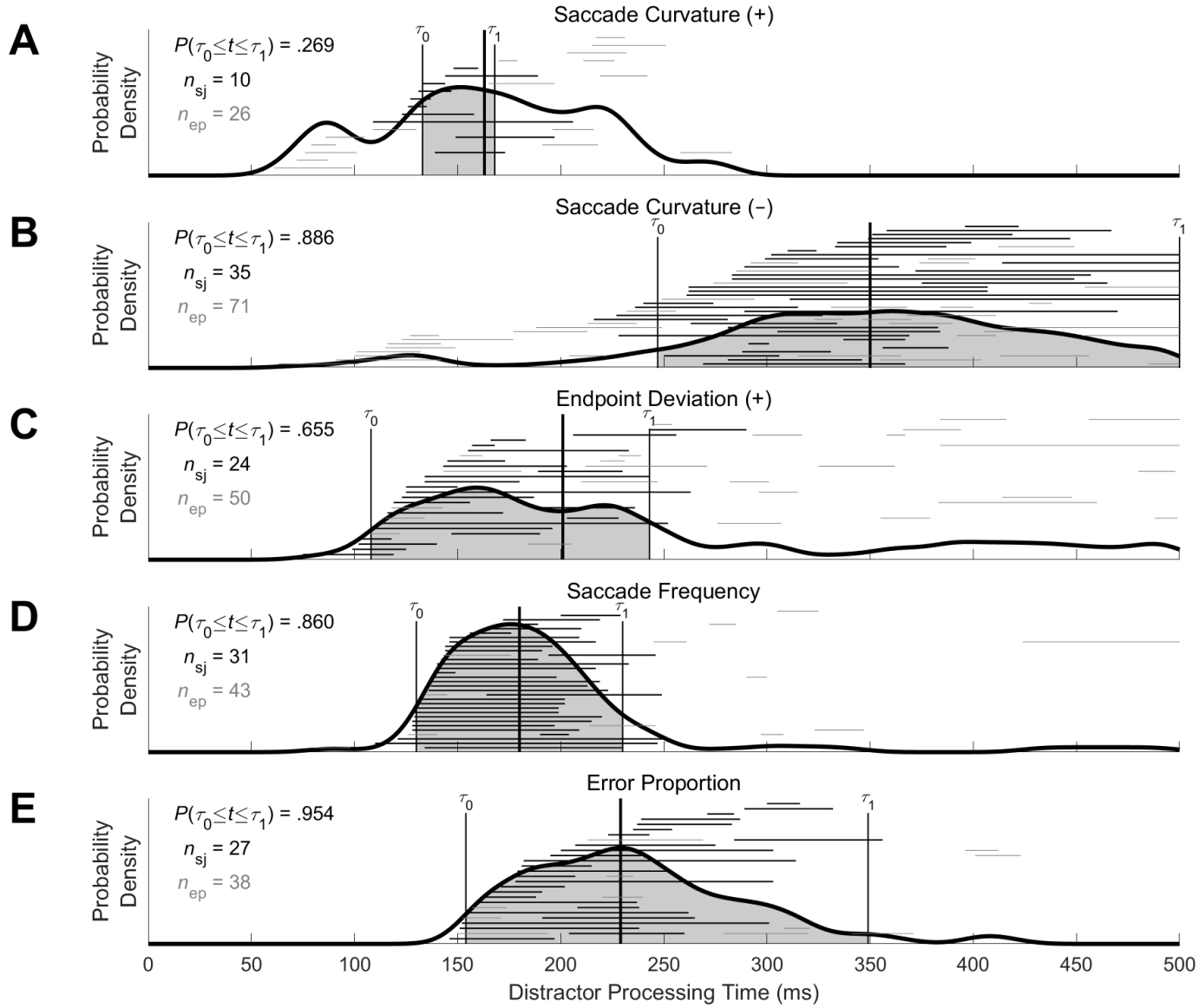

Figure 3.5. Empirical probability density functions of subject-level epochs for the overall data as a function of distractor processing time. Thick, vertical black line indicates the median of the empirical probability density function. τ_0 indicates the effect onset estimated at the group level. τ_1 indicates the effect offset estimated at the group level. The shaded region indicates the probability density of subject-level epochs within the group-level effect

interval, where the probability is indicated by $P(\tau_0 \leq t \leq \tau_1)$. Subject epochs are plotted as horizontal thin lines, where epochs of equal height are observed from the same subject. Subject epochs plotted in black indicate the epoch with maximum overlap of the group interval for a given subject. All remaining subject epochs are plotted in grey. n_{sj} indicates the number of subjects with at least one epoch that overlaps with the group-level epoch. n_{ep} indicates the total number of subject epochs. Epochs that onset < 60 ms after distractor onset were not analyzed. *A*: Saccade curvature excitatory subject epochs. *B*: Saccade curvature inhibitory subject epochs. *C*: Endpoint deviation excitatory subject epochs. *D*: Saccade frequency subject epochs. *E*: Error proportion subject epochs.

Table 3.1. Consistency between subject-level epochs and group-level epochs.

				Subject-Level Epoch Distribution							
		Group-Level Epoch				Probability				Consistent Subjects	
Metric	Effect	Onset (τ_0)	Offset (τ_1)	Median	*SD*	Below	Inside	Above	n_{ep}	n_{sj}	*p*
S Curvature	+	133	168	163	50.86	.263	.269	.468	26	10	0.992
S Curvature	−	247	500	350	88.16	.114	.886	.000	71	35	0.000
E Deviation	+	108	243	201	109.24	.026	.655	.319	50	24	0.008
S Frequency	n/a	130	230	180	62.61	.026	.860	.114	43	31	0.000
E Proportion	n/a	154	349	229	53.22	.010	.954	.036	38	27	0.000

S Curvature: saccade curvature. E Deviation: endpoint deviation. S Frequency: saccade frequency. E Proportion: error proportion. "+": excitatory, positively signed effect. "−": inhibitory, negatively-signed effect. SD: standard deviation. Below: probability of subject-level epochs less than group-level interval, $P(t < \tau_0)$. Inside: probability of subject-level epochs within group-level interval, $P(\tau_0 \leq t \leq \tau_1)$. Above: probability of subject-level epochs greater than group-level interval, $P(t > \tau_1)$. n_{ep}: number of subject-level epochs. n_{sj}: number of subjects with at least one subject-level epoch that overlaps with the group-level interval. *p*: one-tailed binomial exact test of $\binom{35}{n_{sj}}$.

3.5.3. *OS Condition Distractor Processing Differences*

We analyzed the behavioral effects of distractor processing time separately across OS conditions (see Figure 3.6). Positively valued saccade curvature indicates curvature towards the distractor, which is indicative of excitatory distractor processing, while negatively valued saccade curvature indicates curvature away from the distractor, which is indicative of inhibitory

distractor processing. We present but did not analyze distractor processing times <100 ms as the overall analysis demonstrated that any such effects are anticipatory.

For saccade curvature, there was a transient excitatory epoch observed across all OS conditions and the duration of this epoch varied across OS condition (OS1: 144-156 ms; OS3: 132-167 ms; OS5: 134-195 ms) (see Figure 3.6*A*). There was also a secondary transient excitatory epoch uniquely observed in the OS1 condition (220-231 ms). Finally, there was an extended inhibitory epoch that onset first in the OS3 (245-461 ms) and OS5 (247-478 ms) conditions, and later in the OS1 condition (303-482 ms). OS3 and OS5 saccade curvature was more negatively curved than OS1 curvature during the inhibitory delay in the OS1 condition (black line, 275-307 ms). There was a brief period of negative curvature in the OS3 condition preceding the extended inhibitory epoch (OS3: 215-229 ms), which we think reflects the true inhibitory onset in the OS3 condition given both the trend of the data and the observation that the sliding inferential analysis was marginally significant ($.051 \leq p \leq .109$) throughout the interval separating the brief and extended inhibitory epochs (OS3: 216-244 ms).

Positively valued endpoint deviation indicates saccade endpoints biased towards the distractor, which is associated with sustained excitatory distractor processing. Endpoint deviation indicated an excitatory epoch which onset first in the OS5 condition (104-172 ms) and shortly thereafter in the OS1 (116-246 ms) and OS3 conditions (116-218 ms) (see Figure 3.6*B*). Critically, during the excitatory epoch, endpoint deviation was different between OS conditions (black line, 141-160 ms). OS1 endpoint deviation was higher than in OS3 and OS5 conditions concurrent with the secondary excitatory epoch observed for saccade curvature in the OS1 condition (black line, 214-235 ms). Endpoint deviations were otherwise non-significant but for an additional excitatory epoch in the OS1 condition in which OS1 endpoint deviation was greater

than OS3 and OS5 endpoint deviation (black line, 301-323 ms). Interestingly, this epoch somewhat corresponded to the inhibitory delay period between the OS1 condition vs. OS3 and OS5 conditions observed with saccade curvature.

The expectation model provided a good fit to saccade frequency across OS conditions (all $p < .001$) (see Figure 3.6*C*). There was a transient drop in the likelihood of making a saccade across OS conditions (OS1: 136-210 ms; OS3: 137-215 ms; OS5: 125-229 ms). Interestingly, there was a lower frequency of saccades in the OS1 condition than both the OS3 and OS5 conditions (black line, 220-305 ms), coinciding with the secondary excitatory epoch observed uniquely in the OS1 condition and also coinciding with the inhibitory delay observed in the OS1 condition relative to the OS3 and OS5 conditions.

There was a transient increase in error rates with consistent onset latencies across OS conditions but that was sustained in just the OS1 condition (OS1: 157-410; OS3: 167-249 ms; OS5: 157-249 ms) (see Figure 3.6*D*). Errors were consistently higher in the OS1 condition than the OS3 and OS5 conditions (black line, 208-461 ms).

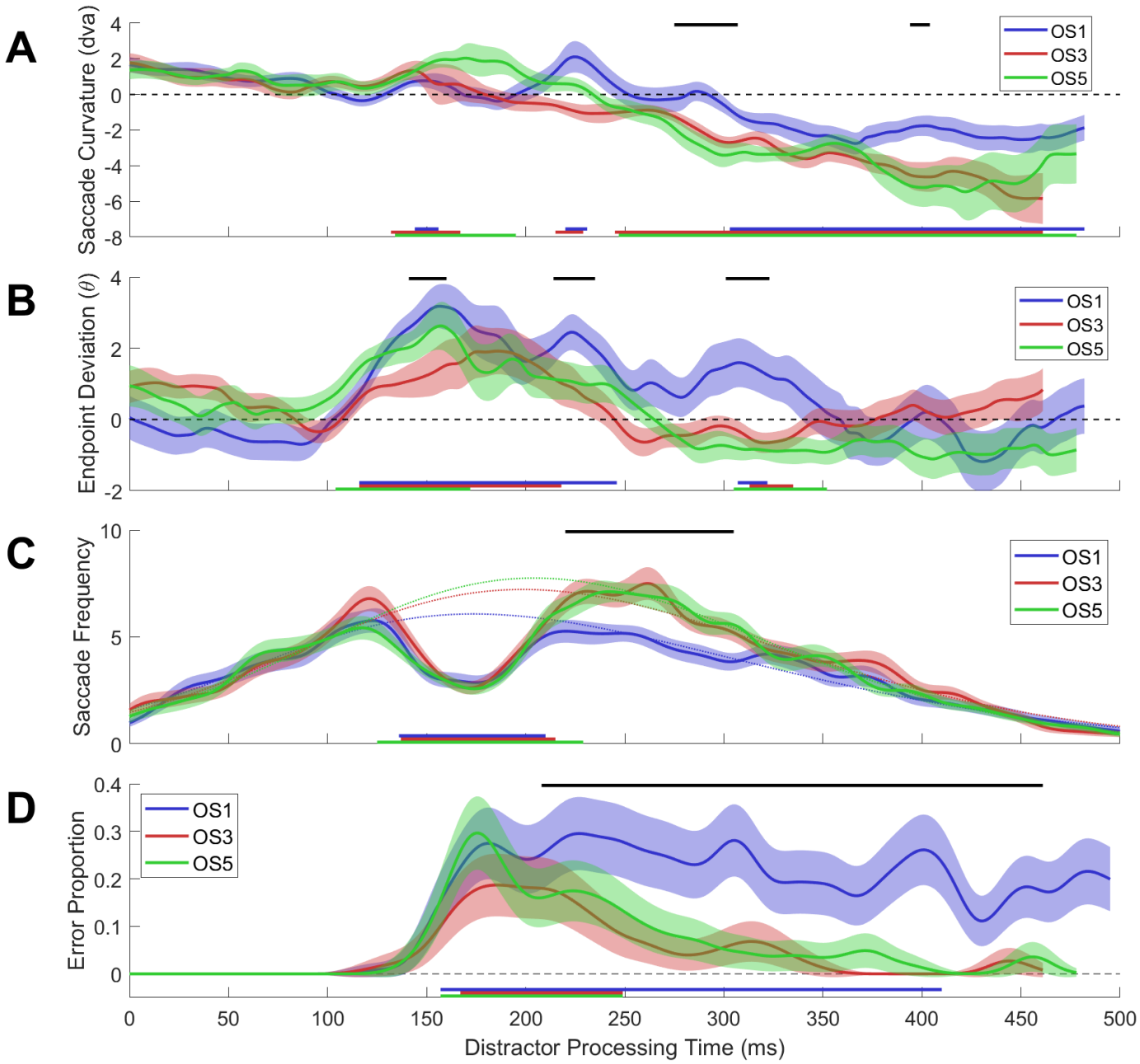

Figure 3.6. Smoothed saccade metrics as a function of distractor processing time in the OS1 (blue), OS3 (red), and OS5 (green) conditions. Shaded error bars represent standard error across subjects (N = 35). Black bars above panels indicate significant differences between conditions (Friedman test). All statistical analyses were considered significant at $p < .05$. *A*, *B*: Colored bars along the abscissa indicate significant differences from zero (two-tailed Wilcoxon signed-rank test). *A*: Mean saccade curvature. *B*: Mean endpoint deviation. *C*: Sum saccade frequency. Dashed lines indicate fitted exponentially-modified Gaussian expectation models. Colored bars along the abscissa indicate significant differences below expectation (one-tailed Wilcoxon signed-rank test). *D*: Proportion of errors.

Colored bars along the abscissa indicate significant differences above the standard error of the proportion (one-tailed Wilcoxon signed-rank test).

3.5.4. *Experimental Block Distractor Processing Differences*

We examined the effects of distractor processing time separately over the early (E), middle (M), and late (L) experimental blocks of the experiment. As in the previous analysis, we present but did not analyze distractor processing times <100 ms as the overall analysis demonstrated that any such effects are anticipatory.

This analysis demonstrated five notable effects (see Figure 3.7): (a) The saccade curvature excitatory response was longest in the early blocks (E: 124-168 ms), reduced in the middle blocks (M: 142-163 ms), and was completely extinguished in the late blocks (see Figure 3.7*A*). (b) The latency of the saccade curvature inhibitory response decreased over the course of the experiment (E: 276 ms; M: 251 ms; L: 240 ms). (c) Endpoint deviation in the initial excitatory epoch was considerably higher in the early blocks than later in the experiment (black line, 164-189 ms) (see Figure 3.7*B*). (d) The latency of the transient drop in saccade likelihood was consistent across experimental blocks (E: 128 ms; M: 130 ms; L: 133 ms; all expectation models $p < .001$) (see Figure 3.7*C*). (e) Errors during the initial excitatory epoch had a shorter latency in the early blocks (E: 153 ms) than in the middle and late blocks (M: 169 ms; L: 169 ms) (see Figure 3.7*D*).

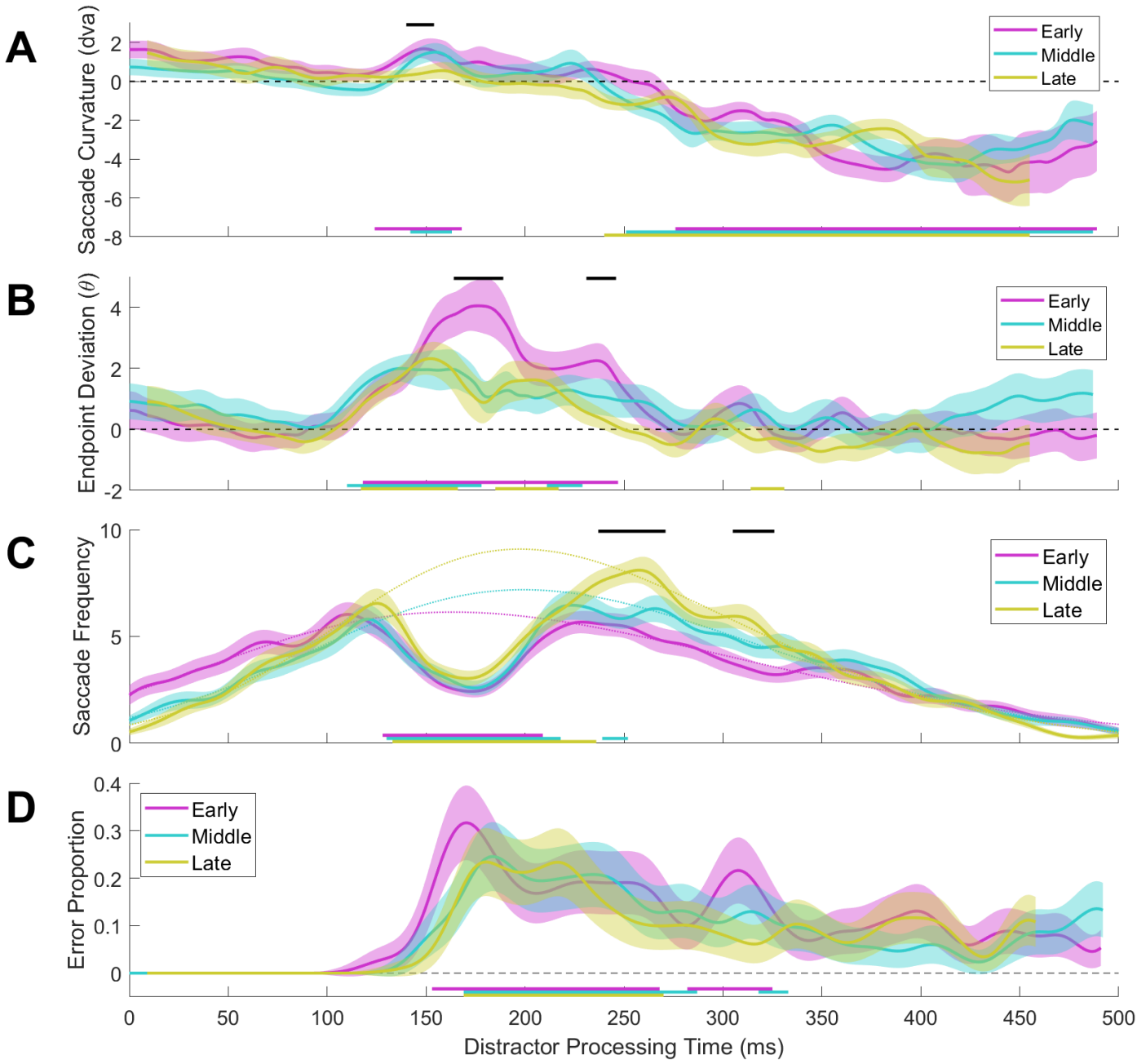

Figure 3.7. Smoothed saccade metrics as a function of distractor processing time in the early (magenta), middle (cyan), and late (yellow) experimental blocks. Shaded error bars represent standard error across subjects (N = 35). Black bars above panels indicate significant differences between conditions (Friedman test). All statistical analyses were considered significant at $p < .05$. *A*, *B*: Colored bars along the abscissa indicate significant differences from zero (two-tailed Wilcoxon signed-rank test). *A*: Mean saccade curvature. *B*: Mean endpoint deviation. *C*: Sum saccade frequency. Dashed lines indicate fitted exponentially-modified Gaussian expectation models. Colored bars along the abscissa indicate significant differences below expectation (one-tailed Wilcoxon signed-rank test). *D*:

Proportion of errors. Colored bars along the abscissa indicate significant differences above the standard error of the proportion (one-tailed Wilcoxon signed-rank test).

3.5.5. *SRT Processing Differences*

3.5.5.1. Mean differences. There were no SRT main effects or interactions between conditions (all $F \leq 1.50$, all $p \geq .127$) (see Figure 3.8). There was a significant effect of DTOA on error proportions ($F[3,1218] = 37.37$, $p < .001$). All pairwise differences were significant (all $F \geq 4.76$, all $p \leq .029$), except for DTOA150 and DTOA100 ($F[1,1218] = 2.59$, $p = .108$). There was a significant effect of OS on error proportions ($F[2,1218] = 51.28$, $p < .001$). All pairwise differences were significant (all $F \geq 55.73$, all $p < .001$), except for OS3 and OS5 ($F[1,1218] = 3.40$, $p = .065$). There were no other error proportion main effects or interactions between conditions.

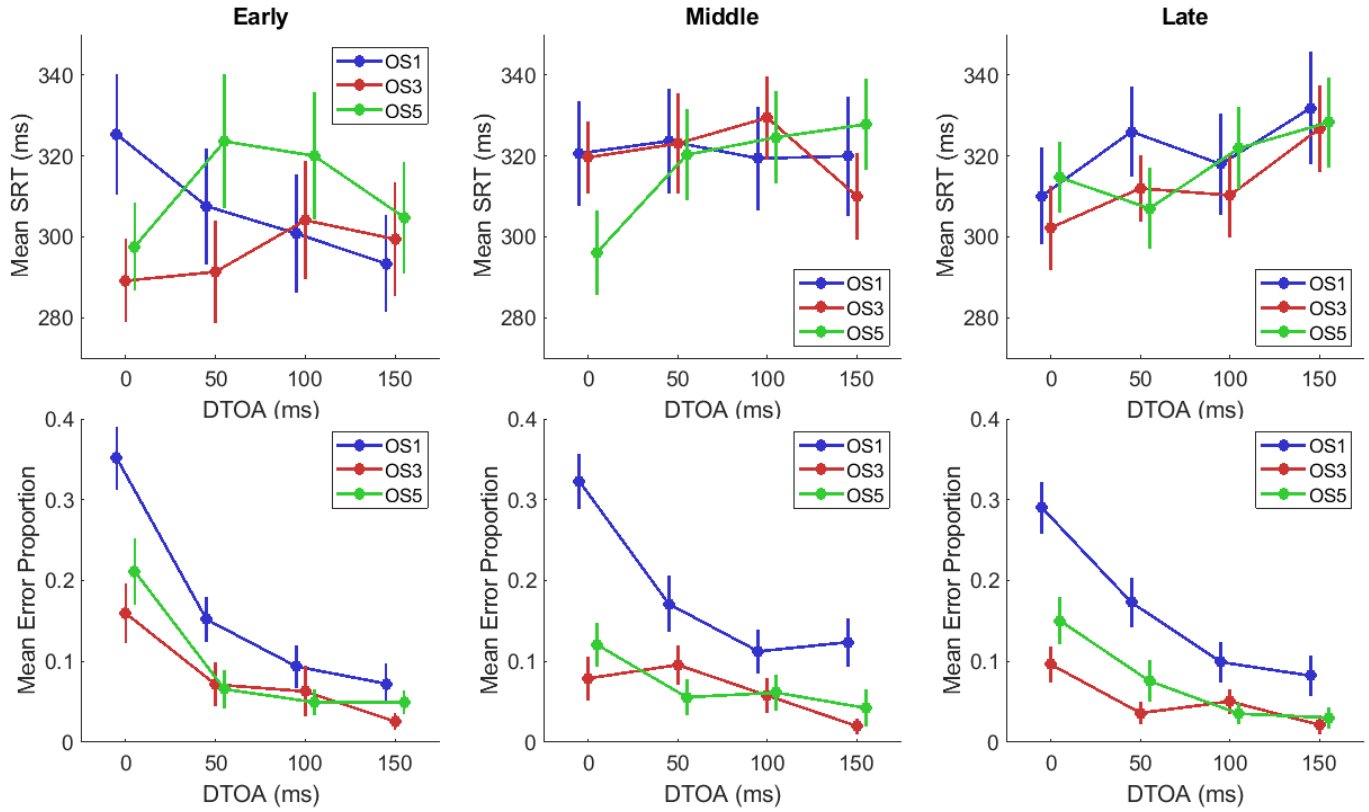

Figure 3.8. Mean SRT (top row) and error proportion (bottom row) differences between DTOA, OS, and experimental block conditions. DTOA is plotted along abscissa. OS conditions are color-coded (OS1 = blue, OS3 = red, OS5 = green). Experimental block conditions are plotted by column (early = left, middle = middle, late = right). Error bars represent standard error across subjects (N = 35).

3.5.5.2. Distractor processing time differences between DTOA conditions. We analyzed the behavioral effects of distractor processing time separately across DTOA conditions and compared them to the group level effects observed for the overall data (see Figure 3.9). The effects of distractor processing time on saccade curvature were consistent across DTOA conditions (see Figure 3.9*A*). Across DTOA conditions, there were consistent positive curvatures after ~140 ms of distractor processing (DTOA0: 139-229 ms; DTOA50: 145-181 ms; DTOA100: 138-159 ms), except in the DTOA150 condition in which the excitatory response failed to meet the 10 ms criterion but was significantly greater than zero for 9 ms (140-148 ms). Additionally, by subjectively examining the trends of the means, the excitatory epoch in the DTOA50 condition does appear to have a slightly longer latency than the remaining conditions falling just outside of the excitatory epoch measured for the overall data (see Figure 3.9*A*). During the excitatory epoch, there were differences between DTOA conditions (black line, 139-220 ms), likely driven by higher saccade curvature in the DTOA0 condition than the remaining conditions. These results indicate that the magnitude of excitatory responses was modulated by DTOA condition, but critically, the latency was highly consistent across DTOA conditions. The onset of inhibition did vary somewhat across DTOA conditions as a function of distractor processing time (DTOA0: 257 ms; DTOA50: 265 ms; DTOA100: 233 ms; DTOA150: 277 ms) but was otherwise indistinguishable between conditions.

Endpoint deviation excitatory epochs were related to distractor processing time and consistent with the overall group estimates (DTOA50: 108 ms; DTOA100: 117 ms; DTOA150: 112 ms) (see Figure 3.9*B*). However, there were insufficient observations in the DTOA0 condition to determine if the excitatory epoch latency was equal to ~110 ms of distractor processing. As with saccade curvature, there were differences between DTOA conditions during the excitatory epoch (black line, 139-168 ms), suggesting that the magnitude of excitatory responses was modulated my DTOA condition, but critically, not the latency.

Saccade frequency distributions were offset by ~50 ms between DTOA conditions (see Figure 3.9*C*). This was expected since splitting the data by distractor onset shifts target onsets by ~50 ms between DTOA conditions (see Figure 3.2*D*). However, across DTOA conditions, there was a drop in saccadic likelihood with latencies clearly related to distractor processing time (DOTA50: 123 ms; DTOA100: 123 ms; DTOA150: 140 ms), except for DTOA0 in which there were too few observations in this range (all expectation models $p < .001$). As expected, the expectation model failed to reproduce the DTOA0 saccade frequency distribution in the 125-250 ms range, as it was fit outside of this range.

Errors onset much earlier in the DTOA0 condition (DTOA0: 132 ms) than in the remaining DTOA conditions (DTOA50: 209 ms; DTOA100: 196 ms; DTOA150: 227 ms) and were initially much higher in the DTOA0 condition than the remaining DTOA conditions (black line, 132-236 ms) (see Figure 3.9*D*). This difference is likely driving the main effect of error proportion on DTOA (see *Mean Differences*). By ~250 ms of distractor processing, error rates were indistinguishable between DTOA conditions.

Taken together, these results show that distractor effect epochs were temporally locked to distractor processing time consistently across DTOA conditions and were also consistent with estimates from the overall data.

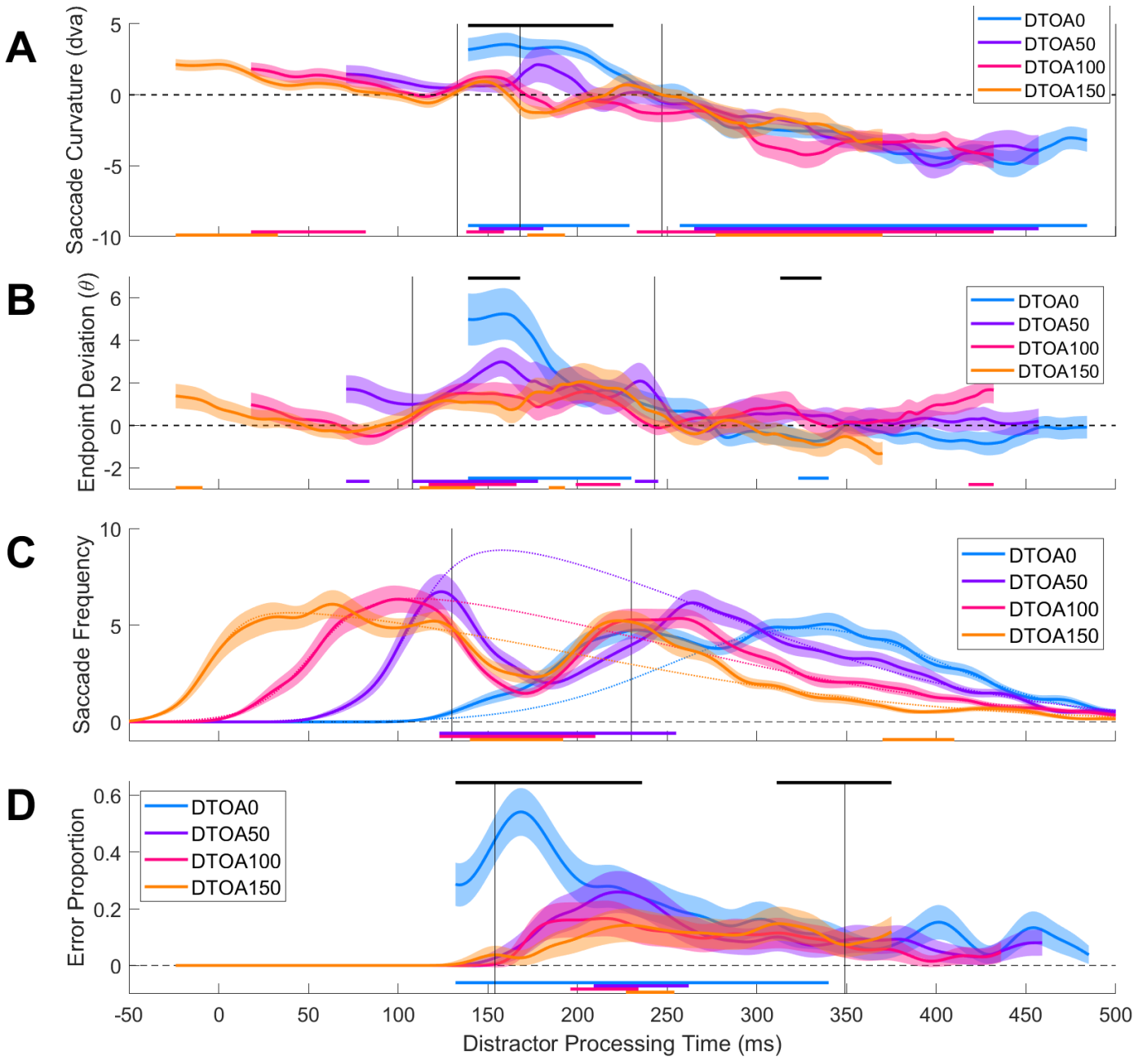

Figure 3.9. Smoothed saccade metrics as a function of distractor processing time in the DTOA0 (teal), DTOA50 (purple), DTOA100 (pink), and DTOA150 (orange) conditions. Shaded error bars represent standard error across subjects (N = 35). Black bars above panels indicate significant differences between conditions (Friedman test). All

statistical analyses were considered significant at $p < .05$. Thin, vertical, black lines indicate the group-level epochs observed for the overall data. *A*, *B*: Colored bars along the abscissa indicate significant differences from zero (two-tailed Wilcoxon signed-rank test). *A*: Mean saccade curvature. *B*: Mean endpoint deviation. *C*: Sum saccade frequency. Dashed lines indicate fitted exponentially-modified Gaussian expectation models. Colored bars along the abscissa indicate significant differences below expectation (one-tailed Wilcoxon signed-rank test). *D*: Proportion of errors. Colored bars along the abscissa indicate significant differences above the standard error of the proportion (one-tailed Wilcoxon signed-rank test).

3.5.5.3. SRT differences between DTOA conditions. Next we analyzed saccade metrics as a function of SRT separately across DTOA conditions (see Figure 3.10). This analysis allowed us to disentangle the effects of SRT and distractor onset on the saccade metrics. Significant epochs with overlapping SRT intervals across DTOA conditions are SRT-related. Significant epochs temporally contingent to the corresponding distractor onset (see colored squares in Figure 3.10) are related to distractor processing time. As we saw effects staggered across DTOA conditions, offset by approximately 50 ms between conditions and in the appropriate order, we concluded that the previously discussed overall effects (see section *Overall Distractor Processing Effects*) were primarily related to distractor processing time.

For saccade curvature, there were effects related to both SRT and distractor onset time (see Figure 3.10*A*). There was consistent positive curvature across DTOA conditions at the earliest SRTs (DTOA0: 139-229 ms; DTOA100: 128-165 ms; DTOA150: 134-189 ms). This SRT-related positive curvature was not significant in the DTOA50 condition, but still qualitatively exhibited the same trend. In the DTOA150 condition, this activity preceded the distractor onset and was therefore definitively anticipatory. In the DTOA100 condition, this activity onset ~30 ms after distractor onset and was therefore also likely anticipatory. Saccades were more positively curved in the DTOA0 condition than the remaining DTOA conditions

during this early SRT epoch (black line, 139-226 ms), perhaps suggesting an additive influence of anticipation and distractor visual processing. However, despite these clear SRT-related effects, there were also distractor-related effects, as excitatory epochs in the DTOA50 and DTOA100 conditions were scaled by differences in distractor onset latency (DTOA50: 202-241 ms; DTOA100: 245-258 ms). It was less clear whether negatively signed saccade curvature was related to SRT or distractor processing time. The onset of negatively signed curvature effects did vary across DTOA conditions (DTOA0: 257 ms; DTOA50: 329 ms; DTOA100: 336 ms; DTOA150: 429 ms) suggesting distractor-related effects. As a consequence, the magnitude of inhibitory processing was greater in the DTOA0 condition relative to the other conditions during the inhibitory epoch (black line, 287-443 ms). However, although inhibition latencies monotonically increased across DTOA conditions, these differences were not linearly scaled with distractor onset as expected by distractor-related effects.

The DTOA100 and DTOA150 conditions also indicated SRT-related anticipatory activity for endpoint deviation (DTOA100: 128-140 ms; DTOA150: 134-148 ms) (see Figure 3.10*B*). However, like saccade curvature, there were excitatory epochs in the DTOA50, DTOA100, and DTOA150 conditions linearly scaled by differences in distractor onset latency (DTOA50: 161-232 ms; DTOA100: 229-276 ms; DTOA150: 277-304 ms).

Saccade frequency clearly indicated excitatory epochs linearly scaled by distractor onset latency (DTOA50: 183-315 ms; DTOA100: 236-317 ms; DTOA150: 299-348 ms; all expectation model *p*s < .001) and no SRT-related activity (see Figure 3.10*C*). Aligning saccade frequency to SRT illustrates that there are no clear boundary differences in the overall SRT distributions between DTOA conditions, consistent with the null main effect of DTOA condition on mean SRT (see *Mean Differences*).

Error proportion also clearly indicated distractor effect epochs with onsets linearly scaled by distractor onset latency (DTOA0: 132 ms; DTOA50: 213 ms; DTOA100: 261 ms) (see Figure 3.10*D*). The number of errors also appears to be linearly related to DTOA condition, consistent with the main effect of DTOA on error proportion discussed earlier (see *Mean Differences*).

Taken together, these results show that although contributed SRT excitatory anticipatory activity and non-linearities in inhibitory processing, excitatory epochs were clearly related to distractor onset latencies.

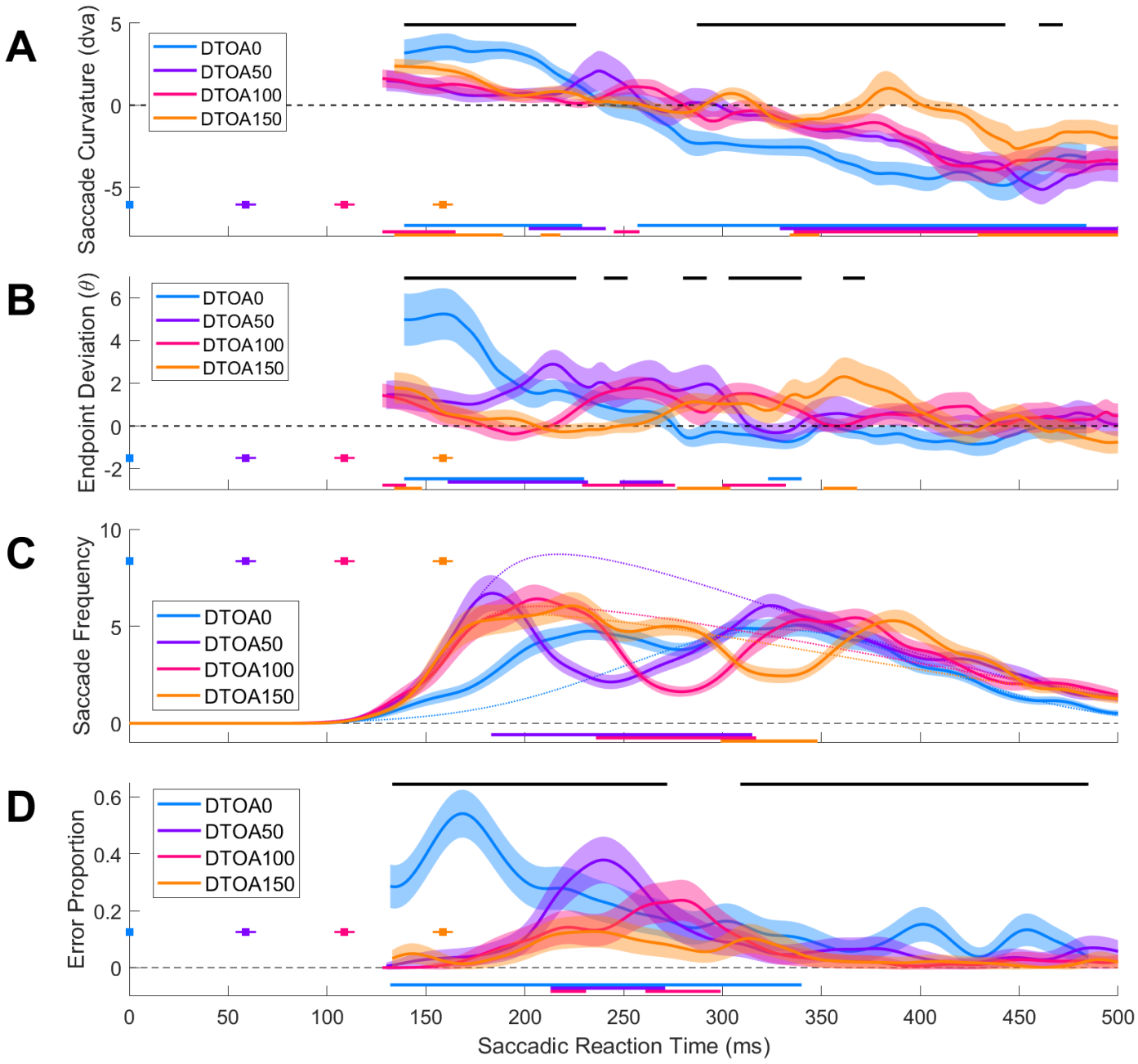

Figure 3.10. Smoothed saccade metrics as a function of saccadic reaction time in the DTOA0 (teal), DTOA50 (purple), DTOA100 (pink), and DTOA150 (orange) conditions. Shaded error bars represent standard error across subjects (N = 35). Black bars above panels indicate significant differences between conditions (Friedman test). All statistical analyses were considered significant at $p < .05$. Colored squares indicate mean distractor onset latency and accompanying error bars indicate distractor onset latency standard deviation. The distractor latencies indicate the degree to which temporal epochs are contingent to distractor onset time in each respective DTOA condition. Temporal effects occurring at consistent SRTs across DTOA conditions are thus unrelated to distractor processing

time. *A*, *B*: Colored bars along the abscissa indicate significant differences from zero (two-tailed Wilcoxon signed-rank test). *A*: Mean saccade curvature. *B*: Mean endpoint deviation. *C*: Sum saccade frequency. Dashed lines indicate fitted exponentially-modified Gaussian expectation models. Colored bars along the abscissa indicate significant differences below expectation (one-tailed Wilcoxon signed-rank test). *D*: Proportion of errors. Colored bars along the abscissa indicate significant differences above the standard error of the proportion (one-tailed Wilcoxon signed-rank test).

3.6. Discussion

We non-invasively measured human saccade curvatures, endpoint deviations, saccade frequencies, and error proportions—indices of oculomotor excitation (Glimcher & Sparks, 1993; McPeek, 2006; McPeek et al., 2003; Munoz & Istvan, 1998; Port & Wurtz, 2003; Reingold & Stampe, 2002; Robinson, 1972; Robinson & Fuchs, 1969; White et al., 2012) and inhibition (Aizawa & Wurtz, 1998; Lee et al., 1988; McPeek & Keller, 2004; Munoz & Istvan, 1998; White et al., 2012)—as a function of time after the abrupt onset of a task-relevant, visually complex distractor. Critically, we ensured distractor feature processing and manipulated the visual similarity between targets and distractors. Based on previous physiological experiments, we hypothesized that distractor onsets would elicit an excitatory, feature-invariant oculomotor vector representation, followed by an inhibitory response encoding target-distractor similarity.

On average, the saccade vector modulation latency was ~135 ms for saccade curvature and ~110 ms for endpoint deviation. This 25 ms difference is consistent with saccade curvature as indicative of competing activity ~20-30 ms prior to saccade execution and endpoint deviation as indicative of competing activity at the time of saccade execution, demonstrating high reliability between these metrics and suggesting that the latency of visually evoked oculomotor excitatory processing was ~110 ms. Visual onset responses measured invasively in oculomotor substrates are typically much faster (reviewed by Boehnke & Munoz, 2008), but can increase as

stimulus features require processing in higher areas of the ventral visual processing hierarchy (e.g., perceptual color space; White et al., 2009) or for extremely low luminance stimuli (e.g., ≤.05 cd/m^2; Bell et al., 2006; Marino et al., 2015). As our stimuli were very high luminance (~125 cd/m^2) and sufficiently complex to require processing in late stages of the ventral visual processing stream, the unusually long visual onset response latency of 110 ms we observed must reflect a delay in cortical feedforward projections into oculomotor substrates to accommodate sufficient visual processing necessary for feature discrimination. As such, our results suggest that, in the context of complex object discrimination, the contribution of the oculomotor substrates to feature-based target selection is limited to selecting the preprocessed object representation with the highest activation as opposed to discriminating the target from distractor(s) on the basis of a local featural analysis. Strong corroboration of this account is the observation that error rates were not different from zero in the first ~150 ms after distractor onset and errors never occurred prior to 125 ms after distractor onset, suggesting that saccadic target selection was guided exclusively by the target representation during this epoch. A 40 ms delay between oculomotor vector representations modulating saccade trajectories versus modulating saccade target choices suggests a buildup of the representational strength of the distractor until it was suprathreshold for eliciting saccades to the distractor, consistent with collicular visual onset bursts eliciting express saccades after sufficient buildup (Marino et al., 2015). We also observed a transient drop in the likelihood of making a saccade ~130 ms after distractor onset. A similar transient drop in saccade frequency occurs ~50-60 ms after a luminance flash on a saccade-to-target task (Reingold & Stampe, 2002). Although analytic differences between experiments prohibit making exact temporal comparisons, the considerably large difference in saccadic inhibition latencies (~75 ms) suggests that this difference is not merely an artefact of our analytic

choices. We therefore interpret this difference as consistent with our account that the delayed oculomotor vector representation onset latency we observed relative to other experiments utilizing simpler visual features and task-demands, reflects the additional time required for sufficient visual processing of stimuli to satisfy the current task demands.

We observed that the initial oculomotor vector representation, conventionally conceptualized as being strictly bottom-up and feature invariant upon invasive examination (Boehnke & Munoz, 2008), was modulated by the behavioral relevance of the distractor: first, saccade endpoints were more biased towards the high similarity distractor than the intermediate similarity distractor 20 ms after the manifestation of the saccade vector representation (130 ms). Second, we observed that the excitatory epoch characterizing the oculomotor vector representation extended longer in time for the high similarity distractor than all other distractors as indicated across all metrics. Uniquely for the high similarity distractor, we observed two sequential excitatory epochs separated by ~80 ms, consistent with the physiological observation of a secondary visual onset burst in SCi VM cells (McPeek & Keller, 2002). Critically, the secondary excitatory epoch occurred prior to the inhibitory processing for the low and intermediate similarity distractors, which suggests that the protracted excitatory epoch encoding high similarity distractors does not merely reflect a delayed onset of inhibition. Since distractor identity could be decoded from the magnitude and duration of excitatory processing related to the distractor onset, this suggests that the oculomotor system dynamically receives preprocessed object representations from relevant visual modules and encodes these objects as dynamically reweighted oculomotor vectors, as we have argued previously (Kehoe & Fallah, 2017; Kehoe et al., 2018a, 2018b).

Saccade curvature indicated that the magnitude of inhibition increased as distractors became increasingly dissimilar to the target, which we have observed previously using the same stimulus set (Kehoe et al., 2018a). This is the opposite pattern of results observed in previous behavioral studies of saccade curvature using opponent color singletons (Ludwig & Gilchrist, 2003; Mulckhuyse et al., 2009). This different pattern of results is likely related to methodological differences: as we utilized a perceptual discrimination here and previously (Kehoe et al., 2018a), other behavioral studies of the effects of visual similarity on saccade curvature utilized spatially guided saccades with task-irrelevant distractors (Ludwig and Gilchrist, 2003; Mulckhuyse et al., 2009). Perhaps on discrimination tasks, saccadic inhibition guides the target selection process itself and is therefore proportional to *perceptual confidence* (see Gold & Shadlen, 2000); while on spatially guided saccade tasks, saccadic inhibition guides saccadic accuracy to spatially preselected targets and is proportional to perceptual interference.

Erroneous saccades to the high similarity distractor persisted across time, while erroneous saccades to the intermediate and low similarity distractors gradually decreased to zero, suggesting that high similarity distractor representations were never successfully pruned from the decision process. As measured by saccade curvature, the onset of inhibition occurred first for the intermediate similarity distractor (215 ms), then the low similarity distractor (247 ms), and finally for the high similarity distractor (303 ms). Taken together, these observations are consistent with attentional facilitation of high similarity distractors within the featural focus of the attended target and intermediate distractors in the inhibitory annulus around the featural focus of the attended target, as would be predicted by the selective tuning model of attention (Tsotsos et al., 1995; Tsotsos, 2011) and a multidimensional (i.e., multi-featural) object-space (Kehoe et al., 2018a).

Splitting the data between the early, middle, and late blocks of the experiment revealed that the initial excitatory epoch, as measured by saccade curvature, was not temporally stable and immutable, but rather that it was reduced in the middle experimental blocks and was eventually extinguished in the late experimental blocks. In the middle blocks, there was an inhibitory response that immediately preceded the excitatory response. This observation suggests a strong influence of perceptual learning and executive function on saccade target selection processing, as executive processing adapted to the consistent latencies of excitatory projections into the oculomotor system and anticipatorily minimized distractor bias on target selection. Perhaps this anticipatory response was eventually well calibrated enough that the excitatory and anticipatory responses nullified one-another thus there was eventually no longer any evidence of either. There was no evidence of oculomotor vector representation attenuation with the remaining saccade metrics. In fact, endpoint deviation, saccade frequency, and error proportion oculomotor vector representation had approximately the same temporal properties as with the overall data across experimental blocks. We discuss this discrepancy in more detail below.

3.6.1. *Computational Modeling of Oculomotor Excitation and Inhibition*

The current experiment demonstrates the versatility of this paradigm for non-invasively estimating the latency of oculomotor excitation and inhibition. There are several main differences between the current experiment and the original implementation in Kehoe & Fallah (2017). First, using far more complicated, task-relevant stimuli increased the latency of the oculomotor vector representation by ~40 ms compared to task-irrelevant luminance- and color-modulated Gabor patches in the original paradigm. This discrepancy is consistent with the discrepancy between visual onset burst latencies in early visual modules and anterior ventral visual processing modules observed in macaques (e.g., V1 vs. V4 or inferotemporal cortex [IT];

Nowak & Bullier, 1997; Schmolesky, 1998). Similarly, we observed that inhibitory processing onset far later and accumulated far slower compared to inhibitory processing of task-irrelevant Gabors. Second, we have utilized three additional behavioral metrics that are independent of saccade curvature, but that are all theoretically indicative of the same underlying oculomotor processes. These metrics provided consistent temporal estimates and have thus strengthened the validity of saccade curvature modeling to infer oculomotor excitation latencies. Third, to ensure that stimulus onset order did not provide useful target information, distractors onset prior to the target on half of the trials. However, SRTs were not different between DTOA conditions and there were strong effects of DTOA on target selection accuracy, suggesting that subjects prioritized speed over accuracy and were seemingly committed to their target choice. Furthermore, we analyzed directly whether visual onset responses were related to SRT or distractor processing time. Despite the fact that SRT modulated the oculomotor vector representation magnitude, we observed reliable oculomotor vector representations with consistent latencies across DTOA conditions demonstrating that oculomotor vector representation latencies are related to distractor processing time independently of SRT. As such, the current analyses can be interpreted as in the original paradigm: the competitive influence of a distractor over time while a saccade is concurrently being planned independently to a target.

All four saccade metrics were indicative of excitatory oculomotor processing. However, three, presumably top-down, executively mediated inhibitory effects were only observed for saccade curvature: first, after the emergence of excitatory oculomotor processing, saccades increasingly began to deviate away from the distractor. The magnitude of this inhibitory response was modulated by SRT (i.e., it was maximum for synchronous target-distractor onsets and was reduced as target lead time increased). Second, at the shortest possible SRTs (100-150 ms),

saccade curvatures were consistently curved towards the distractor. Third, excitatory processing eliciting saccade curvature was gradually extinguished over the time course of the experimental session.

The distinguishing feature of saccade curvature, transience, provides some insight into unique saccade curvature effects. Oculomotor selection circuits are not strictly winner-take-all, as co-active saccade vectors elicit vector-weighted average movements (Robinson & Fuchs, 1969; Robinson, 1972). If co-activation is resolved before saccade initiation, then only an initial portion of the resultant saccade is vector-averaged but the saccade otherwise remains accurate, and the saccade trajectory is therefore curved (McPeek et al., 2003; McPeek, 2006; Port & Wurtz, 2003). Conversely, if co-activation persists to the time of saccade initiation, the entire saccade is vector-averaged (Glimcher & Sparks, 1993). As such, the emergence of unique saccade curvature effects suggests the emergence of transient modulation of the distractor and/or target vector representations immediately preceding saccade execution, while attenuation of saccade curvature effects not apparent with other saccade metrics suggests the cessation of such transient modulation. Critically, the fact that this modulation is constrained to the narrow interval immediately preceding the saccade (White et al., 2012) highlights the top-down nature of such effects, as this temporally coincides with the saccadic go-signal, itself presumably related to the perceptual decision threshold (Ding & Gold, 2010). The shift from saccade curvature directed towards distractors and subsequently away from distractors observed as a function of SRT (Mulckhuyse et al., 2009; White et al., 2012) or distractor processing time (Kehoe & Fallah, 2017) and the attenuation of saccade curvature effects over time must then reflect a systematic shift in *how* saccades are triggered by the voluntary saccadic control system over the time course of individual trials and experimental sessions. For example, saccades may be triggered by direct

excitatory input from dorsal-attentional cortices or indirectly from executive cortices via basal ganglian disinhibition (Hikosaka et al., 2000). Similarly, SNr contains both inhibitory and disinhibitory burst cells imposing concurrent suppressive and facilitatory effects on SCi (Shin & Sommer, 2010). The exact physiological mechanism for top-down effects apparent with saccade curvature can only be speculated given the emerging understanding of the voluntary saccade control system (see Basso & Sommer, 2012). However, it follows from the spatiotemporal interactions that elicit saccade curvature that systematic differences between interactive saccade trigger mechanisms must elicit unique saccade curvature effects. As such, these effects may be instantiated in a narrow window of time physiologically (McPeek, 2006; McPeek et al., 2003; Port & Wurtz, 2003; White et al., 2012), but apparent across an extended window of time behaviorally.

3.6.2. *Putative Neural Mechanism*

Several observations demonstrate that SCi and FEF are necessary for feature-based target selection, which guides both action and perception. The visual features characterizing potential oculomotor targets modulate VM neural activity in SCi (Horwitz & Newsome, 2001; McPeek & Keller, 2002; Shen & Paré, 2012) and FEF (Bichot & Schall, 1999; Thompson et al., 2005). Inactivation of SCi causes feature-based target selection deficits for saccades (McPeek & Keller, 2004) and manual button presses (Lovejoy & Krauzlis, 2010). Conversely, subthreshold microstimulation of SCi or FEF biases feature-based target selection for eye movements (Carello & Krauzlis, 2004; Dorris et al., 2007; McPeek et al., 2003; McPeek, 2006) and facilitates perceptual discriminations (Cavanaugh & Wurtz, 2004; Müller et al., 2005; Moore & Fallah, 2001, 2004) by modulating downstream cortical visual representations (Moore & Armstrong, 2003; Monosov et al., 2011). However, despite these observations, it remains unclear whether

SCi and FEF contribute to feature-based target selection by selecting amongst the feature-weighted object representations in other modules or by actively resolving competition between object representations by locally discriminating features.

Some SCi cells show broad sensitivities for certain visual features such as contrast (Chen et al., 2015; Li & Basso, 2008), orientation and spatial frequency (Chen & Hafed, 2018), motion direction (Horwitz & Newsome, 1999, 2001; Goldberg & Wurtz, 1972), and color (White et al., 2009), while some cells in the strictly visual, superficial layers of the superior colliculus (SCs) encode the presence (Le et al., 2020) and orientation (Nguyen et al., 2014) of faces. In fact, there is new evidence to suggest that selectivity for feature singletons in anterior loci of the visual processing hierarchy arise from collicular processing (Bogadhi et al., 2021). Nevertheless, given the broad tuning for simple feature singletons encoded by SCi neurons, these representations may still be insufficient for fine-tuned feature-based discriminations of complex objects, relying instead on representations in visual cortices. Similarly, visual representations in SCs, such as those encoding face information, must require upstream cortical input as ablation or reversible cooling of visual and associative cortices extinguishes visual responses in SCs altogether (Schiller et al., 1972). Classic studies of the discharge properties of FEF visual and visuomotor cells have shown that visual responses for FEF cells are not differentiated by feature singletons (Bruce & Goldberg, 1985; Mohler et al., 1973; Pigarev et al., 1979). These limitations suggest that SCi and FEF may be insufficient for feature discrimination during target selection in certain contexts, as they may lack the requisite specificity. If so, SCi and FEF would instead require input from outside visual modules specialized for processing task-relevant visual features. If saccade-vector encoding substrates required input from specialized visual modules, then the

latency of visual representations in these oculomotor substrates should increase for more complex stimuli as is seen in the ventral visual processing hierarchy.

There are robust links between the behavioral saccade metrics used in our experiment and neural activation levels in oculomotor substrates SCi (Glimcher & Sparks, 1993; McPeek et al., 2003; Robinson, 1972; Port & Wurtz, 2003; White et al., 2012) and FEF (McPeek, 2006; Robinson & Fuchs, 1969). As such, the latency of saccadic interference effects measured with these metrics should closely correspond to the latency of neural activation in these substrates. As we observed considerably longer saccadic interference effects for complex stimuli than is typically observed for simple stimuli, our data therefore support the interpretation that complex feature discriminations are not performed in oculomotor substrates.

3.6.3. Conclusion

We expanded on our paradigm in which human saccade metrics are non-invasively modeled as a function of time after abrupt distractor onset while a saccade is being independently planned to a target (Kehoe & Fallah, 2017) by utilizing visually complex, novel, and task-relevant stimuli that needed to be perceptually discriminated for successful target selection. We strengthened the validity of this technique by using three additional behavioral metrics indicative of oculomotor excitation independent of saccade curvature and which gave consistent estimates of oculomotor vector representation onset latencies. Our data show that the latencies of oculomotor behavioral plans elicited by complex, task-relevant objects are longer than for simple task-irrelevant stimuli, suggesting that oculomotor substrates may receive direct visual inputs from contextually dependent visual modules specialized for processing task-relevant features. Critically, we provide evidence that initial oculomotor excitatory responses can encode stimulus identity, contrary to influential views of oculomotor processing (Fecteau &

Munoz, 2006). Stimuli were encoded according to perceptual confidence and we observed a strong role of executive perceptual learning in mediating these representations.

Chapter 4. Motion Distractors Perturb Saccade Programming Later in Time than Static Distractors

This manuscript has been published in *Current Research in Neurobiology*:

Kehoe, D. H., Schießer, L., Malik, H., & Fallah, M. (2023). Motion distractors perturb saccade programming later in time than static distractors. *Current Research in Neurobiology*, *4*, 100092. https://doi.org/10.1016/j.crneur.2023.100092

4.1. Abstract

The mechanism that reweights oculomotor vectors based on visual features is unclear. However, the latency of oculomotor visual activations gives insight into their antecedent featural processing. We compared the oculomotor processing time course of grayscale, task-irrelevant static and motion distractors during target selection by continuously measuring a battery of human saccadic behavioral metrics as a function of time after distractor onset. The motion direction was towards or away from the target and the motion speed was fast or slow. We compared static and motion distractors and observed that both distractors elicited curved saccades and shifted endpoints at short latencies (~25 ms). After 50 ms, saccade trajectory biasing elicited by motion distractors lagged static distractor trajectory biasing by 10 ms. There were no such latency differences between distractor motion directions or motion speeds. This pattern suggests that additional processing of motion stimuli occurred prior to the propagation of visual information into the oculomotor system. We examined the interaction of distractor processing time (DPT) with two additional factors: saccadic reaction time (SRT) and saccadic amplitude. Shorter SRTs were associated with shorter DPT latencies of biased saccade trajectories. Both SRT and saccadic amplitude were associated with the magnitude of saccade trajectory biases.

4.2. Highlights

- Motion and static distractors spatially biased saccade trajectories at extremely short latencies (~25 ms).
- After 50 ms, motion distractors spatially biased and inhibited saccades 10 ms later than static distractors.
- The time course did not vary by motion speed or direction.

- The oculomotor system encodes visual stimuli in order of featural complexity.

4.3. Public and Media Statement

We found evidence that planning an eye movement to an object takes intrinsically longer for different visual features that could characterize the object. Eye movements are often directed purposely towards an object with specific visual attributes: if you're looking for something red, you're likely going to scan for red objects and ignore any green objects. Therefore, visual information that provides stimulus identity is critical to execute optimal eye movements. In our experiment, we showed participants a static stimulus and various motion animated stimuli and measured the time it takes the oculomotor system to encode these objects. We found that the time it takes the oculomotor system to encode motion was systematically longer than the time it takes to encode the static stimulus. This suggests that, when determining what is most relevant to look at, the oculomotor system does not utilize a holistic, undifferentiated object representation. Instead, it represents individual features as they become available to it. This would also suggest then that the oculomotor system has a limited role in extracting features from object representations to guide motor behaviors, and that instead, this function is likely then subserved by separate perceptual processing systems.

4.4. Introduction

The role of the oculomotor system in saccadic target selection has been studied extensively (Basso & Wurtz, 1997, 1998; Bichot et al., 1999; Horwitz & Newsome, 1999, 2001; McPeek & Keller, 2002, 2004; Shen & Paré, 2007). However, the role of the oculomotor system in feature extraction and discrimination—a necessary component of target selection in the real-world—receives less attention. As such, it remains unclear whether oculomotor substrates are

sufficient for feature extraction and discrimination during target selection, or alternatively, whether features are extracted and discriminated in specialized visual cortices.

Specialized visual cortical modules exhibit robust visual afferent delay times differences between them (Bodelón et al., 2007; Nowak & Bullier, 1997; Schmolesky et al., 1998). As such, one method to investigate whether visual projections into oculomotor substrates are feature-dependent is to compare the latency of oculomotor activation elicited by features processed in different cortical modules. The dependence account would predict that oculomotor activation latencies mimic those observed in the relevant visual cortices, while the independence account would predict that oculomotor activation latencies are undifferentiated between features. Although the latency of oculomotor activation is modulated by luminance (Bell et al., 2006; Li & Basso 2008a) and chromaticity (Hall & Colby, 2014, 2016) contrast energy, there is evidence that oculomotor activation latencies are dependent on feature-relevant visual afferent processing channels. White et al. (2009) demonstrated that visual onset burst latencies are approximately 30-35 ms faster for maximum-luminance-contrast saccade targets than for maximum-chromaticity-contrast isoluminant color targets in collicular neurons. This difference is remarkably similar to the visual afferent delay time differences observed between these stimuli in the dorsal and ventral processing streams of V1 and V2.

This logic can be applied to experiments with human populations as many experimental paradigms have been developed to non-invasively infer the time course of sensory processing in the oculomotor system. These paradigms typically involve displaying an intervening visual stimulus while an impending movement is in preparation, such as saccadic (Edelman & Xu, 2009; Reingold & Stampe, 2002) or microsaccadic (Buonocore & McIntosh, 2012; Hafed & Ignashchenkova, 2013) inhibition paradigms, compelled saccades (Salinas et al., 2010; Shankar

et al., 2011; Stanford et al., 2010), and double-stepping targets (Becker & Jürgens, 1979; Findley & Harris, 1984; Ludwig et al., 2007). Similarly, Kehoe et al. (2017, 2021) recently developed a paradigm whereby subjects plan and execute a saccade to a target and we abruptly onset a peripheral distractor at some random interval after target onset. This randomizes the duration of time in which the distractor is visually present prior to the saccade. Over hundreds of trials, a rich, wide range of these time intervals are collected and a continuous variable we refer to as distractor processing time emerges. We use a battery of behavioral saccade metrics to examine saccadic perturbations as a function of distractor processing time. Specifically, we analyze saccade trajectory spatial biases, suppressed saccade initiation, and stimulus selection errors (if applicable), as each of these phenomena has a clear neurophysiological antecedent in the intermediate layers of the superior colliculus (SCi) and the frontal eye fields (FEF), two critical oculomotor substrates that determine oculomotor behavior.

Oculomotor substrates encode the direction-amplitude vectors of both eye movements (Robinson et al., 1969, 1972) and visual stimuli (Bruce & Goldberg, 1985; Goldberg & Wurtz, 1972) as increased neural activation on orderly retinotopic maps, whereby the constituent visuomotor (VM) neurons have spatially overlapping motor and visual fields (Marino et al., 2008). The spatiotemporally weighted average of neural activation levels across the vector map determines the resultant saccadic trajectory: in the perisaccadic interval between 30-0 ms prior to saccade execution, increased activation at a distractor locus can curve saccade trajectories (McPeek et al., 2003, 2006; Port & Wurtz, 2003) and shift endpoints (Glimcher & Sparks, 1993; Robinson et al., 1969, 1972) towards the distractor, while decreased activation at the distractor locus can curve saccade trajectories away from the distractor (Aizawa & Wurtz, 1998; White et al., 2012). Upon activation of a saccade vector in SCi, lateral inhibitory networks impose

transient inhibition on neighboring saccade vectors (Munoz & Istvan, 1998), which manifests as lower visual onset burst magnitudes for stimulus dense displays (Basso & Wurtz, 1997, 1998) and a transient drop in saccadic likelihood after the onset of a secondary stimulus (Buonocore & McIntosh, 2012; Edelman & Xu, 2009; Reingold & Stampe, 2002).

There is considerable evidence that the latency of saccadic perturbations in humans reflects the afferent delay time of visual representations in oculomotor substrates. Visual onset burst latencies in SCi are usually ~50 ms as measured by direct physiological observation (reviewed by Boehnke & Munoz, 2008). Consistent saccadic behavior perturbation latency estimates of ~50 ms have been observed across human behavioral paradigms and metrics, such as double-stepping targets biasing saccadic endpoints (Becker & Jürgens, 1979; Findley & Harris, 1984; Ludwig et al., 2007), luminance flashes (Reingold & Stampe, 2002) and distractor onsets (Buonocore & McIntosh, 2012; Edelman & Xu, 2009; Kehoe et al., 2021) suppressing saccadic initiation, and distractor onsets biasing saccade trajectories (Kehoe et al., 2017, 2021). Previously, we observed that luminance-modulated Gabors perturb saccade trajectories approximately 20 ms faster than color-modulated Gabors (Kehoe & Fallah, 2017), consistent with visual onset burst latency differences for similar stimuli (White et al., 2009). More recently, Kehoe et al. (2021) showed that saccadic perturbation latencies were 40 ms longer for task-relevant, pseudo-alphanumeric characters as compared to task irrelevant Gabors. This 40 ms difference is consistent with visual afferent delay time differences in early (e.g., primary visual cortex) and late (e.g., inferotemporal cortex) stages of the cortical visual processing hierarchy.

With our behavioral paradigm, we have not yet examined oculomotor activation latency differences between visual features processed in the same visual modules with visual features processed in separate visual modules using the same subjects. In the current experiment, we

compared saccade perturbation latencies elicited by static, fast-motion, and slow-motion task-irrelevant distractor gratings using our behavioral paradigm. We utilized 8 and 4 °/s as our fast and slow motion speeds given a classic electrophysiologically relevant boundary of 6 °/s delineating fast and slow motion (ffytche et al., 1995). If motion requires additional processing over static gratings (e.g., MT vs. V1), and if the oculomotor system receives visual input after sufficient antecedent featural processing, saccade perturbation latencies should be longer for motion distractors than for static distractors. Since there are no visual processing time differences between these motion speeds (Azzopardi et al., 2003), we do not expect activation latency differences between our fast- and slow-motion distractors. We quantified saccade perturbation as saccade curvature, biased saccade endpoints (herein referred to as endpoint deviation), and a transient drop in saccadic likelihood. Additionally, we compared distractor motion towards and away from the target, as task-irrelevant motion can reflexively bias eye movement in the direction of motion (Fallah & Reynolds, 2012) and because some oculomotor cells preferentially activate for motion directed into their motor field (Horwitz & Newsome, 1999, 2001). We therefore expected a greater magnitude of saccadic trajectory perturbation for distractor motion away from the target, as distractor motion may bias the movement in the direction opposite the target and because motion away may elicit less target activation. We also split the data into upwards and downwards saccades and again compared static and motion distractors to investigate whether processing differences between static and motion distractors generalized across vertical visual hemifields. Given the strong anisotropy in the latency and magnitude of collicular visual responses (Hafed & Chen, 2016), we expect saccade perturbation latencies are shorter and perturbation magnitudes are greater in the upper visual hemifield. Finally, we extensively examined the interaction of saccadic reaction time (SRT) and saccadic amplitude on

measuring saccade perturbations as a function of distractor processing time. This enabled us to disentangle executive processing (SRT) and kinematics (amplitude) from sensory processing (distractor processing time). Based on previous observations using our paradigm, we expected that SRT would affect the magnitude of saccade perturbations but not the latencies (Kehoe et al., 2021). Also, given that a subset of VM cells have open-ended motor fields in which they discharge a motor burst at increasingly longer latencies after movement initiation as saccadic amplitudes increase beyond their preferred amplitude (Munoz & Wurtz, 1995a, 1995b), we expected that saccade perturbation magnitude should be functionally related to saccade amplitude.

4.5. Methods

4.5.1. Participants

31 York University undergraduate students (16-37 years old, 4 male) participated in the experiment for course credit. Participants had normal or corrected-to-normal visual acuity and were naïve to the purpose and design of the experiment. Informed consent was obtained prior to participation. All research was approved by York University's Human Participants Review Committee.

4.5.2. Stimuli

The saccade target was a white (CIE*xy* = [.29, .30], luminance = 122.70 cd/m^2) square that subtended 0.6° × 0.6° and was located 12° above or below central fixation. Distractors were sinusoidal motion animations viewed through an aperture, created offline using MATLAB (MathWorks, Natick, MA). Animation frames consisted of 2D achromatic sinusoidal waves (CIE*xy* = [.31, .33], maximum luminance = 9.33 cd/m^2, minimum luminance = 1.52 cd/m^2) with a spatial frequency of 2°/cycle, a vertical orientation, and were superimposed with a circular

aperture (radius = 1°). Leftward and rightward distractor motion was animated by linearly decreasing or increasing (respectively) sinusoidal phases across successive frames to create fast (8 °/s) and slow (4 °/s) motion. These motion speeds were selected given the electrophysiologically relevant boundary of 6 °/s delineating fast and slow motion (ffytche et al., 1995). All animations had a frame rate of 40 fps and began at a phase of 0. The static distractor consisted of a single frame. Stimuli were imbedded in a grey (CIE*xy* = [.28, .30], luminance = 7.51 cd/m^2) background. The stimuli were displayed on a 21-inch CRT monitor (85 Hz, 1024 × 768). Participants viewed stimuli in a dimly lit room from a viewing distance of 57 cm with a headrest stabilizing their head position.

4.5.3. Apparatus and Measurement

Stimulus presentation was controlled using a computer running Presentation software (Neurobehavioral Systems, Berkeley, CA). Eye position was recorded using infrared eye tracking (500 Hz, EyeLink II, SR Research, Ontario, Canada). The eye tracker was calibrated using a nine-point grid at the beginning and halfway point of each experimental session, and as needed. All data processing and statistical analysis was performed using MATLAB.

4.5.4. Task Procedure

Trials were initiated by maintaining fixation (1.89° square window) to a white (CIE*xy* = [.29, .30], luminance = 122.70 cd/m^2), central fixation cross (0.4°× 0.4°) for 200 ms (see Figure 4.1A). The fixation cross then offset and the target onset 12° above or below fixation. Participants were instructed to fixate the target as soon as it appeared. After an interval of 50, 100, 150, or 200 ms, the distractor onset to the left or right of the target at an eccentricity of 12°. The target and distractor always appeared in the same vertical hemifield, angularly separated by 45°. The distractor feature was (1) fast motion towards the target, (2) slow motion towards the

target, (3) fast motion away from the target, (4) slow motion away from the target, or (5) static. The onset interval between the target and distractor is subsequently referred to as the distractor-target onset asynchrony (DTOA). The trial ended when a saccade was made to the target or 500 ms had elapsed (time-out). Time-out trials were randomly replaced back into the block and were signified with an error tone and message. Trials were separated by a 1000 ms intertrial interval (ITI) with a blank, grey display.

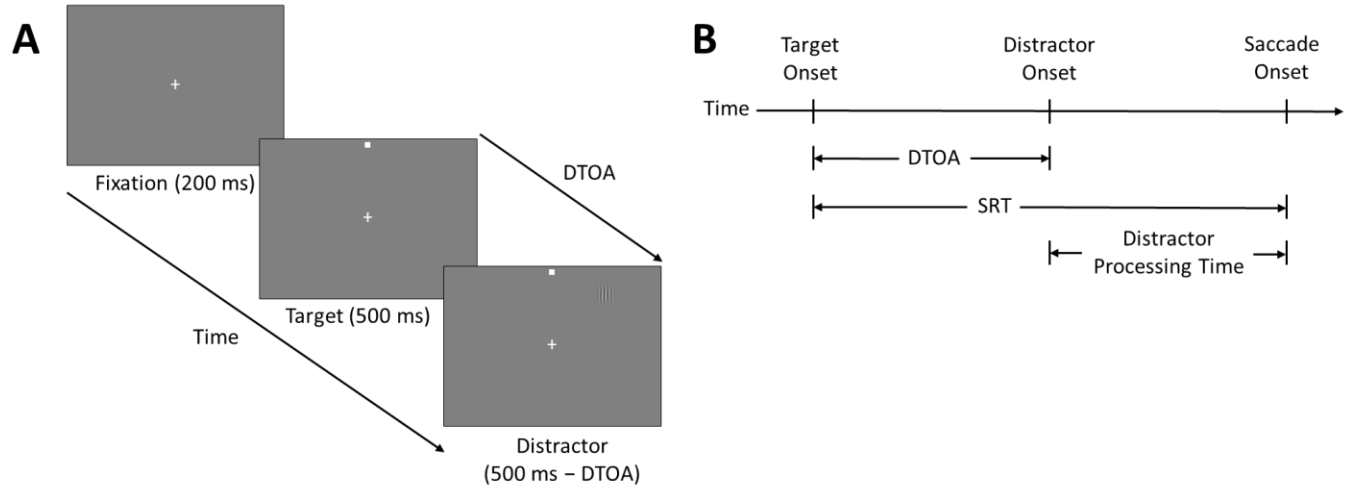

Figure 4.1. Trial temporal schematics. ***A***: Stimuli sequence. After maintaining fixation for 200 ms, the target was presented for 500 ms or until a saccade to the target was detected. The distractor was displayed after a randomized interval, referred to as distractor-target onset asynchrony (DTOA). ***B***: Trial epochs. Trials were parsed into 3 temporal intervals: saccadic reaction time (SRT), DTOA, and distractor processing time. The boundaries of these intervals were defined by 3 temporal events: target onset, distractor onset, and saccade onset. DTOA is an independent variable, while SRT and distractor processing time are dependent variables. Distractor processing time was derived by subtracting DTOA from SRT.

Participants completed 1 session with 10 blocks of 84 trials for a total of 840 trials. Each block contained a randomized ordering of 2×2×4×5+4=84 experimental conditions: target location (up, down) × distractor location (left, right) × DTOA (50, 100, 150, 200 ms) × distractor feature (fast-towards, slow-towards, fast-away, slow-away, static) + two baseline trials without

distractors at each target location.

4.5.5. Saccade Detection

Saccades were detected, visualized, filtered and analyzed offline using customized MATLAB algorithms. Saccades were defined as a velocity exceeding 20 °/s for at least 8 ms and a peak velocity exceeding 50 °/s. Saccadic reaction time (SRT) was defined as the time from target onset to saccade initiation. Saccade amplitude was defined as the Euclidean distance between saccade endpoint and the center of fixation. Trials that contained blinks or sub-velocity-threshold eye movements (4.80%), corrective saccades (0.93%), distractor-directed saccades (0.32%), saccade amplitudes < 1° (0.43%), endpoint deviations > 3° from the center of the target (6.79%), fixation drifts > 0.5° during the pre-saccadic latency period (3.08%), or an SRT < 100 ms (4.88%) were excluded from further analysis leaving 78.76% of the data remaining.

Saccade curvatures were quantified as the sum of all orthogonal deviations between the saccade trajectory and a straight line between the start- and endpoints of saccades in degrees of visual angle. Endpoint deviations were quantified as the angular separation between the saccade endpoint and the center of the target in polar degrees. To reduce idiosyncratic movement, we subtracted mean baseline saccade curvature and endpoint deviation from the data, separately for each participant at each target location. We coded these metrics so that positive values correspond to deviations towards the distractor, while negative values correspond to deviations away from the distractor. We trimmed extreme (4 standard deviations above/below the mean) saccade curvature and endpoint deviation values from the aggregate dataset, removing 194 saccades (0.74%).

4.5.6. Data Analysis

Distractor processing time was defined as the interval of time between distractor and

saccade onsets and was computed by subtracting DTOA from SRT (see Figure 4.1*B*). Distractor processing time is therefore reciprocally distractor time-locked and saccade time-locked, where DTOA−SRT is the time of distractor onset prior to saccade initiation and SRT−DTOA is the time of saccade initiation after distractor onset, both exactly mirrored about a value of zero.

4.5.6.1. Saccade trajectory perturbations. We used Gaussian kernel regression to estimate saccade curvature and endpoint deviation as a function of distractor processing time for each subject in each distractor condition. We used leave-one-out cross-validation (LOOCV) with a least squares loss function to select the optimally predictive bandwidth for each model. Next, we estimated several parameters that describe saccade trajectory perturbations as a function of distractor processing time: the onset latency of saccade trajectory perturbation, the latency of maximum saccade trajectory perturbations, and the magnitude of maximum saccade trajectory perturbations. We refer to these parameters as *onset*, *max*, and *magnitude* herein.

To estimate *onset*, we used a sliding Wilcoxon signed-rank test to determine the earliest distractor processing times at which saccade curvature and endpoint deviation were significantly different than zero for at least 10 ms. To estimate *max* and *magnitude*, we averaged the kernel regressions across subjects and computed the distractor processing time of maximum saccade curvature/endpoint deviation and the maximum saccade curvature/endpoint deviation *per se* (respectively).

These 3 parameters were estimated using the aggregated data across subjects and not on the individual subject level, making direct inferential comparisons impossible between parameters estimated in different conditions. As such, we bootstrapped the raw data b=1000 times and repeated the above analyses for each resample to estimate the sampling distribution of each parameter. We compared each parameter between distractor conditions using exhaustive

pairwise two-tailed distribution tests of the independently resampled distributions. The distribution test empirically evaluates the cutoffs of a computationally approximated joint probability density function of two independent distributions (see Poe et al., 2005 for derivation and overview). For two independent distributions $\mathbf{x} = (x_1, \ldots, x_n)$ and $\mathbf{y} = (y_1, \ldots, y_m)$, the left-tailed cumulative probability is

$$p = \frac{1}{nm}\sum_{i=1}^{n}\sum_{j=1}^{m} z_{ij}, \quad z_{ij} = \begin{cases} 0, & x_i \leq y_j \\ 1, & x_i > y_j \end{cases},$$

and the two-tailed cumulative probability is $2 \times \min\{p, 1-p\}$.

In a final step, we used a sliding Friedman test to determine the distractor processing times at which saccade curvature and endpoint deviation were significantly different between distractor conditions for at least 10 ms. Here, significant epochs separated by less than 5 ms were pooled together.

4.5.6.2. Saccade initiation perturbations. We used Gaussian kernel density estimation (KDE) to estimate the observed probability density of saccades as a function of distractor processing time for each subject in each distractor condition. We used LOOCV with a log-likelihood loss function to select the maximum likelihood bandwidth for each model. Next, we estimated the distractor processing time of a transient drop in saccadic likelihood, which requires some model of expected saccadic likelihood for comparison. However, there is no analytic-form for a random variable such as distractor processing time, which is the difference between two other random variables, one with multiple widely spaced, jittered peaks (DTOA) and one that is a heavily-skewed Gaussian (SRT). Therefore, we computationally generated an expectation model of saccadic likelihood for comparison with observed saccadic likelihood.

To generate our expectation model, we randomly sampled with replacement SRTs

observed on baseline (i.e., distractor absent) trials pooled across participants (with n = 978 trials to sample), and then independently sampled DTOAs observed on valid trials with distractor onsets. The difference of these distributions gave a bootstrapped empirical distribution of expected distractor processing times. We fit this expectation distribution with KDE using the average bandwidth across subjects in each condition.

We used a sliding Wilcoxon signed-rank test to determine the earliest distractor processing time at which observed saccade density was significantly lower than the expectation model, which we herein refer to as *onset*. We repeated the bootstrapping procedure, distribution tests, and sliding Friedman analysis discussed in the previous section.

4.5.6.3. Distractor processing time interactions with SRT and saccade amplitude. We analyzed whether the parameter estimates outlined in the previous 2 sections were consistent across the ranges of SRT and saccade amplitude observed in the data. To this end, we used Gaussian kernel regression to estimate saccade curvature and endpoint deviation as a 2D function of distractor processing time and saccadic reaction time for each subject. We repeated this analysis for 2D functions of distractor processing time and saccade amplitude. We used LOOCV with a least squares loss function to estimate optimally predictive bandwidths for each subject. Similarly, we used Gaussian KDE to estimate saccade probability density as a 2D function of distractor processing time and SRT or distractor processing time and saccade amplitude. We used LOOCV with a log-likelihood loss function to estimate the maximum likelihood bandwidth for each subject.

At each level of SRT (range = [150 ms, 275 ms], scale = 1 ms) or saccade amplitude (range = [10°, 14°], scale = .025°) in the 2D functions, we repeated the 1D distractor processing time analyses outlined in the previous 2 sections. We therefore obtained parameter estimates as a

function of SRT and amplitude. As before, we bootstrapped the raw data b=1000 times to generate a distribution of these parameter estimates as a function of SRT and amplitude. We used a sliding distribution test to determine the SRT or saccade amplitude values at which the 2D parameter distributions were significantly different than the omnibus parameter distributions from the preceding two sections. We used the same sliding inferential analysis conventions as above. Finally, to examine whether there was an overall linear trend of the 2D parameter estimates, we developed a computational linear regression analysis for large distributions. First, for each bootstrap, we used ordinary least squares to fit linear models of parameter estimate as a function of SRT or amplitude. Second, we computed the squared error of all 2D parameter estimates from the fitted models and unitized the variance. Third, we squared the distribution of best-fitting slopes from step 1 and unitized the variance. Last, we compared the squared/unitized distributions of model residuals and slopes from step 2 and step 3 using a one-tailed distribution test. This analysis is analogous to a non-central F-test with degrees of freedom arbitrarily close to infinity.

4.6. Results

4.6.1. Expectation Model

To better illustrate the derivation of the expectation model, we show each expected (bootstrapped) distribution of distractor processing times relative to the observed distribution, split by distractor-target onset time (DTOA) condition (see Figure 4.2). In panels *A* through *D*, the expected distractor processing time (DPT) distributions (DPT = DTOA−SRT; see Figure 4.1*B*) closely resemble the SRT distribution shifted back in time by DTOA ms. The sum of these distributions gives the expectation model (see Figure 4.2*E*). In Figure 4.2, we present these data as count densities to illustrate the relative mass of saccades in each DTOA condition. In the

DTOA=200 ms condition (Figure 4.2*D*), there is a much smaller mass of saccades relative to the remaining conditions, as many of these trials were trimmed from the data since saccades landed on target and ended the trial prior to distractor onset. Note that the same bootstrapped distribution of expected distractor processing times was used to compute the expectation model for every split of the data by distractor condition. In each condition, the expected distribution was fit using the optimal KDE bandwidth for the respective condition, thus creating the distractor-specific expectation model.

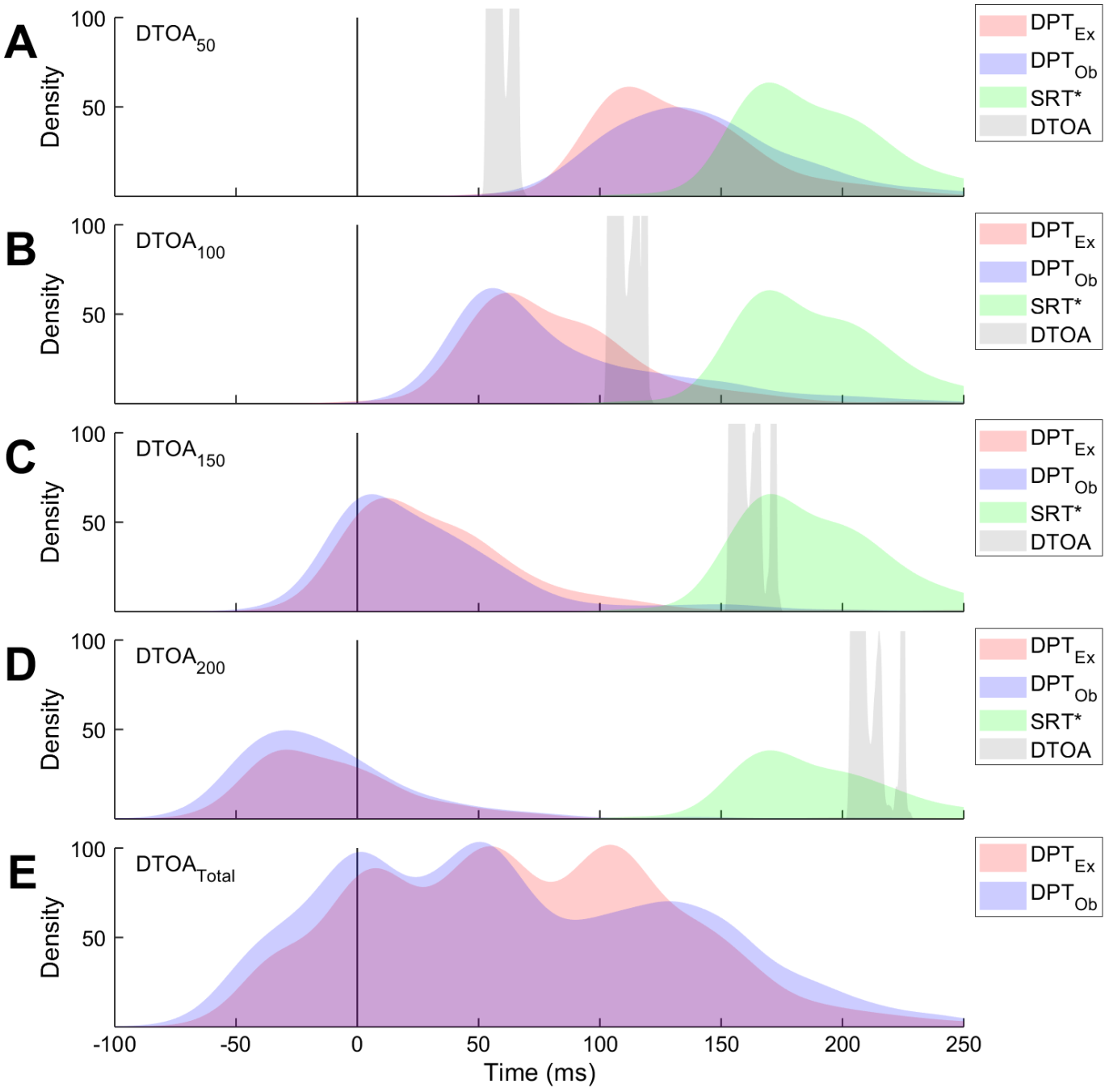

Figure 4.2. Expected vs. observed distractor processing time (DPT) distributions split by distractor-target onset asynchrony (DTOA). Expected DPT distributions are plotted in red. Observed DPT distributions are plotted in blue. Bootstrapped SRT distributions are plotted in green. Observed DTOA distributions are plotted in gray. ***A*:** DTOA = 50 ms. ***B*:** DTOA = 100 ms. ***C*:** DTOA = 150 ms. ***D*:** DTOA = 200 ms. ***E*:** Aggregate of all DTOAs.

4.6.2. Distractor Motion

We compared saccade curvature, endpoint deviation, and saccade density as a function of distractor processing time between static distractors and the aggregate of all motion distractors (see Figure 4.3). Descriptive statistics for the bootstrapped distributions of parameters in the static and motion distractor conditions are in Table 4.1.

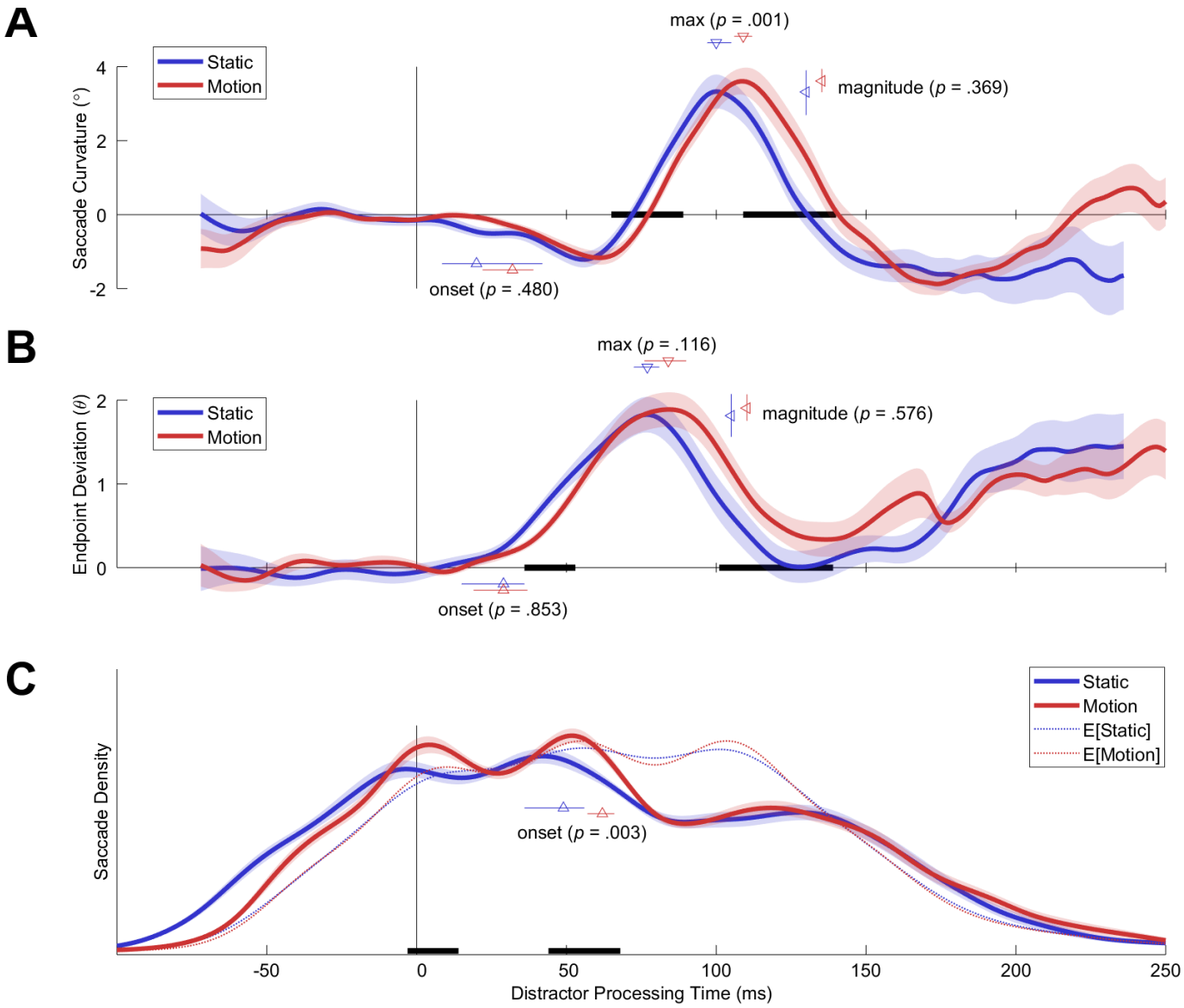

Figure 4.3. Saccade metrics as a function of distractor processing time split by static (blue) and motion (red) distractor types. Mean saccade metrics are plotted with thick, colored lines. Standard error of the mean across subjects (n = 31) is indicated by shading. Black lines along the abscissa in each panel indicate epochs of significant

(p<.05, sliding Friedman test) differences between saccade metrics. Arrowheads indicate the estimated onset latency of saccadic perturbation (▲), the estimated time of maximum saccadic perturbation (▼), and the magnitude of saccadic perturbation (◄). Arrowheads are color-coded to indicate distractor condition. Error bars intersecting the arrowheads indicate the bootstrapped 95% confidence interval of each point estimate. *P* values indicate significance (distribution test) of the difference between bootstrapped point estimates in each condition. ***A*:** Mean saccade curvature as a function of distractor processing time. ***B*:** Mean endpoint deviation as a function of distractor processing time. ***C*:** Mean saccade probability density as a function of distractor processing time. Dotted lines indicate expectation models.

Table 4.1. Descriptive statistics for bootstrapped parameter distributions in all distractor conditions.

		Distractor		95% CI	
Metric	Parameter	Condition	Median	Lower	Upper
Saccade Curvature	*onset*	Static	20	8.00	41.72
		Motion	32	21.55	38.33
		Toward	37	22.33	41.71
		Away	31	23.23	38.20
		Slow	31	17.50	37.43
		Fast	36	23.00	41.97
	max	Static	100	96.67	104.06
		Motion	109	105.23	111.30
		Toward	110	106.11	111.94
		Away	107	103.59	111.16
		Slow	110	106.20	112.82
		Fast	107	102.65	110.44
	magnitude	Static	3.32	2.69	3.89
		Motion	3.62	3.31	3.94
		Toward	3.39	2.97	3.77
		Away	3.68	3.26	4.09
		Slow	3.44	3.06	3.81
		Fast	3.46	3.05	3.90
Endpoint Deviation	*onset*	Static	29	14.42	35.24
		Motion	29	18.55	36.06
		Toward	36	23.33	41.55
		Away	28	14.33	34.64
		Slow	25	15.19	35.14
		Fast	34	27.29	38.63
	max	Static	77	72.00	80.62
		Motion	84	75.25	89.05
		Toward	84	76.17	89.00

		Away	82	74.67	89.54
		Slow	83	73.62	89.89
		Fast	83	78.11	86.52
	magnitude	Static	1.81	1.56	2.07
		Motion	1.90	1.75	2.07
		Toward	1.99	1.76	2.22
		Away	1.76	1.57	1.94
		Slow	1.79	1.60	1.98
		Fast	1.89	1.69	2.08
Saccade Density	*onset*	Static	49	34.67	55.57
		Motion	62	56.50	65.40
		Toward	62	56.12	66.60
		Away	63	56.05	66.75
		Slow	61	53.11	65.05
		Fast	64	56.77	67.35

Note: 95% CI is 95% confidence interval of the bootstrapped parameter distribution. *onset* is the onset latencies saccadic perturbation. *max* is the onset latency of maximum saccadic perturbation. *magnitude* is the magnitude of maximum saccadic perturbation.

For saccade curvature (see Figure 4.3*A*), the *onset* latency was very short (~26 ms) and did not differ between distractor conditions (p = .480). The *max* latency was clearly differentiated between the static (100 ms) and motion distractors (109 ms; p = .001), but the *magnitude* was not (p = .369). The sliding Friedman analysis identified 2 epochs in which saccade curvature was significantly different between distractor conditions: 65-88 ms and 109-139 ms. These epochs closely corresponded to the rising and falling edges of the positively signed curvature effect.

For endpoint deviation (see Figure 4.3*B*), the *onset* latency also had a short latency (~30 ms) and did not differ between distractor conditions (p = .853). The *max* latency was ~80 ms and was not different between conditions (p = .116). Similarly, the *magnitude* was not different between conditions (p = .576). Like saccade curvature, the sliding Friedman analysis identified epochs in which endpoint deviation was significantly different between distractor conditions

coinciding with the rising (36-52 ms) and falling edges (101-138 ms) of the initial endpoint deviation effect.

Next, we examined the latency of saccade density falling below the expectation model (see Figure 4.3*C*). This *onset* latency was shorter in the static condition (49 ms) than in the motion condition (62 ms; $p = .003$). The sliding Friedman analysis identified two early epochs in which saccade density was different between distractor conditions: -3 to 13 ms and 44 to 67 ms. These differences seem to reflect the fact that the static saccade density distribution is flatter in the range of 0 through 70 ms of distractor processing time as compared to the motion saccade density distribution. Beyond 70 ms, however, the two distributions are indistinguishable. This flattening effect in the static condition coincides with an increase of the width of the distribution into the negative distractor processing range as compared to motion distractors. Negative distractor processing times only arise when saccades begin after distractor onset. Since distractor onset times were identical in the static and motion distractor conditions, this increased density in the negative distractor processing range suggests increased SRTs for static distractors. Accordingly, a Wilcoxon signed-rank test confirmed that median SRT across subjects was longer for static distractors ($M = 200.15$ ms, $SE = 3.50$ ms) than for motion distractors ($M = 195.00$ ms, $SE = 3.48$ ms) ($p < .001$). It is unclear whether static distractors slowed SRT or motion distractors speeded SRTs.

4.6.3. Distractor Motion Direction

Next, we compared saccade curvature, endpoint deviation, and saccade density as a function of distractor processing time between static distractors, distractors with motion towards the distractor, and distractors with motion away from the target (see Figure 4.4). Descriptive

statistics for the bootstrapped distributions of parameters in the static, motion towards, and motion away distractor conditions are in Table 4.1.

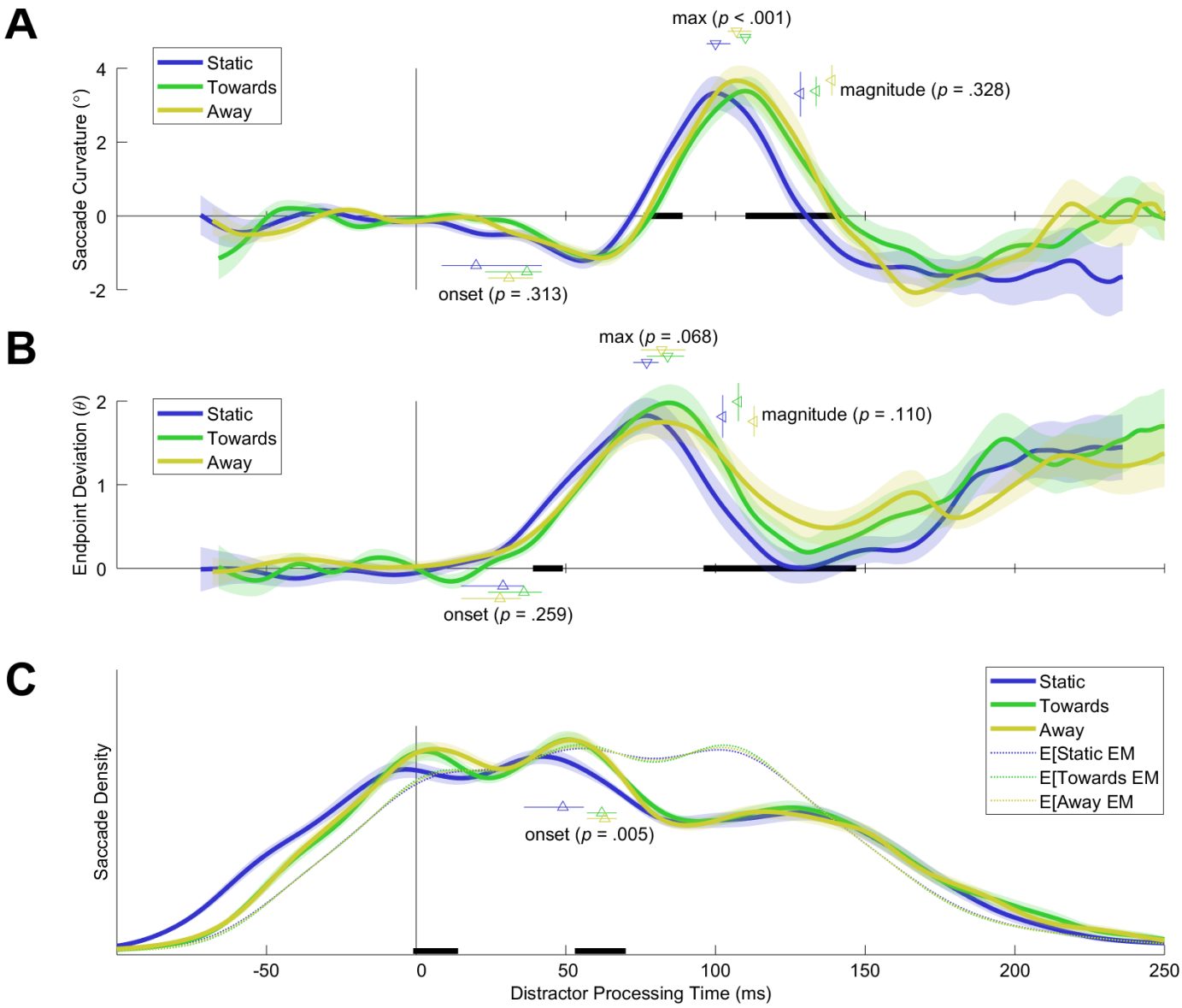

Figure 4.4. Saccade metrics as a function of distractor processing time split by static (blue), motion towards the target (green), and motion away from the target (yellow) distractor types. Mean saccade metrics are plotted with thick, colored lines. Standard error of the mean across subjects (n = 31) is indicated by shading. Black lines along the abscissa in each panel indicate epochs of significant (p<.05, sliding Friedman test) differences between saccade metrics. Arrowheads indicate the estimated onset latency of saccadic perturbation (▲), the estimated time of maximum saccadic perturbation (▼), and the magnitude of saccadic perturbation (◄). Arrowheads are color-coded to indicate distractor condition. Error bars intersecting the arrowheads indicate the bootstrapped 95% confidence interval of each

point estimate. *P* values indicate significance (distribution test) of the difference between bootstrapped point estimates in each condition. ***A*:** Mean saccade curvature as a function of distractor processing time. ***B*:** Mean endpoint deviation as a function of distractor processing time. ***C*:** Mean saccade probability density as a function of distractor processing time. Dotted lines indicate expectation models.

For saccade curvature (see Figure 4.4*A*), the *onset* latency was not different between distractor conditions (all $p \geq .313$). The *max* latency was clearly differentiated between the static (100 ms) and motion towards distractors (110 ms; $p < .001$) and motion away distractors (107 ms; $p = .006$). However, there was no difference between the motion towards and motion away conditions ($p = .278$). The *magnitude* was not different between conditions (all $p \geq .328$). The sliding Friedman analysis identified 2 epochs in which saccade curvature was significantly different between distractor conditions: 76-88 ms and 110-141 ms.

For endpoint deviation (see Figure 4.4*B*), the *onset* latency was not different between distractor conditions (all $p \geq .259$). The *max* latency was marginally different between the static (77 ms) and motion towards distractors (84 ms; $p = .068$) but was otherwise not significantly different between conditions (all $p \geq .161$). The *magnitude* was not different between conditions either (all $p \geq .110$). The sliding Friedman analysis identified 2 epochs in which endpoint deviation was significantly different between distractor conditions: 39-48 ms and 96-146 ms.

The *onset* latency of lower than expectation saccade density was shorter in the static condition (49 ms) than in the motion towards (62 ms; $p = .008$) and motion away (63 ms; $p = .005$) conditions (see Figure 4.4*C*). There was no difference between the motion towards and motion away conditions ($p = .718$). The sliding Friedman analysis identified two epochs in which saccade density was different between distractor conditions: -1 to 13 ms and 53 to 69 ms.

4.6.4. Distractor Motion Speed

We compared saccade curvature, endpoint deviation, and saccade density as a function of distractor processing time between static distractors, distractors with slow motion, and distractors with fast motion (see Figure 4.5). Descriptive statistics for the bootstrapped distributions of parameters in the static, slow motion, and fast motion are in Table 4.1.

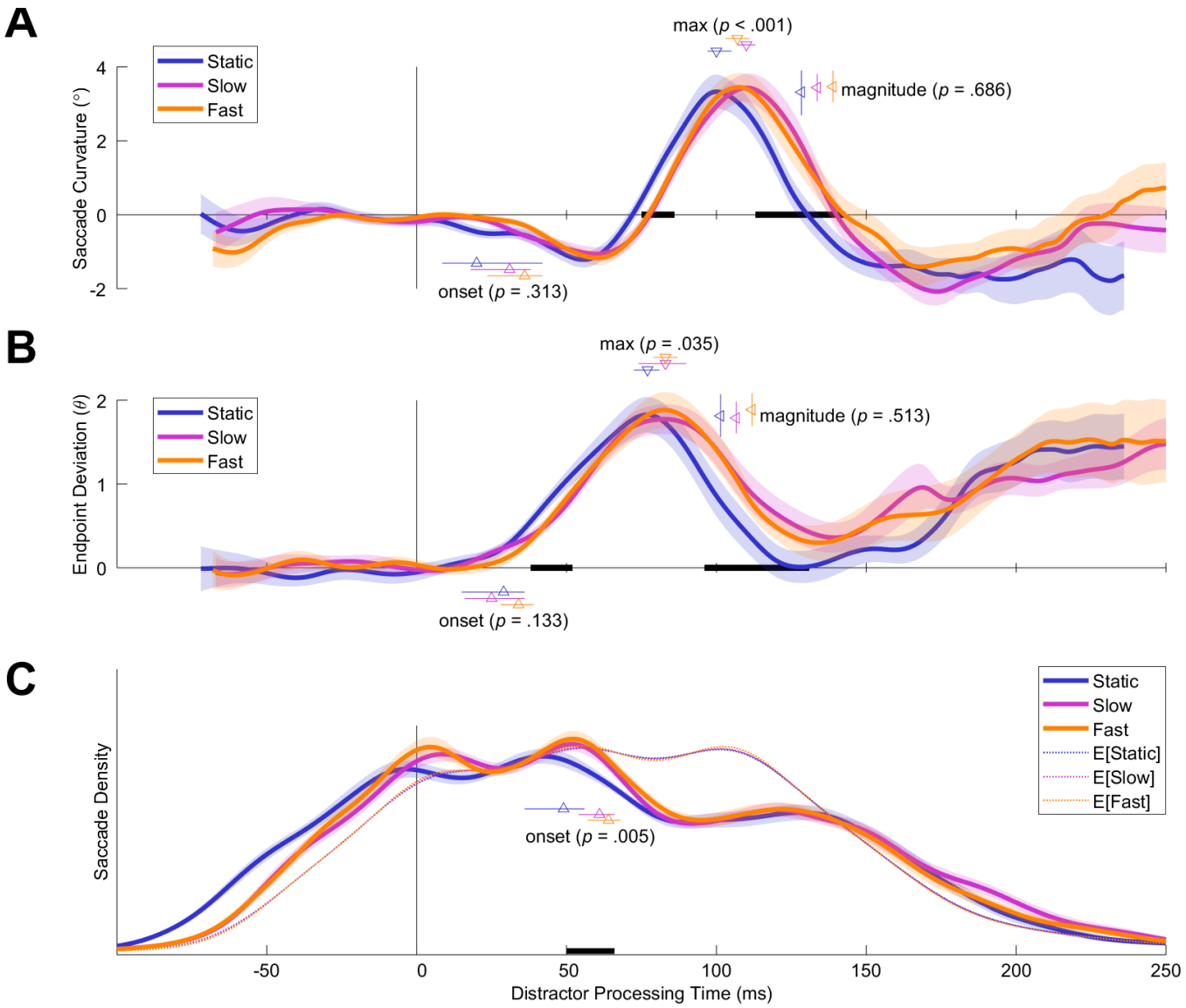

Figure 4.5. Saccade metrics as a function of distractor processing time split by static (blue), slow motion (magenta), and fast motion (orange) distractor types. Mean saccade metrics are plotted with thick, colored lines. Standard error of the mean across subjects (n = 31) is indicated by shading. Black lines along the abscissa in each panel indicate

epochs of significant (p<.05, sliding Friedman test) differences between saccade metrics. Arrowheads indicate the estimated onset latency of saccadic perturbation (▲), the estimated time of maximum saccadic perturbation (▼), and the magnitude of saccadic perturbation (◄). Arrowheads are color-coded to indicate distractor condition. Error bars intersecting the arrowheads indicate the bootstrapped 95% confidence interval of each point estimate. *P* values indicate significance (distribution test) of the difference between bootstrapped point estimates in each condition. ***A*:** Mean saccade curvature as a function of distractor processing time. ***B*:** Mean endpoint deviation as a function of distractor processing time. ***C*:** Mean saccade probability density as a function of distractor processing time. Dotted lines indicate expectation models.

For saccade curvature (see Figure 4.5*A*), the *onset* latency was not different between distractor conditions (all $p \geq .313$). The *max* latency was shorter in the static (100 ms) condition than the slow motion condition (110 ms; $p < .001$) and the fast motion condition (107 ms; $p = .012$). There was no such difference between the slow motion and fast motion conditions ($p = .144$). The *magnitude* was not different between conditions (all $p \geq .686$). The sliding Friedman analysis identified 2 epochs in which saccade curvature was significantly different between distractor conditions: 75-85 ms and 113-142 ms.

For endpoint deviation (see Figure 4.5*B*), the *onset* latency was not different between distractor conditions (all $p \geq .133$). The *max* latency was faster in the static condition (77 ms) than the fast motion condition (83 ms; $p = .035$) but was otherwise not significantly different between conditions (all $p \geq .247$). The *magnitude* was not different between conditions either (all $p \geq .513$). The sliding Friedman analysis identified 3 epochs in which endpoint deviation was significantly different between distractor conditions: 38-51 ms, 96-110, and 116-130 ms.

The *onset* latency of lower than expectation saccade density was shorter in the static condition (49 ms) than in the slow motion (61 ms; $p = .025$) and fast motion (64 ms; $p = .005$) conditions (see Figure 4.5*C*). There was no difference between the motion towards and motion

away conditions (p = .423). The sliding Friedman analysis identified a single epoch in which saccade density was different between distractor conditions (50-65 ms).

4.6.5. Visual Hemifield

We compared saccade curvature, endpoint deviation, and saccade density as a function of distractor processing time between distractor type (static, motion) × vertical visual hemifield (upper, lower) (see Figure 4.6).

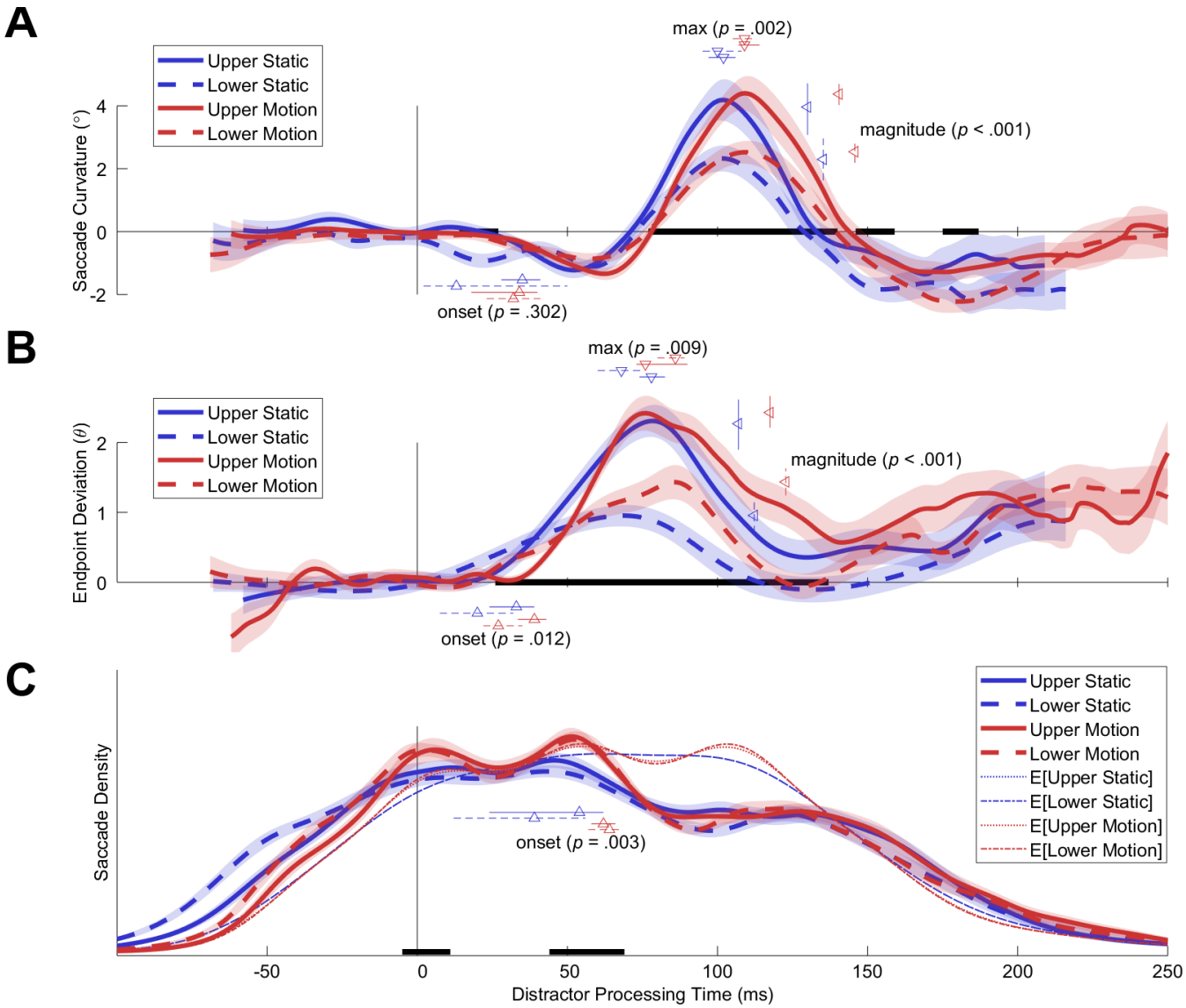

Figure 4.6. Saccade metrics as a function of distractor processing time split by distractor type (static, motion) × vertical visual hemifield (upper, lower). Static is plotted in blue. Motion is plotted in red. Upward saccades are

plotted with solid lines. Downward saccades are plotted with broken lines. Mean saccade metrics are plotted with thick, colored lines. Standard error of the mean across subjects (n = 31) is indicated by shading. Black lines along the abscissa in each panel indicate epochs of significant (p<.05, sliding Friedman test) differences between saccade metrics. Arrowheads indicate the estimated onset latency of saccadic perturbation (▲), the estimated time of maximum saccadic perturbation (▼), and the magnitude of saccadic perturbation (◄). Arrowheads are color-coded to indicate distractor condition. Error bars intersecting the arrowheads indicate the bootstrapped 95% confidence interval of each point estimate. *P* values indicate significance (distribution test) of the difference between bootstrapped point estimates in each condition. ***A*:** Mean saccade curvature as a function of distractor processing time. ***B*:** Mean endpoint deviation as a function of distractor processing time. ***C*:** Mean saccade probability density as a function of distractor processing time. Dotted lines indicate expectation models for upwards saccades. Alternating dashed/dotted lines indicate expectation models for downward saccades.

For saccade curvature (see Figure 4.6*A*), the *onset* latency was not different between distractor conditions (all $p \geq .302$). The *max* latency was shorter for all static distractor conditions than all motion distractor condition regardless of hemifield (all $p \leq .033$). There was no hemifield differences between static ($p = .609$) or motion ($p = .831$) distractors. Conversely, the *magnitude* was lesser for all lower hemifield conditions than all upper hemifield distractors condition regardless of static/motion type (all $p \leq .004$). There were no static/motion differences between lower ($p = .536$) or upper ($p = .339$) visual hemifield distractors. The sliding Friedman analysis indicated that saccade curvature was significantly different between distractor conditions across the full range of the positive saccade curvature epoch: 77-139 ms.

For endpoint deviation (see Figure 4.6*B*), the *onset* latency of the upper motion distractor was surprisingly longer than both lower visual hemifield distractors (all $p \leq .026$). No other distractor condition differences were significant (all $p \geq .079$). The *max* latency was longer for the lower motion distractor than all static distractors (all $p \leq .040$). The *max* latency was shorter

for the lower static distractor than all remaining distractors (all $p \leq .032$). No other distractor condition differences were significant (all $p \geq .193$).

The *magnitude* was different between all conditions (all $p \leq .002$), except between upper static and upper motion ($p = .442$). The sliding Friedman analysis indicated that endpoint deviation was significantly different between distractor conditions across the full range of the positive endpoint deviation epoch: 26-136 ms.

The *onset* latency of lower than expectation saccade density was shorter latency in the lower static condition than in both motion (all $p \leq .003$) conditions (see Figure 4.6*C*). There was no difference between any remaining distractor conditions (all $p \geq .062$). The sliding Friedman analysis identified two epochs in which saccade density was different between distractor conditions: −5-10 ms and 44-68 ms.

4.6.6. Distractor Processing Time Interaction with SRT

We analyzed whether distractor processing time parameters measured continuously as a function of SRT differed from distractor processing time parameters measured using the aggregate of all SRT values (see Figure 4.7). 2D analyses were performed on the data in the motion distractor condition to maximize the amount of data. We only analyzed data within the empirical 90% confidence intervals of the distractor processing time and saccadic reaction time distributions.

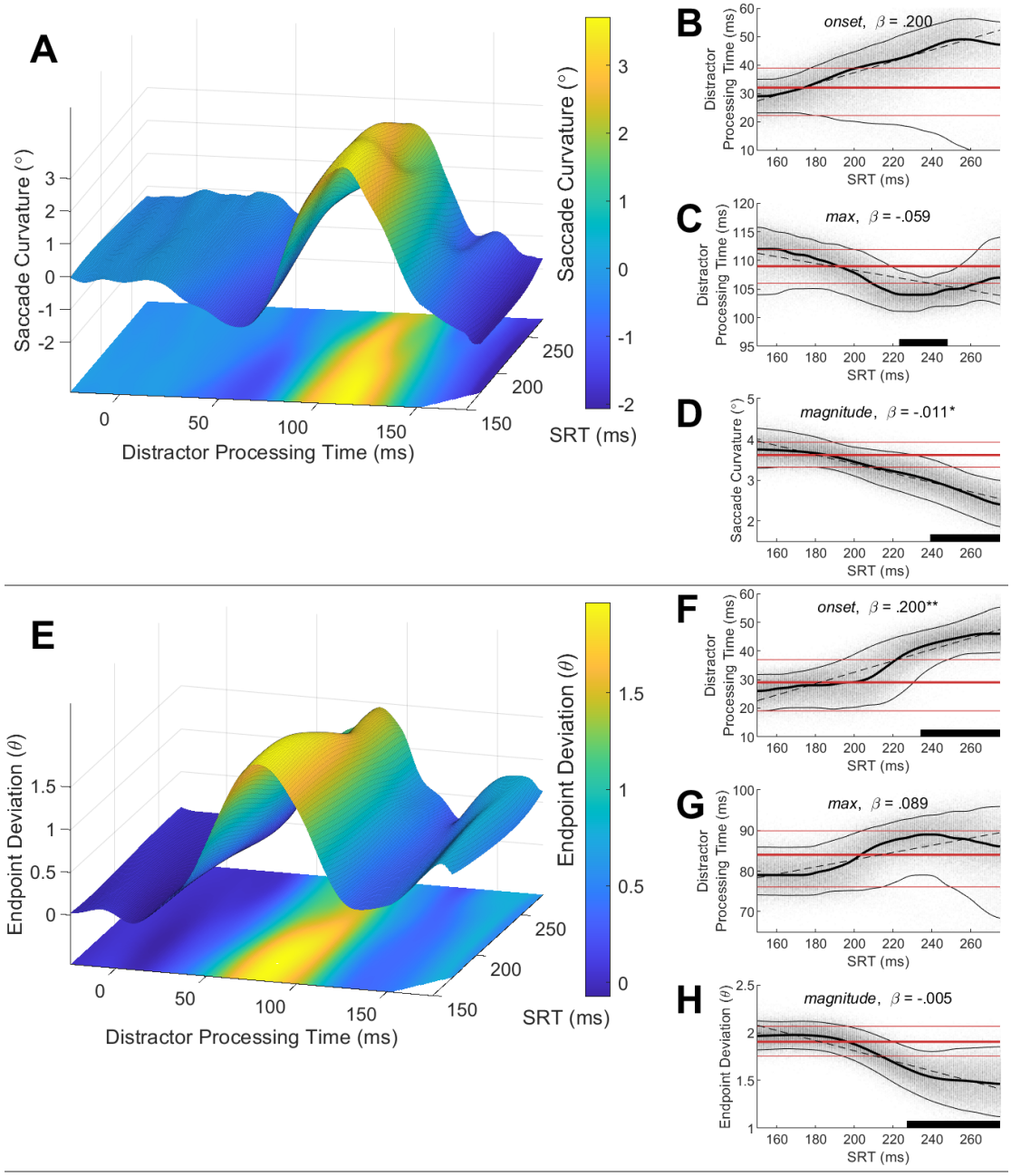
A
Saccade Curvature (°)
Distractor Processing Time (ms)
SRT (ms)
Saccade Curvature (°)
B
onset, β = .200
Distractor Processing Time (ms)
SRT (ms)
C
max, β = -.059
Distractor Processing Time (ms)
SRT (ms)
D
magnitude, β = -.011*
Saccade Curvature (°)
SRT (ms)
E
Endpoint Deviation (θ)
Distractor Processing Time (ms)
SRT (ms)
Endpoint Deviation (θ)
F
onset, β = .200**
Distractor Processing Time (ms)
SRT (ms)
G
max, β = .089
Distractor Processing Time (ms)
SRT (ms)
H
magnitude, β = -.005
Endpoint Deviation (θ)
SRT (ms)
I
Saccade Density
Distractor Processing Time (ms)
SRT (ms)
Saccade Density

Figure 4.7. Saccade metrics as a function of distractor processing time and saccadic reaction time (SRT) in the motion distractor condition. ***Left panels*:** Mean (across subjects, n = 31) saccade metrics as a function of distractor processing time and SRT plotted as a 3D manifold above a 2D heatmap with a colorbar to indicate scaling. ***Right subpanels*:** Distractor processing time parameter estimates as a function of SRT. Black dots indicate parameter estimates at each level of SRT across b=1000 bootstrapped resamples. Thick black line indicates median of bootstrapped distributions as a function of SRT. Thin black lines indicate empirical 95% confidence intervals of bootstrapped distributions as a function of SRT. Dashed black line indicates mean linear model of parameter estimates as a function of SRT fit to each bootstrapped distribution. Text labels indicates parameter type and the mean slope (β) across linear models fit to each bootstrapped distribution. Asterisks indicates significance of a one-tailed distribution test between squared, unitized slope distribution and squared, unitized model residual distribution (*p<.05, **p<.01, ***p<.001). Thick red line indicates median of constant 1D distribution of parameter estimates in the motion distractor condition. Thin red lines indicate empirical 95% confidence interval of constant 1D distribution of parameter estimates in the motion distractor condition. Black rectangles along abscissa indicate the SRT intervals in which the distribution of parameter estimates as a function of SRT was significantly different than the constant 1D distribution of parameter estimates (p<.05; sliding distribution test). ***A*:** Mean saccade curvature as a function of distractor processing time and SRT. ***B*:** Saccade curvature *onset* parameter estimate as a function of SRT. ***C*:** Saccade curvature *max* parameter estimate as a function of SRT. ***D*:** Saccade curvature *magnitude* parameter estimate as a function of SRT. ***E*:** Mean endpoint deviation as a function of distractor processing time and SRT. ***F*:** Endpoint deviation *onset* parameter estimate as a function of SRT. ***G*:** Endpoint deviation *max* parameter estimate as a function of SRT. ***H*:** Endpoint deviation *magnitude* parameter estimate as a function of SRT. ***I*:** Mean saccade density as a function of distractor processing time and SRT.

We first analyzed saccade curvature as a 2D function of distractor processing time and saccadic reaction time (see Figure 4.7*A*). The *onset* parameter was unrelated to SRT (see Figure 4.7*B*). There was no linear trend of the *max* parameter (p = .282; see Figure 4.7*C*) as a function of SRT. However, the *max* parameter as a function of SRT was significantly lower than the aggregate *max* parameter in the SRT interval of 223-248 ms. There was a significant linear trend

of the *magnitude* parameter as a function of SRT (p = .015; see Figure 4.7*D*) and *magnitude* as a function of SRT was significantly lower than the aggregate *magnitude* in the SRT interval of 239-275 ms. Note that 275 ms is the end of the SRT range in our data and that this trend may actually extend further in time.

Next, we analyzed endpoint deviation as a 2D function of distractor processing time and saccadic reaction time (see Figure 4.7*E*). There was no linear trend of the *max* parameter (p = .308; see Figure 4.7*G*) as a function of SRT. There was a significant linear trend of the *onset* (p = .003; see Figure 4.7*F*) and the *magnitude* (p = .049; see Figure 4.7*H*) parameters as a function of SRT. Correspondingly, the *onset* parameter as a function of SRT was significantly higher than the aggregate *onset* parameter in the SRT interval of 234-275 ms and the *magnitude* parameter as a function of SRT was significantly lower than the aggregate *magnitude* parameter in the SRT interval of 227-275 ms.

Finally, we analyzed saccade density as a 2D function of distractor processing time and saccadic reaction time (see Figure 4.7*I*). The LOOCV procedure correctly determined the statistical structure of the data as the 2D saccade density function was parsed into 4 disjoint distributions, one for each DTOA value. As such, we could not compare the 1D expectation model to the distractor processing time data at each level of SRT.

4.6.7. Distractor Processing Time Interaction with Amplitude

We analyzed whether distractor processing time parameters measured continuously as a function of saccade amplitude differed from distractor processing time parameters measured using the aggregate of all saccade amplitude values (see Figure 4.8). 2D analyses were performed on the data in the motion distractor condition to maximize the amount of data. We

only analyzed data within the empirical 90% confidence intervals of the distractor processing time and saccadic amplitude distributions.

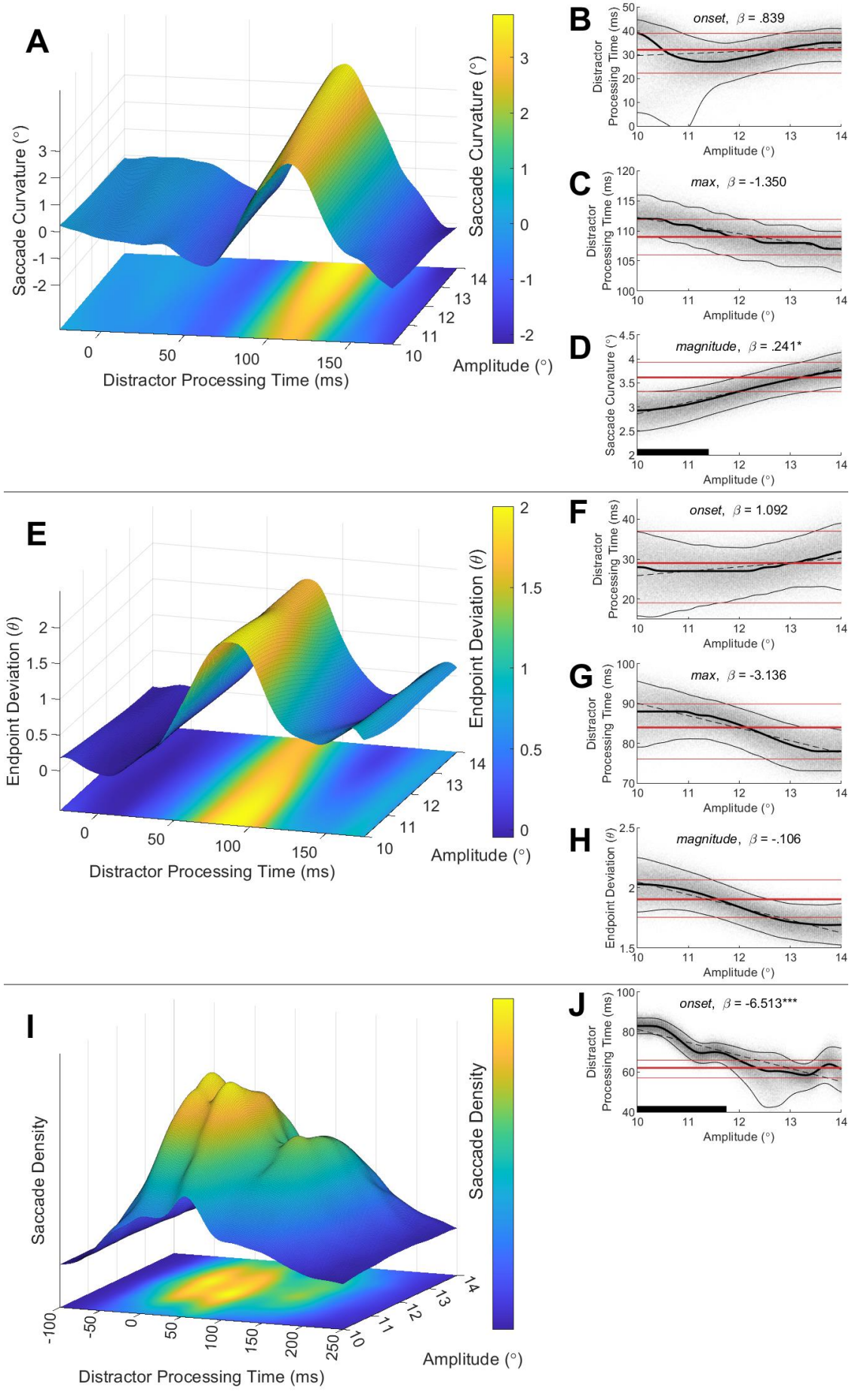
A
Saccade Curvature (°)
Distractor Processing Time (ms)
Amplitude (°)
B
onset, β = .839
C
max, β = -1.350
D
magnitude, β = .241*
E
Endpoint Deviation (θ)
F
onset, β = 1.092
G
max, β = -3.136
H
magnitude, β = -.106
I
Saccade Density
J
onset, β = -6.513***

Figure 4.8. Saccade metrics as a function of distractor processing time and saccade amplitude in the motion distractor condition. ***Left panels*:** Mean (across subjects, n = 31) saccade metrics as a function of distractor processing time and saccade amplitude plotted as a 3D manifold above a 2D heatmap with a colorbar to indicate scaling. ***Right subpanels*:** Distractor processing time parameter estimates as a function of saccade amplitude. Black dots indicate parameter estimates at each level of saccade amplitude across b=1000 bootstrapped resamples. Thick black line indicates median of bootstrapped distributions as a function of saccade amplitude. Thin black lines indicate empirical 95% confidence intervals of bootstrapped distributions as a function of saccade amplitude. Dashed black line indicates mean linear model of parameter estimates as a function of saccade amplitude fit to each bootstrapped distribution. Text labels indicates parameter type and the mean slope (β) across linear models fit to each bootstrapped distribution. Asterisks indicates significance of a one-tailed distribution test between squared, unitized slope distribution and squared, unitized model residual distribution (*p<.05, **p<.01, ***p<.001). Thick red line indicates median of constant 1D distribution of parameter estimates in the motion distractor condition. Thin red lines indicate empirical 95% confidence interval of constant 1D distribution of parameter estimates in the motion distractor condition. Black rectangles along abscissa indicate the saccade amplitude intervals in which the distribution of parameter estimates as a function of saccade amplitude was significantly different than the constant 1D distribution of parameter estimates (p<.05; sliding distribution test). ***A*:** Mean saccade curvature as a function of distractor processing time and saccade amplitude. ***B*:** Saccade curvature *onset* parameter estimate as a function of saccade amplitude. ***C*:** Saccade curvature *max* parameter estimate as a function of saccade amplitude. ***D*:** Saccade curvature *magnitude* parameter estimate as a function of saccade amplitude. ***E*:** Mean endpoint deviation as a function of distractor processing time and saccade amplitude. ***F*:** Endpoint deviation *onset* parameter estimate as a function of saccade amplitude. ***G*:** Endpoint deviation *max* parameter estimate as a function of saccade amplitude. ***H*:** Endpoint deviation *magnitude* parameter estimate as a function of saccade amplitude. ***I*:** Mean saccade density as a function of distractor processing time and saccade amplitude. ***J*:** Saccade density *onset* parameter estimate as a function of saccade amplitude.

We first analyzed saccade curvature as a 2D function of distractor processing time and saccadic amplitude (see Figure 4.8*A*). There was no linear trend of the *onset* (p = .782; see Figure 4.8*B*) or *max* (p = .215; see Figure 4.8*C*) parameters as a function of amplitude. There was a

significant linear trend of the *magnitude* parameter as a function of amplitude (p = .021; see Figure 4.8*D*) and *magnitude* as a function of amplitude was significantly lower than the aggregate *magnitude* parameter in the amplitude interval of 10.0-11.4°.

Next, we analyzed endpoint deviation as a 2D function of distractor processing time and saccadic amplitude (see Figure 4.8*E*). There was no linear trend of the *onset* (p = .629; see Figure 4.8*F*), *max* (p = .171; see Figure 4.8*G*), or *magnitude* (p = .061; see Figure 4.8*H*) parameters as a function of amplitude.

Finally, we analyzed saccade density as a 2D function of distractor processing time and saccadic amplitude (see Figure 4.8*I*). There was a strong linear trend of the *onset* parameter as a function of amplitude (p < .001; see Figure 4.8*J*) and the *onset* parameter as a function of amplitude was significantly higher than the aggregate *onset* parameter in the amplitude interval of 10.0-11.75°.

4.7. Discussion

We examined saccade curvature, endpoint deviation, and saccadic likelihood as a continuous function of time after the onset of task irrelevant static and motion distractors. We observed that the latency of saccade perturbations is longer for motion distractors than for static distractors. Furthermore, the motion distractors were either fast or slow and the motion direction was either towards or away from the target. We observed no differences in the latency or magnitude of saccade perturbations between distractor motion towards or away from the distractor or between fast and slow motion distractors. Finally, we analyzed how saccadic reaction time and saccade amplitude interact with saccade perturbations as a function of distractor processing time. We saw that the latency of saccade perturbations increased with SRT,

the magnitude of saccade perturbations decreased with SRT, and the magnitude of saccade curvature increased with saccade amplitude.

4.7.1. Distractor Features

We observed that the latency of peak saccade perturbations (*max* parameters) was ~10 ms longer for motion distractors than for static distractors. Upon onset, the first motion animation frame and static grating were indistinguishable. If visual representations of static and motion distractors were projected to the oculomotor substrates through identical channels, then no such latency difference would be expected. This latency difference is therefore consistent with our hypothesis that visual stimulus representations are projected into oculomotor substrates from the relevant cortical visual modules specialized for processing the constituent visual features characterizing the stimuli.

Middle temporal (MT) and medial superior temporal (MST) cortices process complex motion, such as the current motion grating distractor, by spatiotemporally summating downstream motion components encoded in V1, such as the current static grating distractor (Movshon et al., 1985, 1996; Zeki, 1974). MT and MST are thus situated higher in the cortical visual hierarchy (Maunsell & Van Essen, 1983) with a visual afferent delay time that is ~10 ms longer than V1 (Schmolesky et al., 1998). Furthermore, processing in MT and MST is necessary for motion perception (Bisley & Pasternak, 2000; Britten et al., 1996; Rudolph & Pasternak, 1999; Salzman et al., 1990, 1992) and certain motor behaviors like pursuit eye movements (Dürsteler et al., 1987, 1988; Komatsu & Wurtz, 1989). Given the direct connection between V1 and MT/MST (Maunsell & Van Essen, 1983), applying the 10 ms rule-of-thumb (Nowak & Bullier, 1997), one expects a 10 ms visual afferent delay latency difference between cells in these areas on average. Since V1 is sufficient for processing the static grating, and since MT is

necessary for processing the motion grating, we reason that the 10 ms latency difference we observed between static and motion distractors reflects oculomotor activation originating from different levels in the cortical processing hierarchy. Although we are unable to ascertain this speculation directly with the current behavioral methodology, this difference cannot be accounted for by other factors such as luminance contrast energy since our distractors were identical in all aspects besides motion energy. Consistent with our account of V1 and MT separately driving visual representations in oculomotor substrates, there are direct connections between V1 and superior colliculus (SC) (Fries, 1984; Lock et al., 2003), MT and SC (Maunsell & Van Essen, 1983), and MT and FEF (Schall et al., 1995b). To corroborate our speculation, future behavioral experiments could examine if these same latency differences manifest for other types of stimuli that also show strong processing ties to areas V1 and MT. For example, random white noise elicits strong activation in V1 (e.g., Pack et al., 2006), while random dot fields elicit strong activation in area MT (Albright, 1984). Like the current stimuli, these stimuli are advantageous as equalizing their contrast energy and spatial locality is trivial.

White et al. (2009) showed that visual burst onset latencies in SCi cells are ~35 ms later for maximum-chromaticity-contrast isoluminant color patches than for maximum-luminance-contrast patches. More recent work has shown that vision is trichromatically encoded in SC (Hall & Colby, 2014, 2016). However, since visual representations in SC are completely extinguished following ablation of striatal and extrastriatal cortices (Schiller et al., 1974), color information in SC must be mediated through the retinogeniculocortical pathway. The work of White et al. therefore suggests that the visual representations encoded by SCi cells were driven separately by the magno- and parvocellular processing streams in early cortex, as these processing streams bear similar visual afferent delay differences between them (Schmolesky et al., 1998) and

because isoluminant color patches would be nearly invisible to the magnocellular pathway (Livingstone & Hubel, 1987, 1988). However, this result does not imply cortical gating per se, as these stimuli were simply projected along parallel pathways with inherently different conduction latencies. In contrast, our data do suggest cortical gating, as our stimuli would very likely be projected through the same processing stream. That is, the latency differences we saw can only be explained by a delay within the magnocellular processing stream, as our grayscale stimuli would elicit very weak activation in the parvocellular processing stream where only 10% of cells are responsive to broadband stimulation (Livingstone & Hubel, 1987, 1988).

We observed no difference between the latencies of saccade trajectory perturbation onset (*onset* parameters) for static and motion distractors. These parameters indicate the earliest evidence of distractor-based spatial biasing of the saccade. For endpoint deviation and saccade curvature, these latencies were both extremely short (~25 ms) and equal across all distractor features. At such low latencies, this must reflect direct retinotectal projections and precludes the first frame being processed in V1 (Schiller & Malpeli, 1977). The earliest evidence of saccade trajectory perturbation as a function of distractor processing time diverging between static and motion distractors was after ~50 ms (i.e., 36 ms for endpoint deviation and 65 ms for saccade curvature). Qualitatively, it appeared as though the motion and static distractor processing time functions were identical in the first 50 ms, then at distractor processing times greater than 50 ms, the motion distractor processing time function was shifted behind the static function by 10 ms. Consistent with this, the drop in saccadic likelihood for static distractors occurred at 50 ms, while for motion distractors, this drop occurred at 60 ms.

These observations suggest that visual information projected into the oculomotor substrates was cascading: first, a feature-invariant retinotectal signal indicated the location of

newly acquired potential saccade targets. Second, a cortically-gated signal carried the featural information about the potential saccade targets. One alternative explanation is that this pattern of results was due to the motion animation delivering luminance transients upon every frame, whereby each new motion animation frame would elicit a rapid retinotectal swell of oculomotor activation bypassing cortex altogether. However, this cannot be the case. First, using our 85 Hz CRT to render a 40 fps animation, the first animation frame is repeated at the 11.8 and 23.5 ms refresh cycles. The second frame is finally delivered on the 35.3 ms refresh cycle. If 25 ms is the minimum retinotectal conduction time as we saw, then the second animation frame at ~35 ms is insufficient to elicit the divergence at 50 ms. Second, this account predicts that the motion distractor processing time function should grow monotonically. However, there were no magnitude differences (*max* parameters) between the static and motion distractor processing time functions. Third, the luminance transient between animation frames should be more intense for the fast motion stimulus than the slow motion stimulus, which predicts a latency or magnitude difference between fast and slow motion distractors. However, we observed no such differences (discussed in more detail below). Given these reasons, the more plausible explanation is that the second motion animation frame engaged motion processing cortical areas that provided much stronger inputs to the oculomotor substrates and/or gated V1 visual projections to oculomotor substrates. Future investigations could test this reasoning by repeating this experiment using a higher refresh rate.

The lack of saccade perturbation latency or magnitude differences between distractor motion towards and away from the target was surprising, as large-field visual motion (Kawano & Miles, 1986; Miles et al., 1986) and small motion patches (Fallah & Reynolds, 2012) can reflexively elicit pursuit eye movements in the direction of the task-irrelevant motion stimulus.

Since directional biasing of saccades and pursuit eye movements can be elicited by microstimulation from within the same oculomotor (Krauzlis & Miles, 1998; Yan et al., 2001) and visual (Groh et al., 1997) substrates, we expected that our motion distractors would also elicit reflexive directional biasing of saccades as with pursuit. If so, saccades would show increased trajectory perturbations towards the distractor for distractor motion directed away from the target, which we did not observe. There are at least two explanations for this: first, reflexive ocular following responses are observed immediately after the execution of saccades terminating in the motion field (Fallah & Reynolds, 2012; Kawano & Miles, 1986; Miles et al., 1986), and therefore, likely arise from motion introducing spatial error signals during post-saccadic retinal stabilization processing. As saccades on our task passed through empty space and terminated on stationary targets, we would not expect dynamic spatial error signals during saccade execution or post-saccade at the saccade termination loci. Future iterations of the task could require observers to saccade through or onto a motion field to test this possibility. Second, perhaps small motion patches may only bias eye movement vectors in the context of competing motion information. Competing motion signals are encoded in MT and MST as a vector-weighted average of the motion directions on short post-stimulus time scales (Groh et al., 1997; Recanzone & Wurtz, 1999, 2000). MT and MST are critical for resolving motion-based competition during oculomotor processing (Dürsteler et al., 1987, 1988; Komatsu & Wurtz, 1989). However, since the current target did not elicit motion competition, perhaps the oculomotor system did not utilize the distractor motion information to reweight the distractor visual representation during target selection on this task. A simple test of this speculation is to repeat this task with motion targets.

A subpopulation of cells in superior colliculus exhibits inherent motion direction sensitivities whereby they discharge higher activation for motion directed into their motor field (Horwitz & Newsome, 1999, 2001). As such, we expected that distractor motion towards the target would elicit higher target activation than distractor motion away from the target. This would bias a vector-weighted average computation in favor of the target for distractor motion towards the target. In such a case, the distractor motion away condition should elicit higher saccade perturbations than the motion towards condition; however, we did not observe this. It could be that the 30% of motion selective cells in the population (Horwitz & Newsome, 2001) which would drive this effect constitute too few of the cells encoding the stimuli to significantly bias the vector average computation.

The current experiment was the first within subjects comparison of features processed in the same cortical modules to features processed in different cortical modules using our behavioral paradigm. Cortical area MT processes fast and slow motion stimuli with no apparent visual afferent delay time differences as a function of motion strength (Azzopardi et al., 2003). As such, comparing the saccade perturbation latencies of fast and slow motion distractor types provided a complimentary test of our hypothesis that visual representations are projected into the oculomotor substrates from relevant cortical modules. As these stimuli are processed in the same cortical module, we did not expect saccadic perturbation latency difference between them, consistent with our results. Additionally, contrasting this observation with the 10 ms difference between motion and static gratings illustrates that our latency effects are related to featural complexity and not simply differences between motion strength. One possibility is that our fast and slow motion speeds were not sufficiently differentiated to elicit a true difference (see ffychte et al., 1995). Although this account is discredited by Azzopardi et al. (2003), it could

nevertheless be investigated in future iterations of this experiment using markedly different motion speeds (e.g., 5 °/s vs. 25 °/s).

4.7.2. Non-Invasive Computational Modelling of Target Selection

We observed clear evidence of an initial epoch of negative curvature preceding the subsequent epoch of positive curvature. We also observed this phenomenon in the previous two investigations of saccade perturbations as a function of distractor processing time and either dismissed this effect (Kehoe & Fallah, 2017) or interpreted it as top-down inhibition (Kehoe et al., 2021). However, the vector-weighted average model of Port and Wurtz (2003) offers a more plausible explanation: saccade trajectories are computed as the instantaneous vector-weighted average of the target and distractor vectors weighted by the activation at the target and distractor loci on the oculomotor map. This computation occurs between approximately 30 to 0 ms prior to saccade execution (McPeek et al., 2003, 2006; Port & Wurtz, 2003; White et al., 2012). As can be seen in Figure 4.9*B*, when distractor processing time begins to exceed 0, the distractor visual onset burst sweeps into the upper bound of the critical epoch. This distractor competition only affects the late portion of the saccade programming, so the saccade is initially straight but then veers towards the distractor in the latter portion. As such, the saccade is curved and the endpoint is biased towards the distractor. However, given our conceptualization of saccade curvature, saccades with this shape are negatively signed, as the deviations are directed away from the distractor with respect to a straight line connecting the beginning and end of the saccade. As can be seen in Figure 4.9C, when distractor processing time increases further, the distractor visual onset burst eventually begins to align with the lower bound of the critical epoch. Therefore, the initial portion of the saccade is heavily biased towards the distractor, while the latter portion of the saccade is less averaged and directed straight towards the target. When this occurs, we see

positively signed saccade curvature as these initial deviations are directed towards the distractor with respect to a straight line connecting the beginning and end of the saccade. Interestingly, this computation also presupposes that saccade deviations directed away from the distractor with respect to a straight line between fixation and the target would require a negative contribution from the distractor, such as inhibition at the distractor locus (see Aizawa & Wurtz, 1998; White et al., 2012). Testing various inhibitory mechanisms as inputs into the vector average model would provide insight into the nature of saccade deviations away from distractors, as we plan to do in future investigations.

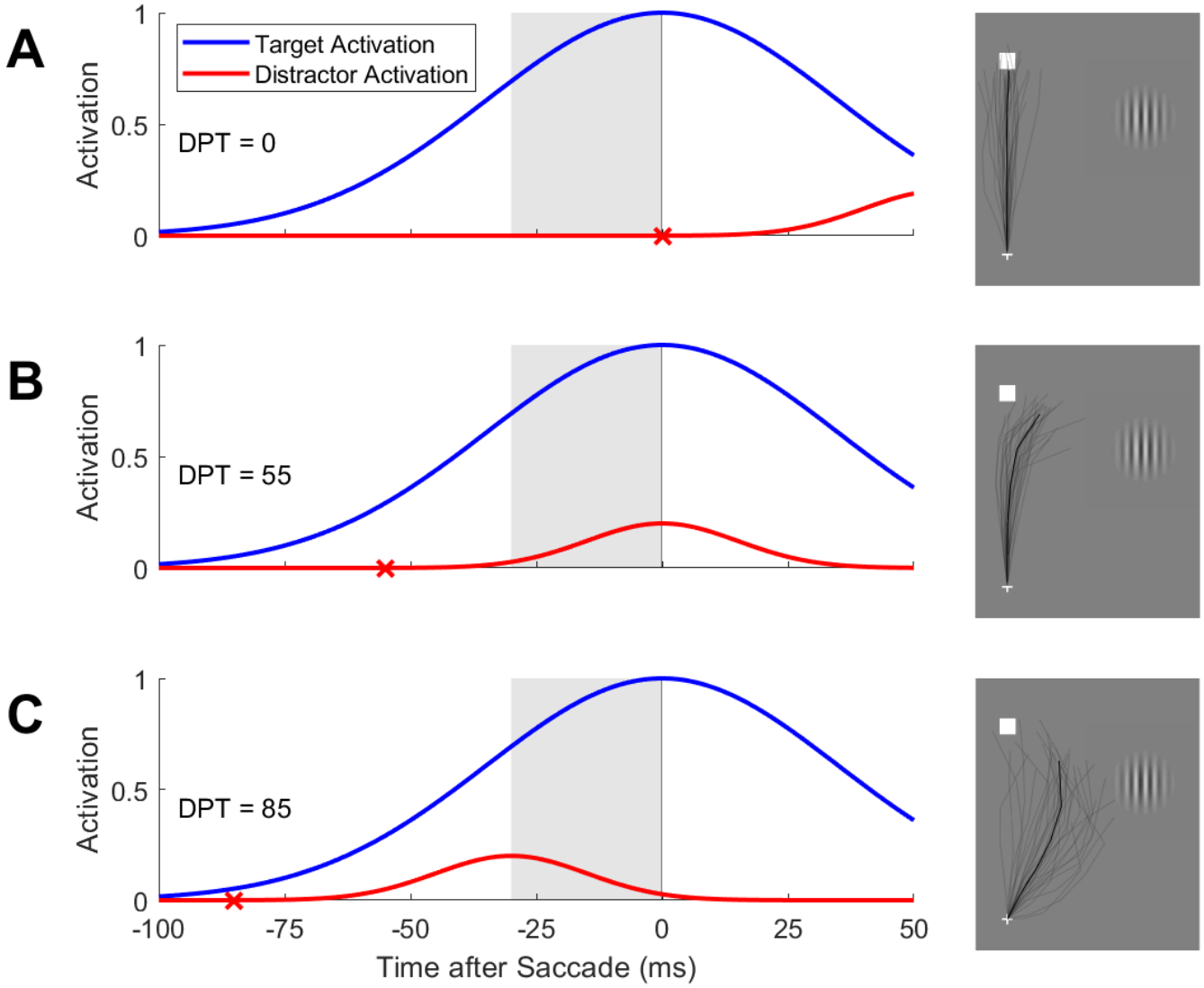

Figure 4.9. Theoretical and empirical saccadic vector-weighted averaging. ***Left panels:*** Hypothetical neural activation as a function of time before saccade initiation for oculomotor cells encoding the target (blue) or the distractor (red). Gray shaded region indicates the critical epoch between 30 and 0 ms prior to saccade initiation. Saccade trajectories are determined by the vector-weighted average of the target and distractor activation functions in the critical epoch. Red "x" indicates the distractor onset time. Text label indicates corresponding distractor processing time (DPT). Distractor activation functions had a 30 ms initial phase as reported elsewhere (McPeek and Keller, 2002) and a lead time of 25 ms after distractor onset as was observed in the current experiment. ***Right panels:*** Example displays with target (square), fixation ("+"), distractor (grating), and observed saccade trajectories (gray and black traces). Gray traces are average saccade trajectories for each subject at the respective distractor processing time (± 5 ms) indicated by the text label in each row. Trajectories were angularly scaled by 10 degrees for illustrative purposes (e.g., a saccade trajectory angled 45 degrees towards the distractor was actually observed as only 4.5 degrees). Black traces are the average saccade trajectories across subjects. ***A:*** Distractor onset occurs at the time of saccade initiation (distractor processing time = 0). The visual onset burst elicited by the distractor is well outside the critical epoch and no averaging should occur. This is consistent with observation as saccades were straight at this DPT. ***B:*** Distractor onset occurs 55 ms before saccade initiation (distractor processing time = 55). The visual onset burst is aligned with the upper portion of the critical epoch. Minimal averaging should occur in the early portion of the saccade, while maximum averaging should occur in the latter portion of the saccade. This is consistent with observation as, at this DPT, saccades were initially straight but then curved towards the distractor in the latter portion. ***C:*** Distractor onset occurs 85 ms before saccade initiation (distractor processing time = 85). The visual onset burst is aligned with the lower portion of the critical epoch. Maximum averaging should occur in the initial portion of the saccade, but minimal averaging should occur in the latter portion of the saccade. This is consistent with observation as, at this DPT, the saccade is initially directed in between the target and distractor, but angles back towards the target in the latter portion.

As in a previous investigation of saccade perturbations as a function of distractor processing time (Kehoe et al., 2021), we corroborated our saccade trajectory perturbation metrics with an additional metric: saccade initiation perturbation, that is, a drop in saccade likelihood relative to an expectation model. Drops in saccade density have been observed ~60 milliseconds

after flashes of light (Reingold & Stampe, 2002) or irrelevant distractor onsets (Bunocore & McIntosh, 2012). This drop in saccadic likelihood may be related to rapid lateral inhibition in SC (Munoz & Istvan, 1998), as a similar drop in microsaccade rates is observed after the onset of a stimulus (Engbert & Kliegl, 2003; Hafed & Ignashchenkova, 2013; Rolfs et al., 2008). However, in the current experiment, we observed that the latency of this drop in saccadic likelihood was ~10 ms longer for motion stimuli than for static stimuli. This observation provides further validation of our saccade trajectory perturbation metrics and corroborates our account that visual input into the oculomotor system is cortically-gated on the basis of features, even when the features are task irrelevant.

We split the data into upwards and downwards saccades and repeated our analysis of static and motion distractors. We observed that the magnitude of saccadic trajectory perturbations was much stronger in the vertical hemifield than the lower hemifield, as expected since visual activations are much stronger in the upper visual hemifield (Hafed & Chen, 2016). For saccade curvature and saccadic likelihood, the overall pattern of latency results generalized across the two vertical hemifields: the motion activation lagged behind the static activation by approximately ~10 ms regardless of hemifield. For endpoint deviation, the results were less clear. We surprisingly saw that the estimated onset latency of endpoint deviation for upper motion distractors was slower than both lower distractors. However, visual activation latencies should be faster in the upper visual field (Hafed & Chen, 2016), which suggests this is likely an artefact.

4.7.3. Saccadic Reaction Time and Amplitude

Previous behavioral studies examining the time-course of saccade perturbations (McSorley et al., 2006; Mulckhuyse et al., 2009) have not disentangled the role of executive

processing (SRT) from sensory processing (distractor processing time). Here, we examined the interaction of distractor processing time and SRT and observed that the qualitative pattern of distractor processing time results is stable across the observed range of SRT, but with certain quantitative differences. First, the magnitude of peak saccade trajectory perturbations as a function of distractor processing time (*max* parameter) monotonically decreased as a function of SRT. In fact, both trajectory perturbation metrics, saccade curvature and endpoint deviation, showed a nearly 50% peak perturbation magnitude reduction between the shortest (150 ms) and longest (275 ms) SRTs. This is consistent with the results from our recent experiment investigating the distractor processing time and SRT interaction elicited by markedly different stimuli: task-relevant, complex objects (Kehoe et al. 2021). This therefore demonstrates that this effect is robust across stimulus categories. Second, the initial onset latency of saccade trajectory perturbation as a function of distractor processing time (*onset* parameter) showed a monotonic increase as a function of SRT whereby at the shortest SRTs, the onset latency of saccade trajectory perturbations was merely 20 ms, and at the longest SRTs, it had increased to 50 ms.

Our results suggest that the magnitude and latency of the visual onset responses encoding distractors were gradually attenuated as a function of SRT. This implicates the role of executive processing in gating sensory input into the oculomotor system. The voluntary control of saccades is largely mediated by the cortico-nigral-tectal pathway, whereby executive cortices modulate basal ganglian activity and the substantia nigra pars reticulata of the basal ganglia (SNr) imposes tonic GABAnergic inhibition on the superior colliculus (reviewed by Hikosaka et al., 2000). This circuit controls the sensitivity of VM cells in SC to sensory stimulation: GABA antagonist injections in SC produce spontaneous, irrepressible saccades into empty regions of space (Hikosaka & Wurtz, 1985a), while GABA agonist injections in SC produce misdirected,

hypometric, long latency, low-velocity saccades and decreased saccadic likelihood (Aizawa & Wurtz, 1998; Hikosaka & Wurtz, 1985a; McPeek & Keller, 2004). These deficits are replicated by pharmacologically deactivating (Hikosaka & Wurtz, 1985b) and microstimulating (Basso & Liu, 2007; Liu & Basso, 2008) SNr (respectively). The sensitivity of SC cells to sensory stimulation is directly related to SRTs as observed in express saccades, whereby visual onset responses themselves reach motor threshold and elicit extremely short latency saccades (Dorris et al., 1997; Marino et al., 2015). This mechanism provides a plausible explanation of the current interaction of SRT and distractor processing time. Perhaps on certain trials the oculomotor system was visually desensitized via tonic inhibition to minimize the competitive influence of the distractor and thus facilitate task performance, which incidentally increased SRT. We suspect that this desensitization would increase over the course of the experiment, as we observed previously that saccade perturbation magnitudes gradually decreased throughout the course of a similar experiment (Kehoe et al., 2021).

We analyzed the interaction of distractor processing time and saccadic amplitude, as saccadic amplitude is indicative of target motor activation independently of distractor visual activation. We observed that peak saccade curvature (*magnitude* parameter) strongly increased as a function of saccadic amplitude. This effect is expected from an open-ended movement field encoding scheme as seen in approximately one third of collicular neurons: saccades of equal or lesser amplitude than the cell's preferred amplitude elicit a motor burst that reaches peak excitability at the time of movement initiation, while for saccades greater than the cell's preferred amplitude, the motor burst reaches peak excitability at increasingly longer latencies after movement initiation (Munoz & Wurtz, 1995a, 1995b). Critically, for such cells encoding the target direction, saccades with a longer-than-preferred amplitude would elicit a motor burst

outside of the perisaccadic interval, the interval between 30 to 0 ms prior to saccade initiation when vector-weighted averaging occurs (McPeek et al., 2003, 2006; Port & Wurtz, 2003; White et al., 2012). Longer-than-preferred amplitude saccades would therefore diminish the target-encoding cells' contribution to the vector-weighted average computation and saccadic spatial biasing towards the distractor should increase, as observed.

We also observed that the onset latency of an abrupt drop in saccadic likelihood (*onset* parameter) strongly decreased with saccadic amplitude. This effect suggests that less lead time of a visual distractor is required for cancelling a longer saccade than for a shorter saccade. Our distractor processing time variable is equal to the distractor lead time prior to saccade onset. As such, the distractor processing time latency of an abrupt drop in saccadic likelihood can be interpreted as the minimum lead time necessary to inhibit an impending saccade. Saccades can be effectively canceled at any point midflight (Robinson et al., 1969, 1972). Since longer saccades extend longer in time, there is a longer effective window for cancelling them.

4.7.5. Conclusions

Oculomotor planning and motion processing are inextricably linked (Dürsteler et al., 1987, 1988; Komatsu & Wurtz, 1989). We utilized our human behavioral paradigm (Kehoe et al., 2017, 2021) to show that during target selection, motion information is encoded by the oculomotor system after a 10 ms delay as compared to static stimuli, even though both stimulus types were task irrelevant. We suggest that this delay therefore reflects an inherent visual encoding property of the oculomotor system: visual representations are cortically gated to accommodate sufficient featural analysis. This gives insight into the process by which visual representations on oculomotor maps are feature-weighted to facilitate accurate target selection of

behaviorally relevant stimuli (Bichot et al., 1999; Horwitz & Newsome, 1999, 2001; McPeek & Keller, 2002; Shen &Paré, 2007).

Chapter 5. Oculomotor Feature Discrimination is Cortically Mediated

This manuscript has been published in *Frontiers in Systems Neuroscience*:

Kehoe, D. H., & Fallah, M. (2023). Oculomotor feature discrimination is cortically mediated. *Frontiers in Systems Neuroscience, 17*, 1251933. https://doi.org/10.3389/fnsys.2023.1251933

This manuscript was written in response to an invitation to contribute to the *Rising Stars in Neuroscience 2022* collection in *Frontiers in Systems Neuroscience*. I elected to submit a *Theory and Perspective* article type. The manuscript synthesizes my previously published manuscripts into a broad theoretical account of how cortical feature processing contributes to oculomotor target selection. As such, I have included this manuscript in my dissertation in the place of an unpublished General Discussion chapter.

5.1. Abstract

Eye movements are often directed towards stimuli with specific features. Decades of neurophysiological research has determined that this behavior is subserved by a feature-reweighting of the neural activation encoding potential eye movements. Despite the considerable body of research examining feature-based target selection, no comprehensive theoretical account of the feature-reweighting mechanism has yet been proposed. Given that such a theory is fundamental to our understanding of the nature of oculomotor processing, we propose an oculomotor feature-reweighting mechanism here. We first summarize the considerable anatomical and functional evidence suggesting that oculomotor substrates that encode potential eye movements rely on the visual cortices for feature information. Next, we highlight the results from our recent behavioral experiments demonstrating that feature information manifests in the oculomotor system in order of featural complexity, regardless of whether the feature information is task-relevant. Based on the available evidence, we propose an oculomotor feature-reweighting mechanism whereby (1) visual information is projected into the oculomotor system only after a visual representation manifests in the highest stage of the cortical visual processing hierarchy necessary to represent the relevant features and (2) these dynamically recruited cortical module(s) then perform feature discrimination via shifting neural feature representations, while also maintaining parity between the feature representations in cortical and oculomotor substrates by dynamically reweighting oculomotor vectors. Finally, we discuss how our behavioral experiments may extend to other areas in vision science and its possible clinical applications.

5.2. Contribution to the Field Statement

Visual features are the elementary constituents of the visual environment (e.g., color, motion, orientation). We routinely and effortlessly move our eyes to objects with specific

features and ignore objects with other features. Yet, surprisingly, a detailed theoretical account of the mechanism that incorporates visual features into eye movements to achieve this behavior is lacking. Here, we posit such a mechanism based on (1) a clear functional dissociation between two neural systems, a perceptual system that processes visual features and an oculomotor system that plans eye movements; and (2) a series of recent experiments illustrating that visual objects are incorporated into eye movements in order of visual complexity. We propose that a visual object engages a particular set of substrates in the perceptual system necessary for representing its constituent features and visual projections into the oculomotor system are bottlenecked until after this representation has manifested. Cognitive mechanisms may then operate on the perceptual representation to satisfy behavioral goals and the perceptual system dynamically updates the feature representations in the oculomotor system to maintain parity. Our theory addresses a decades-long gap in our understanding of oculomotor processing; accounts for a wide range of observations in oculomotor research; and makes clear, testable predictions.

5.3. Introduction

As your eyes scan through your sock drawer looking for your favourite blue socks, you redirect your gaze to each pair of blue socks one-by-one. Although you attempt to ignore all other colors, you occasionally find yourself distracted by the same pair of bright red socks, which repeatedly draw your gaze back to them. Anecdotes like this illustrate how visual features guide our voluntary and reflexive eye movements in our daily lives, a phenomenon also routinely observed in primate vision experiments. For example, when humans or monkeys perform goal-directed search for a previewed target, their eye movement selections (Pomplun et al., 2001; Shen & Paré, 2006; Shen et al., 2000) and saccade trajectories themselves (Kehoe et al., 2018a, 2018b; Giuricich et al., 2023) are biased for objects that share features with the target.

Conversely, during task-free viewing of natural scenes, human (Berg et al., 2009; Parkhurst & Niebur, 2003; Parkhurst et al., 2002; Peters et al., 2005) and monkey (White et al., 2017a) eye movements are disproportionately directed towards areas in the scene with the most salient features. Although feature-guided eye movements are so ubiquitous, surprisingly little research has investigated the cognitive and neural mechanisms that incorporates visual features into impending eye movement programs.

5.4. Feature-Guided Eye Movements

Feature-guided eye movements require several processing steps: the spatial position of potential eye movement targets must be encoded, each potential target must be feature-weighted according to behavioral goals, a winner in the set of potential targets must be selected, and the spatial code of the winner must be converted into movement instructions and sent to the extraocular muscles. All these processing steps are observed in the oculomotor substrates of the primate nervous system.

The primate oculomotor system encodes the loci of visual stimuli and potential eye movements as direction-amplitude vectors on orderly retinotopic motor maps, whereby sufficient activation of a specific vector elicits an eye movement with the corresponding direction and amplitude (Bruce et al., 1985; Robinson & Fuchs, 1969; Robinson, 1972). This is perhaps nowhere more apparent than in the superior colliculus (SC; Mays & Sparks, 1980; Munoz & Wurtz, 1995; Sparks, 1978; Wurtz & Goldberg, 1971, 1972) and frontal eye fields (FEF; Bruce & Goldberg, 1985; Goldberg & Bushnell, 1981; Schall et al., 1995a). In these substrates—SC (Horwitz & Newsome, 1999, 2001; Kim & Basso, 2008; Krauzlis & Dill, 2002; Li & Basso, 2005; McPeek & Keller, 2002; Shen & Pare, 2007, 2014) and FEF (Bichot et al., 1996; Sato & Schall, 2003; Sato et al., 2001; Schall & Hanes, 1993; Schall et al., 1995a; Thompson et al.,

1996)—the featural identity of visual stimuli can be decoded from the neural activity encoding impending eye movements (see Figure 5.1). However, this feature encoding unfolds over time. After the onset of a visual stimulus, oculomotor neurons encode the presence of the stimulus with a rapid swell of activation (reviewed by Boehnke & Munoz, 2008). This early activation is feature invariant but is soon reweighted by the feature-based behavioral relevance and conspicuity of the stimulus, typically between 50 and 100 ms after the start of the visual onset burst (reviewed by Fecteau & Munoz, 2006).

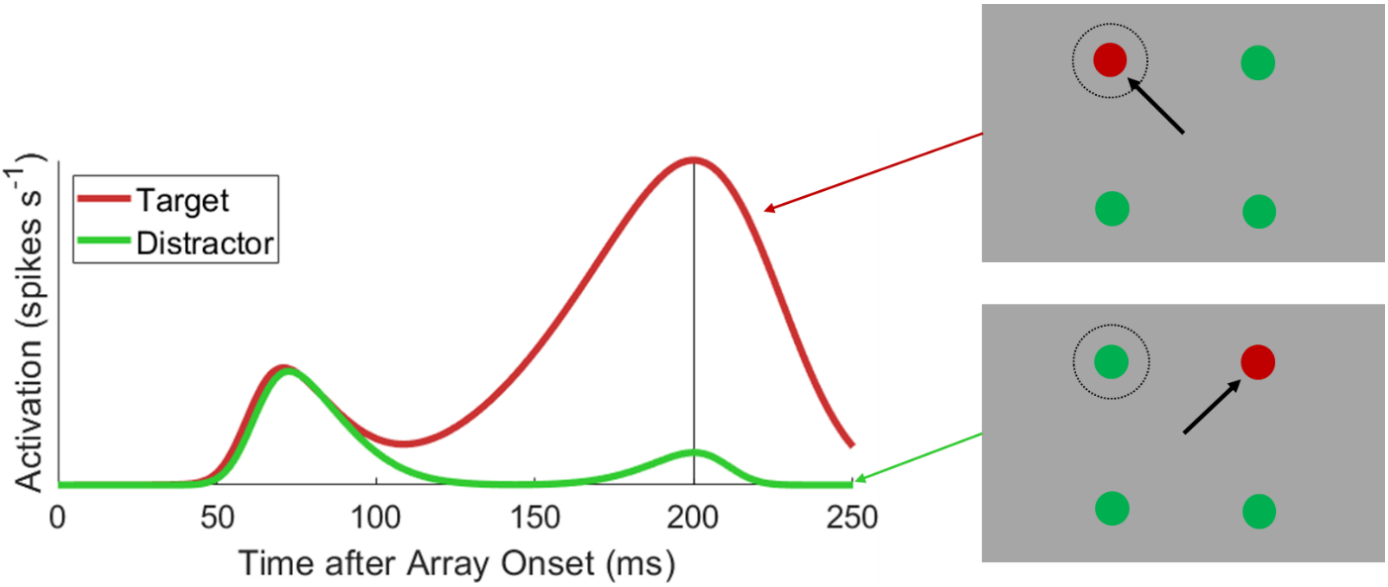

Figure 5.1. Typical visuomotor neural activation during feature-based target selection. Depicted is a hypothetical color-oddity saccade task (right insets), where monkeys saccade to a red target amongst green distractors and spikes are collected from a visuomotor cell whose motorfield aligns to the top-left stimulus position in the search array. Activation is plotted as a function of time after search array onset when either a target (red line) or distractor (green line) is placed into the motorfield. There is a feature invariant visual onset burst approximately 50 ms after array onset. After approximately 100 ms, activation encoding targets and distractors diverges (i.e., discrimination time), where target activation ramps up to a motor burst triggering a target-directed saccade and distractor activation decays to baseline.

Two alternative explanations could account for feature-reweighting of competing

incipient oculomotor programs routinely observed in oculomotor research: oculomotor substrates process visual features independently of and in parallel to the perceptual system, or alternatively, potential eye movements encoded in oculomotor substrates could be dynamically feature-weighted by the perceptual system. Although the latter account is widely held—that feature inputs from the perceptual system are pivotal for feature-guided eye movements (cf. Fecteau & Munoz, 2006; Schall & Cohen, 2011)—a more detailed theory of the mechanism subserving this process is lacking. What are the factors that determine when feature-reweighting occurs during the time course of oculomotor processing? Where in the perceptual system does this feature information originate? Is this featural mechanism task-dependent or fundamental? These questions have been largely unaddressed.

In this article, we have several goals: (1) to dispel the notion that oculomotor substrates are sufficient for feature-guided eye movements, and to argue instead that feature-reweighting of oculomotor vectors is driven by dynamic input from the perceptual system; (2) summarize recent experiments revealing the feature-dependent time scale of visual encoding in the oculomotor system; (3) based on these experiments, propose a broad theoretical account of the interplay between perceptual and oculomotor systems that facilitates top-down feature-guided eye movements and bottom-up feature encoding in oculomotor substrates more broadly; and (4) lastly, to discuss how the same experimental paradigms used to measure the latency of feature information in the oculomotor system can be used to answer other questions in vision science and possibly even offer a practical diagnostic tool in clinical neuropsychology.

5.5. Oculomotor Substrates Are Insufficient for Feature-Reweighting

For neural systems to be even theoretically capable of guiding behavior to specific visual features, they must include feature filters that intrinsically encode specific visual features. In this

section, we summarize experimental evidence spanning decades that demonstrates that oculomotor substrates depend upon cortical inputs for feature information. In this view, oculomotor substrates contribute to target selection by integrating visual feature information onto spatial movement coordinates. If so, oculomotor and perceptual substrates ought to be functionally dissociable. Therefore, in this section we also summarize the evidence from ablation, inactivation, and microstimulation studies supporting this functional dissociation.

5.5.1. Inherent Feature Encoding

The visual perceptual system encodes the size, location, and features of visual stimuli on retinotopic maps widely distributed across a tangled web of cortical modules most famously catalogued by the meticulous work of Van Essen et al. (see Figure 5.2). These classic neuroanatomy studies of the connections between visual cortical modules have revealed a clear hierarchical organization between modules (Felleman & Van Essen, 1991; Van Essen & Maunsell, 1983; Van Essen et al., 1992), the cortical visual hierarchy. The cortical visual hierarchy is primarily organized such that vision is successively projected to increasingly anterior cortical sites along the posterior-to-anterior axis. Intriguingly, the cortical visual hierarchy also exhibits functional hierarchical organization, as the receptive field size, visual onset latency, and representational complexity of visual neurons within modules successively increases at each level of the anatomical hierarchy. Although there is debate about whether the functional-anatomical hierarchical correspondence has meaningful implications for the nature of visual processing more broadly (Bullier & Nowak, 1995; Hegde & Felleman, 2007), the existence of the functional visual hierarchy is undisputed (cf. Hegde & Felleman, 2007). Furthermore, the functional hierarchy is the basis for many successful formal models of visual processing (e.g., Riesenhuber & Poggio, 1999, 2000; Serre et al., 2007). As such, we will herein

used the term cortical visual hierarchy to describe the anatomical and/or functional hierarchy interchangeably.

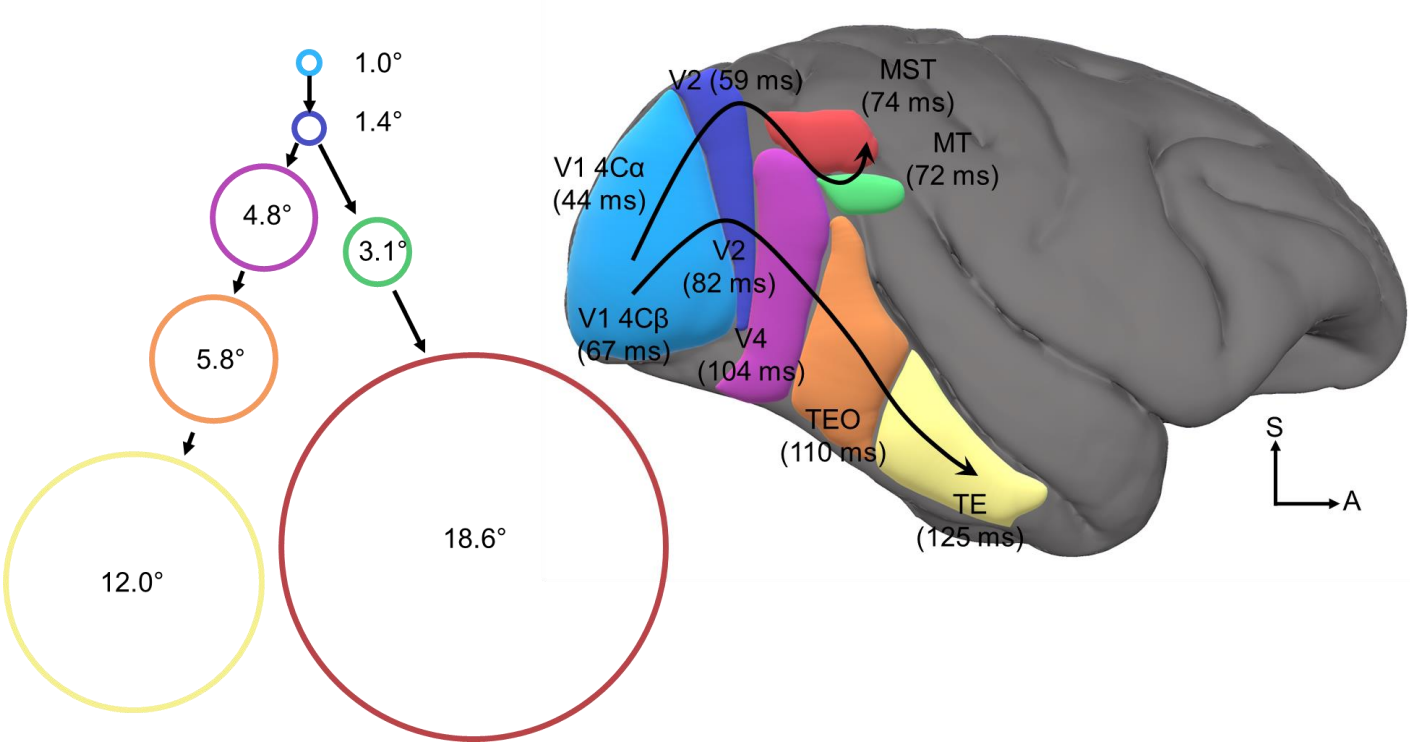

Figure 5.2. Visual cortical hierarchy. Depicted is a right lateral view of macaque cortex with several color-coded and labelled visual cortical areas. Bracketed values indicate average onset latencies as reported by Schmolesky et al. (1998) for V1/V2/V4/MT/MST and Nowak & Bullier (1997) for TEO/TE. Curved black arrows trace the dorsal and ventral processing streams. Circles are color-coded to indicate visual cortical area and scaled in size to indicate average visual receptive field area at the fovea as reported by Kravitz et al. (2013) for V1/V2/V4/TEO/TE and Raiguel et al. (1997) for MT/MST. Accompanying receptive field labels specify the receptive field diameter in degrees of visual angle.

In each module of the cortical visual hierarchy, feature filters extract specific visual attributes (e.g., direction, color, orientation). These feature representations are then projected upstream to the next processing stage where they are pooled or transformed into increasingly complex feature representations (Brincat & Connor, 2004, 2006; Livingstone et al., 2001; Mineault et al., 2012; Yau et al., 2013). As neural projections between cortical modules are

bound by some conduction velocity, the average visual onset latency of neurons increases somewhat linearly in successively higher stages of the hierarchy (Nowak & Bullier, 1997; Schmolesky et al., 1998). It is important to note that ascribing strict representational feature sets and visual onset latencies to specific cortical modules is an oversimplification, but this scheme does serve as a useful and widely adopted heuristic.

Experimentally detecting inherent feature encoding in oculomotor substrates is convoluted in the context of target selection. Target selection refers to the oculomotor behavior whereby a target must be discriminated from distractors and selected for an eye movement. Often, this discrimination is based on visual features (see Figure 5.1). Critically, whether oculomotor vectors are reweighted by visual features per se or simply by behavioral choices is indistinguishable in this context. Single target saccade and passive viewing paradigms circumvents this issue and has indeed revealed several seemingly inherent feature sensitivities in the intermediate (visuomotor) layers of SC: orientation (Chen & Hafed, 2018), spatial frequency (Chen & Hafed, 2017), color (White et al., 2009), motion direction (Davidson & Bender, 1991; Horwitz & Newsome, 2001), and face detection (Le et al., 2020; Nguyen et al., 2014). Similarly, a classic study of FEF visual response properties found that 12% of purely visual FEF neurons show featural sensitivity for color and motion (Mohler et al., 1973), while more recent studies have found that between 31-54% of visuomotor FEF neurons exhibit sensitivity for motion direction and speed (Barborica and Ferrera, 2003; Xiao et al., 2006).

A classic experiment by Schiller et al. (1974) provides some insights into the origin of these seemingly inherent feature sensitivities in oculomotor substrates. They demonstrated that the visual feature sensitivities exhibited by SC neurons must be driven by cortical inputs. After the ablation or cortical cooling of striate and extrastriatal cortices, visual responses, but not

motor responses, in the intermediate layers of SC were completely extinguished. Conversely, visual responses in the superficial (retinotectal) layers of SC were unaffected. Given the feature sensitivities in SC, it is entirely possible that feature discrimination subserving target selection occurs in SC itself. However, this classic experiment by Schiller et al. makes clear that, even if this is true, SC is dependent on cortical input for feature information. Featural sensitivities in FEF have not been examined following cortical cooling/ablation, so it is unclear whether FEF featural sensitivities also rely on downstream feature-specialized cortical modules. However, is this feasible given that FEF is richly interconnected with visual areas spanning the entire cortical processing hierarchy (Barone et al., 1998; Moore and Armstrong, 2003; Schall et al., 1995b). The combined weight of evidence from other ablation, inactivation, and microstimulation studies casts further doubt on the possibility that oculomotor substrates SC and FEF are the seat of feature discrimination subserving target selection.

5.5.2. Dissociating Oculomotor and Perceptual Functions

In systems neuroscience, there is a decades-old double-dissociation between perceptual and motor processing systems (Haxby et al., 1991; Mishkin et al., 1983; Ungerleider & Haxby, 1994). In this section, we summarize a similar double-dissociation that exists between the neural modules that subserves the perception of visual stimulus features from the neural modules necessary to program and execute eye movements.

5.5.2.1. Lesions and inactivation. In humans, lesions of the visual cortices are predominately associated with permanent perceptual deficits but spared motor function. When visual cortical lesions are especially localized, the deficits are amazingly specific; limited to the visual attribute(s) for which the lesioned cortex was specialized. Fascinating examples include achromatopsia and akinetopsia, the inability to perceive color or motion (respectively), reviewed

elsewhere (e.g., Heywood & Cowey, 2013; Zeki, 1991). These observations suggest that the cortical visual hierarchy exhaustively encodes the features we perceive and experience (Zeki & Bartels, 1999). In contrast to these perceptual deficits, visual cortical lesions spar motor functions.

Hemianopic patients with acquired scotomas from damage to the geniculostriate pathway can still readily execute saccades per se; however, to make visually-guided saccades into their lesioned visual field, they reply upon idiosyncratic compensatory strategies that exploit vision from their intact visual field (Barbur et al., 1988; Meienberg et al., 1981). Similarly, when hemianopic patients make saccades into the intact visual field, peripheral distractors in the lesioned field do not elicit saccadic interference (Walker et al., 2000), as is seen in healthy adults (Buonocore & McIntosh, 2012; Edelman & Xu, 2009; Hafed & Ignashchenkova, 2013).

In contrast to visual cortical lesions, ablations of oculomotor substrates are associated with deficits in saccadic production and selection. SC and FEF are reciprocally connected but independently project to the brainstem motor circuitry (Huerta et al., 1986; Moschovakis et al., 1988; Schnyder et al., 1985; Segraves & Goldberg, 1987; Segraves, 1992; Sommer & Wurtz, 2004; Staton et al., 1988). As such, SC and FEF form parallel pathways necessary for planning and executing eye movements, as ablation of both SC and FEF produces permanent deficits in visually guided saccades (Schiller et al., 1979, 1980), while ablation of a single module spares this function (Mohler & Wurtz, 1977; Schiller et al., 1987; Schiller, 1977; but see Hanes & Wurtz, 2001).

Reversible inactivation of oculomotor substrates impairs perceptual discriminations indicated with saccades (McPeek & Keller, 2004; Monosov et al., 2011) and even for manual button responses (Lovejoy & Krauzlis, 2010) or reaching movements (Song et al., 2011, 2015).

However, these behavioral deficits are likely related to an acquired attentional neglect scotoma and do not necessarily imply a perceptual deficit more broadly. Case studies of human localized SC lesions are exceedingly rare, but results from at least one such human case study does support this reasoning. One patient reportedly did develop visuospatial neglect contralateral to a localized lesion of SC; however, the authors did not report whether the perceptual capabilities of the patient were intact (see Nyffeler et al., 2021).

5.5.2.2. Microstimulation. Microstimulation reveals the functional encoding scheme of neural populations in a complementary manner to lesion and inactivation studies. If the oculomotor substrates rely upon featural representations in the visual cortical hierarchy to program feature-guided eye movements, then microstimulation of either the visual cortices or oculomotor substrates should bias eye movements to the stimulated feature during target selection. Additionally, microstimulation of the visual cortices should elicit perceptual phenomena.

A fascinating human case study by (Lee et al., 2000) reports a variety of visual hallucinations evoked by electrocorticographical stimulation across occipital, occipital-parietal, and occipital-temporal cortices. Patients experienced seeing flashes, primitive shapes, formless "blobs", complex objects including faces and animals, and even entire scenes, where objects were either moving or stationary, and objects appeared in various colors and textures. Schiller et al. (2011) showed that visual perceptual phenomena elicited by microstimulation of monkey visual cortices can be inferred with clever behavioral paradigms, likely inspired by the elegant somatosensory experiments of Romo et al. (1998). Their research suggested that monkeys experienced seeing a small, low-contrast colored dot after microstimulation was delivered to striate cortex.

Eye movements can be elicited from microstimulation of striate cortex, where the current threshold drops as a function of the cortical penetration depth (Tehovnik et al., 2003). This is consistent with much earlier experiments showing that striatially-evoked eye movements arise from current propagating through the direct connection between striate cortex and SC, as these striatally-evoked eye movements are abolished when SC is ablated (Schiller, 1977). Microstimulation of the oculomotor substrates elicits eye movements at relatively low currents (Bruce et al., 1985; Robinson and Fuchs, 1969; Robinson, 1972). At even lower subthreshold currents, microstimulation of the oculomotor substrates mimics the behavioral and neural effects of visuospatial attentional deployment, namely speeded processing and lowered perceptual detection thresholds (Carello & Krauzlis, 2004; Cavanaugh & Wurtz, 2004; Moore & Fallah, 2001, 2004) and downstream neural gain modulation (Armstrong et al., 2006; Moore & Armstrong, 2003). Similarly, speeded detection times and perceptual biases are elicited from microstimulating visual cortices, such as medial temporal (MT) (Bisley et al., 2001; Britten & van Wezel, 1998; Celebrini & Newsome, 1995; DeAngelis et al., 1998; Ditterich et al., 2003; Salzman et al., 1990, 1992) and V4 (Kienitz et al., 2022). Critically, these perceptual biases are incorporated into eye movements, as pursuit eye movements intended to track a moving stimulus are biased in the cortically (i.e., MT) microstimulated movement direction (Born et al., 2000; Groh et al, 1997; Komatsu & Wurtz, 1989).

Taken together, these results demonstrate that oculomotor substrates lack cortically-independent inherent feature representations, while inactivation and stimulation studies show that they functionally subserve attentional selection and eye movement generation, but not perception. Conversely, the cortical visual hierarchy is the seat of visual feature-encoding in the nervous system: inactivation and stimulation studies show that visual cortices are necessary for

the perception of visual features, and critically, these feature representations bias feature-guided oculomotor behavior.

5.6. Feature Dependent Visual Onset Latencies

A basic property of the cortical visual hierarchy is that increased featural complexity requires additional featural processing in higher stages of the hierarchy and thus additional processing time. The behavioral consequence of this encoding scheme is that the time required to perceive features is proportional to their complexity (Bodelón et al., 2007). Similarly then, if oculomotor vectors are dynamically feature-reweighted by inputs from the perceptual system, then increasing the featural complexity of a potential eye movement target should increase the latency of its feature-reweighing.

Guided by this logic, we have recently conducted a series of behavioral experiments in which we (1) non-invasively infer the oculomotor encoding time course of a visual stimulus and (2) compare this time course between different visual features that constitute the visual stimulus (see Figure 5.3).

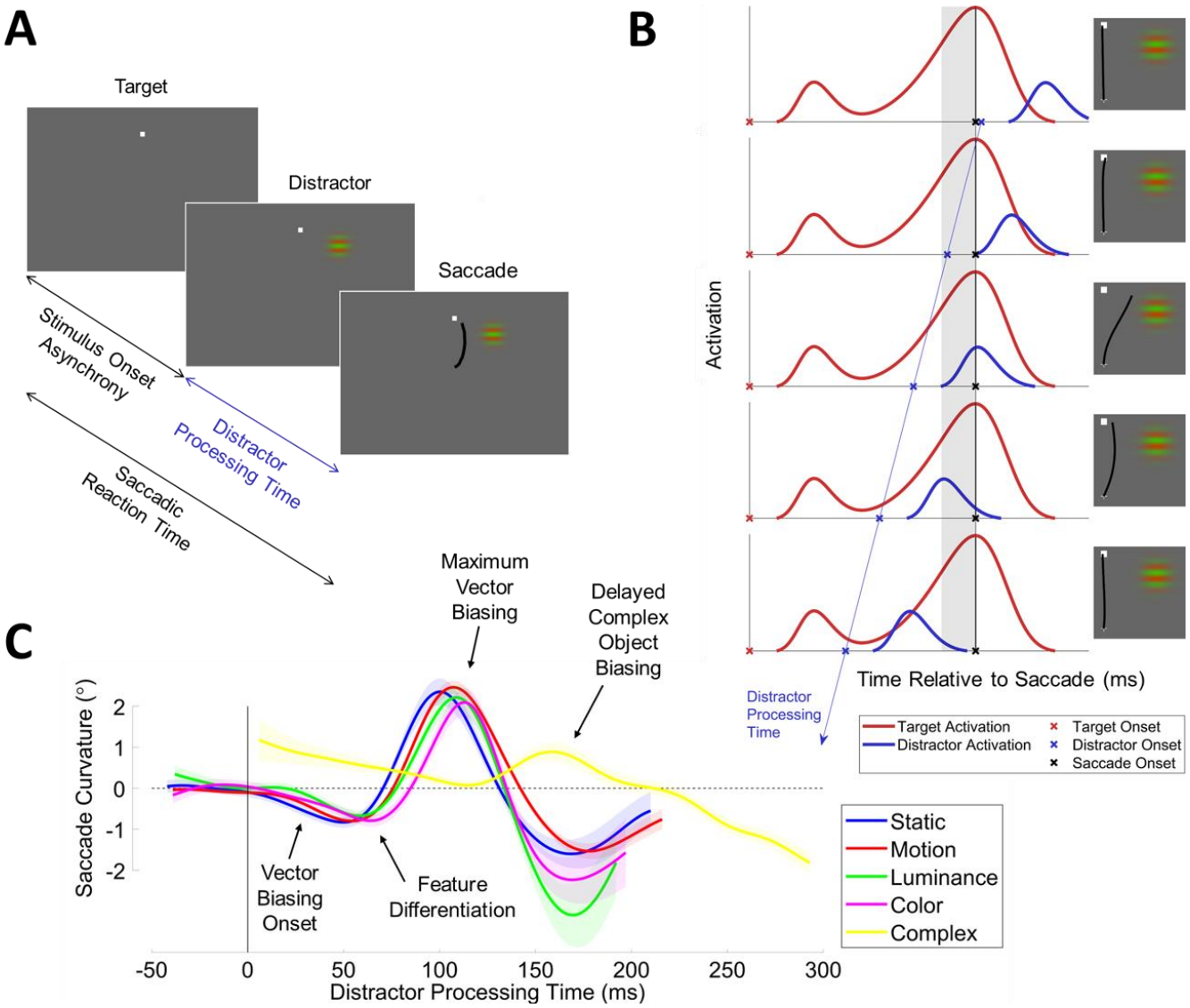

Figure 5.3. The distractor-saccade onset asynchrony (SDOA) paradigm. ***A*:** Task procedure schematic. Targets are displayed at some random interval before the distractor (stimulus onset asynchrony). Participants elicit target-directed saccades sometime after distractor onset (distractor processing time). ***B*:** Putative neural underpinnings. Depicted is the hypothetical activation of visuomotor neurons elicited when the target (red line) or distractor (blue line) are in the motorfield of the cell. Activation is plotted as a function of time relative to the saccade. The onset of the saccade is indicated by the black vertical line and black "X"s. In the perisaccadic interval immediately prior to the saccade (gray shaded region), the incipient motor plan for target-directed saccades may become biased by unresolved distractor activation. The target is displayed sometime prior to the saccade (red "X"s). In this contrived example, the saccadic reaction time is constant. The target onset elicits a visual onset burst time-locked to stimulus

onset and a motor burst time-locked to the saccade. The distractor onset (blue "X"s) is stochastic and can occur at any time relative to the saccade. The distractor onset elicits a visual onset burst time-locked to stimulus onset. In this example, we systematically increase the distractor processing time (i.e., the duration of time between distractor onset and subsequent saccade), illustrated by the blue line with arrowhead. As such, the distractor-related visual onset burst sweeps through the perisaccadic interval. Right insets depict hypothetical saccades elicited by the distractor visual onset burst given its position in time relative to the perisaccadic interval. ***C*:** The results across iterations of the SDOA paradigm. Saccade curvature (vector biasing) is plotted as a function of distractor processing time for all examined distractor features: static-gratings (blue), motion-gratings (red) (Kehoe et al., 2023); luminance-modulated Gabors (green), color-modulated Gabors (magenta) (Kehoe & Fallah, 2017); and complex pseudo-alphanumeric characters during discrimination (yellow) (Kehoe et al., 2021). We highlight notable effects with text-labelled arrows: (1) for simple gratings, vector biasing onsets after just 25 ms of distractor processing time; (2) features begin to differentiate after approximately 50 ms of distractor processing time; (3) the maximum vector biasing occurs after approximately 100 ms of distractor processing time; and (4) discriminated complex objects elicit vector biasing very late, after approximately 110 ms. Note that these data from prior publications have been replotted onto a common figure.

In our paradigm (Kehoe & Fallah, 2017; Kehoe et al., 2021, 2023), human participants plan and execute a saccade to a target, and at some randomized interval after the onset of the target, we onset a peripheral distractor (see Figure 5.3A). Critically, we constrain the randomized interval between target and distractor onset so to maximize the likelihood that the distractor onsets prior to the saccade. As such, we have referred to this behavioral paradigm as the saccade-distractor onset asynchrony (SDOA) paradigm. Here, we will subsequently refer to the interval between distractor onset and saccade initiation as distractor processing time, as it corresponds to the duration of time afforded to visual processing of the distractor. We then measure a battery of human saccade metrics to examine the effect of the distractor on the target-directed saccade across a continuous range of distractor processing times.

Several recurring patterns of behavior were observed using this paradigm (see Figure 5.3C): (1) at the shortest distractor processing times, the distractor has no discernable effect on the target-directed saccade; (2) after approximately 25 ms of distractor processing time, saccade trajectories and endpoints curved towards the distractor; (3) by approximately 50 ms of distractor processing time, we saw the onset of a transient drop in the likelihood of generating a saccade; and (4) by approximately 100 ms of distractor processing time, trajectory spatial biasing and the drop in saccade likelihood both reached their maximum extent. These results are generally consistent with other behavioral paradigms that utilize an intervening stimulus during saccade planning to a target (Buonocore & McIntosh, 2012; Edelman & Xu, 2009; Hafed & Ignashchenkova, 2013; Reingold & Stampe, 2002) or double-stepping targets (Becker & Jürgens, 1979; Findlay & Harris, 1984).

The most clear and parsimonious interpretation of these behavioral results is that, in oculomotor substrates like SC, the visual onset burst encoding the distractor was spatially averaged with the developing target-directed saccade program (see Figure 5.3B). First, visual onset bursts observed in oculomotor substrates generally occur with a latency of ~50 ms after stimulus onset (Boehke & Munoz 2008), consistent with a broad set of behavioral results. Second, invasive microstimulation (Glimcher & Sparks, 1993; McPeek, 2006; McPeek et al., 2003) and dual recordings (Port & Wurtz, 2003) have confirmed that unresolved distractor activation does indeed spatially bias saccades according to a vector average of the target and distractor vectors.

5.6.1. Luminance and Color

The most intriguing results from our SDOA paradigm arose when we compared the saccadic perturbation (i.e., spatial biasing and drop in saccadic likelihood) time course between

different distractor visual features. In the original implementation (Kehoe & Fallah, 2017), we compared luminance- and color-modulated Gabors and observed that saccade curvature elicited by color lagged behind saccadic curvature elicited by luminance (see Figure 5.3C). The lag was approximately 20 ms, consistent with a neurophysiological study measuring a 30 ms difference between the visual onset bursts of collicular neurons encoding similar visual stimuli (White et al., 2009). Given this close correspondence, we interpreted our result through the lens of the same underlying neural mechanism.

A 20-30 ms lag between color and luminance encoding is consistent with the visual onset latency differences observed in the magnocellular and parvocellular layers of the lateral geniculate nucleus (LGN), between layers 4B/4Cα and 4Cβ in V1, or between the thick and pale thin layers of V2 (Nowak et al., 1995; Schmolesky et al., 1998). The anatomical divisions in these early visual substrates are highly functionally segregated and form parallel processing streams of disjoint feature sets (reviewed by Livingstone and Hubel, 1988), including luminance and color in particular. This experiment therefore confirms our reasoning: specific visual features should elicit visual onset latencies associated with specific visual processing modules specialized for processing those features. As such, the results of Kehoe & Fallah (2017) and White et al. (2009) taken together strongly imply that the representations of potential eye movement targets in oculomotor substrates are dynamically feature-weighted by the relevant modules in the perceptual system.

6.5.2. Non-motion and Motion

The results of Kehoe and Fallah (2017) suggest that feature information is projected into the oculomotor system from the relevant processing channels of the cortical visual hierarchy. But it remained difficult to determine whether feature information is projected into the oculomotor

system from the relevant stage of processing in the cortical visual hierarchy. We therefore recently repeated the original paradigm replacing the distractor features with static and motion-animated gratings (Kehoe et al., 2023). Unlike luminance and color information, which are processed in parallel channels within the same cortices and subcortical nuclei, grayscale static and motion stimuli are encoded within the same processing channel, which is distributed between and within cortices. For example, V1 encodes simple motion components and projects these upstream to MT where they are summated into complex motion representations (Movshon et al., 1996). In V1, direction-selective complex cells encode motion direction by spatiotemporally summating input from phase-selective simple cells (De Valois & Cottaris, 1998). Therefore, by using a grayscale static and motion feature set in the SDOA paradigm, any oculomotor encoding delays between features would suggest that feature information projected into the oculomotor system was bottlenecked to accommodate the appropriate stage of cortical feature processing.

In this experiment (Kehoe et al., 2023), we made several interesting findings: (1) at the earliest distractor processing times (<50 ms), saccadic perturbation was feature invariant; (2) after 50 ms of distractor processing time, saccadic perturbation elicited by motion gratings lagged behind saccadic perturbation elicited by static gratings by 10 ms; and (3) this temporal lag was not accompanied by any saccadic perturbation magnitude differences between features (see Figure 5.3C).

The biasing of saccade trajectories observed for distractor processing times between 25-50 ms suggests that our behavioral paradigm is sensitive to oculomotor processing occurring at the theoretical lower bound of visual afferent latencies. The direct connections from the retina to the superior colliculus—constituting a relatively small number of retinal ganglian projections—is

the only known mechanism to support these conduction latencies (Hubel et al., 1975; Schiller & Malpeli, 1977). Visual onset bursts in collicular neurons are not typically seen at latencies less than ~50 ms after visual stimulus onset (Boehnke & Munoz, 2008). These results may therefore suggest a gentle increase of baseline collicular activity that directly upregulated upstream brainstem oculomotor nuclei in a passthrough manner, but this speculation warrants investigation.

The saccade trajectory biasing time course became differentiated between static and motion distractors after 50 ms, where the effects of motion distractors lagged those of static distractors by 10 ms. Similarly, a rapid drop in saccadic likelihood began at 50 ms for static distractors and later at 60 ms for motion distractors. Saccadic inhibition immediately following visual stimulation is likely due to rapid lateral inhibition networks in colliculus, whereby activation of a saccade vector near instantaneously inhibits neighboring saccade vectors (Munoz & Istvan, 1998). This is suggested by the facts that (1) visual onsets elicit transient collicular bursts and visually-evoked saccadic inhibition is also transient and (2) visual onset bursts and saccadic inhibition occur after the same latency (Buonocore & McIntosh, 2012; Edelman & Xu, 2009; Hafed & Ignashchenkova, 2013; Reingold & Stampe, 2002). Given that the feature-dependent saccade inhibition effect was very likely driven by collicular visual onset bursts encoding the distractor, then by extension, the trajectory biasing divergence occurring simultaneously was likely then also driven by collicular visual onset bursts.

The feature-dependent saccade perturbation latencies we saw further corroborates our account that visual feature information projected into the oculomotor system is bottlenecked to afford the requisite processing in the appropriate substrates of the cortical visual hierarchy. Furthermore, we did not see any differences in the magnitude of saccadic vector averaging

between features. Therefore, it is unlikely that the time course erroneously appeared differentiated because the motion burst continued to intensify after the static burst reached its maximum intensity.

5.6.3. Complex Object Discrimination

The most compelling evidence of bottlenecked visual projections into the oculomotor system was when we examined the oculomotor encoding time course of complex, novel objects during a discrimination task (Kehoe et al., 2021). On this task, participants were shown a target preview and told to discriminate this target from a distractor with a saccade to indicate their choice. These stimuli resembled pseudo-alphanumeric characters that were not meaningful to English speakers. As in other iterations of our behavioral paradigm, we randomized the stimulus onset asynchrony between targets and distractors. However, to ensure that stimulus order did not provide reliable target information, the distractor onset prior to the target on 50% of trials. We were able to analyze distractor processing time as before by concentrating our analyses on trials with targets leading distractors and distractors leading saccades. We were therefore able to measure saccade trajectory biases, saccadic inhibition, and error rates as a function of distractor processing time.

Fascinatingly, we observed that the earliest evidence of trajectory biasing, saccade inhibition, and selection errors was at distractor processing times of at least 110 ms, in stark contrast to the 50 ms effects we saw for simple, task-irrelevant gratings. The discrimination of these stimuli would very likely recruit substrates in the higher stages of the cortical processing hierarchy, specifically inferortemporal cortex (IT) where simple geometric subunits represented in downstream modules are concatenated into coherent objects (Brincat & Connor, 2004, 2006). At these later stages in the hierarchy, visual onset latencies are typically over 100 ms (Nowak &

Bullier, 1997). As such, the clearest explanation of our results is that visual encoding of the complex objects was absent within the oculomotor substrates until these objects were visually represented in the higher stages of the cortical visual hierarchy, the necessary substrates for complex object discrimination.

5.7. Mechanism for Feature Representations in Oculomotor Substrates

Our experiments suggest that visual encoding in the oculomotor system is extremely contextual. A combination of the task requirements and the visual feature set determines the latency of visual encoding in the oculomotor system. Since the oculomotor system relies upon cortical input for visual feature information (Schiller et al., 1974), we argue that these latency differences reflect the highest stage of processing in the cortical visual hierarchy that was recruited in each experimental context to successfully satisfy feature discrimination. In this view, only after visual representations have manifested in these task- and feature-dependent cortical substrates does the oculomotor system receive cortical inputs to reweight eye movement vectors. As there are systematic differences between the visual onset latencies across the cortical visual hierarchy, the onset latency of visual representations in the oculomotor system is also feature-dependent and increases with featural complexity. This framework is inspired by classic cognitive theories stipulating that a base representation (Ullman, 1984) or raw primal sketch (Marr, 1982) must be constructed before cognitive mechanisms or visual routines (Ullman, 1984) can operate on the visual information so to satisfy relevant visual task demands.

Neurophysiological investigations of saccadic target selection typically utilize discriminations between different features of the same visual attribute (e.g., a red target amongst green distractors, where all stimuli are color singletons). In these experiments, oculomotor visual onset bursts for targets and distractors have identical latencies. Shortly thereafter however, the

activation level of the target gradually increases, while the activation level of distractors gradually decreases (Fecteau & Munoz, 2006). These observations suggest that, after visual input first arrives in the oculomotor substrates, feature-dependent cortical inputs must continue to dynamically reweight the saccade vector over time. This likely reflects the fact that in the recruited cortical modules, visual discriminations unfold over time by way of gradually shifting neuronal feature representations, akin to the process Ullman (1984) has termed incremental representations. When observers encounter stimuli sharing just one attribute (e.g., all stimuli are color singletons), then the same cortical module(s) are recruited to encode all visual stimuli. Thus, the cortical bottleneck applies equally to all stimuli in this context. We therefore do not expect a visual onset burst latency difference between stimuli, as is seen. After the feature-dependent cortical modules are recruited for the task and begin representing the visual stimuli, the cortical feature discrimination process begins. Once commenced, these relevant cortical module(s) dynamically reweight the oculomotor vectors to maintain parity between oculomotor and cortical feature representations. Thus, we observe target features activate and distractor features deactivate over time in oculomotor substrates during target selection.

Another critical implication from our behavioral work is that this putative neural mechanism is not specifically a mechanism for feature discrimination in oculomotor substrates, but more broadly feature representation in oculomotor substrates. In two of our experiments (Kehoe & Fallah, 2017; Kehoe et al., 2023), we observed saccadic perturbation latency differences between distractor features that were wholly task-irrelevant, as these distractors always appeared at target invalid spatial locations. Feature discriminating these targets from distractors was not necessary for the task and discrimination could have been achieved more simply with spatial processing. Despite this, we still observed that saccadic perturbation latencies

were contingent on featural complexity. This suggests that our putative neural mechanism does not just subserve feature-based oculomotor target selection but instead describes a fundamental processing regime connecting the oculomotor and perceptual systems.

5.8. Caveats and Alternatives

5.8.1. Categorizing Neural Substrates

In this review, we have focused on SC and FEF as the critical substrates of the oculomotor system. However, these substrates are just two of many substrates widely considered part of a broad oculomotor network (Corbetta et al., 1998; Fecteau and Munoz, 2006; Schall and Cohen, 2011). For example, the lateral bank of the intraparietal sulcus (LIP) is widely considered a critical substrate subserving saccadic behavior (Andersen et al., 1992; Goldberg et al., 2006) because, like in SC and FEF, it encodes both spatial and feature information during saccadic target selection (Buschman & Miller, 2007; Constantinidis & Steinmetz, 2001; Subaramanian & Colby, 2014), lesions to LIP produce attentional neglect scotomas (Driver & Mattingley, 1998; Parton et al., 2004), eye movements are evoked from weak microstimulation (Tehovnik et al., 2003), and it exhibits perisaccadic receptive field remapping (Duhamel et al., 1992). However, these properties are not unique to LIP and are observable, to at least some extent, in several clearly visual cortices such as V1 [task-modulated feature discriminability (Chen & Seidemann, 2012; Motter, 1993), post-lesion scotomas (Weiskrantz, 1996), evoked saccades (Tehovnik et al., 2003), perisaccadic receptive field remapping (Merriam et al., 2007; Nakamura & Colby, 2002)]. What does seem to be unique about SC and FEF—and why we mainly focus on these substrates when discussing critical oculomotor substrates here—is that they are directly connected to the brainstem pulse generators (Schiller & Tehovnik, 2005).

In a complimentary manner, the question arises whether SC and/or FEF are visual areas.

There are compelling reasons to draw this conclusion, as recently summarized by Hafed et al. (2023) concerning SC in particular. For example, the optic tectum phylogenetically precedes visual cortex altogether and is the primary mechanism for vision in some organisms. As summarized previously, there has recently emerged a broad understanding of the rich feature processing capabilities of the SC. Finally, SC is richly interconnected with most of cortex and subcortex linking it to structures specialized for visual and cognitive processing. Granting SC as a visual area given these interesting considerations, SC is certainly still an oculomotor substrate in primates given its privileged synaptic proximity to the brainstem, as discussed above. As such, although there is a growing appreciation for SC as a both a visual and oculomotor substrate, it is, nevertheless, still oculomotor.

5.8.2. Interpreting Absolute Latencies

Several studies have specifically examined the latency of visual onsets in oculomotor areas during passive free-viewing (Mayo & Sommer, 2012; Mohler et al., 1973; Pouget et al., 2005; Schall, 1991; Schmolesky et al., 1998). Comparing the average visual onset latencies in oculomotor substrates (typically 50-60 ms) observed in these studies to the average visual onset latencies observed across the cortical visual hierarchy in other studies (see Nowak & Bullier, 1997) seems to suggest that visual onset latencies in oculomotor substrates are faster than those observed in many modules of the cortical visual hierarchy. However, this is a complex comparison to make as latencies are inherently variable; sensitive to individual differences between organisms, states (e.g., anesthetized vs. awake), tasks, and myriad stimulus parameters (e.g., contrast, size, position).

Circumventing this issue, one neuronal chronometry study by Schmolesky et al. (1998) recorded visual onset latencies across cortical modules—mostly visual but also including FEF—

within the same anesthetized monkeys. They observed that there was no difference in the average visual onset time between FEF neurons and neurons in higher areas of the dorsal cortical processing stream, namely areas V3, MT, and MST. Additionally, visual onset latencies were actually faster in FEF than in the pale thin layers of V2 and in V4. However, it is not clear from this study whether this pattern of results is specific to the task and stimulus set that was used. For example, in the context of planning a saccade to a single high contrast spot of light, why would FEF wait for visual input from V4 when visual input from LGN or V1 is likely sufficient to provide FEF with the necessary visual information? Indeed, our own behavioral experiments suggest that oculomotor visual onset latencies are stimulus-dependent, so it is entirely possible that FEF visual responses are slower than those in V4 for some other task/stimulus set.

Yet another possibility is that visual onset latencies are absolute and the mechanism that reweights oculomotor vectors based on features is by virtue of cascading visual input into oculomotor substrates. As SC and FEF are reciprocally innervated by nearly the entire visual brain, perhaps visual input from across all nodes of the visual cortical hierarchy is projected into the oculomotor substrates sequentially. For example, perhaps visual responses in FEF are initially driven by inputs from V1, then driven by V2 10 ms later, thus visual onset latencies in FEF are faster than in V2. This also is consistent with previous neuronal chronometry experiments showing a very wide range of visual onset latencies between cells in oculomotor substrates (30-120 ms) (Mayo & Sommer, 2012; Mohler et al., 1973; Pouget et al., 2005; Schall, 1991; Schmolesky et al., 1998) similarly observed across modules of the cortical visual hierarchy (Nowak & Bullier, 1997). As such, the simplest explanation linking these observations could be that the oculomotor visual response latencies are driven by the fastest early sensory responses.

Another important consideration is that examining the onset of feature sensitivities as

opposed to visual onset latencies likely provides a better indication of when feature information arrives in oculomotor substrates. As discussed, oculomotor stimulus encoding evident in neural spikes is usually feature invariant for the initial ~100 ms after stimulus onset (Boehnke & Munoz, 2008). Our own behavioral experiment shows that stimulus information is decodable from saccade metrics in as little as 25 ms, and unsurprisingly, is also feature invariant (Kehoe et al., 2023). If this initial visual encoding is entirely spatial (see Fecteau & Munoz, 2006), then it is the wrong metric to compare the latency of feature information between visual and oculomotor modules. For example, White et al. (2009) compared SC visual onset latencies evoked by isoluminant color targets to those evoked by luminance targets on a simple saccade-to-target task. They observed that visual onsets for color targets lagged luminance targets by at least 30 ms. Critically, however, they also observed that the color responses exhibited tuning in DKL colorspace and thus necessarily conveyed feature information and not merely spatial information. As such, this is a very robust comparison of feature information latency differences and provides an extremely useful example of how to easily test our theoretical account posited here.

5.8.3. Reciprocal Processing

We argued strongly that feature information manifests in oculomotor substrates only after antecedent featural processing in cortical substrates. However, a number of studies suggest that this relationship is far more reciprocal than has been outlined here. In a seminal experiment, Moore & Armstrong (2003) microstimulated FEF while also recording from downstream neurons in V4 with overlapping or non-overlapping receptive fields. They observed that neuronal visual activity in V4 was enhanced by stimulation of retinotopically congruent loci in FEF and was suppressed by stimulation of retinotopically incongruent loci. In a complimentary experiment, Noudoost et al. (2014) showed that inactivation of FEF increased presaccadic

enhancement of V4 activity and decreased feature-based discriminability of V4 visual responses. That is, V4 began strongly encoding the direction of saccades and exhibited a reduced sensitivity to encode the features of visual stimuli.

These observations clearly and elegantly demonstrate that feature representations in visual cortices are modulated by reciprocal feedback from upstream oculomotor substrates. What is less clear from these experiments is whether the modulation of downstream sensory representations is feature-based or purely spatial. Afterall, microstimulating FEF also produces behavioral effects akin to exogenously cueing spatial attention (Moore & Fallah, 2001, 2004), so FEF modulation of V4 feature representations in these experiments can be accounted for by spatial processing and may be entirely unrelated to feature processing in FEF.

Other experiments have provided evidence of feature processing in oculomotor substrates manifesting earlier than in select visual cortices. Zhou & Desimone (2011) showed that feature discrimination occurs in FEF 30-50 ms before it occurs in V4 during cued visual search for complex objects. Similarly, White et al. (2017b) recently showed that task-irrelevant salience (i.e., orientation contrast) is encoded in SC approximately 10 ms earlier than in V1 during a simple saccade-to-target task. These observations raise several potential explanations.

First, it is entirely possible that the choice of visual modules on these tasks were higher in the visual hierarchy than was sufficient to discriminate the stimuli. That is, perhaps if an earlier module was recorded from, feature discrimination would occur earlier in the visual module than in the oculomotor module. For example, substituting V2 for V4 in the case of Zhou and Desimone (2011) or LGN with V1 in the case of White et al. (2017b). This possibility cannot yet be ruled out but poses a difficult experimental challenge. Second, perhaps a primary function of oculomotor substrates is as a comparator. In the case of SC, previous authors have long argued

that its function is to agnostically pool feature representations from sensory cortices and compute salience based on disparate feature codes (Fecteau & Munoz, 2006; White et al., 2017a, 2017b). In the case of FEF, there is also strong evidence of salience encoding (Sato & Schall, 2003; Thompson & Bichot, 2005). In this comparator view, perhaps feature discrimination is delayed in sensory cortices relative to oculomotor modules because feature discrimination in sensory cortices is delayed until salience information is reciprocally propagated by oculomotor substrates back into sensory cortices.

Clearly, reciprocal interactions between oculomotor substrates and sensory cortices are well-supported experimentally. However, reciprocal sensorimotor interactions are not mutually exclusive with the theory posited here. Future investigations could examine potential latency differences between stimulus attribute types (e.g., luminance vs. color) and may discover that although feature discrimination in oculomotor substrates does precede feature discrimination in visual cortices (e.g., FEF before V4), discrimination for more complex features occurs later than simpler features within those oculomotor substrates.

5.9. Extensions of the SDOA Paradigm

The SDOA paradigm can be used to answer a broad range of questions in vision and cognitive science and has many clinical applications. Inferring stages of processing has been a central theme of vision and cognitive science throughout the entire contemporary period (e.g., Marr, 1982; Neisser, 1967; Treisman & Gelade, 1980; Ullman, 1984). Our paradigm offers a robust tool to assess the processing stage of a stimulus across time, but its applicability is also not limited to inferences of feedforward visual processing in the cortical visual hierarchy. The advantage of examining behavior, as with the SDOA paradigm, is that it reflects the output of the entire cognitive information processing pipeline, including executive, memory, sensory, and

affective subsystems. Critically, the output of these various subsystems is encoded by eye movements (Belopolsky & Theeuwes, 2011; Schmidt et al., 2012; Takikawa et al., 2002; Theeuwes et al., 2005) and neural activation within oculomotor substrates (Hanes et al., 1998; Ikeda & Hikosaka, 2003; Johnston & Everling, 2006, 2008; Paré & Hanes, 2003). As such, the SDOA paradigm examines how the output of these various cognitive subsystems is encoded into oculomotor programs over time.

There is a clinical tradition of using eye movements for early diagnosis of neurological disease and abnormality (for review, see Anderson & MacAskill, 2013; Antoniades & Kennard, 2015), as eye movement tasks are quick, non-invasive, computationally light, and inexpensive to administer. However, although abnormal eye movements are indicative of neurological disorders, they do not differentiate between neurological disorders. The SDOA paradigm examines eye movements across stages of processing and can selectively focus on specific cognitive subsystems. Therefore, our paradigm lends itself to differential and more sensitive diagnosis. Furthermore, the SDOA paradigm is an effective means to trace disease or rehabilitative progress, without the need for more difficult, costly, and invasive medical surveillance methods.

5.10. Conclusions

Visual features often guide primate eye movements (Pomplun et al., 2001; Shen et al., 2000; Shen & Paré, 2006) and can be decoded from neural activation encoding potential eye movements (Boehnke & Munoz, 2008). However, oculomotor research has overlooked the mechanism that feature-reweights potential eye movements. Here, we have summarized functional and anatomical evidence that strongly suggests the oculomotor system is insufficient to extract visual features that guide target selection, and instead, relies upon the substrates of the

cortical visual hierarchy for feature information. The cortical visual hierarchy is functionally organized (Fellemen & Van Essen, 1991) such that specific visual feature sets are represented in specific modules. Similarly, the onset latency of vision is systematically different between these modules (Nowak & Bullier, 1997; Schmolesky et al., 1998). As such, our account of oculomotor feature-reweighting predicts that feature information should manifest in the oculomotor system with the same latency as in the relevant cortical modules specialized for processing the respective features. Consistent with this prediction, we have conducted a series of innovative behavioral experiments showing that visual features manifest in the oculomotor system in order of visual complexity regardless of whether the features are task-relevant. We therefore proposed a theory of oculomotor feature-reweighting whereby visual feature sets engage a specific set of cortical modules and visual projections into the oculomotor system are delayed until after these cortical modules generate visual representations. During the process of feature discrimination in the recruited cortical module(s), the evolving feature representations are projected to oculomotor substrates where they continuously and dynamically reweight the active eye movement vectors. This theory accounts for many observations in oculomotor research, offers a more detailed account of how oculomotor vectors are feature-reweighted during target selection, and makes a series of easily testable predictions. Finally, we briefly discussed the applicability of the SDOA paradigm to address broader questions in vision and cognitive science and its potential utility as a clinical diagnostic tool.

Chapter 6. References

Aizawa, H., & Wurtz, R. H. (1998). Reversible inactivation of monkey superior colliculus. I. Curvature of saccadic trajectory. *Journal of Neurophysiology*, *79*(4), 2082-2096. https://doi.org/10.1152/jn.1998.79.4.2082

Albright, T. D. (1984). Direction and orientation selectivity of neurons in visual area MT of the macaque. *Journal of Neurophysiology*, *52*(6), 1106–1130. https://doi.org/10.1152/jn.1984.52.6.1106

Andersen, R. A., Brotchie, P. R., & Mazzoni, P. (1992). Evidence for the lateral intraparietal area as the parietal eye field. *Current Opinion in Neurobiology*, *2*(6), 840-846. https://doi.org/10.1016/0959-4388(92)90143-9

Anderson, R. W., Keller, E. L., Gandhi, N. J., & Das, S. (1998). Two-dimensional saccade-related population activity in superior colliculus in monkey. *Journal of Neurophysiology*, *80*(2), 798-817. https://doi.org/10.1152/jn.1998.80.2.798

Anderson, T., MacAskill, M. (2013). Eye movements in patients with neurodegenerative disorders. *Nature Reviews Neurology*, *9*(2), 74-85. https:doi.org/doi:10.1038/nrneurol.2012.273

Antoniades, C., Kennard, C. (2015). Ocular motor abnormalities in neurodegenerative disorders. *Eye*, *29*(2), 200-207. https://doi.org/10.1038/eye.2014.276

Armstrong, K. M., Fitzgerald, J. K., & Moore, T. (2006). Changes in visual receptive fields with microstimulation of frontal cortex. *Neuron*, *50*(5), 791-798. https://doi.org/10.1016/j.neuron.2006.05.010

Awh, E., Armstrong, K. M., & Moore, T. (2006). Visual and oculomotor selection: links, causes and implications for spatial attention. *Trends in Cognitive Sciences*, *10*(3), 124-130. https://doi.org/10.1016/j.tics.2006.01.001

Azzopardi, P., Fallah, M., Gross, C. G., & Rodman, H. R. (2003). Response latencies of neurons in visual areas MT and MST of monkeys with striate cortex lesions. *Neuropsychologia*, *41*(13), 1738–1756. https://doi.org/10.1016/S0028-3932(03)00176-3

Bahill, A. T., & Stark, L. (1975). Neurological control of horizontal and vertical components of oblique saccadic eye movements. *Mathematical Biosciences*, *27*(3-4), 287–298. https://doi.org/10.1016/0025-5564(75)90107-8

Barborica, A., & Ferrera, V. J. (2003). Estimating invisible target speed from neuronal activity in monkey frontal eye field. *Nat Neuroscience*, *6*(1), 66-74. https://doi.org/10.1038/nn990

Barbur, J. L., Forsyth, P. M., & Findlay, J. M. (1988). Human saccadic eye movements in the absence of the geniculocalcarine projection. *Brain*, *111*, 63-82. https://doi.org/10.1093/brain/111.1.63

Barone, P., Batardiere, A., Knoblauch, K., & Kennedy, H. (2000). Laminar distribution of neurons in extrastriate areas projecting to visual areas V1 and V4 correlates with the hierarchical rank and indicates the operation of a distance rule. *Journal of Neuroscience*, *20*(9), 3263-3281. https://doi.org/10.1523/JNEUROSCI.20-09-03263.2000

Basso, M. A., & Liu, P. (2007). Context-dependent effects of substantia nigra stimulation on eye movements. *Journal of Neurophysiology*, *97*(6), 4129-4142. https://doi.org/10.1152/jn.00094.2007

Basso, M. A., & Sommer, M. A. (2012). Exploring the role of the substantia nigra pars reticulata in eye movements. *Neuroscience, 198,* 205–212. https://doi.org/10.1016/j.neuroscience.2011.08.026

Basso, M. A., & Wurtz, R. H. (1997). Modulation of neuronal activity by target uncertainty. *Nature*, *389*(6646), 66–69. https://doi.org/10.1038/37975

Basso, M. A., & Wurtz, R. H. (1998). Modulation of neuronal activity in superior colliculus by changes in target probability. *Journal of Neuroscience, 18*(18), 7519–7534. https://doi.org/10.1523/JNEUROSCI.18-18-07519.1998

Bauer, B., Jolicoeur, P., & Cowan, W. B. (1996a). Distractor heterogeneity versus linear separability in colour visual search. *Perception*, *25*(11), 1281–1293. https://doi.org/10.1068/p251281

Bauer, B., Jolicoeur, P., & Cowan, W. B. (1996b). Visual search for colour targets that are or are not linearly separable from distractors. *Vision Research*, *36*(10), 1439–1465. https://doi.org/10.1016/0042-6989(95)00207-3

Bauer, B., Jolicoeur, P., & Cowan, W. B. (1998). The linear separability effect in color visual search: Ruling out the additive color hypothesis. *Perception & Psychophysics*, *60*(6), 1083–1093. https://doi.org/10.3758/BF03211941

Becker, W., & Jürgens, R. (1979). An analysis of the saccadic system by means of double step stimuli. *Vision Research*, *19*(9), 967-983. https://doi.org/10.1016/0042-6989(79)90222-0

Bell, A. H., Meredith, M. A., Van Opstal, A. J., & Munoz, D. P. (2006). Stimulus intensity modifies saccadic reaction time and visual response latency in the superior colliculus. *Experimental Brain Research*, 174, 53–59. https://doi.org/10.1007/s00221-006-0420-z

Belopolsky, A. V., & Theeuwes, J. (2011). Selection within visual memory representations activates the oculomotor system. *Neuropsychologia*, *49*(6), 1605–1610. https://doi.org/10.1016/j.neuropsychologia.2010.12.045

Belopolsky, A. V., & Van der Stigchel, S. (2013). Saccades curve away from previously inhibited locations: evidence for the role of priming in oculomotor competition. *Journal of Neurophysiology*, *110*(10), 2370-2377. https://doi.org/10.1152/jn.00293.2013

Benson, N. C., Jamison, K. W., Arcaro, M. J., Vu, A. T., Glasser, M. F., Coalson, T. S., Van Essen, D. C., Yacoub, E., Ugurbil, K., Winawer, J., & Kay, K. (2018). The Human Connectome Project 7 Tesla retinotopy dataset: Description and population receptive field analysis. *Journal of Vision*, *18*(13), 23-23. https://doi.org/10.1167/18.13.23

Berg, D. J., Boehnke, S. E., Marino, R. A., Munoz, D. P., & Itti, L. (2009). Free viewing of dynamic stimuli by humans and monkeys. *Journal of Vision*, *9*(5), 19-19. https://doi.org/10.1167/9.5.19

Bichot, N. P., & Schall, J. D. (1999). Effects of similarity and history on neural mechanisms of visual selection. *Nature Neuroscience*, *2*(6), 549–554. https://doi.org/10.1038/9205

Bichot, N. P., Schall, J. D., & Thompson, K. G. (1996). Visual feature selectivity in frontal eye fields induced by experience in mature macaques. *Nature*, *381*(6584), 697-699. https://doi.org/10.1038/381697a0

Bisley, J. W., & Pasternak, T. (2000). The multiple roles of visual cortical areas MT/MST in remembering the direction of visual motion. *Cerebral Cortex*, *10*(11), 1053–1065. https://doi.org/10.1093/cercor/10.11.1053

Bisley, J. W., Zaksas, D., & Pasternak, T. (2001). Microstimulation of cortical area MT affects performance on a visual working memory task. *Journal of Neurophysiology*, *85*(1), 187-196. https://doi.org/10.1152/jn.2001.85.1.187

Blizzard, S., Fierro-Rojas, A., & Fallah, M. (2017). Response inhibition is facilitated by a change to red over green in the stop signal paradigm. *Frontiers in Human Neuroscience*, *10*, 655. https://doi.org/10.3389/fnhum.2016.00655

Bodelón, C., Fallah, M., & Reynolds, J. H. (2007). Temporal resolution for the perception of features and conjunctions. *Journal of Neuroscience*, *27*(4), 725–730. https://doi.org/10.1523/JNEUROSCI.3860-06.2007

Boehler, C. N., Tsotsos, J. K., Schoenfeld, M. A., Heinze, H.-J., & Hopf, J.-M. (2009). The center-surround profile of the focus of attention arises from recurrent processing in visual cortex. *Cerebral Cortex*, *19*(4), 982–991. https://doi.org/10.1093/cercor/bhn139

Boehnke, S. E., & Munoz, D. P. (2008). On the importance of the transient visual response in the superior colliculus. *Current Opinion in Neurobiology*, *18*(6), 544-551. https://doi.org/10.1016/j.conb.2008.11.004

Bogadhi, A. R., Katz, L. N., Bollimunta, A., Leopold, D. A., & Krauzlis, R. J. (2021). Midbrain activity shapes high-level visual properties in the primate temporal cortex. *Neuron*, *109*(4), 690–699. https://doi.org/10.1016/j.neuron.2020.11.023

Born, R. T., Groh, J. M., Zhao, R., & Lukasewycz, S. J. (2000). Segregation of object and background motion in visual area MT: effects of microstimulation on eye movements. *Neuron, 26*(3), 725-734. https://doi.org/10.1016/S0896-6273(00)81208-8

Brincat, S. L., & Connor, C. E. (2004). Underlying principles of visual shape selectivity in posterior inferotemporal cortex. *Nature Neuroscience, 7*(8), 880-886. https://doi.org/10.1038/nn1278

Brincat, S. L., & Connor, C. E. (2006). Dynamic shape synthesis in posterior inferotemporal cortex. *Neuron, 49*(1), 17-24. https://doi.org/10.1016/j.neuron.2005.11.026

Britten, K. H., & van Wezel, R. J. (1998). Electrical microstimulation of cortical area MST biases heading perception in monkeys. *Nature Neuroscience, 1*(1), 59-63. https://doi.org/10.1038/259

Britten, K. H., Newsome, W. T., Shadlen, M. N., Celebrini, S., & Movshon, J. A. (1996). A relationship between behavioral choice and the visual responses of neurons in macaque MT. *Visual Neuroscience, 13*(1), 87–100. https://doi.org/10.1017/S095252380000715X

Bruce, C. J., Goldberg, M. E., Bushnell, M. C., & Stanton, G. B. (1985). Primate frontal eye fields. II. Physiological and anatomical correlates of electrically evoked eye movements. *Journal of Neurophysiology, 54*(3), 714-734. https://doi.org/10.1152/jn.1985.54.3.714

Bruce, C.J., & Goldberg, M.E. (1985). Primate frontal eye fields. I. Single neurons discharging before saccades. *Journal of Neurophysiology, 53*(3), 603–635. https://doi.org/10.1152/jn.1985.53.3.603

Buffalo, E. A., Fries, P., Landman, R., Liang, H., & Desimone, R. (2010). A backward progression of attentional effects in the ventral stream. *Proceedings of the National Academy of Sciences of the United States of America*, *107*(1), 361–365. https://doi.org/10.1073/pnas.0907658106

Bullier, J., & Nowak, L. G. (1995). Parallel versus serial processing: new vistas on the distributed organization of the visual system. *Current Opinion in Neurobiology*, *5*(4), 497-503. https://doi.org/10.1016/0959-4388(95)80011-5

Buonocore, A., & McIntosh, R. D. (2012). Modulation of saccadic inhibition by distractor size and location. *Vision Research*, *69*(15), 32–41. https://doi.org/10.1016/j.visres.2012.07.010

Buschman, T. J., & Miller, E. K. (2007). Top-down versus bottom-up control of attention in the prefrontal and posterior parietal cortices. *Science*, *315*(5820), 1860-1862. https://doi.org/10.1126/science.1138071

Carello, C. D., & Krauzlis, R. J. (2004). Manipulating intent: evidence for a causal role of the superior colliculus in target selection. *Neuron*, *43*(4), 575-583. https://doi.org/10.1016/j.neuron.2004.07.026

Cavanaugh, J., & Wurtz, R. H. (2004). Subcortical modulation of attention counters change blindness. *Journal of Neuroscience*, *24*(50), 11236-11243. https://doi.org/10.1523/JNEUROSCI.3724-04.2004

Celebrini, S., & Newsome, W. T. (1995). Microstimulation of extrastriate area MST influences performance on a direction discrimination task. *Journal of Neurophysiology, 73*(2), 437-448. https://doi.org/10.1152/jn.1995.73.2.437

Chen, C. Y., & Hafed, Z. M. (2017). A neural locus for spatial-frequency specific saccadic suppression in visual-motor neurons of the primate superior colliculus. *Journal of Neurophysiology*, *117*(4), 1657-1673. https://doi.org/10.1152/jn.00911.2016

Chen, C. Y., & Hafed, Z. M. (2018). Orientation and contrast tuning properties and temporal flicker fusion characteristics of primate superior colliculus neurons. *Frontiers in Neural Circuits*, *12*, 58. https://doi.org/10.3389/fncir.2018.00058

Chen, C. Y., Ignashchenkova, A., Their, P., & Hafed, Z. M. (2015). Neuronal response gain enhancement prior to microsaccades. *Current Biology*, *25*(16), 2065–2074. https://doi.org/10.1016/j.cub.2015.06.022

Chen, Y., & Seidemann, E. (2012). Attentional modulations related to spatial gating but not to allocation of limited resources in primate V1. *Neuron*, *74*(3), 557-566. https://doi.org/10.1016/j.neuron.2012.03.033

Chen, Y., Byrne, P., & Crawford, J.D. (2011). Time course of allocentric decay, egocentric decay, and allocentric-to-egocentric conversion in memory-guided reach. *Neuropsychologia*, *49*(1), 49–60. https://doi.org/10.1016/j.neuropsychologia.2010.10.031

Coëffé, C., & ORegan, J. K. (1987). Reducing the influence of non-target stimuli on saccade accuracy: Predictability and latency effects. *Vision Research*, *27*(2), 227-240. https://doi.org/10.1016/0042-6989(87)90185-4

Connor, C. E., Gallant, J. L., Preddie, D. C., & Van Essen, D. C. (1996). Responses in area V4 depend on the spatial relationship between stimulus and attention. *Journal of Neurophysiology*, *75*(3), 1306-1308. https://doi.org/10.1152/jn.1996.75.3.1306

Connor, C. E., Preddie, D. C., Gallant, J. L., & Van Essen, D. C. (1997). Spatial attention effects in macaque area V4. *Journal of Neuroscience*, *17*(9), 3201-3214. https://doi.org/10.1523/JNEUROSCI.17-09-03201.1997

Constantinidis, C., & Steinmetz, M. A. (2001). Neuronal responses in area 7a to multiple-stimulus displays: I. Neurons encode the location of the salient stimulus. *Cerebral Cortex*, *11*(7), 581-591. https://doi.org/10.1093/cercor/11.7.581

Conway, B. R., & Livingstone, M. S. (2006). Spatial and temporal properties of cone signals in alert macaque primary visual cortex. *Journal of Neuroscience*, *26*(42), 10826–10846. https://doi.org/10.1523/JNEUROSCI.2091-06.2006

Conway, B. R., Moeller, S., & Tsao, D. Y. (2007). Specialized color modules in macaque extrastriate cortex. *Neuron*, *56*(3), 560–573. https://doi.org/10.1016/j.neuron.2007.10.008

Corbetta, M., & Shulman, G. L. (2002). Control of goal-directed and stimulus-driven attention in the brain. *Nature Reviews Neuroscience*, *3*(3), 201-215. https://doi.org/10.1038/nrn755

Corbetta, M., Akbudak, E., Conturo, T. E., Snyder, A. Z., Ollinger, J. M., Drury, H. A., ... & Shulman, G. L. (1998). A common network of functional areas for attention and eye movements. *Neuron*, *21*(4), 761-773. https://doi.org/10.1016/S0896-6273(00)80593-0

Curcio, C. A., Sloan, K. R., Kalina, R. E., & Hendrickson, A. E. (1990). Human photoreceptor topography. *The Journal of Comparative Neurology*, *292*(4), 497–523. https://doi.org/10.1002/cne.902920402.

D'Zmura, M. (1991). Color in visual search. *Vision Research*, *31*(6), 951–966. https://doi.org/10.1016/0042-6989(91)90203-H

Dassonville, P., Schlag, J., & Schlag-Rey, M. (1992). The frontal eye field provides the goal of saccadic eye movement. *Experimental Brain Research*, *89*, 300–310. https://doi.org/10.1007/BF00228246

Davidson, R. M., & Bender, D. B. (1991). Selectivity for relative motion in the monkey superior colliculus. *Journal of Neurophysiology*, *65*(5), 1115-1133. https://doi.org/10.1152/jn.1991.65.5.1115

De Valois R. L., & De Valois, K. K. (1993). A multi-stage color model. *Vision Research*, *33*(8), 1053–1065. https://doi.org/10.1016/0042-6989(93)90240-W

De Valois, R. L., & Cottaris, N. P. (1998). Inputs to directionally selective simple cells in macaque striate cortex. *Proceedings of the National Academy of Sciences of the United States of America*, *95*(24), 14488-14493. https://doi.org/10.1073/pnas.95.24.14488

De Vries, J. P., Van der Stigchel, S., Hooge, I. T., & Verstraten, F. A. (2018). The lifetime of salience extends beyond the initial saccade. *Perception*, *47*(2), 125-142. https://doi.org/10.1177/0301006617735726

DeAngelis, G. C., Cumming, B. G., & Newsome, W. T. (1998). Cortical area MT and the perception of stereoscopic depth. *Nature, 394*(6694), 677-680. https://doi.org/10.1038/29299

Derrington, A. M, Krauskopf, J., & Lennie, P. (1984). Chromatic mechanisms in lateral geniculate nucleus of macaque. *Journal of Physiology*, *357*(1), 241–265. https://doi.org/10.1113/jphysiol.1984.sp015499

Deuble, H., Wolf, W., & Hauske, G. (1984). The evaluation of the oculomotor error signal. In A. G. Gale & F. Johnston (Eds.), *Theoretical and Applied Aspects of Eye Movement Research* (pp. 55–62). North-Holland/Elsevier Science. https://doi.org/10.1016/S0166-4115(08)61818-X

DeYoe, E. A., & Van Essen, D. C. (1988). Concurrent processing streams in monkey visual cortex. *Trends in Neurosciences*, *11*(5), 219-226. https://doi.org/10.1016/0166-2236(88)90130-0

DiCarlo, J. J., Zoccolan, D., & Rust, N. C. (2012). How does the brain solve visual object recognition?. *Neuron*, *73*(3), 415-434. https://doi.org/10.1016/j.neuron.2012.01.010

Ding, L., & Gold, J.I. (2010). Caudate encodes multiple computations for perceptual decisions. *Journal of Neuroscience*, *30*(47), 15747–15759. https://doi.org/10.1523/JNEUROSCI.2894-10.2010

Ditterich, J., Mazurek, M. E., & Shadlen, M. N. (2003). Microstimulation of visual cortex affects the speed of perceptual decisions. *Nature Neuroscience*, *6*(8), 891–898. https://doi.org/10.1038/nn1094

Dorris, M. C., Olivier, E., & Munoz, D. P. (2007). Competitive integration of visual and preparatory signals in the superior colliculus during saccadic programming. *Journal of Neurosci*ence, *27*(19), 5053–5062. https://doi.org/10.1523/JNEUROSCI.4212-06.2007

Dorris, M. C., Pare, M., & Munoz, D. P. (1997). Neuronal activity in monkey superior colliculus related to the initiation of saccadic eye movements. *Journal of Neuroscience*, *17*(21), 8566-8579. https://doi.org/10.1523/JNEUROSCI.17-21-08566.1997

Doyle, M., & Walker, R. (2001). Curved saccade trajectories: Voluntary and reflexive saccades curve away from irrelevant distractors. *Experimental Brain Research*, *139*(3), 333-344. https://doi.org/10.1007/s002210100742

Driver, J., & Mattingley, J. B. (1998). Parietal neglect and visual awareness. *Nature Neuroscience*, *1*(1), 17-22. https://doi.org/10.1038/217

Duhamel, J. R., Colby, C. L., & Goldberg, M. E. (1992). The updating of the representation of visual space in parietal cortex by intended eye movements. *Science*, *255*(5040), 90-92. https://doi.org/10.1126/science.1553535

Dürsteler, M. R., & Wurtz, R. H. (1988). Pursuit and optokinetic deficits following chemical lesions of cortical areas MT and MST. *Journal of Neurophysiology*, *60*(3), 940–965. https://doi.org/10.1152/jn.1988.60.3.940

Dürsteler, M. R., Wurtz, R. H., & Newsome, W. T. (1987). Directional pursuit deficits following lesions of the foveal representation within the superior temporal sulcus of the macaque monkey. *Journal of Neurophysiology*, *57*(5), 1262–1287. https://doi.org/10.1152/jn.1987.57.5.1262

Edelman, J. A., & Xu, K. Z. (2009). Inhibition of voluntary saccadic eye movement commands by abrupt visual onsets. *Journal of Neurophysiology, 101*(3), 1222–1234. https://doi.org/10.1152/jn.90708.2008

Engbert, R., & Kliegl, R. (2003). Microsaccades uncover the orientation of covert attention. *Vision Research, 43*(9), 1035-1045. https://doi.org/10.1016/S0042-6989(03)00084-1

Fallah, M., & Reynolds, J. H. (2012). Contrast dependence of smooth pursuit eye movements following a saccade to superimposed targets. *PLoS One, 7*, e37888. https://doi.org/10.1371/journal.pone.0037888

Fecteau, J. H., & Munoz, D. P. (2006). Salience, relevance, and firing: a priority map for target selection. *Trends in Cognitive Sciences, 10*(8), 382-390. https://doi.org/10.1016/j.tics.2006.06.011

Felleman, D. J., & Van Essen, D. C. (1991). Distributed hierarchical processing in the primate cerebral cortex. *Cerebral Cortex, 1*(1), 1-47. https://doi.org/10.1093/cercor/1.1.1.

ffytche, D. H., Guy, C. N., & Zeki, S. (1995). The parallel visual motion inputs into areas V1 and V5 of human cerebral cortex. *Brain, 118*(6), 1375–1394. https://doi.org/10.1093/brain/118.6.1375

Findlay, J. M, & Harris, L. R. (1984). Small saccades to double-stepped targets moving in two dimensions. In A. G. Gale & F. Johnson (Eds.), *Theoretical and Applied Aspects of Eye Movement Research* (pp. 71–78). North-Holland/Elsevier Science. https://doi.org/10.1016/S0166-4115(08)61820-8

Findlay, J. M. (1982). Global visual processing for saccadic eye movements. *Vision Research, 22*(8), 1033-1045. https://doi.org/10.1016/0042-6989(82)90040-2

Findlay, J. M., & Blythe, H. I. (2009). Saccade target selection: Do distractors affect saccade accuracy? *Vision Research, 49*(10), 1267-1274. https://doi.org/10.1016/j.visres.2008.07.005

Findlay, J. M., & Kapoula, Z. (1992). Scrutinization, spatial attention, and the spatial programming of saccadic eye movements. *The Quarterly Journal of Experimental Psychology*, *45*(4), 633-647. https://doi.org/10.1080/14640749208401336

Folk, C. L., Remington, R. W., & Johnston, J. C. (1992). Involuntary covert orienting is contingent on attentional control settings. *Journal of Experimental Psychology: Human Perception and Performance*, *18*(4), 1030–1044. https://doi.org/10.1037/0096-1523.18.4.1030

Folk, C. L., Remington, R. W., & Wright, J. H. (1994). The structure of attentional control: contingent attentional capture by apparent motion, abrupt onset, and color. *Journal of Experimental Psychology: Human Perception and Performance*, *20*(2), 317–329. https://doi.org/10.1037/0096-1523.20.2.317

Fries, W. (1984). Cortical projections to the superior colliculus in the macaque monkey: a retrograde study using horseradish peroxidase. *Journal of Comparative Neurology*, *230*(1), 55–76. https://doi.org/10.1002/cne.902300106

Georgopoulos, A. P., Kalaska, J. F., Caminiti, R., & Massey, J. T. (1982). On the relations between the direction of two-dimensional arm movements and cell discharge in primate motor cortex. *Journal of Neuroscience*, *2*(11), 1527–1537. https://doi.org/10.1523/JNEUROSCI.02-11-01527.1982.

Georgopoulos, A. P., Kettner, R. E., & Schwartz, A. B. (1988). Primate motor cortex and free arm movements to visual targets in three-dimensional space. II. Coding of the direction of movement by a neuronal population. *Journal of Neuroscience*, *8*(8), 2928-2937. https://doi.org/10.1523/JNEUROSCI.08-08-02928.1988.

Giuricich, C., Green, R. J., Jordan, H., & Fallah, M. (2023). Target-distractor competition modulates saccade trajectories in space and object space. *eNeuro*, *10*(6). https://doi.org/10.1523/ENEURO.0450-22.2023

Glimcher, P. W., & Sparks, D. L. (1992). Movement selection in advance of action in the superior colliculus. *Nature*, *355*(6360), 542-545. https://doi.org/10.1038/355542a0

Glimcher, P. W., & Sparks, D. L. (1993). Effects of low-frequency stimulation of the superior colliculus on spontaneous and visually guided saccades. *Journal of Neurophysiology*, *69*(3), 953-964. https://doi.org/10.1152/jn.1993.69.3.953

Gold, J. I., & Shadlen, M. N. (2000). Representation of a perceptual decision in developing oculomotor commands. *Nature*, *404*(6776), 390-394. https://doi.org/10.1038/35006062

Gold, J. I., Bennett, P. J., & Sekuler, A. B. (1999). Signal but not noise changes with perceptual learning. *Nature*, *402*(6758), 176–178. https://doi.org/10.1038/46027

Goldberg, M. E., & Bushnell, M. C. (1981). Behavioral enhancement of visual responses in monkey cerebral cortex. II. Modulation in frontal eye fields specifically related to saccades. *Journal of Neurophysiology*, *46*(4), 773-787. https://doi.org/10.1152/jn.1981.46.4.773

Goldberg, M. E., & Wurtz, R. H. (1972). Activity of superior colliculus in behaving monkey. I. Visual receptive fields of single neurons. *Journal of Neurophysiology*, *35*(4), 542-559. https://doi.org/10.1152/jn.1972.35.4.542

Goldberg, M. E., Bisley, J. W., Powell, K. D., & Gottlieb, J. (2006). Saccades, salience and attention: the role of the lateral intraparietal area in visual behavior. *Progress in Brain Research*, *155*(B), 157-175. https://doi.org/10.1016/S0079-6123(06)55010-1

Goldman-Rakic, P. S. (1995). Cellular basis of working memory. *Neuron*, *14*(3), 477–485. https://doi.org/10.1016/0896-6273(95)90304-6

Gottlieb, J. P., Bruce, C. J., & MacAvoy, M. G. (1993). Smooth eye movements elicited by microstimulation in the primate frontal eye field. *Journal of Neurophysiology*, *69*(3), 786-799. https://doi.org/10.1152/jn.1993.69.3.786.

Green, B. F., & Anderson, L. K. (1956). Color coding in a visual search task. *Journal of Experimental Psychology*, *51*(1), 19–24. https://doi.org/10.1037/h0047484

Groh, J. M., Born, R. T., & Newsome, W. T. (1997). How is a sensory map read out? Effects of microstimulation in visual area MT on saccades and smooth pursuit eye movements. *Journal of Neuroscience*, *17*(11), 4312-4330. https://doi.org/10.1523/JNEUROSCI.17-11-04312.1997

Hafed, Z. M., & Chen, C. Y. (2016). Sharper, stronger, faster upper visual field representation in primate superior colliculus. *Current Biology, 26*(13), 1647–1658. https://doi.org/10.1016/j.cub.2016.04.059

Hafed, Z. M., & Clark, J. J. (2002). Microsaccades as an overt measure of covert attention shifts. *Vision Research, 42*(22), 2533-2545. https://doi.org/10.1016/S0042-6989(02)00263-8

Hafed, Z. M., & Ignashchenkova, A. (2013). On the dissociation between microsaccade rate and direction after peripheral cues: microsaccadic inhibition revisited. *Journal of Neuroscience*, *33*(41), 16220–16235. https://doi.org/10.1523/JNEUROSCI.2240-13.2013

Hafed, Z. M., Hoffmann, K. P., Chen, C. Y., & Bogadhi, A. R. (2023). Visual functions of the primate superior colliculus. *Annual Review of Vision Science, 9*, 361-383. https://doi.org/10.1146/annurev-vision-111022-123817

Hall, N. J., & Colby, C. L. (2014). S-cone visual stimuli activate superior colliculus neurons in old world monkeys: implications for understanding blindsight. *Journal of Cognitive Neuroscience*, *26*(6), 1234–1256. https://doi.org/10.1162/jocn_a_00555

Hall, N. J., & Colby, C. L. (2016). Express saccades and superior colliculus responses are sensitive to short-wavelength cone contrast. *Proceedings of the National Academy of Sciences of the United States of America*, *113*(24), 6743–6748. https://doi.org/10.1073/pnas.1600095113

Hanes, D. P., & Schall, J. D. (1996). Neural control of voluntary movement initiation. *Science*, *274*(5286), 427–430. https://doi.org/10.1126/science.274.5286.427

Hanes, D. P., & Wurtz, R. H. (2001). Interaction of the frontal eye field and superior colliculus for saccade generation. *Journal of Neurophysiology*, *85*(2), 804-815. https://doi.org/10.1152/jn.2001.85.2.804

Hanes, D. P., Patterson, W. F., & Schall, J. D. (1998). Role of frontal eye fields in countermanding saccades: visual, movement, and fixation activity. *Journal of Neurophysiology*, *79*(2), 817-834. https://doi.org/10.1152/jn.1998.79.2.817

Haxby, J. V., Grady, C. L., Horwitz, B., Ungerleider, L. G., Mishkin, M., Carson, R. E., ... & Rapoport, S. I. (1991). Dissociation of object and spatial visual processing pathways in human extrastriate cortex. *Proceedings of the National Academy of Sciences of the United States of America*, *88*(5), 1621-1625.

He, P., & Kowler, E. (1989). The role of location probability in the programming of saccades: Implications for "center-of-gravity" tendencies. *Vision Research*, *29*(9), 1165-1181. https://doi.org/10.1016/0042-6989(89)90063-1

Heeman, J., Theeuwes, J., & Van der Stigchel, S. (2014). The time course of top-down control on saccade averaging. *Vision Research*, *100*, 29-37. https://doi.org/10.1016/j.visres.2014.03.007

Heeman, J., Van der Stigchel, S., & Theeuwes J. (2017). The influence of distractors on express saccades. *Journal of Vision*, *17*(1), 1–17. https://doi.org/10.1167/17.1.35

Hegde, J., & Felleman, D. J. (2007). Reappraising the functional implications of the primate visual anatomical hierarchy. *The Neuroscientist*, *13*(5), 416-421. https://doi.org/10.1177/1073858407305201

Herman, J. P., & Krauzlis, R. J. (2017). Color-Change Detection Activity in the Primate Superior Colliculus. *eNeuro*, *4*(2). http://doi.org/10.1523/ENEURO.0046-17.2017

Heywood, C. A., & Cowey, A. (2013). Cerebral achromatopsia. In G. W. Humphreys (Ed.), *Case Studies in the Neuropsychology of Vision* (pp. 17-39). Psychology Press.

Hikosaka, O., & Wurtz, R. H. (1985a). Modification of saccadic eye movements by GABA-related substances. I. Effect of muscimol and bicuculline in monkey superior colliculus. *Journal of Neurophysiology*, *53*(1), 266–291. https://doi.org/10.1152/jn.1985.53.1.266

Hikosaka, O., & Wurtz, R.H. (1985b). Modification of saccadic eye movements by GABA-related substances. II. Effects of muscimol in monkey substantia nigra pars reticulata. *Journal of Neurophysiology*, *53*(1), 292–308. https://doi.org/10.1152/jn.1985.53.1.292

Hikosaka, O., Takikawa, Y., & Kawagoe, R. (2000). Role of the basal ganglia in the control of purposive saccadic eye movements. *Physiological Review*, *80*(3), 953–978. https://doi.org/10.1152/physrev.2000.80.3.953

Hopf, J.-M., Boehler, C.N., Luck, S.J., Tsotsos, J.K., Heinze, H.-J., & Schoenfeld, M.A. (2006). Direct neurophysiological evidence for spatial suppression surrounding the focus of attention in vision. *Proceedings of the National Academy of Sciences of the United States of America*, *103*(4), 1053–1058. https://doi.org/10.1073/pnas.0507746103

Hopf, J.-M., Boehler, C.N., Schoenfeld, M.A., Heinze, H.-J., & Tsotsos, J.K. (2010). The spatial profile of the focus of attention in visual search: Insights from MEG recordings. *Vision Research*, *50*(14), 1312–1320. https://doi.org/10.1016/j.visres.2010.01.015

Horwitz, G. D., & Newsome, W. T. (1999). Separate signals for target selection and movement specification in the superior colliculus. *Science, 284*(5417), 1158-1161. https://doi.org/10.1126/science.284.5417.1158

Horwitz, G. D., & Newsome, W. T. (2001). Target selection for saccadic eye movements: Direction-selective visual responses in the superior colliculus. *Journal of Neurophysiology, 86*(5), 2527-2542. https://doi.org/10.1152/jn.2001.86.5.2527

Hubel, D. H., LeVay, S., & Wiesel, T. N. (1975). Mode of termination of retinotectal fibers in macaque monkey: an autoradiographic study. *Brain Research*, *96*(1), 25-40. https://doi.org/10.1016/0006-8993(75)90567-3

Huerta, M. F., Krubitzer, L. A., & Kaas, J. H. (1986). Frontal eye field as defined by intracortical microstimulation in squirrel monkeys, owl monkeys, and macaque monkeys: I. Subcortical connections. *Journal of Comparative Neurology*, *253*(4), 415-439. https://doi.org/10.1002/cne.902530402

Ikeda, T., & Hikosaka, O. (2003). Reward-dependent gain and bias of visual responses in primate superior colliculus. *Neuron, 39*(4), 693-700. https://doi.org/10.1016/S0896-6273(03)00464-1

Ishihara, S. (2006). *The series of plates designed as a test for colour deficiency* (Concise ed.). Tokyo: Kanehara Trading Inc.

Itti, L., & Koch, C. (2000). A saliency-based search mechanism for overt and covert shifts of visual attention. *Vision Research, 40*(10-12), 1489-1506. https://doi.org/10.1016/S0042-6989(99)00163-7

Itti, L., Koch, C., & Niebur, E. (1998). A model of saliency-based visual attention for rapid scene analysis. *IEEE Transactions on Pattern Analysis and Machine Intelligence*, *20*(11), 1254-1259. https://doi.org/10.1109/34.730558

Johnston, K., & Everling, S. (2006). Monkey dorsolateral prefrontal cortex sends task-selective signals directly to the superior colliculus. *Journal of Neuroscience*, *26*(48), 12471-12478. https://doi.org/10.1523/JNEUROSCI.4101-06.2006

Johnston, K., & Everling, S. (2008). Task-relevant output signals are sent from monkey dorsolateral prefrontal cortex to the superior colliculus during a visuospatial working memory task. *Journal of Cognitive Neuroscience*, *21*(5), 1023-1038. https://doi.org/10.1162/jocn.2009.21067

Jonikaitis, D., & Belopolsky, A. V. (2014). Target–distractor competition in the oculomotor system is spatiotopic. *Journal of Neuroscience*, *34*(19), 6687-6691. https://doi.org/10.1523/JNEUROSCI.4453-13.2014

Kastner, S., DeSimone, K., Konen, C. S., Szczepanski, S. M., Weiner, K. S., & Schneider, K. A. (2007). Topographic maps in human frontal cortex revealed in memory-guided saccade and spatial working-memory tasks. *Journal of Neurophysiology*, *97*(5), 3494–3507. https://doi.org/10.1152/jn.00010.2007

Kawano, K., & Miles, F.A. (1986). Short-latency ocular following responses of monkey. II. Dependence on a prior saccadic eye movement. *Journal of Neurophysiology*, *56*(5), 1355-1380. https://doi.org/10.1152/jn.1986.56.5.1355

Kehoe, D. H., & Fallah, M. (2017). Rapid accumulation of inhibition accounts for saccades curved away from distractors. *The Journal of Neurophysiology, 118*(2), 832–844. https://doi.org/10.1152/jn.00742.2016

Kehoe, D. H., Aybulut, S., & Fallah, M. (2018a). Higher order, multifeatural object encoding by the oculomotor system. *Journal of Neurophysiology*, *120*(6), 3042–3062. https://doi.org/10.1152/ jn.00834.2017

Kehoe, D. H., Lewis, J., & Fallah, M. (2021). Oculomotor target selection is mediated by complex objects. *Journal of Neurophysiology*, *126*(3), 845-863. https://doi.org/10.1152/jn.00580.2020

Kehoe, D. H., Rahimi, M., & Fallah, M. (2018b). Perceptual color space representations in the oculomotor system are modulated by surround suppression and biased selection. *Frontiers in Systems Neuroscience*, *12*, 1. https://doi.org/10.3389/fnsys.2018.00001

Kehoe, D. H., Schießer, L., Malik, H., & Fallah, M. (2023). Motion distractors perturb saccade programming later in time than static distractors. *Current Research in Neurobiology*, *4*, 100092. https://doi.org/10.1016/j.crneur.2023.100092

Kettner, R. E., Schwartz, A. B., & Georgopoulos, A. P. (1988). Primate motor cortex and free arm movements to visual targets in three-dimensional space. III. Positional gradients and population coding of movement direction from various movement origins. *Journal of Neuroscience*, *8*(8), 2938-2947. https://doi.org/10.1523/JNEUROSCI.08-08-02938.1988

Kienitz, R., Kouroupaki, K., & Schmid, M. C. (2022). Microstimulation of visual area V4 improves visual stimulus detection. *Cell Reports*, *40*(12), 111392. https://doi.org/10.1016/j.celrep.2022.111392

Kim, B., & Basso, M. A. (2008). Saccade target selection in the superior colliculus: a signal detection theory approach. *Journal of Neuroscience*, *28*(12), 2991-3007. https://doi.org/10.1523/JNEUROSCI.5424-07.2008

Komatsu, H., & Wurtz, R. H. (1989). Modulation of pursuit eye movements by stimulation of cortical areas MT and MST. *Journal of Neurophysiology*, *62*(1), 31–47. https://doi.org/10.1152/jn.1989.62.1.31

Krauzlis, R. J., & Dill, N. (2002). Neural correlates of target choice for pursuit and saccades in the primate superior colliculus. *Neuron*, *35*(2), 355-363. https://doi.org/10.1016/S0896-6273(02)00756-0

Krauzlis, R. J., & Miles, F. A. (1998). Role of the oculomotor vermis in generating pursuit and saccades: effects of microstimulation. *Journal of Neurophysiology*, *80*(4), 2046–62. https://doi.org/10.1152/jn.1998.80.4.2046

Krauzlis, R.J. (2005). The control of voluntary eye movements: New perspectives. *The Neuroscientist*, *11*(2), 124–137. https://doi.org/10.1177/1073858404271196

Kravitz, D. J., Saleem, K. S., Baker, C. I., Ungerleider, L. G., & Mishkin, M. (2013). The ventral visual pathway: an expanded neural framework for the processing of object quality. *Trends in Cognitive Sciences*, *17*(1), 26-49. https://doi.org/10.1016/j.tics.2012.10.011

Laidlaw, K. E., Badiudeen, T. A., Zhu, M. J., & Kingstone, A. (2015). A fresh look at saccadic trajectories and task irrelevant stimuli: Social relevance matters. *Vision Research*, *111*(A), 82-90. https://doi.org/10.1016/j.visres.2015.03.024

Le, Q. V., Nishimaru, H., Matsumoto, J., Takamura, Y., Hori, E., Maior, R. S., Tomaz, C., Ono, T., & Nishijo, H. (2020). A prototypical template for rapid face detection is embedded in the monkey superior colliculus. *Frontiers in System Neuroscience*, *14*, 5. https://doi.org/10.3389/fnsys.2020.00005

Lee, C., Rohrer, W. H., & Sparks, D. L. (1988). Population coding of saccadic eye movements by neurons in the superior colliculus. *Nature*, *332*(6162), 357-360. https://doi.org/10.1038/332357a0

Lee, H. W., Hong, S. B., Seo, D. W., Tae, W. S., & Hong, S. C. (2000). Mapping of functional organization in human visual cortex: electrical cortical stimulation. *Neurology*, *54*(4), 849-854. https://doi.org/10.1212/WNL.54.4.849

Lee, H., Simpson, G. V., Logothetis, N. K., & Rainer, G. (2005). Phase locking of single neuron activity to theta oscillations during working memory in monkey extrastriate visual cortex. *Neuron*, *45*(1), 147–156. https://doi.org/10.1016/j.neuron.2004.12.025

Li, X., & Basso, M. A. (2005). Competitive stimulus interactions within single response fields of superior colliculus neurons. *Journal of Neuroscience*, *25*(49), 11357-11373. https://doi.org/10.1523/JNEUROSCI.3825-05.2005

Li, X., & Basso, M. A. (2008). Preparing to move increases the sensitivity of superior colliculus neurons. *Journal of Neuroscience*, *28*(17), 4561–77. https://doi.org/10.1523/JNEUROSCI.5683-07.2008

Lindsey, D. T., Brown, A. M., Reijnen, E., Rich, A. N., Kuzmova, Y. I., & Wolfe, J. M. (2010). Color channels, not color appearance or color categories, guide visual search for desaturated color targets. *Psychological Science*, *21*(9), 1208–1214. https://doi.org/10.1177/0956797610379861

Liu, P., & Basso, M. A. (2008). Substantia nigra stimulation influences monkey superior colliculus neuronal activity bilaterally. *Journal of Neurophysiology*, *100*(2), 1098–1112. https://doi.org/10.1152/jn.01043.2007

Livingstone, M. S., & Hubel, D. H. (1987). Psychophysical evidence for separate channels for the perception of form, color, movement, and depth. *Journal of Neuroscience*, *7*(11), 3416–3468. https://doi.org/10.1523/JNEUROSCI.07-11-03416.1987

Livingstone, M. S., & Hubel, D. H. (1988). Segregation of form, color, movement, and depth: anatomy, physiology, and perception. *Science*, *240*(4853), 740–749. https://doi.org/10.1126/science.3283936

Livingstone, M. S., Pack, C. C., & Born, R. T. (2001). Two-dimensional substructure of MT receptive fields. *Neuron*, *30*(3), 781-793. https://doi.org/10.1016/S0896-6273(01)00313-0

Loach, D., Frischen, A., Bruce, N., & Tsotsos, J. K. (2010). An attentional mechanism for selecting appropriate actions afforded by graspable objects. *Psychological Science*, *19*(12), 1253–1257. https://doi.org/10.1111/j.1467-9280.2008.02234.x

Lock, T. M., Baizer, J. S., Bender, D. B. (2003). Distribution of corticotectal cells in macaque. *Experimental Brain Research*, 151, 455–470. https://doi.org/10.1007/s00221-003-1500-y

Lovejoy, L. P., & Krauzlis, R. J. (2010). Inactivation of primate superior colliculus impairs covert selection of signals for perceptual judgments. *Nature Neuroscience*, *13*(2), 261-266. https://doi.org/10.1038/nn.2470

Lowe, K. A., & Schall, J. D. (2018). Functional categories of visuomotor neurons in macaque frontal eye field. *eNeuro*, *5*(5). https://doi.org/10.1523/ENEURO.0131-18.2018

Luck, S. J. (2014). *An introduction to the event-related potential technique* (2nd ed.). MIT Press.

Ludwig, C. J. H., & Gilchrist, I. D. (2002). Measuring saccade curvature: A curve-fitting approach. *Behavior Research Methods, Instruments, & Computers*, *34*(4), 618-624. https://doi.org/10.3758/BF03195490

Ludwig, C. J. H., & Gilchrist, I. D. (2003). Target similarity affects saccade curvature away from irrelevant onsets. *Experimental Brain Research*, *152*(1), 60-69. https://doi.org/10.1007/s00221-003-1520-7

Ludwig, C. J. H., Mildinhall, J. W., & Gilchrist, I. D. (2007). A population coding account for systematic variation in saccadic dead time. *Journal of Neurophysiology*, *97*(1), 795-805. https://doi.org/10.1152/jn.00652.2006

Marino, R. A., Levy, R., & Munoz, D. P. (2015). Linking express saccade occurrence to stimulus properties and sensorimotor integration in the superior colliculus. *Journal of Neurophysiology*, 114(2), 879–892. https://doi.org/10.1152/jn.00047.2015

Marino, R. A., Rodgers, C. K., Levy, R., & Munoz, D. P. (2008). Spatial relationships of visuomotor transformations in the superior colliculus map. *Journal of Neurophysiology*, 100(5), 2564–2576. https://doi.org/10.1152/jn.90688.2008

Marr, D. (1982). *Vision: A computational investigation into the human representation and processing of visual information*. Freeman and Company.

Martinez-Trujillo, J. C., & Treue, S. (2004). Feature-based attention increases the selectivity of population responses in primate visual cortex. *Current Biology, 14*(9), 744-751. https://doi.org/10.1016/j.cub.2004.04.028

Maunsell, J. H. R., & Van Essen, D. C. (1983). The connections of the middle temporal visual area (MT) and their relationship to a cortical hierarchy in the macaque monkey. *Journal of Neuroscience, 3*(12), 2563–2586. https://doi.org/10.1523/JNEUROSCI.03-12-02563.1983

Mayo, J. P., & Sommer, M. A. (2013). Neuronal correlates of visual time perception at brief timescales [Supplemental material]. *Proceedings of the National Academy of Sciences of the United States of America*, *110*(4), 1506-1511. https://doi.org/10.1073/pnas.1217177110

Mays, L. E., & Sparks, D. L. (1980). Dissociation of visual and saccade-related responses in superior colliculus neurons. *Journal of Neurophysiology*, *43*(1), 207-232. https://doi.org/10.1152/jn.1980.43.1.207

McAdams, C. J., & Maunsell, J. H. (1999a). Effects of attention on the reliability of individual neurons in monkey visual cortex. *Neuron*, *23*(4), 765-773. https://doi.org/10.1016/S0896-6273(01)80034-9

McAdams, C. J., & Maunsell, J. H. (1999b). Effects of attention on orientation-tuning functions of single neurons in macaque cortical area V4. *Journal of Neuroscience*, *19*(1), 431-441. https://doi.org/10.1523/JNEUROSCI.19-01-00431.1999

McPeek, R. M. (2006). Incomplete suppression of distractor-related activity in the frontal eye field results in curved saccades. *Journal of Neurophysiology*, *96*(5), 2699-2711. https://doi.org/10.1152/jn.00564.2006

McPeek, R. M., & Keller, E. L. (2001). Short-term priming, concurrent processing, and saccade curvature during a target selection task in the monkey. *Vision Research*, *41*(6), 785–800. https://doi.org/10.1016/S0042-6989(00)00287-X

McPeek, R. M., & Keller, E. L. (2002). Saccade target selection in the superior colliculus during a visual search task. *Journal of Neurophysiology*, *88*(4), 2019-2034. https://doi.org/10.1152/jn.2002.88.4.2019

McPeek, R. M., & Keller, E. L. (2004). Deficits in saccade target selection after inactivation of superior colliculus. *Nature Neuroscience*, *7*(7), 757-763. https://doi.org/10.1038/nn1269

McPeek, R. M., Han, J. H., & Keller, E. L. (2003). Competition between saccade goals in the superior colliculus produces saccade curvature. *Journal of Neurophysiology*, *89*(5), 2577-2590. https://doi.org/10.1152/jn.00657.2002

McSorley, E., Haggard, P., & Walker, R. (2004). Distractor modulation of saccade trajectories: Spatial separation and symmetry effects. *Experimental Brain Research, 155*(3), 320-333. https://doi.org/10.1007/s00221-003-1729-5

McSorley, E., Haggard, P., & Walker, R. (2006). Time course of oculomotor inhibition revealed by saccade trajectory modulation. *Journal of Neurophysiology, 96*(3), 1420-1424. https://doi.org/10.1152/jn.00315.2006

McSorley, E., Haggard, P., & Walker, R. (2009). The spatial and temporal shape of oculomotor inhibition. *Vision Research, 49*(6), 608–614. https://doi.org/10.1016/j.visres.2009.01.015

Mehta, A. D., Ulbert, I., & Schroeder, C. E. (2000). Intermodal selective attention in monkeys. I: Distribution and timing of effects across visual areas. *Cerebral Cortex, 10*(4), 343–358. https://doi.org/10.1093/cercor/10.4.343

Meienberg, O., Zangemeister, W. H., Rosenberg, M., Hoyt, W. F., & Stark, L. (1981). Saccadic eye movement strategies in patients with homonymous hemianopia. *Annals of Neurology*, *9*(6), 537-544. https://doi.org/10.1002/ana.410090605

Merriam, E. P., Genovese, C. R., & Colby, C. L. (2007). Remapping in human visual cortex. *Journal of Neurophysiology*, *97*(2), 1738-1755. https://doi.org/10.1152/jn.00189.2006

Miles, F. A, Kawano, K., & Optican, L. M. (1986). Short-latency ocular following responses of monkey. I. Dependence on temporospatial properties of visual input. *Journal of Neurophysiology*, *56*(5), 1321-1354. https://doi.org/10.1152/jn.1986.56.5.1321

Mineault, P. J., Khawaja, F. A., Butts, D. A., & Pack, C. C. (2012). Hierarchical processing of complex motion along the primate dorsal visual pathway. *Proceedings of the National Academy of Sciences of the United States*, *109*(16), E972-E980. https://doi.org/10.1073/pnas.1115685109

Mishkin, M., & Ungerleider, L. G. (1982). Contribution of striate inputs to the visuospatial functions of parieto-preoccipital cortex in monkeys. *Behavioural Brain Research*, *6*(1), 57-77. https://doi.org/10.1016/0166-4328(82)90081-X

Mishkin, M., Ungerleider, L. G., & Macko, K. A. (1983). Object vision and spatial vision: Two cortical pathways. *Trends in Neurosciences*, *6*, 414-417. https://doi.org/10.1016/0166-2236(83)90190-X

Miyashita, N., & Hikosaka, O. (1996). Minimal synaptic delay in the saccadic output pathway of the superior colliculus studied in awake monkey. *Experimental Brain Research*, *112*(2), 187-196. https://doi.org/10.1007/BF00227637

Mohler, C. W, & Wurtz, R. H. (1977). Role of striate cortex and superior colliculus in visual guidance of saccadic eye movements in monkeys. *Journal of Neurophysiology*, 40(1), 74–94. https://doi.org/10.1152/jn.1977.40.1.74

Mohler, C. W., Goldberg., M. E., & Wurtz, R. H. (1973). Visual receptive fields of frontal eye field neurons. *Brain Research*, *61*, 385–389. https://doi.org/10.1016/0006-8993(73)90543-X

Monosov, I. E., Sheinberg, D. L., & Thompson, K. G. (2011). The effects of prefrontal cortex inactivation on object responses of single neurons in the inferotemporal cortex during visual search. *Journal of Neuroscience*, *31*(44), 15956-15961. https://doi.org/10.1523/JNEUROSCI.2995-11.2011

Moore, T., & Armstrong, K. M. (2003). Selective gating of visual signals by microstimulation of frontal cortex. *Nature*, *421*(6921), 370-373. https://doi.org/10.1038/nature01341

Moore, T., & Fallah, M. (2001). Control of eye movements and spatial attention. *Proceedings of the National Academy of Sciences of the United States of America*, *98*(3), 1273-1276. https://doi.org/10.1152/jn.00741.2002

Moore, T., & Fallah, M. (2004). Microstimulation of the frontal eye field and its effects on covert spatial attention. *Journal of Neurophysiology*, *91*(1), 152-162. https://doi.org/10.1073/pnas.98.3.1273

Moore, T., Armstrong, K. M., & Fallah, M. (2003). Visuomotor origins of covert spatial attention. *Neuron*, *40*(4), 671-683. https://doi.org/10.1016/S0896-6273(03)00716-5

Moschovakis, A. K., Karabelas, A. B., & Highstein, S. M. (1988). Structure-function relationships in the primate superior colliculus. II. Morphological identity of presaccadic neurons. *Journal of Neurophysiology*, *60*(1), 263-302. https://doi.org/10.1152/jn.1988.60.1.263

Motter, B. C. (1993). Focal attention produces spatially selective processing in visual cortical areas V1, V2, and V4 in the presence of competing stimuli. *Journal of Neurophysiology*, *70*(3), 909-919. https://doi.org/10.1152/jn.1993.70.3.909

Movshon, J. A., & Newsome, W. T. (1996). Visual response properties of striate cortical neurons projecting to area MT in macaque monkeys. *Journal of Neuroscience*, *16*(23), 7733–7741. https://doi.org/10.1523/JNEUROSCI.16-23-07733.1996

Movshon, J. A., Adelson, E. H., Gizzi, M. S., & Newsome, W. T. (1985). The analysis of moving visual patterns. In C. Chagas, R. Gattass, & C. Gross (Eds.), *Pattern Recognition Mechanisms* (pp. 117-151). Vatican Press.

Mulckhuyse, M., Van der Stigchel, S., & Theeuwes, J. (2009). Early and late modulation of saccade deviations by target distractor similarity. *Journal of Neurophysiology*, *102*(3), 1451-1458. https://doi.org/10.1152/jn.00068.2009

Müller, J. R., Philiastides, M. G., & Newsome, W. T. (2005). Microstimulation of the superior colliculus focuses attention without moving the eyes. *Proceedings of the National Academy of Sciences of the United States of America*, *102*(3), 524-529. https://doi.org/10.1073/pnas.0408311101

Müller, N. G., & Kleinschmidt, A. (2004). The attentional 'spotlight's' penumbra: Center-surround modulation in striate cortex. *NeuroReport*, *15*(6), 977–980. https://doi.org/10.1097/00001756-200404290-00009

Munoz, D. P., & Istvan, P. J. (1998). Lateral inhibitory interactions in the intermediate layers of the monkey superior colliculus. *Journal of Neurophysiology*, *79*(3), 1193-1209. https://doi.org/10.1152/jn.1998.79.3.1193

Munoz, D. P., & Wurtz, R. H. (1993). Fixation cells in monkey superior colliculus. I. Characteristics of cell discharge. *Journal of Neurophysiology*, *70*(2), 559-575. https://doi.org/10.1152/jn.1993.70.2.559

Munoz, D. P., & Wurtz, R. H. (1995a). Saccade-related activity in monkey superior colliculus. I. Characteristics of burst and buildup cells. *Journal of Neurophysiology*, *73*(6), 2313-2333. https://doi.org/10.1152/jn.1995.73.6.2313

Munoz, D. P., & Wurtz, R. H. (1995b). Saccade-related activity in monkey superior colliculus. II. Spread of activity during saccades. *Journal of Neurophysiology*, 73(6), 2334-2348. https://doi.org/10.1152/jn.1995.73.6.2334

Nakamura, K., & Colby, C. L. (2002). Updating of the visual representation in monkey striate and extrastriate cortex during saccades. *Proceedings of the National Academy of Sciences of the United States of America*, *99*(6), 4026-4031. https://doi.org/10.1073/pnas.052379899

Neisser, U. (1967). *Cognitive psychology*. Prentice-Hall.

Nguyen, M. N., Nishimaru, H., Matsumoto, J., Van Le, Q., Hori, E., Maior, R. S., Tomaz, C., Ono, T., & Nishijo, H. (2016). Population coding of facial information in the monkey superior colliculus and pulvinar. *Frontiers in Neuroscience*, *10*, 1. https://doi.org/10.3389/fnins.2016.00583

Nguyen, M.N., Matsumoto, J., Hori, E., Maior, R.S., Tomaz, C., Tran, A.H., Ono, T. and Nishijo, H. (2014). Neuronal responses to face-like and facial stimuli in the monkey superior colliculus. *Frontiers in Behavioral Neuroscience*, *8*, 85. https://doi.org/10.3389/fnbeh.2014.00085

Noudoost, B., Clark, K. L., & Moore, T. (2014). A distinct contribution of the frontal eye field to the visual representation of saccadic targets. *Journal of Neuroscience*, *34*(10), 3687-3698. https://doi.org/10.1523/JNEUROSCI.3824-13.2014

Nowak, L. G., & Bullier, J. (1997). The timing of information transfer in the visual system. In K. S. Rockland, J. H. Kaas, & A. Peters (Eds.), *Cerebral Cortex: Extrastriate Cortex in Primates* (pp. 205–241). Plenum Press.

Nowak, L. G., Munk, M. H. J., Girard, P., & Bullier, J. (1995). Visual latencies in areas V1 and V2 of the macaque monkey. *Visual Neuroscience*, *12*(2), 371-384. https://doi.org/10.1017/S095252380000804X

Nyffeler, T., Kaufmann, B. C., & Cazzoli, D. (2021). Visual neglect after an isolated lesion of the superior colliculus. *Journal of the America Medical Association: Neurology*, *78*(12), 1531-1533. https://doi.org/10.1001/jamaneurol.2021.3863

Ottes, F. P., Van Gisbergen, J. A., & Eggermont, J. J. (1986). Visuomotor fields of the superior colliculus: a quantitative model. *Vision Research*, *26*(6), 857-873. https://doi.org/10.1016/0042-6989(86)90144-6

Pack, C. C., Conway, B. R., Born, R. T., & Livingstone, M. S. (2006). Spatiotemporal structure of nonlinear subunits in macaque visual cortex. *Journal of Neuroscience*, *26*(3), 893-907. https://doi.org/10.1523/JNEUROSCI.3226-05.2006

Palmer, S. E. (1978). Structural aspects of visual similarity. *Memory & Cognition*, *6*(2), 91-97. https://doi.org/10.3758/BF03197433

Paré, M., & Hanes, D. P. (2003). Controlled movement processing: superior colliculus activity associated with countermanded saccades. *Journal of Neuroscience*, *23*(16), 6480-6489. https://doi.org/10.1523/JNEUROSCI.23-16-06480.2003

Parkhurst, D., & Niebur, E. (2003). Scene content selected by active vision. *Spatial Vision*, *16*(2), 125-154. https://doi.org/10.1163/15685680360511645

Parkhurst, D., Law, K., & Niebur, E. (2002). Modeling the role of salience in the allocation of overt visual attention. *Vision Research*, *42*(1), 107-123. https://doi.org/10.1016/S0042-6989(01)00250-4

Parton, A., Malhotra, P., & Husain, M. (2004). Hemispatial neglect. *Journal of Neurology, Neurosurgery & Psychiatry*, *75*(1), 13-21. https://doi.org/10.1007/springerreference_115726

Perry, C. J., Sergio, L. E., Crawford, J. D., & Fallah, M. (2015). Hand placement near the visual stimulus improves orientation selectivity in V2 neurons. *Journal of Neurophysiology*, *113*(7), 2859-2870. https://doi.org/10.1152/jn.00919.2013

Peters, R. J., Iyer, A., Itti, L., & Koch, C. (2005). Components of bottom-up gaze allocation in natural images. *Vision Research*, *45*(18), 2397-2416. https://doi.org/10.1016/j.visres.2005.03.019

Pigarev, I. N., Rizzolatti, G., & Scandolara, C. (1979). Neurons responding to visual stimuli in the frontal lobe of macaque monkeys. *Neuroscience Letters*, *12*(2-3), 207–212. https://doi.org/10.1016/0304-3940(79)96063-4

Poe, G.L., Giraud, K.L., & Loomis, J. B. (2005). Computational methods for measuring the difference of empirical distributions. *American Journal of Agricultural Economics*, *87*(2), 353–365. https://doi.org/10.1111/j.1467-8276.2005.00727.x

Pomerleau, V.J., Fortier-Gauthier, U., Corriveau, I., Dell'Acqua, R., & Jolicoeur, P. (2014). Colour-specific differences in attentional deployment for equiluminant pop-colours: Evidence from lateralized potentials. *International Journal of Psychophysiology*, *91*(3), 194–205. https://doi.org/10.1016/j.ijpsycho.2013.10.016

Pomplun, M., Reingold, E. M., & Shen, J. (2001). Peripheral and parafoveal cueing and masking effects on saccadic selectivity in a gaze-contingent window paradigm. *Vision Research*, *41*(21), 2757-2769. https://doi.org/10.1016/S0042-6989(01)00145-6

Port, N. L., & Wurtz, R. H. (2003). Sequential activity of simultaneously recorded neurons in the superior colliculus during curved saccades. *Journal of Neurophysiology*, *90*(3), 1887-1903. https://doi.org/10.1152/jn.01151.2002

Pouget, P., Emeric, E. E., Stuphorn, V., Reis, K., & Schall, J. D. (2005). Chronometry of visual responses in frontal eye field, supplementary eye field, and anterior cingulate cortex. *Journal of Neurophysiology*, *94*(3), 2086-2092. https://doi.org/10.1152/jn.01097.2004

Raiguel, S., Van Hulle, M. M., Xiao, D. K., Marcar, V. L., Lagae, L., & Orban, G. A. (1997). Size and shape of receptive fields in the medial superior temporal area (MST) of the macaque. *NeuroReport*, *8*(12), 2803-2808. https://doi.org/10.1097/00001756-199708180-00030

Recanzone, G. H., & Wurtz, R. H. (2000). Effects of attention on MT and MST neuronal activity during pursuit initiation. *Journal of Neurophysiology*, *83*(2), 777-790. https://doi.org/10.1152/jn.2000.83.2.777

Reingold, E. M., & Stampe, D. M. (2002). Saccadic inhibition in voluntary and reflexive saccades. *Journal of Cognitive Neuroscience, 14*(3), 371-388. https://doi.org/10.1162/089892902317361903

Reynolds, J. H., Pasternak, T., & Desimone, R. (2000). Attention increases sensitivity of V4 neurons. *Neuron*, *26*(3), 703-714. https://doi.org/10.1016/S0896-6273(00)81206-4

Riesenhuber, M., & Poggio, T. (1999). Hierarchical models of object recognition in cortex. *Nature Neuroscience*, *2*(11), 1019-1025. https://doi.org/10.1038/14819

Riesenhuber, M., & Poggio, T. (2000). Models of object recognition. *Nature Neuroscience*, *3*(11), 1199-1204. https://doi.org/10.1038/81479

Robinson, D. A. (1972). Eye movements evoked by collicular stimulation in the alert monkey. *Vision Research, 12*(11), 1795-1808. https://doi.org/10.1016/0042-6989(72)90070-3

Robinson, D. A., & Fuchs, A. F. (1969). Eye movements evoked by stimulation of frontal eye fields. *Journal of Neurophysiology, 32*(5), 637-648. https://doi.org/10.1152/jn.1969.32.5.637

Rodgers, C. K., Munoz, D. P., Scott, S. H., & Paré, M. (2006). Discharge properties of monkey tectoreticular neurons. *Journal of Neurophysiology, 95*(6), 3502-3511. https://doi.org/10.1152/jn.00908.2005

Roelfsema, P. R., Tolboom, M., & Khayat, P. S. (2007). Different processing phases for features, figures, and selective attention in the primary visual cortex. *Neuron, 56*(5), 785–792. https://doi.org/10.1016/j.neuron.2007.10.006

Rolfs, M., Kliegl, R., & Engbert, R. (2008). Toward a model of microsaccade generation: The case of microsaccadic inhibition. *Journal of Vision, 8*(11), 1-23. https://doi.org/10.1167/8.11.5

Romo, R., Hernández, A., Zainos, A., & Salinas, E. (1998). Somatosensory discrimination based on cortical microstimulation. *Nature, 392*(6674), 387-390. https://doi.org/10.1038/32891

Romo, R., Hernández, A., Zainos, A., & Salinas, E. (2003). Correlated neuronal discharges that increase coding efficiency during perceptual discrimination. *Neuron, 38*(4), 649–657. https://doi.org/10.1016/S0896-6273(03)00287-3

Rudolph, K., & Pasternak, T. (1999). Transient and permanent deficits in motion perception after lesions of cortical areas MT and MST in the macaque monkey. *Cerebral Cortex*, *9*(1), 90-100. https://doi.org/10.1093/cercor/9.1.90

Salinas, E., Shankar, S., Costello, M. G., Zhu, D., & Stanford, T. R. (2010). Waiting is the hardest part: comparison of two computational strategies for performing a compelled-response task. *Frontiers in Computational Neuroscience*, *4*, 154. https://doi.org/10.3389/fncom.2010.00153

Salzman, C. D., Britten, K. H., & Newsome, W. T. (1990). Cortical microstimulation influences perceptual judgements of motion direction. *Nature*, *346*(6280), 174-177. https://doi.org/10.1038/346174a0

Salzman, C. D., Murasugi, C. M., Britten, K. H., Newsome, W. T. (1992). Microstimulation in visual area MT: Effects on direction discrimination performance. *Journal of Neuroscience*, *12*(6), 2331-2355. https://doi.org/10.1523/JNEUROSCI.12-06-02331.1992

Sato, T. R., & Schall, J. D. (2003). Effects of stimulus-response compatibility on neural selection in frontal eye field. *Neuron*, *38*(4), 637-648. https://doi.org/10.1016/S0896-6273(03)00237-X

Sato, T. R., Watanabe, K., Thompson, K. G., & Schall, J. D. (2003). Effect of target-distractor similarity on FEF visual selection in the absence of the target. *Experimental Brain Research*, *151*(3), 356-363. https://doi.org/10.1007/s00221-003-1461-1

Sato, T., Murthy, A., Thompson, K. G., & Schall, J. D. (2001). Search efficiency but not response interference affects visual selection in frontal eye field. *Neuron*, *30*(2), 583-591. https://doi.org/10.1016/S0896-6273(01)00304-X

Sawaguchi, T., & Goldman-Rakic, P. S. (1991). D1 dopamine receptors in prefrontal cortex: Involvement in working memory. *Science*, *251*(4996), 947–951. https://doi.org/10.1126/science.1825731

Sawaguchi, T., & Goldman-Rakic, P. S. (1994). The role of the D1-dopamine receptor in working memory: Local injections of dopamine antagonists into the prefrontal cortex of rhesus monkeys performing an oculomotor delayed-response task. *Journal of Neurophysiology*, *71*(2), 515–528. https://doi.org/10.1152/jn.1994.71.2.515

Schall, J. D. (1991). Neuronal activity related to visually guided saccades in the frontal eye fields of rhesus monkeys: comparison with supplementary eye fields. *Journal of Neurophysiology*, *66*(2), 559-579. https://doi.org/10.1152/jn.1991.66.2.559

Schall, J. D. (2004). On the role of frontal eye field in guiding attention and saccades. *Vision Research*, *44*(12), 1453–1467. https://doi.org/10.1016/j.visres.2003.10.025

Schall, J. D., & Hanes, D. P. (1993). Neural basis of saccade target selection in frontal eye field during visual search. *Nature*, *366*(6454), 467-469. https://doi.org/10.1038/366467a0

Schall, J. D., Hanes, D. P., Thompson, K. G., & King, D. J. (1995a). Saccade target selection in frontal eye field of macaque. I. Visual and premovement activation. *Journal of Neuroscience*, *15*(10), 6905-6918. https://doi.org/10.1523/JNEUROSCI.15-10-06905.1995

Schall, J. D., Morel, A., King, D. J., & Bullier J. (1995b). Topography of visual cortex connections with frontal eye field in macaque: Convergence and segregation of processing streams. *Journal of Neuroscience, 15*(6), 4464–4487. https://doi.org/10.1523/JNEUROSCI.15-06-04464.1995

Schall, J. D., Sato, T. R., Thompson, K. G., Vaughn, A. A., & Juan, C. H. (2004). Effects of search efficiency on surround suppression during visual selection in frontal eye field. *Journal of Neurophysiology*, *91*(6), 2765-2769. https://doi.org/10.1152/jn.00780.2003

Schall, J., D, & Cohen, J., Y. (2011). The neural basis of saccade target selection. In S. P. Liversedge, I. D. Gilchrist, & S. Everling (Eds.), *The Oxford Handbook of Eye Movements* (pp. 357–381). Oxford University Press.

Schein, S.J., & Desimone, R. (1990). Spectral properties of V4 neurons in the macaque. *Journal of Neuroscience*, *10*(10), 3369–3389. https://doi.org/10.1523/JNEUROSCI.10-10-03369.1990

Schiller, P. H. (1977). The effect of superior colliculus ablation on saccades elicited by cortical stimulation. *Brain Research*, *122*(1), 154–156. https://doi.org/10.1016/0006-8993(77)90672-2

Schiller, P. H., & Malpeli, J. G. (1977). Properties and tectal projections of monkey retinal ganglion cells. *Journal of Neurophysiology*, *40*(2), 428-445. https://doi.org/10.1152/jn.1977.40.2.428

Schiller, P. H., & Tehovnik, E. J. (2001). Look and see: How the brain moves your eyes about. *Progress in Brain Research*, *134*, 127–142. https://doi.org/10.1016/S0079-6123(01)34010-4

Schiller, P. H., & Tehovnik, E. J. (2005). Neural mechanisms underlying target selection with saccadic eye movements. *Progress in Brain Research*, *149*, 157-171. https://doi.org/10.1016/S0079-6123(05)49012-3

Schiller, P. H., Sandell, J. H., & Maunsell, J. H. (1987). The effect of frontal eye field and superior colliculus lesions on saccadic latencies in the rhesus monkey. *Journal of Neurophysiology*, *57*(4), 1033-1049. https://doi.org/10.1152/jn.1987.57.4.1033

Schiller, P. H., Slocum, W. M., Kwak, M. C., Kendall, G. L., & Tehovnik, E. J. (2011). New methods devised specify the size and color of the spots monkeys see when striate cortex (area V1) is electrically stimulated. *Proceedings of the National Academy of Sciences of the United States of America*, *108*(43), 17809-17814. https://doi.org/10.1073/pnas.1108337108

Schiller, P. H., Stryker, M., Cyander, M., & Berman, N. (1974). Response characteristics of single cells in the monkey superior colliculus following ablatio or cooling of visual cortex. *Journal of Neurophysiology*, *37*(1), 181–194. https://doi.org/10.1152/jn.1974.37.1.181

Schiller, P. H., True, S. D., & Conway, J. L. (1979). Effects of frontal eye field and superior colliculus ablations on eye movements. *Science*, *206*(4418), 590-592. https://doi.org/10.1126/science.115091

Schiller, P. H., True, S. D., & Conway, J. L. (1980). Deficits in eye movements following frontal eye-field and superior colliculus ablations. *Journal of Neurophysiology*, *44*(6), 1175-1189. https://doi.org/10.1152/jn.1980.44.6.1175

Schlag-Rey, M., Schlag, J., & Dassonville, P. (1992). How the frontal eye field can impose a saccade goal on superior colliculus neurons. *Journal of Neurophysiology*, *67*(4), 1003–1005. https://doi.org/10.1152/jn.1992.67.4.1003

Schmidt, L. J., Belopolsky, A. V., & Theeuwes, J. (2012). The presence of threat affects saccade trajectories. *Visual Cognition*, *20*(3), 284-299. https://doi.org/10.1080/13506285.2012.658885

Schmolesky, M. T., Wang, Y., Hanes, D. P., Thompson, K. G., Leutgeb, S., Schall, J. D., & Leventhal, A. G. (1998). Signal timing across the macaque visual system. *Journal of Neurophysiology*, *79*(6), 3272-3278. https://doi.org/10.1152/jn.1998.79.6.3272

Schnyder, H., Reisine, H., Hepp, K., & Henn, V. (1985). Frontal eye field projection to the paramedian pontine reticular formation traced with wheat germ agglutinin in the monkey. *Brain Research*, *329*(1-2), 151-160. https://doi.org/10.1016/0006-8993(85)90520-7

Schwartz, A. B., Kettner, R. E., & Georgopoulos, A. P. (1988). Primate motor cortex and free arm movements to visual targets in three-dimensional space. I. Relations between single cell discharge and direction of movement. *Journal of Neuroscience*, *8*(8), 2913-2927. https://doi.org/10.1523/jneurosci.08-08-02913.1988

Segraves, M. A. (1992). Activity of monkey frontal eye field neurons projecting to oculomotor regions of the pons. *Journal of Neurophysiology*, *68*(6), 1967-1985. https://doi.org/10.1152/jn.1992.68.6.1967

Segraves, M. A., & Goldberg, M. E. (1987). Functional properties of corticotectal neurons in the monkey's frontal eye field. *Journal of Neurophysiology*, *58*(6), 1387-1419. https://doi.org/10.1152/jn.1987.58.6.1387

Serences, J. T., & Yantis, S. (2006). Selective visual attention and perceptual coherence. *Trends in Cognitive Sciences*, *10*(1), 38-45. https://doi.org/10.1016/j.tics.2005.11.008

Serences, J. T., & Yantis, S. (2007). Spatially selective representations of voluntary and stimulus-driven attentional priority in human occipital, parietal, and frontal cortex. *Cerebral Cortex*, *17*(2), 284-293. https://doi.org/10.1093/cercor/bhj146

Serences, J. T., Shomstein, S., Leber, A. B., Golay, X., Egeth, H. E., & Yantis, S. (2005). Coordination of voluntary and stimulus-driven attentional control in human cortex. *Psychological Science*, *16*(2), 114-122. https://doi.org/10.1111/j.0956-7976.2005.00791.x

Serre, T., Oliva, A., & Poggio, T. (2007). A feedforward architecture accounts for rapid categorization. *Proceedings of the National Academy of Sciences of the United States of America*, *104*(15), 6424-6429. https://doi.org/10.1073/pnas.070062210

Shankar, S., Massoglia, D. P., Zhu, D., Costello, M.G., Stanford, T.R., & Salinas, E. (2011). Tracking the temporal evolution of a perceptual judgment using a compelled-response task. *Journal of Neuroscience*, *31*(23), 8406–8421. https://doi.org/10.1523/JNEUROSCI.1419-11.2011

Sheliga, B. M., Riggio, L., & Rizzolatti, G. (1994). Orienting of attention and eye movements. *Experimental Brain Research*, *98*(3), 507-522. https://doi.org/10.1007/BF00233988

Sheliga, B. M., Riggio, L., & Rizzolatti, G. (1995a). Spatial attention and eye movements. *Experimental Brain Research*, *105*(2), 261-275. https://doi.org/10.1007/BF00240962

Sheliga, B. M., Riggio, L., Craighero, L., & Rizzolatti, G. (1995b). Spatial attention-determined modifications in saccade trajectories. *NeuroReport*, *6*(3), 585–588. https://doi.org/10.1097/00001756-199502000-00044

Shen, J., Reingold, E. M., & Pomplun, M. (2000). Distractor ratio influences patterns of eye movements during visual search. *Perception*, *29*(2), 241-250. https://doi.org/10.1068/p2933

Shen, K. & Paré, M. (2006). Guidance of eye movements during visual conjunction search: Local and global contextual effects on target discriminability. *Journal of Neurophysiology*, *95*, 2845-2855. https://doi.org/10.1152/jn.00898.2005

Shen, K., & Paré, M. (2007). Neuronal activity in superior colliculus signals both stimulus identity and saccade goals during visual conjunction search. *Journal of Vision*, *7*(5), 1-13. https://doi.org/10.1167/7.5.15

Shen, K., & Paré, M. (2012). Neural basis of feature-based contextual effects on visual search behavior. *Frontiers in Behavioral Neuroscience*, *5*, 91. https://doi.org/10.3389/fnbeh.2011.00091

Shen, K., & Paré, M. (2014). Predictive saccade target selection in superior colliculus during visual search. *Journal of Neuroscience*, *34*(16), 5640-5648. https://doi.org/10.1523/JNEUROSCI.3880-13.2014

Shin, S., & Sommer, M. A. (2010). Activity of neurons in monkey globus pallidus during oculomotor behavior compared with that in substantia nigra pars reticulata. *Journal of Neurophysiology*, *103*(4), 1874–1887. https://doi.org/10.1152/jn.00101.2009

Slotnick, S., Hopfinger, J.B., Klein, S., & Sutter, E.E. (2002). Darkness beyond the light: Attentional inhibition surround the classic spotlight. *NeuroReport*, *13*(6), 773–778. https://doi.org/10.1097/00001756-200205070-00008

Sommer, M. A., & Wurtz, R. H. (2004). What the brain stem tells the frontal cortex. I. Oculomotor signals sent from superior colliculus to frontal eye field via mediodorsal thalamus. *Journal of Neurophysiology*, *91*(3), 1381-1402. https://doi.org/10.1152/jn.00738.2003

Song, J. H., & McPeek, R. M. (2015). Neural correlates of target selection for reaching movements in superior colliculus. *Journal of Neurophysiology*, *113*(5), 1414-1422. https://doi.org/10.1152/jn.00417.2014

Song, J. H., Rafal, R. D., & McPeek, R. M. (2011). Deficits in reach target selection during inactivation of the midbrain superior colliculus. *Proceedings of the National Academy of Sciences of the United States of America*, *108*(51), E1433-E1440. https://doi.org/10.1073/pnas.1109656108

Sparks, D. L. (1978). Functional properties of neurons in the monkey superior colliculus: coupling of neuronal activity and saccade onset. *Brain Research*, *156*(1), 1-16. https://doi.org/10.1016/0006-8993(78)90075-6

Sparks, D. L. (2002). The brainstem control of saccadic eye movements. *Nature Reviews Neuroscience*, *3*(12), 952-964. https://doi.org/10.1038/nrn986

Spector, R. H. (1990). Visual fields. In H. K. Walker, W. D. Hall, & J. W. Hurst (Eds.), *Clinical methods: The history, physical, and laboratory examinations* (3rd edition, pp. 565–572). Butterworth.

Spitzer, H., Desimone, R., & Moran, J. (1988). Increased attention enhances both behavioral and neuronal performance. *Science*, *240*(4850), 338-340. https://doi.org/10.1126/science.3353728

Stanford, T. R., Shankar, S., Massoglia, D. P., Costello, M. G., & Salinas, E. (2010). Perceptual decision making in less than 30 milliseconds. *Nature Neuroscience*, *13*(3), 379–385. https://doi.org/10.1038/nn.2485

Stanton, G. B., Goldberg, M. E., & Bruce, C. J. (1988). Frontal eye field efferents in the macaque monkey: II. Topography of terminal fields in midbrain and pons. *Journal of Comparative Neurology*, *271*(4), 493-506. https://doi.org/10.1002/cne.902710403

Störmer, V. S., & Alvarez, G. A. (2014). Feature-based attention elicits surround suppression in feature space. *Current Biology*, *24*(17), 1985–1988. https://doi.org/10.1016/j.cub.2014.07.030

Subramanian, J., & Colby, C. L. (2014). Shape selectivity and remapping in dorsal stream visual area LIP. *Journal of Neurophysiology*, *111*(3), 613-627. https://doi.org/10.1152/jn.00841.2011

Supèr, H., Spekreijse, H., & Lamme, V. A. F. (2001). A neural correlate of working memory in the monkey primary visual cortex. *Science*, *293*(5527), 120–124. https://doi.org/10.1126/science.1060496

Takikawa, Y., Kawagoe, R., Itoh, H., Nakahara, H., & Hikosaka, O. (2002). Modulation of saccadic eye movements by predicted reward outcome. *Experimental Brain Research*, *142*, 284-291. https://doi.org/10.1007/s00221-001-0928-1

Tchernikov, I. & Fallah, M. (2010). A color hierarchy for automatic target selection. PLoS One, *5*(2), e9338. https://doi.org/10.1371/journal.pone.0009338

Tehovnik, E. J., Slocum, W. M., & Schiller, P. H. (2002). Differential effects of laminar stimulation of V1 cortex on target selection by macaque monkeys. *European Journal of Neuroscience*, *16*(4), 751-760. https://doi.org/10.1046/j.1460-9568.2002.02123.x

Tehovnik, E. J., Slocum, W. M., & Schiller, P. H. (2003). Saccadic eye movements evoked by microstimulation of striate cortex. *European Journal of Neuroscience*, *17*(4), 870-878. https://doi.org/10.1046/j.1460-9568.2003.02489.x

Theeuwes, J., Kramer, A. F., Hahn, S., & Irwin, D. E. (1998). Our eyes do not always go where we want them to go: Capture of the eyes by new objects. *Psychological Science*, *9*(5), 379-385. https://doi.org/10.1111/1467-9280.00071

Theeuwes, J., Olivers, C. N., & Chizk, C. L. (2005). Remembering a location makes the eyes curve away. *Psychological Science*, *16*(3), 196-199. https://doi.org/10.1111/j.0956-7976.2005.00803.x

Thompson, K. G., & Bichot, N. P. (2005). A visual salience map in the primate frontal eye field. *Progress in Brain Research*, *147*, 249-262. https://doi.org/10.1016/S0079-6123(04)47019-8

Thompson, K. G., Bichot, N. P., & Sato, T. R. (2005). Frontal eye field activity before visual search errors reveals the integration of bottom-up and top-down salience. *Journal of Neurophysiology*, *93*(1), 337-351. https://doi.org/10.1152/jn.00330.2004

Thompson, K. G., Hanes, D. P., Bichot, N. P., & Schall, J. D. (1996). Perceptual and motor processing stages identified in the activity of macaque frontal eye field neurons during visual search. *Journal of Neurophysiology*, *76*(6), 4040-4055. https://doi.org/10.1152/jn.1996.76.6.4040

Thompson, K.G., Biscoe, K.L., & Sato, T.R. (2005). Neuronal basis of covert spatial attention in the frontal eye field. *Journal of Neuroscience*, *25*(41), 9487–9479. https://doi.org/10.1523/JNEUROSCI.0741-05.2005

Tipper, S. P., Howard, L. A., & Jackson, S. R. (1997). Selective reaching to grasp: Evidence for distractor interference effects. *Visual Cognition*, *4*(1), 1–38, 1997. https://doi.org/10.1080/713756749

Tipper, S. P., Howard, L. A., & Paul, M. A. (2001). Reaching affects saccade trajectories. *Experimental Brain Research*, *136*(2), 241-249. https://doi.org/10.1007/s002210000577

Tombu, M., & Tsotsos, J. K. (2008). Attending to orientation results in an inhibitory surround in orientation space. *Perception & Psychophysics*, *70*(1), 30–35. https://doi.org/10.3758/PP.70.1.30

Treisman, A. M., & Gelade, G. (1980). A feature-integration theory of attention. *Cognitive Psychology, 12*(1), 97-136. https://doi.org/10.1016/0010-0285(80)90005-5

Treue, S., & Maunsell, J. H. (1996). Attentional modulation of visual motion processing in cortical areas MT and MST. *Nature*, *382*(6591), 539-541. https://doi.org/10.1038/382539a0

Treue, S., & Trujillo, J. C. M. (1999). Feature-based attention influences motion processing gain in macaque visual cortex. *Nature*, *399*(6736), 575-579. https://doi.org/10.1038/21176

Tsotsos, J. K. (1990). Analyzing vision at the complexity level. *Behavioral and Brain Sciences*, *13*(3), 423–469. https://doi.org/10.1017/S0140525X00079577

Tsotsos, J. K. (2011). *A computational perspective on visual attention*. MIT Press.

Tsotsos, J. K., Culhane, S. M., Wai, W. Y. K., Lai, Y., Davis, N., & Nuflo, F. (1995). Modeling visual attention via selective tuning. *Artificial Intelligence, 78*(1-2), 507–545. https://doi.org/10.1016/0004-3702(95)00025-9

Tudge, L., Brandt, S. A., & Schubert, T. (2018). Salience from multiple feature contrast: Evidence from saccade trajectories. *Attention, Perception, & Psychophysics*, *80*(3), 677-690. https://doi.org/10.3758/s13414-017-1480-9

Tudge, L., McSorley, E., Brandt, S. A., & Schubert, T. (2017). Setting things straight: A comparison of measures of saccade trajectory deviation. *Behavior Research Methods*, *49*(6), 2127-2145. https://doi.org/10.3758/s13428-016-0846-6

Ullman, S. (1984). Visual routines. *Cognition*, *18*(1-3). https://doi.org/10.1016/B978-0-08-051581-6.50035-0

Ungerleider, L. G., & Haxby, J. V. (1994). 'What' and 'where' in the human brain. *Current Opinion in Neurobiology*, *4*(2), 157-165. https://doi.org/10.1016/0959-4388(94)90066-3

Van der Stigchel, S., & Nijboer, T. C. W. (2013). How global is the global effect? The spatial characteristics of saccade averaging. *Vision Research*, *84*, 6-15. https://doi.org/10.1016/j.visres.2013.03.006

Van der Stigchel, S., & Theeuwes, J. (2005). Relation between saccade trajectories and spatial distractor locations. *Cognitive Brain Research*, *25*(2), 579-582. https://doi.org/10.1016/j.cogbrainres.2005.08.001

Van der Stigchel, S., de Vries, J. P., Bethlehem, R., & Theeuwes, J. (2011). A global effect of capture saccades. *Experimental Brain Research, 210*(1), 57–65. https://doi.org/10.1007/s00221-011-2602-6

Van der Stigchel, S., Heeman, J., & Nijboer, T. C. W. (2012). Averaging is not everything: The saccade global effect weakens with increasing stimulus size. *Vision Research, 62*, 108-115. https://doi.org/10.1016/j.visres.2012.04.003

Van Essen, D. C., & Maunsell, J. H. (1983). Hierarchical organization and functional streams in the visual cortex. *Trends in Neurosciences, 6*, 370-375. https://doi.org/10.1016/0166-2236(83)90167-4

Van Essen, D. C., Anderson, C. H., & Felleman, D. J. (1992). Information processing in the primate visual system: an integrated systems perspective. *Science, 255*(5043), 419-423. https://doi.org/10.1126/science.1734518

Van Gisbergen, J. A. M., Van Opstal, A. J., & Tax, A. A. M. (1987). Collicular ensemble coding of saccades based on vector summation. *Neuroscience, 21*(2), 541-555. https://doi.org/10.1016/0306-4522(87)90140-0

Van Opstal, A. J., & Van Gisbergen, J. A. M. (1989). A nonlinear model for collicular spatial interactions underlying the metrical properties of electrically elicited saccades. *Biological Cybernetics, 60*(3), 171-183. https://doi.org/10.1007/BF00207285

van Zoest, W., Donk, M., & Van der Stigchel, S. (2012). Stimulus-salience and the time-course of saccade trajectory deviations. *Journal of Vision, 12*(8), 1-13. https://doi.org/10.1167/12.8.16

Verghese, P. (2001). Visual search and attention: A signal detection theory approach. *Neuron*, *31*(4), 523–535. https://doi.org/10.1016/S0896-6273(01)00392-0

Verghese, P., & Nakayama, K. (1994). Stimulus discriminability in visual search. *Vision Research*, 34(18), 2453–2467. https://doi.org/10.1016/0042-6989(94)90289-5

Walker, R., Deubel, H., Schneider, W. X., & Findlay, J. M. (1997). Effect of remote distractors on saccade programming: Evidence for an extended fixation zone. *Journal of Neurophysiology, 78*(2), 1108-1119. https://doi.org/10.1152/jn.1997.78.2.1108

Walker, R., Mannan, S., Maurer, D., Pambakian, A. L. M., & Kennard, C. (2000). The oculomotor distractor effect in normal and hemianopic vision. *Proceedings of the Royal Society of London. Series B: Biological Sciences*, *267*(1442), 431-438. https://doi.org/10.1098/rspb.2000.1018

Walker, R., McSorley, E., & Haggard, P. (2006). The control of saccade trajectories: Direction of curvature depends on prior knowledge of target location and saccade latency. *Perception & Psychophysics*, *68*(1), 129-138. https://doi.org/10.3758/BF03193663

Weaver, M. D., Lauwereyns, J., & Theeuwes, J. (2011). The effect of semantic information on saccade trajectory deviations. *Vision Research*, *51*(10), 1124-1128. https://doi.org/10.1016/j.visres.2011.03.005

Weiskrantz, L. (1996). Blindsight revisited. *Current Opinion in Neurobiology*, *6*(2), 215-220. https://doi.org/10.1016/S0959-4388(96)80075-4

White, B. J., & Munoz, D. P. (2011). A computational perspective on visual attention. In S. P. Liversedge, I. D. Gilchrist, & S. Everling (Eds.), *The Oxford Handbook of Eye Movements* (pp. 195–213). Oxford University Press.

White, B. J., Berg, D. J., Kan, J. Y., Marino, R. A., Itti, L., & Munoz, D. P. (2017a). Superior colliculus neurons encode a visual saliency map during free viewing of natural dynamic video. *Nature Communications*, *8*(1), 14263. https://doi.org/10.1038/ncomms14263

White, B. J., Boehnke, S. E., Marino, R. A., Itti, L., & Munoz, D. P. (2009). Color-related signals in the primate superior colliculus. *Journal of Neuroscience*, *29*(39), 12159-12166. doi.org/10.1523/JNEUROSCI.1986-09.2009

White, B. J., Kan, J. Y., Levy, R., Itti, L., & Munoz, D. P. (2017b). Superior colliculus encodes visual saliency before the primary visual cortex. *Proceedings of the National Academy of Sciences of the United States of America*, *114*(35), 9451-9456. https://doi.org/10.1073/pnas.1701003114

White, B. J., Theeuwes, J., & Munoz, D. P. (2012). Interaction between visual-and goal-related neuronal signals on the trajectories of saccadic eye movements. *Journal of Cognitive Neuroscience*, *24*(3), 707-717. https://doi.org/10.1162/jocn_a_00162

Williams, G. V., & Goldman-Rakic, P. S. (1995). Modulation of memory fields by dopamine D1 receptors in prefrontal cortex. *Nature*, *376*(6541), 572–575. https://doi.org/10.1038/376572a0

Wolfe, J. M. (1994). Guided search 2.0 a revised model of visual search. *Psychonomic Bulletin & Review*, *1*(2), 202-238. https://doi.org/10.3758/BF03200774

Wolfe, J. M., Cave, K. R., & Franzel, S. L. (1989). Guided search: An alternative to the feature integration model for visual search. *Journal of Experimental Psychology: Human Perception and Performance*, *15*(3), 419-433. https://doi.org/10.1037/0096-1523.15.3.419

Wolfe, J.M., & Horowitz, T.S. (2004). What attributes guide the deployment of visual attention and how do they do it? *Nature Reviews Neuroscience*, *5*(6), 495–501. https://doi.org/10.1038/nrn1411

Wurtz, R. H., & Goldberg, M. E. (1971). Superior colliculus cell responses related to eye movements in awake monkeys. *Science*, *171*(3966), 82-84. https://doi.org/10.1126/science.171.3966.82

Wurtz, R. H., & Goldberg, M. E. (1972). Activity of superior colliculus in behaving monkey. III. Cells discharging before eye movements. *Journal of Neurophysiology*, *35*(4), 575-586. https://doi.org/10.1152/jn.1972.35.4.575

Wurtz, R. H., & Mohler, C. W. (1976). Organization of monkey superior colliculus: Enhanced visual response of superficial layer cells. *Journal of Neurophysiology*, *39*(4), 745-765. https://doi.org/10.1152/jn.1976.39.4.745

Xiao, Q., Barborica, A., & Ferrera, V. P. (2006). Radial motion bias in macaque frontal eye field. *Visual Neuroscience*, *23*(1), 49-60. https://doi.org/10.1017/S0952523806231055

Yan, Y.J., Cui, D. M., & Lynch, J. C. (2001). Overlap of saccadic and pursuit eye movement systems in the brain stem reticular formation. *Journal of Neurophysiology*, *86*(6), 3056–3060. https://doi.org/10.1152/jn.2001.86.6.3056

Yantis, S., & Jonides, J. (1984). Abrupt visual onsets and selective attention: Evidence from visual search. *Journal of Experimental Psychology: Human Perception and Performance, 10*(5), 601-624. https://doi.org/10.1037/0096-1523.10.5.601

Yantis, S., Schwarzbach, J., Serences, J. T., Carlson, R. L., Steinmetz, M. A., Pekar, J. J., & Courtney, S. M. (2002). Transient neural activity in human parietal cortex during spatial attention shifts. *Nature Neuroscience, 5*(10), 995-1002. https://doi.org/10.1038/nn921

Yau, J. M., Pasupathy, A., Brincat, S. L., & Connor, C. E. (2013). Curvature processing dynamics in macaque area V4. *Cerebral Cortex, 23*(1), 198-209. https://doi.org/10.1093/cercor/bhs004

Zeki, S. (1991). Cerebral akinetopsia (visual motion blindness) a review. *Brain, 114*(2), 811-824. https://doi.org/10.1093/brain/114.2.811

Zeki, S. M. (1974). Functional organization of a visual area in the posterior bank of the superior temporal sulcus of the rhesus monkey. *Journal of Physiology, 236*(3), 549–573. https://doi.org/10.1113/jphysiol.1974.sp010452

Zeki, S., & Bartels, A. (1999). Toward a theory of visual consciousness. *Consciousness and Cognition, 8*(2), 225-259. https://doi.org/10.1006/ccog.1999.0390

Zhou, H., & Desimone, R. (2011). Feature-based attention in the frontal eye field and area V4 during visual search. *Neuron, 70*(6), 1205-1217. https://doi.org/10.1016/j.neuron.2011.04.032